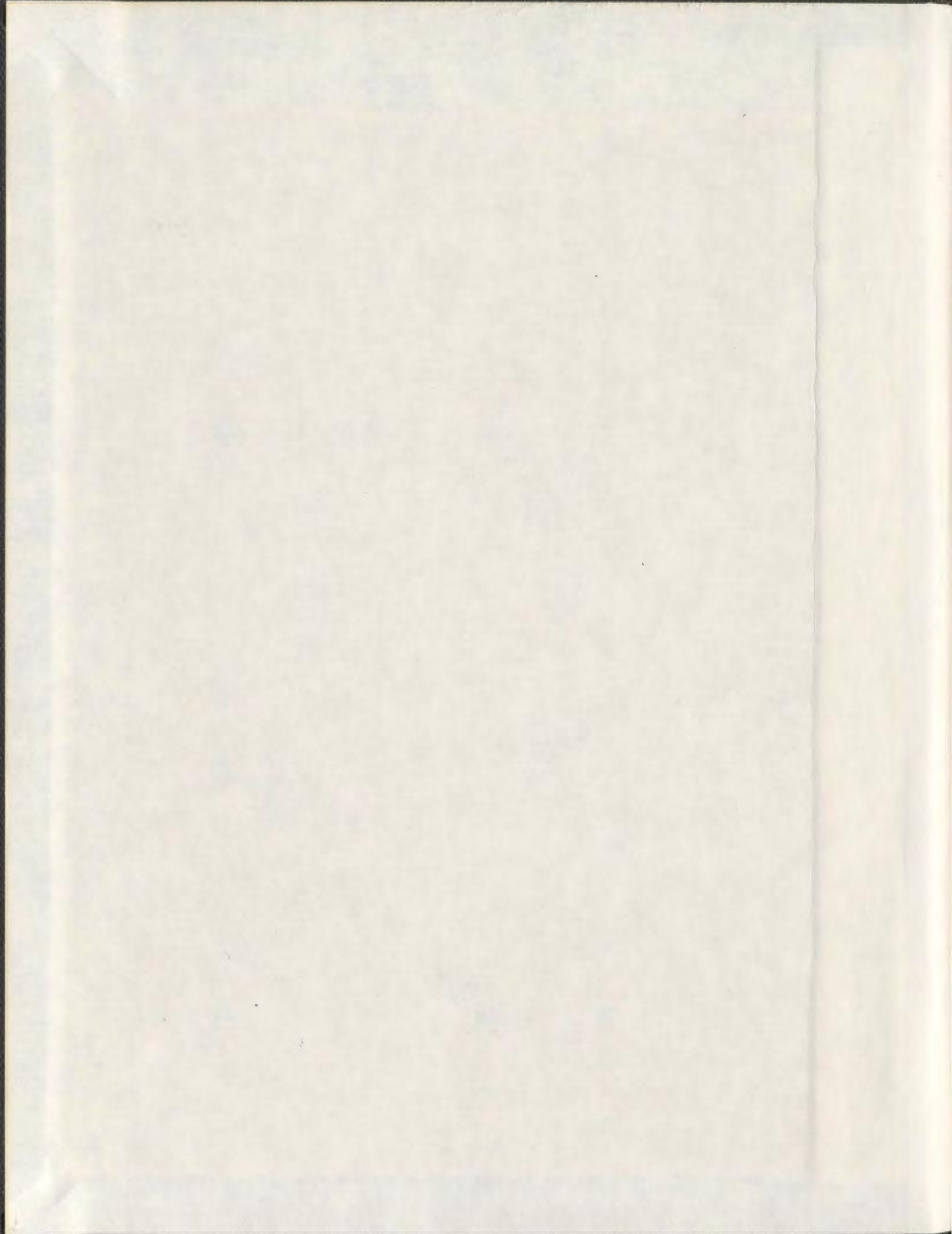


STRUCTURAL CHANGES WITHIN THE AMORPHOUS
AND CRYSTALLINE DOMAINS OF C-TYPE STARCHES
SUBJECTED TO HEAT MOISTURE TREATMENT AT
DIFFERENT TEMPERATURES

PRIYATHARINI AMBIGAIPALAN



**STRUCTURAL CHANGES WITHIN THE AMORPHOUS AND CRYSTALLINE
DOMAINS OF C-TYPE STARCHES SUBJECTED TO HEAT MOISTURE
TREATMENT AT DIFFERENT TEMPERATURES**

by

©Priyatharini Ambigaipalan

A thesis submitted to the

School of Graduate Studies

in partial fulfillment of the requirements for the degree of

Doctor of Philosophy

Department of Biochemistry

Memorial University of Newfoundland

October 2013

St. John's

Newfoundland and Labrador

Canada

Abstract

The structure (granular, supramolecular, molecular) and physicochemical properties of starches isolated from newly introduced Canadian cultivars of faba bean (FB), black bean (BB) and pinto bean (PB) were examined. The structure and physicochemical properties were determined by microscopy, High performance anion exchange chromatography with pulsed amperometric detection (HPAEC-PAD), Attenuated total reflectance Fourier transform infra-red spectroscopy (ATR-FTIR), Wide angle X-ray diffraction (WAXS), ^{13}C cross polarization magic angle spinning nuclear magnetic resonance (^{13}C CP/MAS NMR), Differential scanning calorimetry (DSC), Rapid visco analyzer (RVA), susceptibility towards enzyme and acid hydrolysis and turbidity. FB starches exhibited cracked granules, whereas the surface of PB and BB starches showed no evidence of cracks or indentations. All starches exhibited a 'C' type X-ray pattern. Molecular order near the granule surface followed the order: BB~PB>FB. Differences in amylopectin chain length distribution among FB, BB and PB starches and among cultivars were marginal. FB starches significantly ($P<0.05$) differed from BB and PB starches with respect to amylose leaching, swelling factor, gelatinization temperatures, enthalpy of gelatinization, susceptibility towards acid hydrolysis and nutritional fractions. Retrogradation characteristics of FB, BB and PB starches monitored by turbidity, FTIR, DSC, ^{13}C CP/MAS NMR and X-ray followed the order: FB>BB~PB, PB>BB>FB, PB~BB~FB, PB~BB~FB and PB~BB~FB, respectively. Retrograded FB starches were hydrolyzed by α -amylase to a greater extent than BB and PB (BB>PB) starches.

FB, BB and PB starches were heat-moisture treated (HMT) at 80°, 100° and 120°C for 12h at a moisture content of ~23%. Structural changes with HMT were monitored by microscopy, HPAEC-PAD, ATR-FTIR, WAXS, DSC, RVA, susceptibility towards acid hydrolysis and *in-vitro* digestibility. Amylopectin chain length distribution and gelatinization enthalpy remained unchanged in all starches with HMT. In all starches, HMT increased crystallinity (FB>BB>PB), gelatinization temperatures (FB~PB~BB), gelatinization temperature range (FB>BB>PB), SDS (FB~BB>PB) and RS (PB>BB>FB) contents, and decreased birefringence, set-back (FB>BB>PB), peak viscosity (FB>BB~PB) and the amount of B-type crystallites (FB~BB~PB). The results of this study showed that the structural reorganization of starch chains during HMT at different temperatures was influenced by changes to starch chain flexibility, amylose-amylopectin interactions and crystalline stability of the native granules.

Acknowledgements

I would like to express my sincere gratitude to my supervisor Dr. R. Hoover for the continuous support of my PhD study and research, for his patience, motivation, enthusiasm, and immense knowledge. I also appreciate Dr. R. Bertolo, and Dr. R. McGowan for serving on my supervisory committee and for the time and effort they spent on my behalf. I would like to acknowledge the Department of Biochemistry and the School of Graduate Studies for providing financial assistance. Financial support from Dr. R. Hoover is also acknowledged.

My sincere thanks also extended to Dr. Q. Liu (HPAEC-PAD, FTIR, RVA), Ms. E. Donner, Dr. R. N. Chibbar (HPSEC), Dr. S. Jaiswal, Dr. K. Seetharaman, K. K. M. Nantanga, Dr. K. Stapleton, Dr. C. Schnider and Dr. M. Shaffer for their help in some of the analytical techniques described in the thesis. I would like to express my sincere thanks to Dr. A. Yethiraj (Dept. of Physics and Physical Oceanography) for assistance with confocal laser scanning and polarized microscopy techniques. Thanks also to CREAT unit (Memorial University of Newfoundland) [SEM, DSC, WAXS, ^{13}C CP/MAS NMR] and to Dr. Kirstin Bett (University of Saskatchewan), Dr. Brent Barlow (University of Saskatchewan) and T. Rupert (Agriculture and Agri-Food Canada, Guelph) for the supply of pulse seeds. I also thank my colleagues V. Varathan and S. Maaran.

Thanks also extended to Varathans' family, Lalanis' family, Huberts' family and all my friends in St. John's for helping me in all possible ways to succeed. Finally I am so thankful to my beloved Parents and my sisters for their courage and support throughout my PhD study.

Table of contents

Abstract	ii
Acknowledgements.....	iv
Table of contents.....	v
List of Tables	xi
List of Figures	xiii
List of Abbreviations	xvii
Chapter 1	1
Introduction and Overview	1
Chapter 2.....	7
Literature Review.....	7
2.1 Starch	7
2.2 Starch biosynthesis.....	9
2.3 Granule morphology and size	14
2.4 Molecular architecture of starch.....	17
2.5 Molecular composition of starch granules	20
2.5.1 Amylose.....	23
2.5.1.1 Fine structure of amylose	23
2.5.1.2 Conformation of amylose.....	24
2.5.1.3 Location of amylose	27
2.5.1.4 Amylose-inclusion complex.....	31
2.5.1.5 Determination of amylose content.....	34
2.5.2 Amylopectin.....	35
2.5.2.1 Fine structure of amylopectin.....	35

2.5.2.2 Unit chain distribution of amylopectin.....	35
2.5.2.3 Branch structure and the polymorphism of starch granule	38
2.5.2.4 Starch crystallinity.....	45
2.5.3 Protein.....	49
2.5.4 Lipid.....	49
2.5.5 Phosphorus.....	50
2.6 Starch properties.....	53
2.6.1 Granular swelling and amylose leaching	53
2.6.2 Gelatinization.....	55
2.6.3 Pasting.....	62
2.6.4 Retrogradation	63
2.6.5 Acid hydrolysis of starch	66
2.6.6 Enzyme hydrolysis of starch.....	70
2.6.7 Nutritional fractions	76
2.7 Heat-moisture treatment.....	78
2.7.1 Impact of HMT on granule morphology.....	82
2.7.2 Impact of HMT on granule structure	83
2.7.2.1 Starch polymorphism and X-ray diffraction pattern.....	83
2.7.2.2 Peak intensity and relative crystallinity.....	86
2.7.2.3 Molecular order at the granular surface.....	88
2.7.2.4 Lamellar organization.....	88
2.7.2.5 Amylose-lipid complex formation	89
2.7.3 Impact of HMT on starch properties.....	89
2.7.3.1 Granular swelling	89
2.7.3.2 Amylose leaching.....	90
2.7.3.3 Gelatinization	91
2.7.3.4 Pasting	93
2.7.3.5 Acid hydrolysis	94
2.7.3.6 Enzyme hydrolysis	95
2.7.3.7 Nutritional fractions	96
2.7.4 Applications of HMT starch	98
Chapter 3	100
Materials and Methods.....	100

3.1 Materials.....	100
3.2 Methods.....	101
3.2.1 Starch isolation	101
3.2.2 Heat moisture treatment.....	102
3.2.3 Starch damage.....	102
3.2.4 Chemical composition	103
3.2.4.1 Moisture content	103
3.2.4.2 Ash content	104
3.2.4.3 Nitrogen content	104
3.2.4.4 Phosphorus content	105
3.2.4.5 Apparent amylose content.....	107
3.2.4.5.1 High performance size exclusion chromatography (HPSEC)	107
3.2.4.5.2 Colorimetry	108
3.2.4.6 Lipid content.....	108
3.2.4.6.1 Surface lipid	108
3.2.4.6.2 Bound lipid.....	109
3.2.4.6.3 Crude lipid purification	109
3.2.5 Granule morphology and particle size distribution.....	110
3.2.5.1 Starch granule size distribution	110
3.2.5.2 Polarized light microscopy	111
3.2.5.3 Scanning electron microscopy.....	111
3.2.5.4 Confocal laser scanning microscopy	111
3.2.6 Starch structure	112
3.2.6.1 Determination of amylopectin chain length distribution by high-performance anion-exchange chromatography with pulsed amperometric detection (HPAEC-PAD).....	112
3.2.6.2 Determination of short range molecular order by attenuated total reflectance fourier transform infrared spectroscopy (ATR-FTIR)	114
3.2.6.3 Wide angle X-ray diffraction (WAXS)	114
3.2.6.3 Determination of double helical content by ¹³ C cross polarization magic angle spinning nuclear magnetic resonance spectroscopy (¹³ C CP/MAS NMR)	115
3.2.6 Starch properties	116
3.2.5.1 Amylose leaching (AML)	116
3.2.6.2 Swelling factor (SF)	117
3.2.6.3 Differential scanning calorimetry (DSC)	118

3.2.6.4 Rapid Visco Analyzer (RVA)	119
3.2.6.5 α -amylase hydrolysis	119
3.2.6.6 Acid hydrolysis	120
3.2.6.7 <i>In-vitro</i> starch digestibility and expected glycemic index (eGI)	121
3.2.7 Retrogradation	123
3.2.7.1 Turbidity.....	123
3.2.7.2 Gel preparation.....	123
3.2.8 Statistical analysis.....	124
Chapter 4	125
Results and Discussion	125
4.1 Structure of faba bean, black bean and pinto bean starches at different levels of granule organization and their physicochemical properties.....	125
4.1.1 Composition	125
4.1.2. Granule characteristics	128
4.1.3. Amylopectin chain length distribution.....	133
4.1.4. Attenuated total reflectance Fourier transform infrared spectroscopy (ATR-FTIR)	135
4.1.5. X-ray Diffraction.....	138
4.1.6. Amylose leaching (AML) and Swelling factor (SF).....	141
4.1.7. Pasting properties	144
4.1.8. Gelatinization characteristics	148
4.1.9. <i>In-vitro</i> digestibility	151
4.1.10. Acid hydrolysis	159
4.1.11. Retrogradation studies on pulse starches	162
4.1.11. 1 Turbidity measurements.....	162
4.1.11. 2 Differential scanning calorimetry (DSC).....	166
4.1.11. 3 Attenuated total reflectance Fourier transform infrared spectroscopy (ATR-FTIR)	171
4.1.11.4 Solid state ^{13}C cross-polarization / magic angle spinning nuclear magnetic spectroscopy (^{13}C CP/MAS NMR).....	175
4.1.11.5 Wide angle X-ray diffraction (WAXS).....	179

4.11.6 Enzyme hydrolysis of retrograded starches	184
4.2. Impact of heat-moisture treatment on pulse starch structure and properties	187
4.2.1 Birefringence.....	187
4.2.2 Amylopectin chain length distribution (HPAEC-PAD).....	190
4.2.3 Attenuated total reflectance Fourier transform Infra-red Spectroscopy (ATR-FTIR)	192
4.2.4 X-ray diffraction, patterns and crystallinity	195
4.2.5 Differential scanning calorimetry (DSC)	199
4.2.6 Swelling factor (SF) and amylose leaching (AML)	204
4.2.7 Pasting characteristics	207
4.2.8 Acid Hydrolysis	209
4.2.9 Nutritional Fractions	212
4.2.9.1 Granule morphology of native and HMT80 starches before and after amylolysis..	220
Chapter 5	224
5.1 Summary and conclusions	224
5.2 Novelty and Significance	227
5.3 Directions for future research	230
References.....	231
List of refereed publications and conference proceedings.....	275
Academic Honors, Awards and Fellowships	277
APPENDICES	278
Appendix I	279
Appendix II	280
Appendix III.....	281

Appendix IV.....	282
Appendix V.....	283
Appendix VI.....	284
Appendix VII.....	285

List of Tables

Table 2.1 Shape and size of starch granules from different botanical origins	16
Table 2.2 Proximate composition of starches	22
Table 2.3 Double helical content of starches determined by ¹³ C CP/MAS NMR.....	46
Table 2.4 HMT parameters of pulse starches.....	81
Table 4.1 Chemical composition (%) of faba, black and pinto bean starches	127
Table 4.2 Amylopectin chain length distribution of faba, black and pinto bean starches	134
Table 4.3 Short-range molecular order of faba, black and pinto bean starches.....	137
Table 4.4 Gelatinization parameters of faba, black and pinto bean starches	150
Table 4.5 Nutritional fractions, hydrolysis index and expected glycemic index of native faba, black and pinto bean starches determined by <i>in vitro</i> hydrolysis	157
Table 4.6 Retrogradation transition temperatures of faba bean, black bean and pinto bean starches.....	169
Table 4.7 Short range molecular order of retrograded faba, black and pinto bean starches measured by attenuated total reflectance–Fourier-transform infrared spectroscopy	174
Table 4.8 ¹³ C CPMAS/NMR C-4 peak intensity of native, gelatinized, 2 days retrograded and 25 days retrograded faba bean, black bean and pinto bean starches	177
Table 4.9 Relative crystallinity and B polymorphic content of retrograded faba, black and pinto bean starches measured by wide angle X-ray diffraction.....	182

Table 4.10 Amylase hydrolysis of 25 days retrograded fabab bean, black bean and pinto bean starches	186
Table 4.11 Amylopectin chain length distribution of native and HMT faba bean, black bean and pinto bean starches determined by HPAEC-PAD	191
Table 4.12 Gelatinization transition parameters of native and HMT faba bean, black bean and pinto bean starches	198
Table 4.13 Relative crystallinity and B polymorphic content of native and heat moisture treated faba, black and pinto bean starches.....	203
Table 4.14 Swelling factor and amylose leaching at 80 °C for native and HMT faba bean, black bean and pinto bean starches	206
Table 4.15 Nutritional fractions, hydrolysis index and expected glycemic index of native and HMT faba bean, black bean and pinto bean starches determined by <i>in vitro</i> hydrolysis	218

List of Figures

Figure 2.1 Food and non-food applications of starches	8
Figure 2.2 A proposed pathway of starch biosynthesis in seed storage tissue (A) and in a cereal endosperm cell (B)	13
Figure 2.3 Schematic representation of the several level of ultrastructure of starch	18
Figure 2.4 Schematic representation of the arrangement of blocklets in starch granules..	19
Figure 2.5 Schematic diagram of amylose and amylopectin	21
Figure 2.6 Models proposed for amylose conformation in aqueous solution.....	26
Figure 2.7 Amylose chain localization in amylopectin clusters	29
Figure 2.8 A proposed model of starch granule organization in pea starch.....	30
Figure 2.9 Schematic representation of amylose inclusion complexes	33
Figure 2.10 A cluster model for amylopectin	37
Figure 2.11 Double helices arrangement of A-type and B-type crystallites in starch granules	41
Figure 2.12 Proposed models for A-(waxy maize starch) and B- (potato starch) type amylopectin branching patterns	42
Figure 2.13 Proposed model for blocklet arrangement of A and B –type starches	43
Figure 2.14 Schematic representation of a two-directional backbone model of amylopectin.....	44

Figure 2.15 ^{13}C CP/MAS NMR spectrum of a native starch	47
Figure 2.16 X-ray diffraction patterns of A-, B-, C- and V- type starches	48
Figure 2.17 A molecular model of phosphorylated starch (crystalline domain)	52
Figure 2.18 Liquid-crystalline model of starch gelatinization	58
Figure 2.19 A typical DSC thermal curve (50%) solid of a cereal starch showing the different melting transitions	61
Figure 2.20 Mechanism of acid hydrolysis	67
Figure 2.21 Proposed mechanisms involved in the hydrolysis of glycosidic linkages.....	74
Figure 2.22 Glucose-binding subsites at the active-site of four endo-acting α -amylases.	75
Figure 2.23 A schematic representation of some possible changes occur during HMT	79
Figure 2.24 A proposed model of the polymorphic transformation from B-type to A-type unit cell in the solid state	85
Figure 4.1 Granule morphology of faba, black and pinto bean starches	131
Figure 4.2 Starch granule size distribution of faba, black and pinto bean starches	132
Figure 4.3 X ray diffraction patterns, relative crystallinity (RC) and B-polymorphic content of faba, black and pinto bean starches.....	140
Figure 4.4 Amylose leaching and swelling factor of faba, black and pinto bean starches	143
Figure 4.5 Pasting profiles of faba, black and pinto bean starches.....	147

Figure 4.6 Digestibility profile of faba, black and pinto bean starches	158
Figure 4.7 Acid hydrolysis profile of faba, black and pinto bean starches.....	161
Figure 4.8 Turbidity profiles of faba bean(A), black bean(B) and pinto bean(C) starches stored at 25 °C.....	165
Figure 4.9 Enthalpy profile of retrograded faba bean(A), black bean(B) and pinto bean(C) starches stored at 25 °C.....	170
Figure 4.10 ¹³ C CPMAS/NMR spectra of native (N), gelatinized (G), 2 days retrograded (R2) and 25 days retrograded (R25) Faba bean, Black bean and Pinto bean starches.....	178
Figure 4.11 X-ray diffraction patterns of retrograded faba bean(A), black bean(B) and pinto bean(C) starches stored at 25 °C.....	183
Figure 4.12 Polarized light microscopy (× 200) images of native (a), HMT80 (b), HMT100 (c), HMT120 (d) FB (Fatima; 1), BB (Expresso; 2) and PB (AC Pintoba; 3) starches, respectively.	189
Figure 4.13 Structural changes during the time course of heat moisture treatment.....	194
Figure 4.14 Degree of molecular order at the granular surface (1048/1016 cm ⁻¹) of native and HMT FB, BB and PB starches determined by ATR-FTIR spectroscopy.	197
Figure 4.15 X-ray pattern of native and HMT cultivars of FB (Fatima), BB (Expresso) and PB (AC pintoba).....	202
Figure 4.16 Pasting profiles of native and HMT FB, BB and PB starches determined by Rapid Visco Analyzer.	208

Figure 4.17 Acid hydrolysis (2.2N HCl) profiles of native and HMT FB, BB and PB starches.....	211
Figure 4.18 <i>In-vitro</i> digestibility profiles of native and HMT FB, BB and PB starches subjected to hydrolysis by mixture of pancreat in and amyloglucosidase.....	219
Figure 4.19 Scanning electron microscopy images of FB (Fatima, 4.19.1), BB (Expresso, 4.19.2) and PB (AC pintoba, 4.19.3; Pecos, 4.19.4) starches in their native (a,b,c) and HMT80 (d,e,f) states before and after amylolysis (30 min [b,e] and 16 h [c,f]).	223

List of Abbreviations

ADP	-	Adenosine di-phosphate
AFM	-	Atomic force microscopy
AM	-	Amylose
AML	-	Amylose leaching
AP	-	Amylopectin
APCLD	-	Amylopectin chain length distribution
APTS	-	8-aminopyrene-1,3,6-trisulfonic acid
ATR-FTIR	-	Attenuated total reflectance Fourier transform Infrared spectroscopy
¹³ C CP/MAS NMR	-	Cross-polarization magic angle spinning carbon-13 nuclear magnetic resonance
CL	-	Chain length
CLSM	-	Confocal laser scanning microscopy
CVD	-	Cardiovascular disease
db	-	Dry basis
DMSO	-	Dimethyl sulfoxide
DP _n	-	Degree of polymerization
DSC	-	Differential scanning calorimetry
FACE	-	Fluorophore-assisted carbohydrate electrophoresis
FAO	-	Food and Agriculture Organization
FFA	-	Free fatty acids
GI	-	Glycemic index
GWD	-	α-glucan water dikinase

HMT	-	Heat-moisture treatment
HPAEC-PAD	-	High performance anion exchange chromatography with pulsed amperometric detection
HPSEC	-	High performance size exclusion chromatography
LPL	-	Lysophospholipid
PLM	-	Polarized light microscopy
PPA	-	Porcine pancreatic α -amylase
RDS	-	Rapidly digestible starch
RS	-	Resistant starch
RVA	-	Rapid visco analyser
SCLCP	-	Side chain liquid crystalline polymer
SDS	-	Slowly digestible starch
SEC	-	Size exclusion chromatography
SEM	-	Scanning electron microscopy
SF	-	Swelling factor
SS	-	Starch synthase
SBE	-	Starch branching enzyme
TEM	-	Transmission electron microscopy
T _g	-	Glass transition temperature
T _m	-	Melting temperature
XRD	-	X-ray diffraction
WAXS	-	Wide angle X-ray diffraction

Chapter 1

Introduction and Overview

Pulses are the dicotyledonous seed of plants that belong to the Leguminosae family, which are the dry edible seeds (peas, lentils, chickpea and dry bean) of legumes. Global production of pulses reached 40.5 million tonnes in 2006-2007. Pulses have become the fifth largest crop produced in Canada in terms of volume after wheat, barley, canola and corn (FAO, 2007). Canada is the second largest producer of pulses and the world's largest exporter of peas and lentils and a world leader in chickpea and bean exports (FAO, 2007). The top pulse export markets include India, China, Turkey, Pakistan, Spain and Mexico (Saskatchewan Pulse Growers, 2013). Canada is the greatest producer of peas, second largest producer of lentils and ninth largest global producer of chickpeas. Canada produces many types of beans including black bean, pinto bean, faba bean, navy bean, kidney bean and great northern bean (Pulse Canada, 2010). The greatest proportion of bean production is in Southern Ontario and Manitoba, with lesser amounts grown in Alberta and Quebec (Pulse Canada, 2010). About 70% of Canadian pulses are exported each year (Pulse Canada, 2010). World production of dry faba bean ranged from 4.9 to 5.1 million tonnes from 2003-2006. The majority of faba bean production in Canada is in Manitoba (80%), Alberta and Saskatchewan. Pinto bean production in Canada accounts for 40 percent of annual production in North America along with 65 percent of the annual production being in Alberta (Saskatchewan Pulse Growers, 2013). Black bean is an important cash crop for bean growers in south western Ontario. In 2002, Ontario colored dry bean growers produced approximately 8,400 tonnes of black beans.

Pulses play an important role in human diet. Pulses are rich in protein and fiber, and are low in fat and have high levels of minerals such as iron, zinc, and phosphorus as well as folate and other B-vitamins (Hoover et al., 2010). In addition, pulses are inherently gluten-free, and can boost the nutritional profile of gluten-free baked foods. Starch is the most abundant carbohydrate in the pulse seed (22 – 45% [Hoover and Sosulski, 1985]). Pulse starches provide unique properties to food systems, such as high gelation temperature, resistance to shear thinning, fast retrogradation, high resistant starch and high elasticity of gel, owing to their higher amylose content compared to cereal starches (Sandhu and Lim, 2008). Thus, the utilization of their components as new ingredients in the food industry has drawn the attention of researchers. However, native starches from various plant species have poor functionality and are thus not directly suitable for food applications. For example, amylose-rich starches form rigid opaque gels on cooling (due to retrogradation), which on storage lose water (syneresis). Whereas, amylopectin-rich starches (waxy-type) form soft gels (Tharanathan, 2005). Consequently, native starches are physically and/or chemically modified by a variety of modification methods to meet the desired functional properties.

A review of the literature revealed that there is a dearth of information on the structure of pulse starches at the different levels of structural organization (granular, supramolecular and molecular). Consequently, it is difficult in many instances, to interpret the variation in properties among pulse starches reported in the literature. Furthermore, there is very little information on pulse starches with respect to susceptibility towards acid and enzyme hydrolysis, polymorphic composition, rate and extent of retrogradation and on the levels

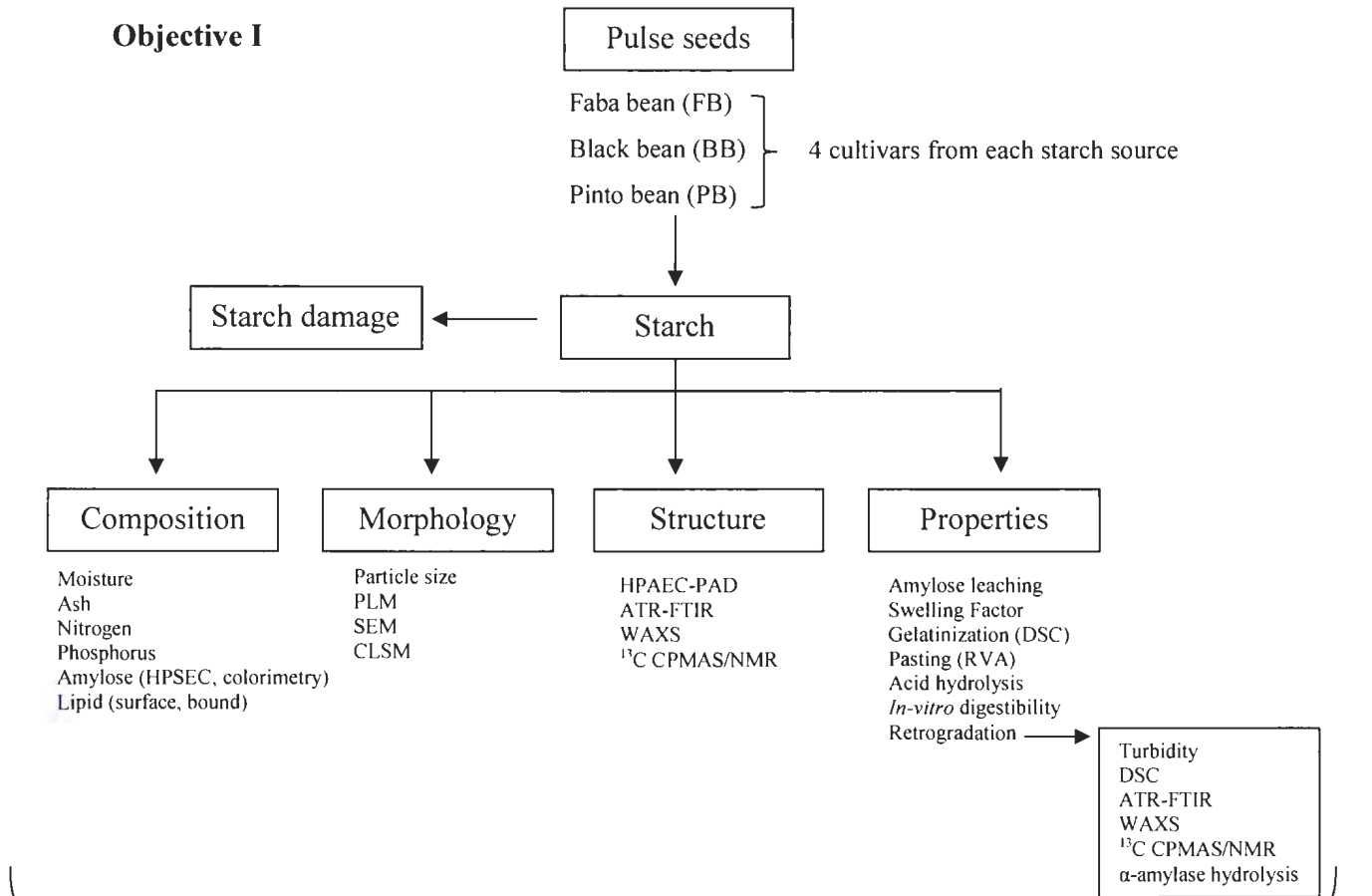
of rapidly digestible starch, slowly digestible starch and resistant starch. Retrogradation characteristics of pulse starches (contain both A and B-type unit cells in different proportions) have been determined mainly by syneresis (exudation of water when a frozen gelatinized starch gel is thawed at room temperature), differential scanning calorimetry (DSC), wide angle X-ray diffraction (WAXS) and turbidity measurements have been used only to a limited extent. Syneresis data on pulse starches is difficult to compare, since starch to water ratios, storage temperatures, number of freeze-thaw cycles and centrifugal speed and time have been different. Many of the studies on pulse starches have been on single cultivars. Consequently, it is difficult to ascertain whether the structure-property relationships reported for a particular cultivar is truly representative of the biotype. Thus, the first objective of this study was **to determine the morphology, composition, structure (at different levels of granule organization) and physicochemical properties of starches isolated by wet milling from 4 newly introduced cultivars of faba bean (*Vicia faba*), black bean (*Phaseolus vulgaris* L.) and pinto bean (*Phaseolus vulgaris* L.) starches.** Recognition of variation in starch properties among cultivars could be useful for plant breeders, who may wish to develop or select potentially useful cultivars with certain functional properties of their starches. The results of the first phase would form the basis for further investigation on the influence of heat-moisture treatment to improve the physicochemical properties of the above starches.

Heat-moisture treatment (HMT) is a physical modification technique where starch granules at low moisture levels (< 35 % H₂O, w/w) are heated at a temperature above the

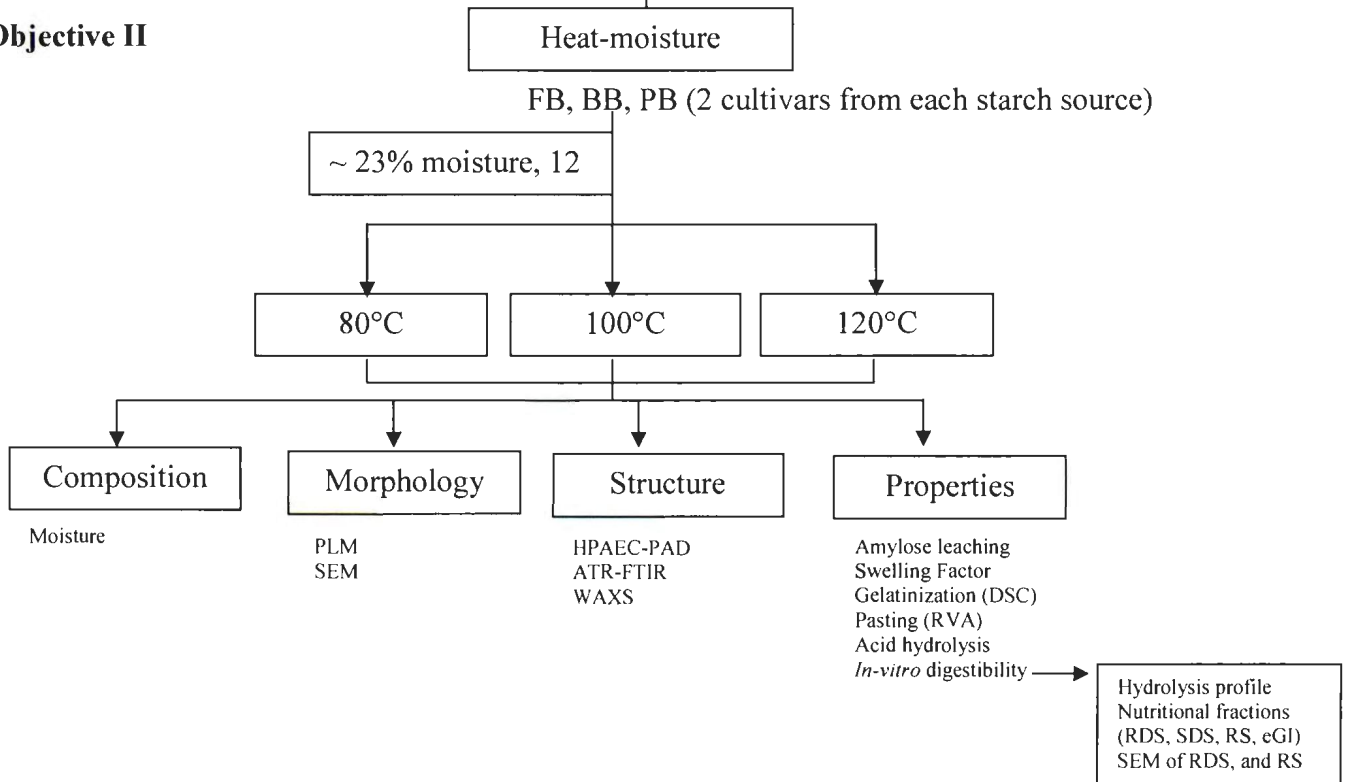
glass transition (T_g) but below the gelatinization temperature for a fixed period of time varying from 15 min to 16 h. HMT facilitates starch chain interactions within the amorphous and crystalline region without destroying its granular structure. Several studies have shown that HMT influences granule morphology, X-ray diffraction pattern, gelatinization parameters, crystallinity, granule swelling, amylose leaching, gelatinization parameters, viscosity, retrogradation and susceptibility towards acid and α -amylase hydrolysis (Hoover and Vasanthan, 1994; Chung, Liu and Hoover, 2009; Varatharajan et al., 2010; Zavareze and Dias, 2011). The type and extent of change has been shown to vary with botanical origin, starch composition and HMT conditions (Hoover, 2010). Published data on HMT starches have involved studies on a single starch source or comparative studies on starches differing widely in amylopectin chain length distribution (APCLD) and amylose content. Consequently, it is difficult to ascertain the extent to which APCLD and amylose content influence structural changes with HMT. The influence of HMT on the structure and properties of cereal and tuber starches that contain pure A- and B- type crystallites, respectively is well documented. However, similar studies on C-type pulse starches that contain varying proportions of both A- and B-type crystallites are fragmentary. Furthermore, the impact of HMT on starch nutritional fractions (slowly digestible starch [SDS] and resistant starch [RS] contents), acid and enzyme hydrolysis, crystallinity, granule morphology, short range molecular order is not well documented. HMT of pulse starches has been mainly studied only at one temperature [$\geq 100^\circ\text{C}$] (Hoover and Manuel, 1996a; Lawal and Adebowale; 2005a, b; Chung, Liu and Hoover, 2009, 2010; Guzel and Sayar, 2010). In addition, changes to the granular surface and the degradation pathway into the granular interior of RDS and RS

have not been studied for pulse starches. Furthermore, the extent to which amylose [AM] chains influence structural changes with HMT is still dispute. Thus, the second objective of this study was **to unravel the structural changes (at molecular [HPAEC-PAD, ATR-FTIR, ¹³C CP/MAS NMR] and supramolecular levels [WAXS]) that occur in FB, BB and PB starches with HMT (~23% moisture) at 80°, 100° and 120°C, and their impact on physicochemical properties.** Therefore, it is hypothesized that structural changes with HMT may reflect the interplay among the following factors: 1) packing density (loose or compact) of AM and AP chains within native granules, 2) extent of association between AM and AP within the native granules and 3) differences in polymorphic composition. This study will not only widen the knowledge base on HMT, but also provides a less costly and more efficient means of increasing starch nutritional fractions (SDS and RS contents) and thermal and freeze-thaw stability. It is anticipated, that this study will add value to pulse starch production in Canada that primarily relies on the sale of the raw material.

Research outline



Objective II



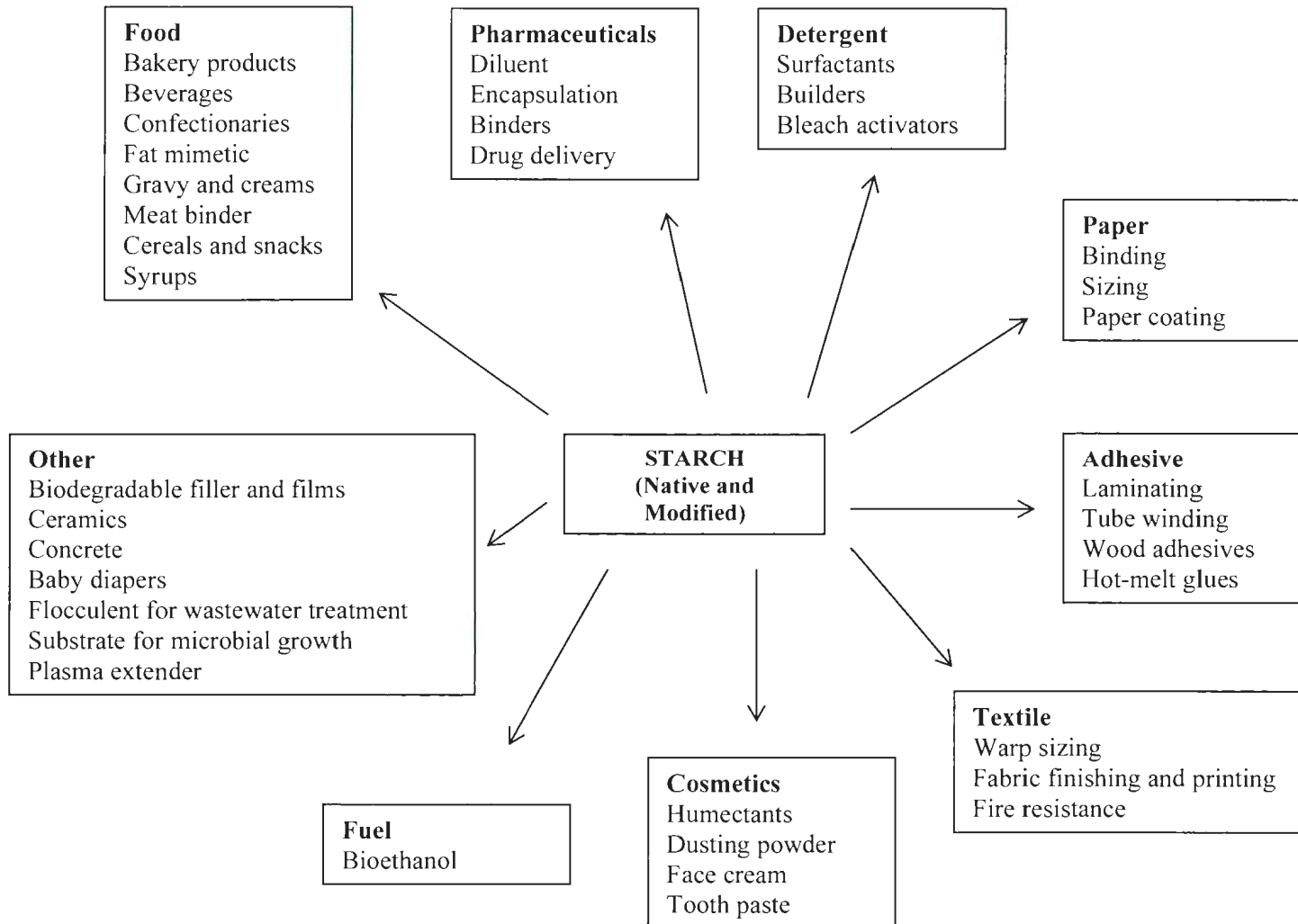
Chapter 2

Literature Review

2.1 Starch

Starch is the predominant food reserve substance in plants. It is an essential component of food providing a large proportion of the daily calorific intake and is important in non-food uses such as in adhesives (Burrell, 2003). It provides 70-80 % of the calories consumed by humans worldwide (Whistler and BeMiller, 1997). Starch granules are mainly found in seeds, roots and tubers, as well as in stems, leaves, fruits and pollen. Food starches are mainly derived from cereal grains (rice, wheat, maize, barley, sorghum etc.), tubers (potato, sweet potato, yam), roots (cassava, taro) and seeds of beans (pulses). Worldwide, the main sources of starch are maize (82%), wheat (8%), potatoes (5%), and cassava (5%) from which tapioca starch is derived (Angellier et al., 2004). In the food industry, starch is a valuable ingredient contributing to nutrition, texture, appearance, sensory characteristics and functional properties. It is also a key ingredient in animal feed and has many industrial applications outside the food industry, such as in paper manufacture, packaging and the production of biofuels. The above characteristics are primarily governed by gelation, gelatinization, pasting, solubility, swelling and digestibility of starch. Food and non-food application of starches are shown in Fig. 2.1.

Figure 2.1 Food and non-food applications of starches (Davis et al., 2003; Ellis et al., 1998)



2.2 Starch biosynthesis

Biosynthesis of starch granules is initiated at the hilum, and the granules grow by apposition (Perez and Bertoft, 2010). The biosynthesis of starch involves not only the production of the composite glucans but also their arrangement into an organized form within the starch granule (Martin and Smith, 1995). Transitory starch synthesis in higher plants occurs in chloroplasts during photosynthesis, which is degraded and transported as sucrose to amyloplasts of storage organs, where it is incorporated into storage starch (Zeeman, Smith and Smith, 2007). Sucrose is the starting point for alpha-glucan deposition. Major amyloplast-based enzymes responsible for biosynthetic process are ADP-glucose pyrophosphorylase (AGPase), starch synthase [SS], starch branching enzymes [SBE] and starch debranching enzyme [DBE] (Jeon et al., 2010; Tetlow, 2011). The generalized pathway of sucrose-to-starch conversion in a typical non-photosynthetic cell (e.g. from potato tuber) (A) and in a cereal endosperm cell (B) is shown in Fig 2.2. In all plant tissues, AGPase is responsible for the synthesis of the ADP-glucose, the primary sugar nucleotide donor of glucose residues for starch biosynthesis (Smith, Denyer and Martin, 1997). Starch synthases catalyze the transfer of the glucosyl moiety of the soluble precursor ADP-glucose to the non-reducing end of a pre-existing α -(1 \rightarrow 4)-O-linked glucan primer to synthesize glucan polymers (Tetlow, 2011). Amylose is synthesized by granular-bound starch synthase (GBSS), which differs from amylopectin synthesized by soluble starch synthase (Jane, 2006). Plants possess multiple isoforms of starch synthases, containing at least five isoforms including GBSSI, GBSSII, SSI, SSII, SSIII and SSIV (Tetlow, 2011). GBSSI, encoded by the waxy (Wx) gene, is responsible for the amylose

biosynthesis (Tetlow, Morell and Emes, 2004). SSI is primarily responsible for the synthesis of the shortest glucan chains ($DP < 10$) whereas SSII and SSIII are responsible for extension of longer glucan chains (Tetlow, Morell and Emes, 2004). The SS III and SS IV have recently been discovered to be responsible for starch granule initiation (Szydlowski et al., 2009)

Amylopectin (AP) is synthesized from linear chains by SBE's which hydrolyzes an α -(1 \rightarrow 4)-linkage within a chain and joins the reducing ends created to an α -(1 \rightarrow 4)-linked chain by an α -(1 \rightarrow 6)-linkage (Tetlow, Morell and Emes, 2004; Jeon et al., 2010). Starch synthases can extend branched chains, which may then be further branched by branching enzymes (Burton et al., 1995). Branching of AP is the result of the balanced activities of SBE. SBE are present in multiple isoforms in all plants examined (Preiss and Sivak, 1996). The isoforms SBEI and SBEII are distinguished by their deduced amino acid sequences (Burton et al., 1995). Tetlow, Morell and Emes (2004) reported that they differ in terms of the length of the glucan chains transferred and their substrate specificities. Each isoform exhibits a unique developmental time of peak activity and a different length of amylose chain transferred (Smith, Denyer and Martin, 1995). Variation in levels of branching enzymes may result in starch with novel branching patterns (McCue et al., 2002). Burton et al. (1995) reported that the absence of SBEI can limit the rate of synthesis of starch in developing pea embryos in a way that cannot be compensated for by SBEII. It also indicates that SBEI may be responsible for the synthesis of about 75% of the AP found in the starch granules of mature embryos. The genes encoding the two

isoforms are also differentially expressed during embryo development and this can be correlated to qualitative differences in the AP formed during embryo development (Burton et al., 1995).

Pea SBEI is most similar to maize SBEII (77% identity) and pea SBEII is 72% identical to SBEI from maize (Burton et al. 1995). Burton et al. (1995) suggested that SBEI from pea, SBEIII from rice and SBEII from maize belong to one starch branching enzyme family (family A) and the other family (family B) contains all but one of the other SBE reported, including SBEII from pea and SBEI from maize. SBEI is significantly more active than SBEII in pea embryo development, and that SBEII activity increases later in embryo development (Smith, 1988; Burton et al., 1995). The basis for these developmental changes is reported due to the changing gene expression (Burton et al., 1995). No differential expression of rice branching enzyme isoforms has been reported (Mizuno et al., 1992). This could be taken to mean that branching of starch in endosperm (unlike pea embryo) does not undergo changes in the nature of its branching enzyme activity through development (Burton et al., 1995). SBE of potato has been identified as similar to SBEI from maize and rice (Poulson and Kreiberg, 1993). In maize, SBEI has higher activity on amylose and SBEII has higher activity on AP (Guan and Preiss, 1993). The change from SBEI activity to a mixture of SBEI and II activity during pea embryo development is accompanied by a change in the structure of amylopectin molecules, suggesting that the two isoforms transfer chains of different lengths *in vivo*. Takeda, Guan and Preiss (1993) showed that the latter transfers shorter branches than the former during branching of maize amylose *in vivo*. Burton et al. (1995) showed that AP of

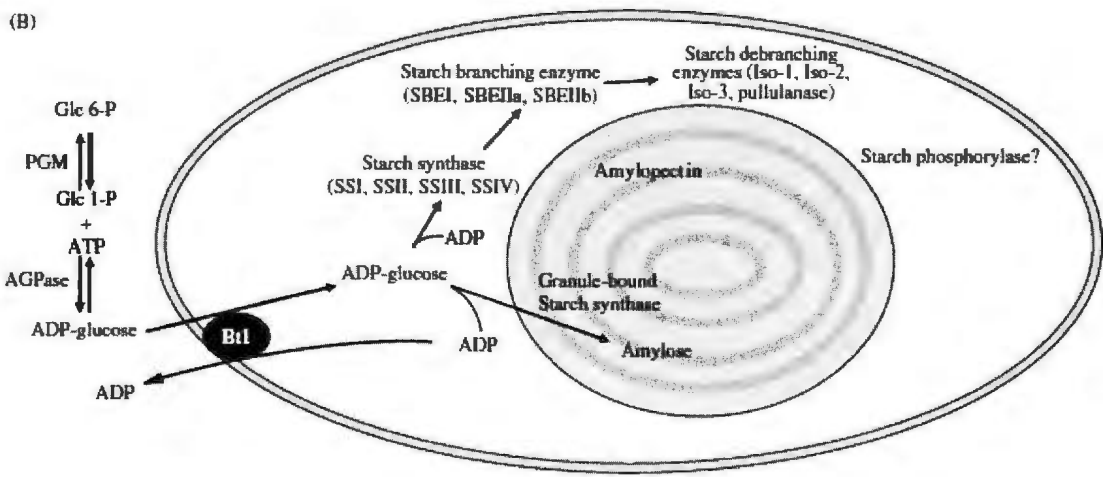
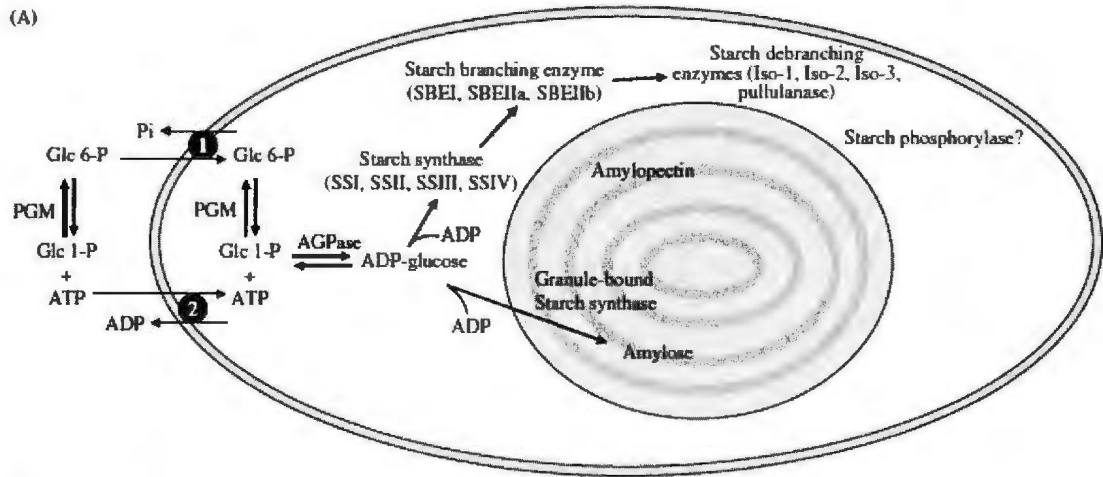
young pea embryos gave a shorter average branch length than AP of older embryos. SBE of families A and B play different roles in determining the structure of AP in storage organs. Differences in the balance of the two isoforms, both in overall activity and contributions during development, could also determine qualitative differences in starch between different plant species (Burton et al., 1995). Crystalline polymorphism is determined by the length of AP side chains. In peas SBEI is active during the early stages of embryo development which produces short side chains and high number of branches. Therefore it produces A-type polymorphs at early stages. The activity of SBEI decreases eventually and SBEII activity increases at latter stage of embryo development. SBEII produces long side chains and forms B-type polymorphs. Therefore, the centers of pea starch granules are rich in B-type whilst peripheral regions are rich in A-type polymorphs (Wang et al., 2012). Potato starch has only SBEII, produces B-type polymorphs. SBEI is responsible for AP synthesis in maize, which produces A-type polymorphs.

Two groups of DBE (isoamylase and the pullulanase) exist in plant, which are responsible for the removal of inappropriately positioned branches (pre-amylopectin) generated at the surface of the growing starch granules, which would otherwise prevent crystallization (Tetlow, 2011). α -glucan-water dikinase (phosphorylates glucose residues at the C6 position in amylopectin) and phospho- α -glucan-water dikinase (involved in phosphorylating amylopectin at the C3 position of glucose residues pre-phosphorylated) probably preparing the polymer for degradation by hydrolytic enzymes (Ritte et al., 2004; Zeeman, Kossmann and Smith, 2010).

Figure 2.2 A proposed pathway of starch biosynthesis in seed storage tissue (A) and in a cereal endosperm cell (B) (Tetlow, 2011, Copyright Cambridge University Press, reproduced with permission)

(A) In storage tissues of dicots AGPase is responsible for the synthesis of ADP-glucose, is exclusively localized in the plastid stroma. Hexose-phosphates and ATP for this reaction are imported into the plastid from the cytosol via, respectively, the Glc 6-P/Pi antiporter (1) and the ATP/ADP transporter (2) located in the inner envelope membrane of the plastid. Cytosolic and plastidial isoforms of phosphoglucomutase (PGM) interconvert Glc 6-P and Glc 1-P. The antiport substrates for these transporters are generated from plastidial reactions involved in starch synthesis; Pi is generated from pyrophosphate produced by AGPase, and ADP is a by-product of the starch synthase (SS) reaction. ADP-glucose is utilized by the SSs, and the glucan chain branched and debranched by starch branching enzymes (SBE) and debranching enzymes, respectively, to form amylopectin. Granule-bound starch synthase also uses ADP-glucose, and is exclusively involved in amylose synthesis.

(B) The pathway of starch synthesis operating in the endosperms of monocots such as cereals. These plants possess a cytosolic form of AGPase and import ADP-glucose from the cytosol via an ADP-glucose/ADP transporter termed Bt1. Monocots also possess a plastidial form of AGPase (as seen in A), but much of the AGPase in these tissues is extra-plastidial.



2.3 Granule morphology and size

The shape and size of the starch granules differ according to the botanical source and the environmental conditions under which a crop is grown (Jackson, 2003). Every variety of starch has its own characteristic shape ranging from spherical to ellipsoidal, lenticular to polyhedral, and average size (Bergthaller and Hollmann, 2007). Diameters of starch granules vary from submicrons (amaranth) to 100 μm (canna starch) (Jane, 2006; Perez and Bertoft, 2010). Granule morphology is characterized using light microscopy, scanning electron microscopy (SEM), transmission electron microscopy (TEM), atomic force microscopy (AFM) and confocal laser scanning microscopy (CLSM) (Jane et al., 1994; Gallant, Bouchet and Baldwin, 1997; Glaring, Koch and Blennow, 2006). Cereal starches are generally small and polyhedric with a concentric hilum. Whereas, tuber starches are generally large, ellipsoid or spherical where, apparent shells are around an eccentric hilum (Tester, Karkalas and Qi, 2004).

Pulse starches have been shown to vary in shape (oval, round, spherical, elliptical, irregular), width (5 to 55 μm) and length (5 to 70 μm) (Hoover et al., 2010). Most pulse starches are composed of simple granules (Hoover et al., 2010). However, there are cases where more than one granule is produced simultaneously in a single amyloplast. Consequently, they are more difficult to separate (Perez and Bertoft, 2010). These compound granules have been reported in smooth pea (Bertoft and Qin, 1993) and wrinkled pea (Colonna and Mercier, 1984; Zhou, Hoover and Liu, 2004). Internal cracks have been shown in mung bean starch (van de Velde, van Riel and Tromp, 2002).

Cracking in maize is primarily radial, suggesting less stability in the interactions between the radially arranged amylopectin molecules. In general, many larger granules exhibit internal cracks regardless of the botanical origin, suggesting an increasing strain on amylopectin structure during granule growth (Glaring, Koch and Blennow, 2006). Variation in shape and size of starch granules from different botanical origins are presented in Table 2.1.

Table 2.1 Shape and size of starch granules from different botanical origins

Starch	Shape	Size (μm)	Reference
Cereal			
Maize (waxy & normal)	Spherical/polyhedral	2 - 30	Tester and Karkalas (2002)
Amylomaize	Irregular	2 - 30	Tester and Karkalas (2002)
Rice	Polyhedral	3 - 8 (single) 150 (compound)	Tester and Karkalas (2002)
Wheat	Lenticular (A-type)	15 - 35	Tester and Karkalas (2002)
	Spherical (B-type)	2 - 10	Tester and Karkalas (2002)
Barley	Lenticular (A-type)	15-25	Tester and Karkalas (2002)
	Spherical (B-type)	2-5	Tester and Karkalas (2002)
Root and Tuber			
Potato	Lenticular	5-100	Tester and Karkalas (2002)
Tapioca	Spherical/lenticular	5-45	Tester and Karkalas (2002)
Pulse			
Adzuki bean	Oval/kidney	20-70	Tjahjadi and Breene (1984)
Black bean	Oval/round/spherical	7-55	Hoover and Ratnayake (2002)
Black gram	Oval/elliptical	14-23	Sandhu and Lim (2008)
Chickpea	Oval/spherical	9-30	Hoover and Ratnayake (2002)
Cowpea	Oval/spherical	3-64	Okechukwu and Rao (1996a)
Fababean	Oval/spherical	9-48	Haase and Shi (1991)
Grasspea	Oval/round/elliptical/irregular	26-34	Jayakody et al. (2007)
Jack bean	Oval/round	12-34	Lawal and Adebawale (2005a)
Kidney bean	Oval/round/elliptical	5-35	Yoshida et al. (2003)
Lentil	Oval/round/elliptical	6-37	Hoover and Manuel (1995)
Mung bean	Oval/round	7-32	Hoover et al. (1997)
Moth bean	Oval/round	6-28	Wankhede and Ramtehe (1982)
Navy bean	Oval/round/elliptical	14-32	Hoover and Ratnayake (2002)
Northern bean	Oval/round/irregular	12-62	Hoover and Sosulski (1985)
Smooth pea	Oval/round/irregular	2-50	Ratnayake et al. (2001)
Wrinkled pea	Round	5-37	Zhou, Hoover and Liu (2004)
Pinto bean	Oval/round/irregular	6-42	Zhou, Hoover and Liu (2004)
Yam bean	Oval/round/irregular	5-35	Forsyth et al. (2002)

Source: Hoover et al. (2010); Tester and Karkalas (2002)

2.4 Molecular architecture of starch

Starch is considered to be structured on five different length scales (Fig. 2.3): 1) whole granule architecture (1-100 μm), 2) growth rings (120–400 nm), 3) blocklets (20–500 nm), 4) amorphous and crystalline lamellae (9 nm) and 5) amylopectin and amylose chains (0.1–1.0 nm) (Tester, Karkalas and Qi, 2004; Perez and Bertoft, 2010). Amylose and amylopectin are organized into a complex, alternating semi-crystalline (hard) and amorphous (soft) shells (Fig. 2.3a). The growth ring consists of alternating amorphous and semi-crystalline shells. Blocklet structures (Fig. 2.3b) are present in both hard and soft shells. These blocklets are described to have alternative crystalline and amorphous lamellae (Fig. 2.3c). The crystalline regions of the lamellae are formed mainly by double helices of amylopectin side chains packed laterally into a crystalline lattice, whereas the amorphous regions of the granule contain the branch points of amylopectin molecules (Dona et al., 2010). Dang and Copeland (2003) proposed an arrangement of blocklets within starch granule using atomic force microscopy (Fig 2.4). The blocklets have been shown to have an average size of 100 nm, and comprise approximately 280 amylopectin side chain clusters.

Figure 2.3 Schematic representation of the several levels of ultrastructure of starch: (a) starch granule showing growth rings; (b) blocklets in semi-crystalline and amorphous rings; (c) blocklet; (d) amorphous and crystalline lamellae in a stack and part of an amorphous growth ring; (e) aligned double helices (from amylopectin side chains) within a crystalline lamella and amylopectin branch points within an amorphous lamella (adapted from Perez and Bertoft, 2010).

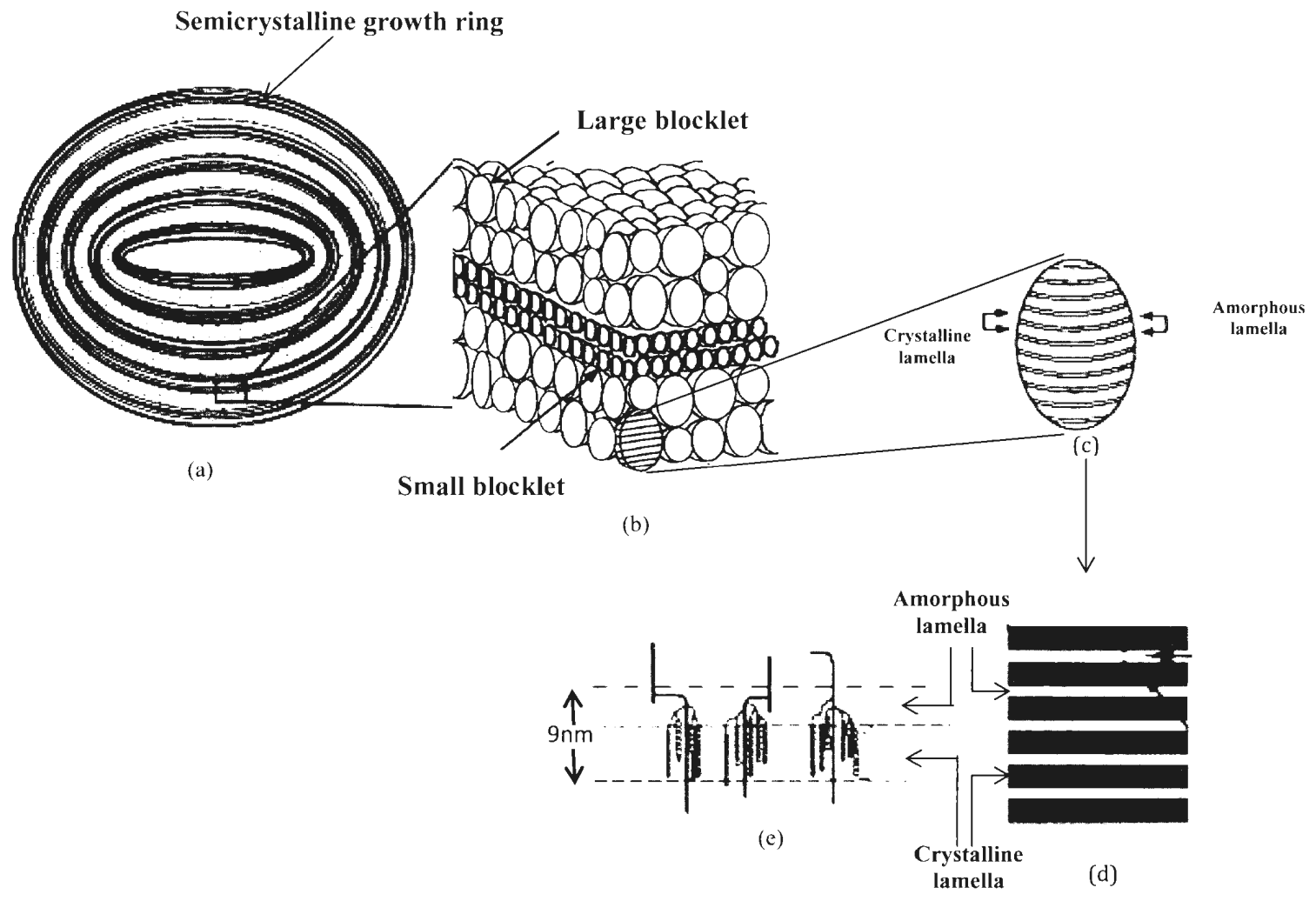
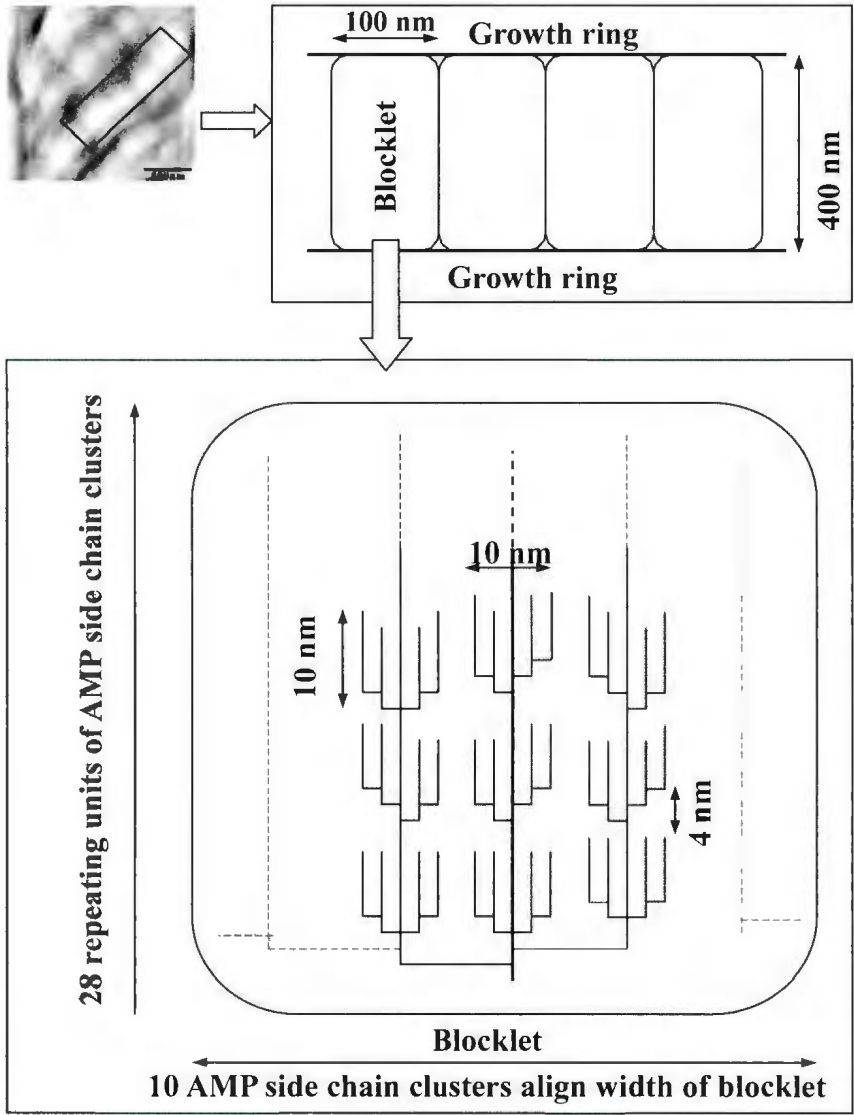


Figure 2.4 Schematic representations of the arrangement of blocklets in starch granules and the proposed arrangement of amylopectin side chain clusters within each blocklet using atomic force microscopy. Dashed lines indicate extension of the diagrammatic representation (Dang and Copeland, 2003, Copyright Elsevier, reproduced with permission).



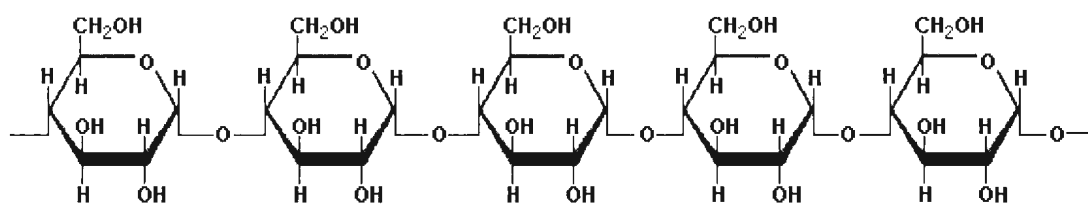
2.5 Molecular composition of starch granules

Starch is made up of polymerized glucose molecules organized into two types of α -(1→4) glucans, amylose and amylopectin (Fig 2.5). Amylose is mainly linear with very few branches whereas amylopectin chains are branched every 20-30 glucose residues by α -(1→4) linkages. The ratio of the two polysaccharides varies according to the botanical origin of the starch (Tester, Karkalas and Qi, 2004; Jane, 2006). Normal starches, such as corn and rice consist of about 70-80% amylopectin and 20-30% amylose (Jane et al. 2006). The 'waxy' starches (lacking GBSS activity) contain less than 15% amylose and 'high' amylose starches (*ae* mutant) greater than 40% (Tester, Karkalas and Qi, 2004). The approximate composition of starches of different botanical origin is presented in Table 2.2.

Intermediate materials having structures and properties between the linear amylose molecules and the large amylopectin are also found in starch granules (Perez and Bertoft, 2010). Intermediate materials have been reported in high amylose maize cultivars (Buléon et al., 1998; Yuan, Thompson and Boyer, 1993) and wrinkled pea (Bertoft and Qin, 1993). Phytoglycogen, a water soluble polysaccharide, is found in sugary-1 maize (*su* mutant) endosperms (Boyer, Simpson and Damewood, 1982; Perez and Bertoft, 2010). In addition to the major polysaccharide components, starch granules also contain very small amounts of proteins, lipids and phosphorus (Tester, Karkalas and Qi, 2004).

Figure 2.5 Schematic diagram of amylose (a) and amylopectin (b) (Adapted from Robyt, 2009)

(a)



(b)

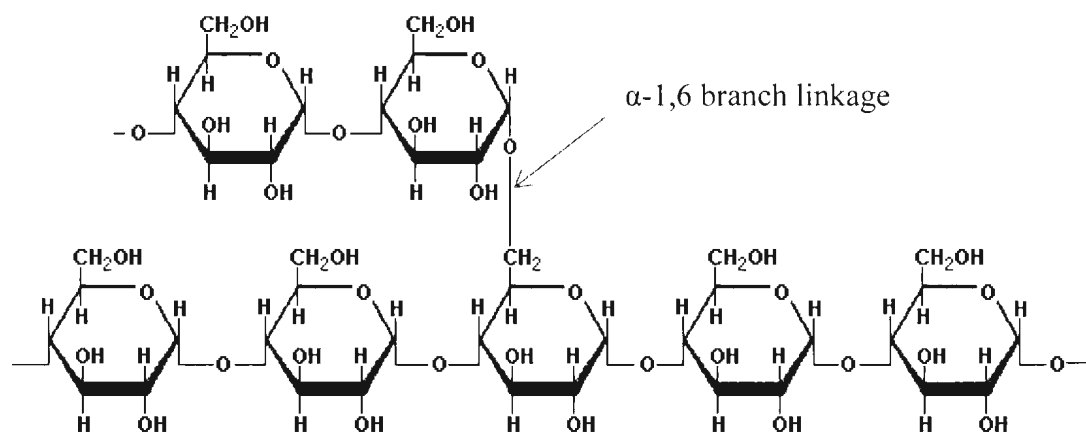


Table 2.2 Proximate composition of starches

Starch	Amylose (%)	Lipid (%)	Nitrogen (%)	Phosphorus (%)	Reference
Cereal					
Normal maize	29.9	0.75	0.02	-	Hoover and Manuel (1996b)
Waxy maize	1.20	0.22	0.02	-	Hoover and Manuel (1996b)
Amylomaize	65.5	0.95	0.03	-	Hoover and Manuel (1996b)
Rice					
Wheat	27.30	0.7	0.04	-	Hoover and Vasanthan (1994a)
Barley	23.6-29.0	0.91	0.30	0.02-0.06	Tester (1997); Li et al. (2001)
Root and Tuber					
Potato	28.10	0.20	0.09	0.10	Gunaratne and Hoover (2002)
Tapioca	33.4	-	-	0.02	Atichokudomchai and Varavinit (2003)
Pulse					
Adzuki bean	17.6-34.9	0.03-0.60	0.01-0.07	-	Tjahjadi and Breene (1984)
Black bean	27.2-39.3	0.20-0.50	0.04-0.07	-	Zhou, Hoover and Liu (2004)
Black gram	30.7-34.6	0.08-0.14	0.10-0.15	-	Singh et al. (2004)
Chickpea	30.4-35.0	0.10-0.50	0.08-0.10	-	Hughes et al. (2009)
Cowpea	25.8-33.0	0.20-1.33	0.06-0.09	-	Huang et al. (2007)
Fababean	17.0-42.0	0.08-1.40	0.33-0.43	-	Haase and Shi (1991)
Grasspea	35.2-38.3	0.12	0.04-0.09	-	Jayakody et al. (2007)
Jack bean	37.5	0.12-0.14	0.09-0.16	-	Lawal and Adebawale (2005a)
Kidney bean	34.0-41.5	0.18	0.02-0.05	-	Yoshida et al. (2003)
Lentil	23.5-32.3	0.01-0.08	0.03-0.09	-	Hoover and Ratnayake (2002)
Mung bean	33-45.3	0.04-0.32	0.02-0.05	-	Hoover et al. (1997)
Moth bean	27.0	0.16	0.06	-	Kevate et al. (2007)
Navy bean	28.6-41.4	0.09-0.60	0.02-0.05	-	Hoover and Ratnayake (2002)
Northern bean	31.6-41.0	0.2-0.5	0.06-0.16	-	Sathe and Salunke (1981)
Smooth pea	24.0-49.0	0.02-0.08	0.02-0.07	-	Chung et al. (2008)
Wrinkled pea	60.5-88.0	0.80-0.84	0.05-0.08	-	Ratnayake et al. (2001)
Pinto bean	31.3-37.4	0.12	0.05-0.07	-	Hoover et al. (2010)
Yam bean	11.6-23.6	-	-	-	Melo et al. (2003)

2.5.1 Amylose

2.5.1.1 Fine structure of amylose

Amylose is defined as a linear molecule of (1→4) linked α -D -glucopyranosyl units, but it is now well established that some molecules (potato, maize) are slightly branched (~1%) by (1→6)- α -linkages (Buléon et al. 1998). Most starches contain a mixture of linear and branched amyloses (Hizukuri et al., 1981; Takeda, Maruta and Hizukuri, 1992). The molecular weight of amylose varies from 1×10^5 to 1×10^6 g/mol (Biliaderis, 1998; Buléon et al., 1998; You et al., 2002) and a number degree of polymerization (DP_n , 324–4920) with around 9–20 branch points equivalent to 3–11 chains per molecule (Hizukuri et al., 1981; Takeda et al., 1987; Yoshimoto et al., 2000; Tester, Karkalas and Qi, 2004). Each chain contains approximately 200–700 glucose residues equivalent to a molecular weight of 32,400–113,400 (Morrison and Karkalas, 1990; Tester and Karkalas, 2002).

Linearity of amylose is defined by susceptibility of the molecule to hydrolysis towards β -amylase. This enzyme splits the (1→4) bonds from the non-reducing end of a chain releasing β -maltosyl units, but cannot cleave the (1→6) bonds (Buléon et al., 1998). When degraded by pure β -amylase, linear macromolecules are completely converted into maltose, whereas branched chains yield maltose and one β -limit dextrin consisting of the remaining inner core polysaccharide structure (Bank and Greenwood, 1975; Buléon et al., 1998). The β -amylolysis limit of amylose varies from 72-95% compared to 55-61% for amylopectin (Jane, 2009).

2.5.1.2 Conformation of amylose

Amylose conformations are generally denoted as double helical A and B, and single helical V-amylose types, with different configurations of water molecules and crystal orientations (Schnupf et al., 2009). The most recent models for A and B amylose structures are based upon 6-fold left-handed double helices with a pitch height of 2.08–2.38 nm (Buléon et al., 1998). A minimum CL of DP 10 is required for double helix formation in a pure oligosaccharide solution (Greenwell et al., 1985; Gidley and Bulpin, 1987; Pfannemuller, 1987). V-amylose is a generic term for amyloses obtained as left-handed helices with an internal cavity where the complexed ligand such as iodine, dimethyl sulfoxide (DMSO), alcohols or fatty acids can reside (Saenger, 1984; Buléon et al., 1998). The conformation of amylose in solution has been shown to vary from helical to an interrupted helix to a random coil (Banks and Greenwood, 1971; Yamamoto et al., 1982). Proposed models for amylose structure in aqueous solution are shown in Fig. 2.6. In a freshly prepared aqueous solution, the amylose chain adopts an unstable random coil structure (Hayashi, Kinoshita and Miyake, 1981) whereas the helical conformation is attained in neutral or alkaline solutions in the presence of complexing agents (lipids, iodine) (Banks and Greenwood, 1971). Interrupted helix conformation consists of regions of loose and extended helices, which alternate with shorter random coil segments (Senior and Hamori, 1973). The helical portions are thought to be stabilized by intramolecular hydrogen bonds (Cheetham and Tao, 1998). With the addition of water, the intramolecular hydrogen bonding in amylose is gradually replaced by amylose-water intermolecular hydrogen bonds, leading to conformational changes (Cheetham and Tao,

1998). The helix formation is induced by the lower energy of the ligand in the helix cavity and the driving force for the creation of these complex structures has been attributed to the tendency of amylose to minimize its interaction with water (Heinemann et al., 2001; Putseys et al., 2010).

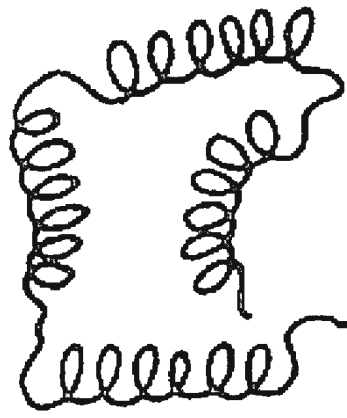
Figure 2.6 Models proposed for amylose conformation in aqueous solution (adapted from

Banks and Greenwood, 1975; Yamamoto et al., 1982)

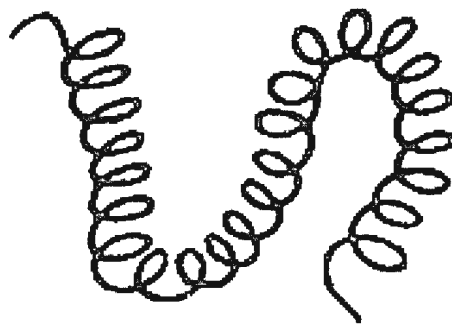
- (a) Random coil
- (b) Interrupted helix
- (c) Tightly wound helix



(a)



(b)



(c)

2.5.1.3 Location of amylose

The location of amylose in the starch granule is not well understood. Earlier studies postulated that amylose is located in bundles between amylopectin clusters (Nikuni, 1978; Blanshard, 1986; Zobel 1992) and randomly interspersed among amylopectin clusters in both the amorphous and crystalline regions (Jane, Radosavljevic and Seib, 1992).

Jane and Shen (1993) proposed (based on cold gelatinization in the presence of CaCl_2), that amylose is more concentrated in the periphery of the potato starch granule. In contrast, Tatge et al. (1999) (based on amylose synthesis in transgenic potato starch granules) suggested that amylose is largely confined to a central region of the granule. Jenkins and Donald (1995) (based on small angle X-ray scattering studies) hypothesized that amylose in maize, barley and pea starches is predominantly located in the amorphous growth rings, and that the interaction between amylose and amylopectin in these amorphous regions may be the cause of decreased crystallinity. Enzyme-gold labeling studies combined with iodine staining of hydrated maize and potato granules indicated that amylose is localized in distinct amorphous regions around the hilum (Atkin et al., 1999). The above finding was supported (Blennow et al., 2003; Gray and BeMiller, 2004; Glaring, Koch and Blennow, 2006) APTS (8-aminopyrene-1,3,6-trisulfonic acid) staining. APTS forms a covalent link with the reducing end of starch molecules. Perez and Bertoft (2010) reported that amylose chains in A-type starches (maize) are believed to be in a single helical state, although a small proportion may be involved in lipid

complexes. Some of the larger (non-leachable) amylose chains may be involved in double-helical interactions with amylopectin.

Zobel (1988a) postulated that amylose chains are probably co-crystallized (Fig 2.7b) with amylopectin chains in potato starches (based on water leaching, iodine reaction, complex formation with lipid, enzyme attack, set-back character and DMSO solubility studies). Later, Jane (2007) showed that amylopectin clusters may contain amylose tie chains, which are portions of macromolecules that connect with the crystalline lamella and have elongated (straightened) conformations inside the crystalline lamellae and an unordered conformation after extending from crystalline to amorphous lamellae (Fig 2.7c). Co-crystallization between amylose and amylopectin chains and penetration of amylose tie chains into amorphous regions has been suggested to disrupt the packing arrangement of crystalline lamellae based on small angle X-ray scattering studies of maize and barley starches (Jenkins and Donalds, 1995). However, amylose helices may contribute to the crystallinity in high amylose starches (Buléon et al., 1998; Hoover, 2001). Recently, Wang et al. (2012) postulated that in pea starches (C-type polymorph), the majority of amylose is localized at the center of the granules (Fig. 2.8), whereas the outer part of the granules is predominantly composed of amylopectin interspersed with some amylose molecules.

Figure 2.7 (a) Amylopectin structure with no amylose present – small packing by amylose
(Jenkins and Donald, 1995, Copyright Elsevier, reproduced with permission)

(b) co-crystallinity between amylose and amylopectin moves a number of amylopectin chains out of register – increase crystalline lamellar size (Jenkins and Donald, 1995, Copyright Elsevier, reproduced with permission)

(c) A model for amylose tie chains localization in amylopectin cluster
(adapted from Yuryev et al., 2007)

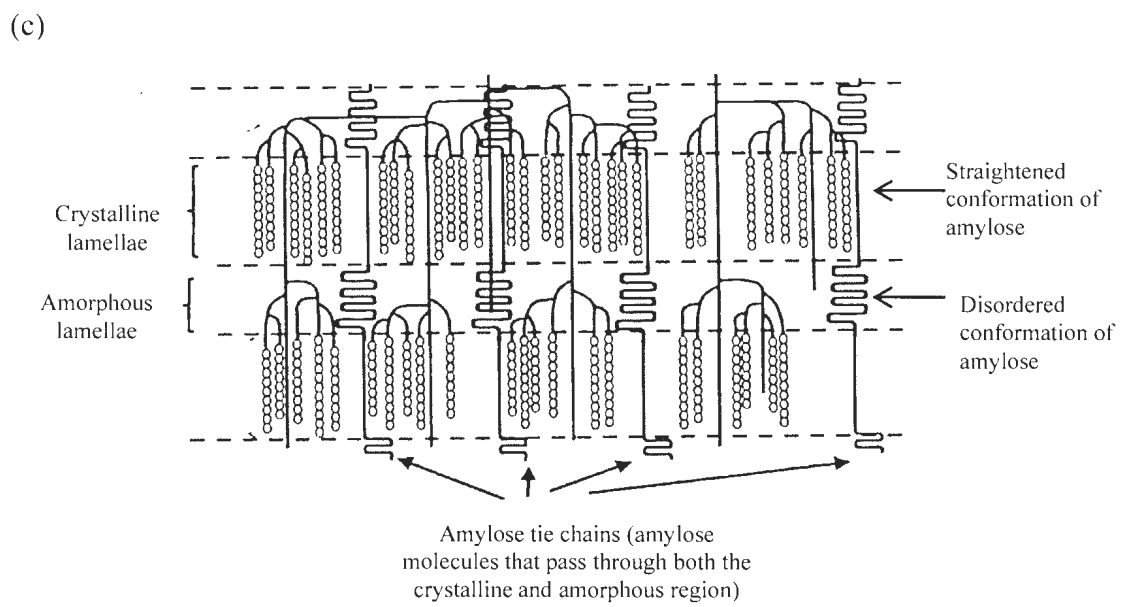
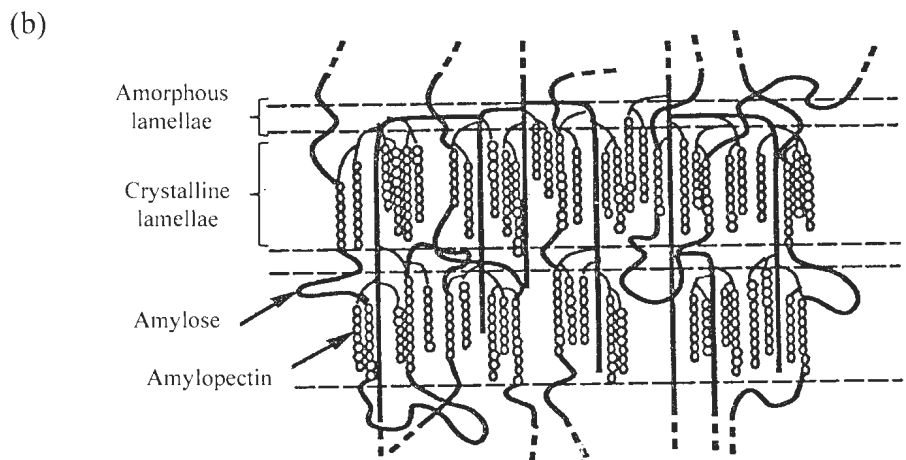
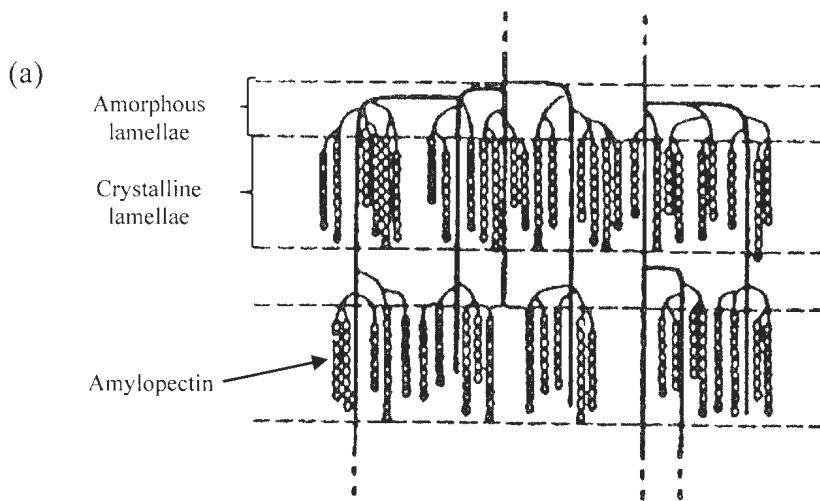
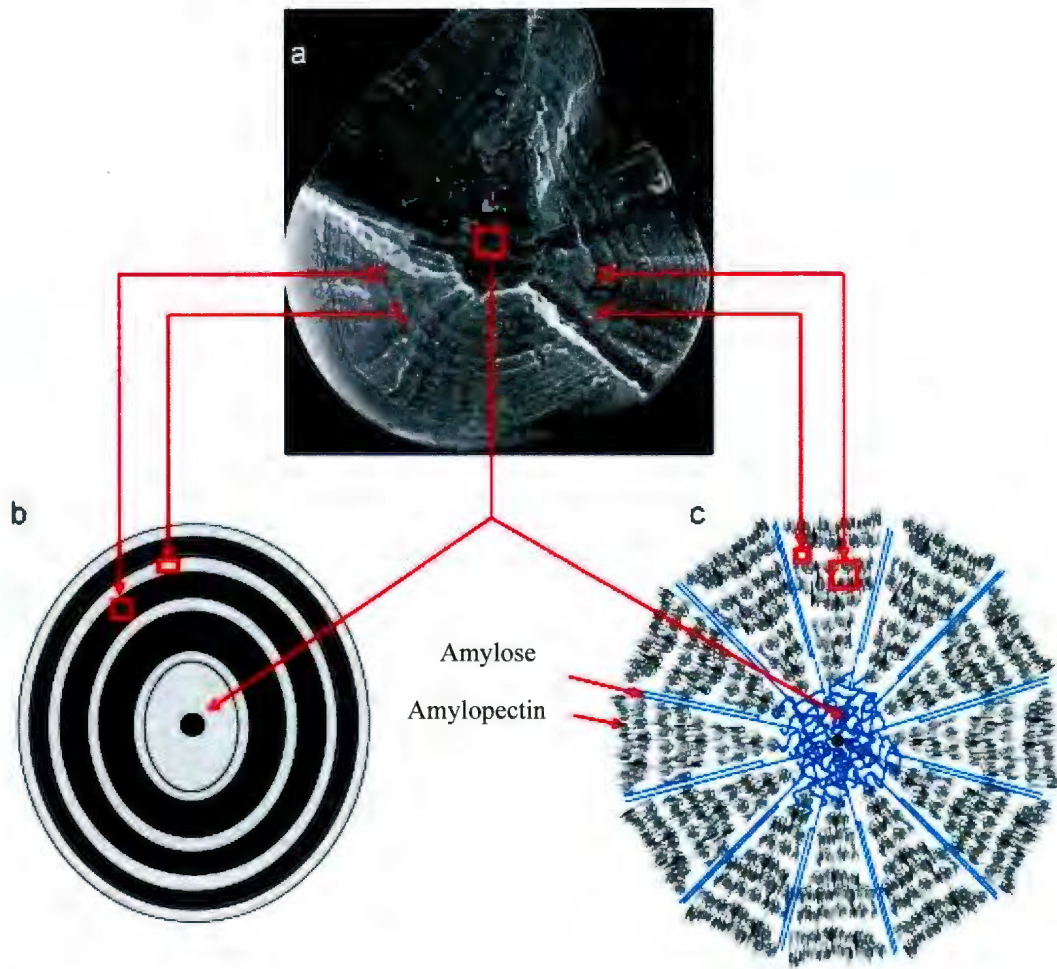


Figure 2.8 A proposed model of starch granule organization in pea starch (Wang et al., 2012, Copyright Elsevier, reproduced with permission).

a - SEM image of a pea starch granule after 2 days of acid (2.2N HCl) hydrolysis

b - Starch granule according to the growth ring model

c - Chain distribution model



2.5.1.4 Amylose-inclusion complex

Amylose has a helical structure where the interior of the helix contains hydrogen atoms, while the hydroxyl groups remain on the outside (Buléon et al., 1998). The hydrophobic helical cavity which provides a high affinity site for the apolar (part of the) ligand (Rutschmann and Solms, 1990; Whittam et al., 1989). Complex between amylose and an inclusion compound is a reversible process (Biliaderis, 1998). Depending on the size of these complexing agents, the amylose chain can take up a helical structure having either six, seven or eight glucose units per turn (Perez and Bertoft, 2010). Amylose complexation occurs with iodine (Rundle and French, 1943), potassium hydroxide (Sarko and Biloski, 1980), DMSO (Simpson, Dintzis and Taylor, 1972) and monoacyl glycerols (Ghiasi, Varriano-Marston and Hosney, 1982).

The amylose–lipid complexes (Fig. 2.9a) can be crystalline or amorphous depending on the temperature at which they form (Biliaderis, 1992; Godet, Bizot and Buléon, 1995). In the native starch granule, the starch–lipid complex is in an amorphous state and it can be annealed into a more ordered semi-crystalline form, which displays a V-type X-ray diffraction pattern (Perez and Bertoft, 2010). Generally 18–24 glucose units are required for the complexation of one lipid molecule (i.e. fatty acid or monoacyl glycerol with 14, 16, 18,... carbon atoms in its tail), organized in three turns, each containing six or eight glucose residues per pitch (Carlson et al., 1979). However, Godet et al. (1996) stated that amylose chains of DP 20 are too short to complex with a lipid. ¹³C-cross polarization/magic angle spinning NMR showed that up to 43 % of amylose in non-waxy

rice starch, 33% in oat starch, and 22% in normal maize and wheat starch granules are complexed with lipids with a single helical conformation (Morrison, Law and Snape, 1993).

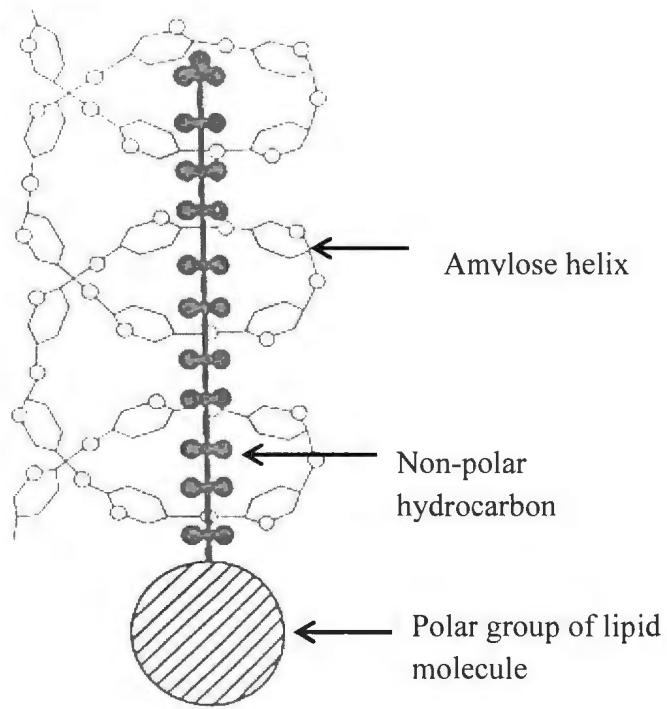
The starch-iodine complex (Fig. 2.9b) has been shown to consist of a linear array of iodine atoms occupying the cavity of a helical polysaccharide molecule (Hanes, 1937). This was later confirmed by X-ray diffraction analysis by Rundle and French (1943). The complex produces a deep blue color, which is used to identify amylose-containing starches and to measure quantitatively the level of amylose in starch either by color intensity or potentiometrically (Schoch, 1964). The primary structures of the polyiodide chains are composed of I_3^- and I_5^- subunits, combined to form four dominant polyiodide chains (I_9^{3-} , I_{11}^{3-} , I_{13}^{3-} and I_{15}^{3-}) which give different absorbance spectra when complexing with amylose (Yu, Houtman and Atalla, 1996). Absorbance maxima of those spectra are 480–510, 610–640, 690–720 and 730–760 nm, respectively. The length of the 1→4 α -glucan chains available for complex formation and molecular size of amylose influences the relative proportions of the individual spectra (Knutson, 2000). The color of the amylose-iodine complex has been reported as brown (DP 21–24), red (DP 25–29), red-violet (DP 30–38), blue-violet (DP 39–46), and blue (DP > 47) (John, Schmidt and Kneifel, 1983).

Figure 2.9 Schematic representations of amylose inclusion complexes (Adapted from

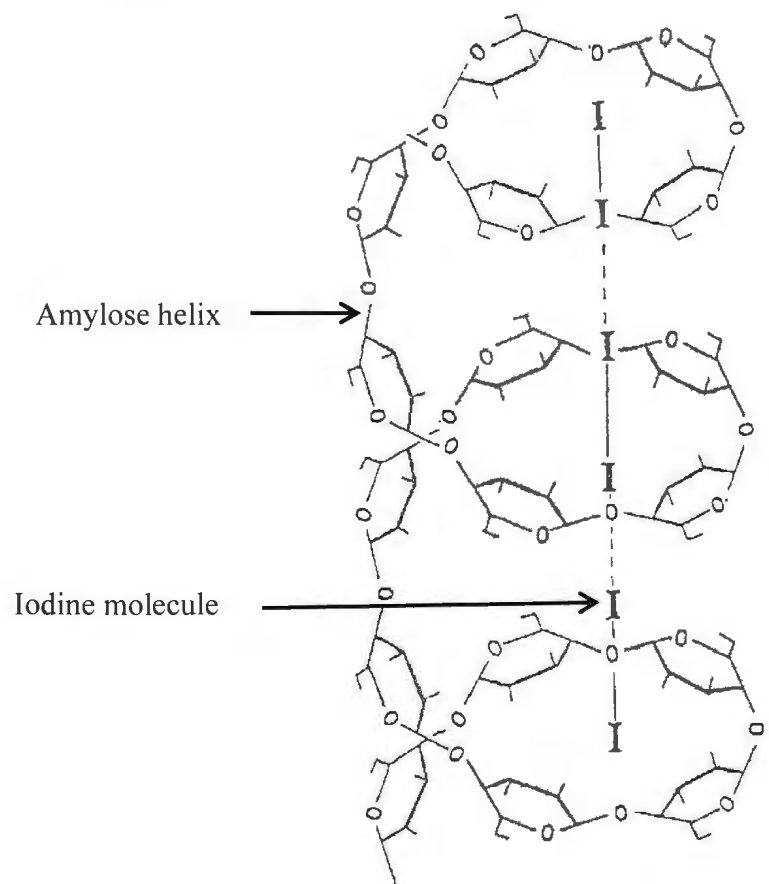
Carlson et al., 1979; Calabrese and Khan, 1999)

(a) Amylose – lipid complex

(b) Amylose - iodine complex



(a)



(b)

2.5.1.5 Determination of amylose content

The amylose content of pulse starches has been shown to range from 24-88 % (Hoover et al., 2010). The amylose content and the amylose-amylopectin ratio in starches have traditionally been measured by iodine-binding procedures, whether amperometric (Larson, Gilles and Jenness, 1953), potentiometric (Banks and Greenwood, 1975), or spectrophotometric (Morrison and Laignelet, 1983). These procedures are based on the amylose-iodine complex, which exhibit a blue color characterized by a maximum absorption wavelength (λ_{\max}) above 620 nm (Herrero-Martínez, Schoenmakers and Kok, 2004). However, amylopectin also forms complexes with iodine which absorb at similar wavelengths ($\lambda_{\max} \approx 540$ nm) and have been shown to interfere with amylose-iodine absorption in colorimetric methods (Banks and Greenwood, 1975; Takeda, Hizukuri and Juliano, 1987). Knutson (2000) reported that only linear branches of amylopectin that are long enough to form a helix can develop a complex with iodine in the same manner of amylose; but the short length of these branches originates unstable purple to red color complexes (Rundle and French, 1944). The iodine-binding capacity of pure amylose is reported to be 19-22% of its weight (Banks, Greenwood and Khan, 1971), whereas for amylopectin it is about 1% (Gerardet al., 2001a). Other techniques for measuring amylose content include concanavalin A binding (Matheson and Welsh, 1988), differential scanning calorimetry (DSC) which measures the energy that evolves from melting of the amylose-lipid complexes (Mestres et al., 1996), size exclusion chromatography (SEC) (Yamada and Taki, 1976; Hanashiro, Shinohara and Takeda, 2003) and more recently, asymmetric flow field flow fractionation (Kim et al., 2007).

However, recently Fitzgerald et al. (2009) compared various techniques used for amylose measurement of rice and suggested the need to revisit and standardize of amylose determination methods.

2.5.2 Amylopectin

2.5.2.1 Fine structure of amylopectin

Amylopectin is the highly branched component of starch: it is formed through chains of α -D -glucopyranosyl residues linked together mainly by (1→4) linkages but with 5–6% of (1→6) bonds at the branch points (Buléon et al., 1998). Amylopectin is a much larger macromolecule than amylose with a molecular weight of 1×10^7 – 1×10^9 (Banks, Greenwood and Walker, 1970; Morrison and Karkalas, 1990; Mua and Jackson, 1997; Buléon et al., 1998; Biliaderis, 1998). The DP_n ranges between 9600–15,900 and comprises three major species with DP_n 13,400–26,500, 4400–8400 and 700–2100 (Takeda, Shibahara and Hanashiro, 2003).

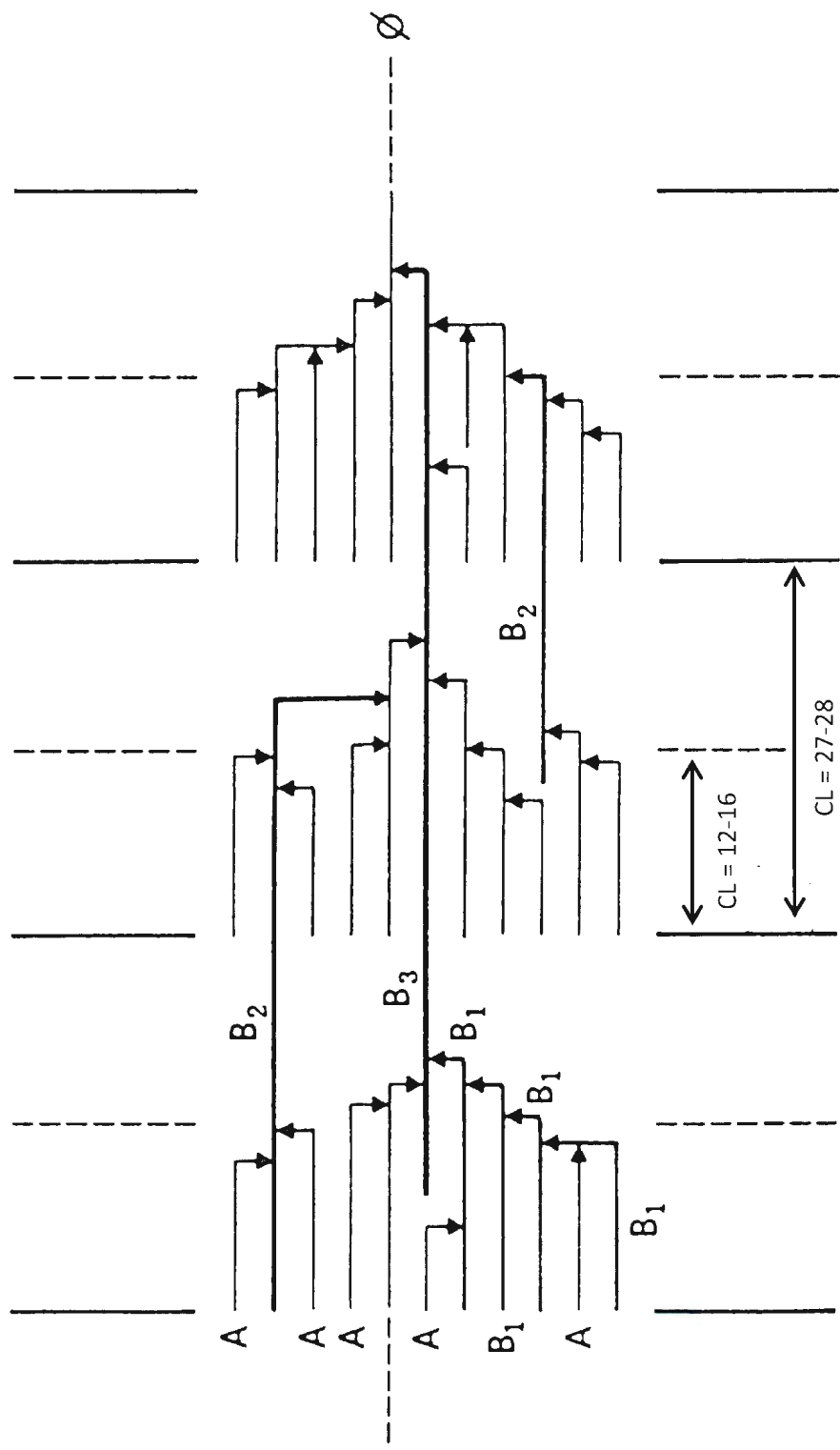
2.5.2.2 Unit chain distribution of amylopectin

Peat et al. (1952) defined the basic organization of the chains as A, B and C chains. The individual chains can be specifically classified in terms of their chain lengths (CL) and position within starch granules (Hizukuri, 1985; 1986). A chains are unbranched and linked to the macromolecule by their reducing end. In contrast, B chains are highly branched. Depending on the CL and correspondingly the number of (radial) clusters

traversed within the native granule, B-chains are referred to as B₁–B₄ (one to four clusters) (Hizukuri, 1986; Tester, Karkalas and Qi, 2004). The A and B₁ chains (Fig. 2.10) are the most external (exterior) and form double helices (and crystallites) within the native granules (Tester, Karkalas and Qi, 2004). In addition, each macromolecule contains a single C-chain, which carries the sole reducing end group.

Typical CLs for A, B₁–B₄ chains for different starches (after debranching with isoamylase) are 12–16, 20–24, 42–48, 69–75 and 101–119, respectively (Hizukuri, 1986; Wang and White, 1994). Hanashiro et al. (2002) described the distribution of C-chains after labelling with a fluorescent dye and reported that the chains covered the DP range 10–130, possessing a peak in size-exclusion chromatograms at DP 40 for several amylopectin samples (Perez and Bertoft, 2010). The ratio of A- to B-chains depends on the starch source and is typically of the order of < 1:1 to > 2:1 on a molar basis or < 0.5:1 to > 1:1 on a weight basis (Morrison and Karkalas, 1990; Tester and Karkalas, 2002). A type starches (most cereals) have shorter CL on average than B type starches (like potato) (Hizukuri, 1985; Li et al., 2001).

Figure 2.10 A cluster model for amylopectin with A, and B1-B3 chains. Φ – reducing end; CL – chain length in degree of polymerization (Adapted from Hizukuri, 1986)



High-performance size-exclusion chromatography (HPSEC) with a differential refractometer and high-performance anion-exchange chromatography with pulsed amperometric detection (HPAEC–PAD) have been frequently used for the examination of the amylopectin chain length distribution (Tomlinson, Lloyd and Smith, 1997; Hanashiro et al., 2002). HPSEC provides a description of all chains in the debranched starch dispersion but cannot resolve peaks for any particular DP (Yuan, Thompson and Boyer, 1993; Klucinec and Thompson, 1998). Fluorophore-assisted carbohydrate electrophoresis (FACE) has been applied in starch structure analysis (O’Shea et al., 1998). HPAEC-PAD has the capability to quantitatively describe the chains longer than DP 50, while FACE has no such capability (Yao, Guiltinan and Thompson, 2005). However, FACE has the advantage in more precisely quantifying short chains ranging from DP 6-12 (Yao, Guiltinan and Thompson, 2005).

2.5.2.3 Branch structure and the polymorphism of starch granule

Double helices are formed by winding two amylopectin branch chains together and are packed in the crystalline lamellae of the starch granule into two different patterns, which are called A- and B-type polymorphic structures. The C-type polymorphic starch is a mixture of A-type and B-type polymorphic structures. A-type polymorphs are found in cereal starches such as wheat, corn and barley, while B-type polymorphs are found in tuber starches such as potato and high amylose cereal starches (Singh and Ali, 2000). The C-type polymorph is characteristic of most pulse starches (Hoover et al. 2010). The double helices within the two polymorphic forms are identical with respect to helical

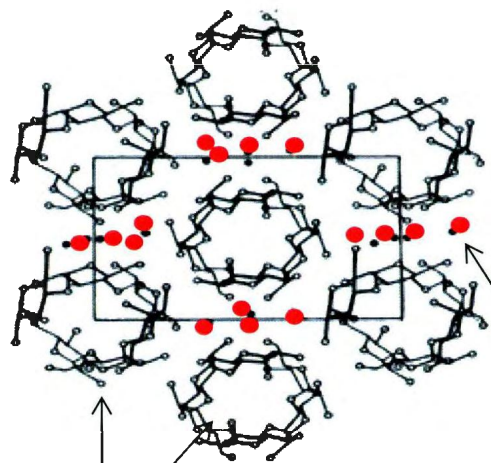
structure (Gidley, 1987; Tester, Karkalas and Qi, 2004). The A-type polymorphic structure is relatively compact with a low water content (4 H₂O molecules), whilst the B-type polymorph has a more open structure containing a hydrated (36 H₂O molecules) helical core (Fig. 2.11). A-polymorph chains are crystallized into a monoclinic lattice with maltotriose as a repeating unit whereas the B-polymorph crystallizes into a more open hexagonal unit cell with maltose as a repeating unit (Imberty and Perez, 1988; Imberty et al., 1988). In addition, in A-type starches, the α (1 \rightarrow 6) branch linkages are located within the crystalline and amorphous areas, whereas in B-type starches the branches are located solely within the amorphous area, which produces an inferior crystalline structure (Fig. 2.12) (Tester, Karkalas and Qi, 2004).

In B-type starches, due to their high amylose content, double helices in crystallites are formed to a larger extent, by the intertwining of linear amylose chains, whereas in A-type starches double helices in crystallites are formed mainly by the intertwining of the outer branches of amylopectin (Jayakody and Hoover, 2002). Therefore, double helices in the B-type starches would be more tightly packed due to strong interactions, via hydrogen bonding and Van der Waals forces, between linear amylose chains than those present in A-type starches (Jayakody and Hoover, 2002). The inner diameter of the double helix cavity is 0.35 nm, while the outer diameter is 1.03 nm (Biliaderis, 1998). The average chain length of A-type starches has been shown to be shorter than that of C- and B-type polymorphic starches. A-type polymorphic starch has a greater population of short branch chains whereas the B-polymorphic starch has more long branch chains (Jane, 2006).

Recently, Xijung et al. (2012) proposed a model for the organization of blocklet in A and B type starches (Fig. 2.13). Bertoft and Wiik (2004) proposed a two directional backbone model (Fig. 2.14) of the clustered structure of amylopectin based on the acid treatment of maize and potato starches. They observed that regardless of the polymorphic type (maize [A type], potato [B type]), long amylopectin chains are completely hydrolyzed by 2.2 N HCl after 2 days. Based on the observation, they suggested that amylose molecules and long chains of amylopectin ($DP > 34$) are probably present within the amorphous region. Double helices of amylopectin are built up from an amorphous backbone of long chains ($DP > 34$) onto which side chain clusters are attached (Bertoft and Wiik, 2004).

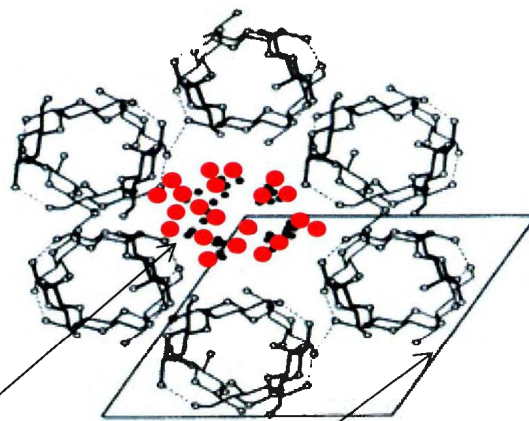
Figure 2.11 Double helices arrangement of A-type and B-type crystallites in starch granules (adapted from Wu and Sarko, 1978a; 1978b).

A-type unit cell



Double helices

B-type unit cell

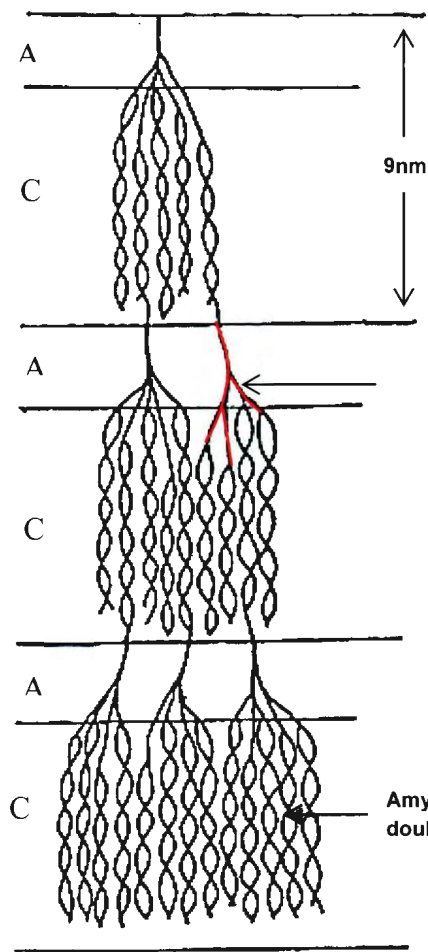


Double helices

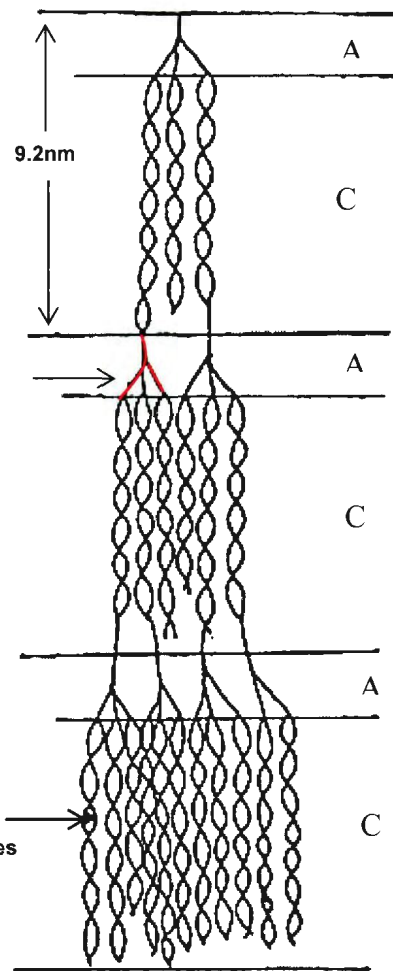
Water molecules

Figure 2.12 Proposed models for A-(waxy maize starch) and B- (potato starch) type amylopectin branching patterns (adapted from Jane, Wong and McPherson, 1997).

**A-type starch
(Waxy maize starch)**



**B-type starch
(Potato starch)**



Amylopectin
double helices

A: Amorphous

C: Crystalline

Figure 2.13 Proposed models for blocklet arrangement of A and B –type starches (Xijun et al., 2012, Copyright Elsevier, reproduced with permission).

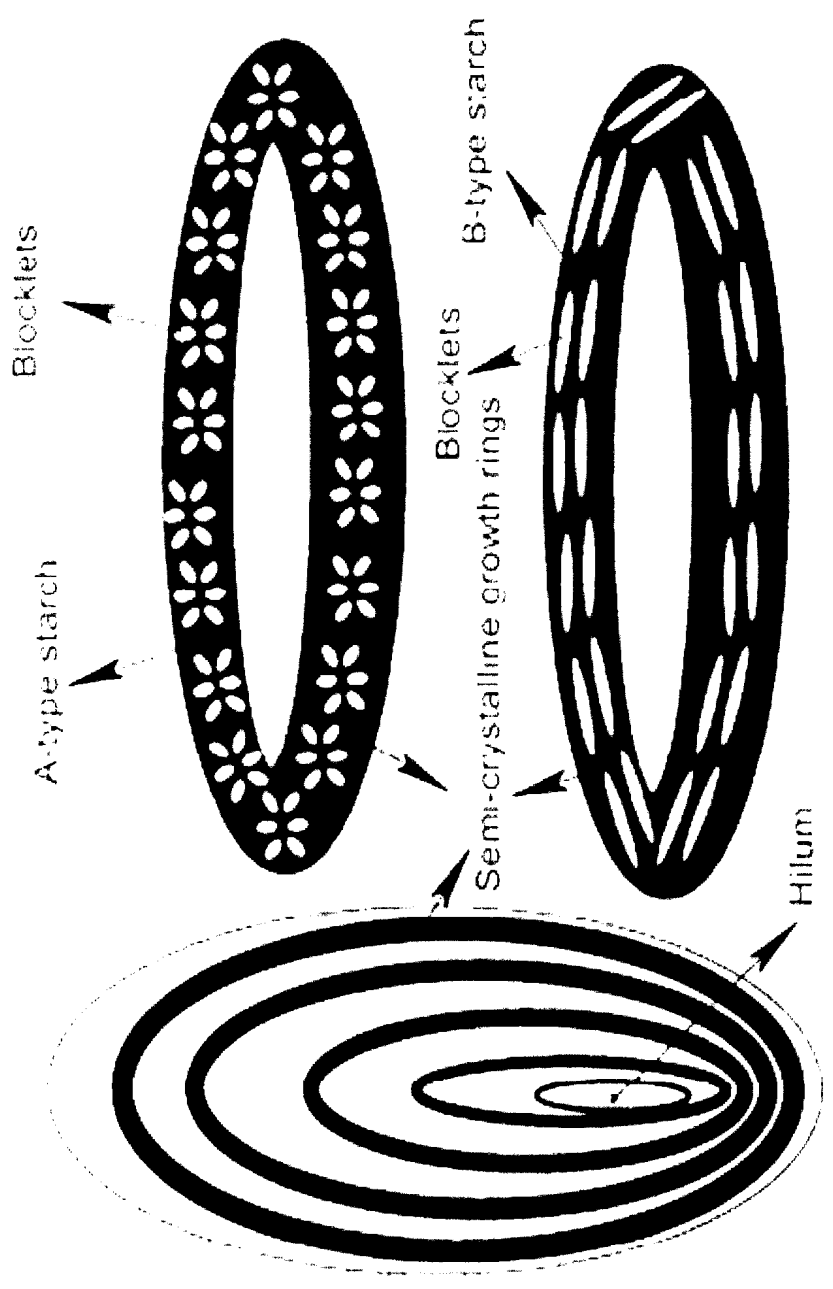
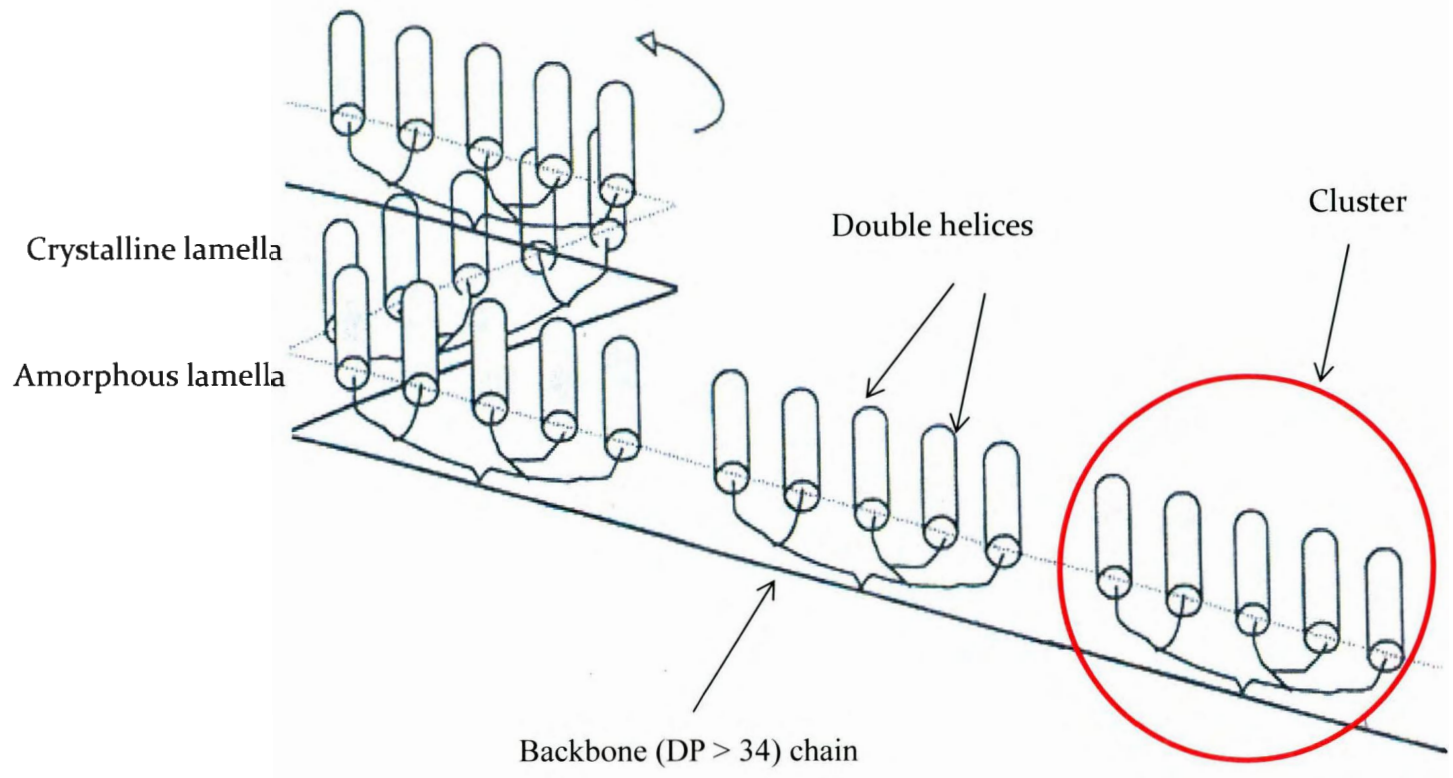


Figure 2.14 Schematic representation of a two-directional backbone model of amylopectin. Double helices (cylinders) of the clusters are found in the crystalline lamella (above thin dotted line). The left handed arrow represents how the macromolecule could be turned into a left-handed super helix (adapted from Bertoft and Wiik, 2004).



2.5.2.4 Starch crystallinity

The crystalline nature of starch depends on both genetic control and climatic conditions during the plant growth (Buléon et al., 1998). The crystalline structure of starch is attributed to structural elements of amylopectin. Hence, the short chains with polymerization degrees ranging between 15 and 18 probably have a double helical conformation (Buléon et al., 1998). According to the Imberty and Perez (1988) model, in the 9 nm repeat distance (crystalline and amorphous lamellae), the crystalline region represents 5 – 6 nm. Native starch crystallinity ranges between 15 – 45 % (Jane, 2006). Hizukuri et al. (1997) suggested that the chain length involved in the crystalline phase and the branching pattern in amylopectin molecules influence the crystallinity and the crystalline type. However, temperature and hydration conditions during the plant growth have also been shown to induce some important changes in the A:B composition (Buléon et al., 1998). Dry and warm condition favors formation of A type crystallite whereas B type crystallite formation is favored in wet and cold conditions (Buléon et al., 1982).

Double helical content (Table 2.3) in starch has been determined by ^{13}C cross polarization magic angle spinning nuclear magnetic resonance (^{13}C CP/MAS NMR) (Bogacheva, Wang and Hedley, 2001; Paris et al., 2001; Tan et al., 2007; Lopez-Rubio et al., 2008). NMR is considered a short distance range probe, measuring order at the level of individual helices (Fig. 2.15), i.e., it distinguishes helices either in or out of crystalline registry (Tan et al., 2007). Wide angle X-ray scattering (WAXS) provides distinctive X-

ray scattering patterns for different starch polymorphs (Fig. 2.16). The X-ray diffraction pattern of starch granules is due to the regular crystalline arrangement of ordered, tightly packed parallel glucan helices of amylopectin molecules (Bergthaller and Hollmann, 2007). The crystalline V-form characteristic of amylose complexed with fatty acids and monoacylglycerols arise from single helices of amylose (Lopez-Rubio et al., 2008; Saibene et al., 2008).

Table 2.3

Double helical content of starches determined by ^{13}C CP/MAS NMR

Starch	Double helical content (%)
Waxy maize	46-47
Normal maize	33-37
Gelose 50	18
Gelose 80	18-26
Rice	38
Barley	21
Wheat	22-31
Potato	44-48
Waxy potato	50.9
Pea	39.7
Low amylose pea	48.6

Sources: Bogracheva, Wang and Hedley (2001), Tan et al. (2007), Lopez-Rubio et al. (2008)

Figure 2.15 ^{13}C CP/MAS NMR spectrum of a native starch

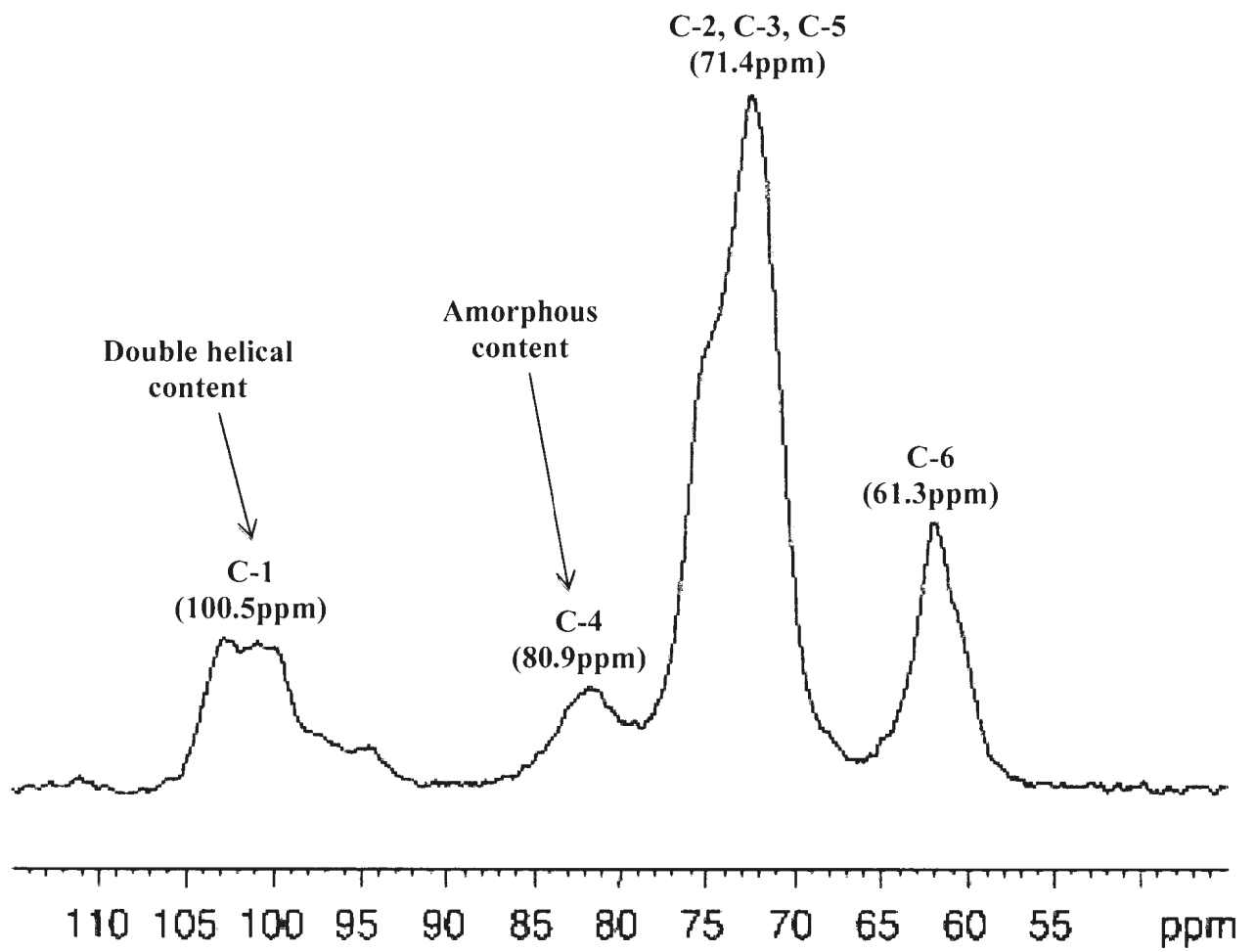
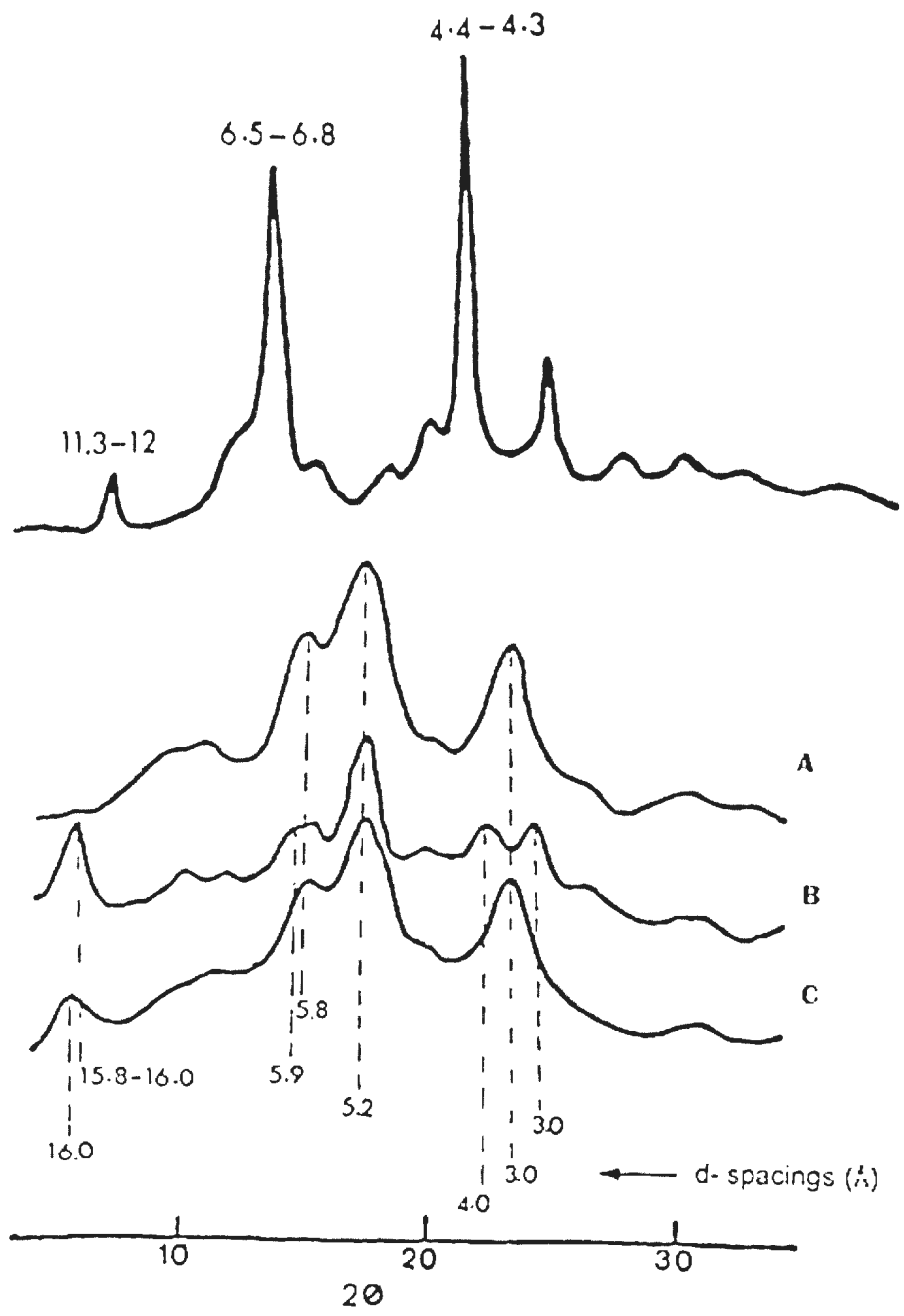


Figure 2.16 X-ray diffraction patterns of A-, B-, C- and V- type starches with their characteristic d-spacings (adapted from Zobel, 1988a, b)



2.5.3 Protein

The protein content of native starch granules varies from 0.1–0.7% by weight (Biliaderis, Grant and Vose, 1981). Granule-bound proteins are found on the granule surface and within the interior [integral proteins] (Perez and Bertoft, 2010). Baldwin (2001) reported that starch granule associated proteins may be associated with lipids on granule surfaces. Integral proteins (include residues of enzymes involved in starch biosynthesis, especially starch synthase) have a higher molecular weight (50–150 kDa) than surface proteins (15–30 kDa) and (Baldwin, 2001). The amount of protein associated with starch granules depends on both the botanical origin of the starch and its degree of purification during extraction (Baldwin, 2001). However, a typical well-washed cereal starch sample contains ~ 0.25 % protein (Skerritt et al., 1990), whilst a typical protein content of pulse starches has been reported to be generally in the range of 0.06-0.43 % (Hoover et al., 2010). In wheat, the starch surface protein, friabilin, has received much attention because of its proposed association with grain hardness (Greenwell and Schofield, 1986; Oda and Schofield, 1997; Baldwin, 2001; Tester, Karkalas and Qi, 2004).

2.5.4 Lipid

Generally, cereal starches (corn, wheat, rice) contain relatively high levels of lipid (0.2-0.8%) while, tuber (potato) and root (tapioca) starches have lower levels of lipids (0.1-0.2%) (Table 2.2). Lipids associated with isolated cereal starch granules have been found to occur on the surface as well as inside the granule (Morrison, 1981). Integral lipids of

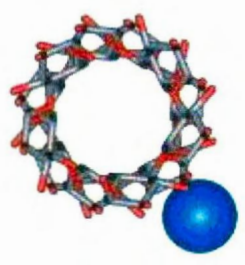
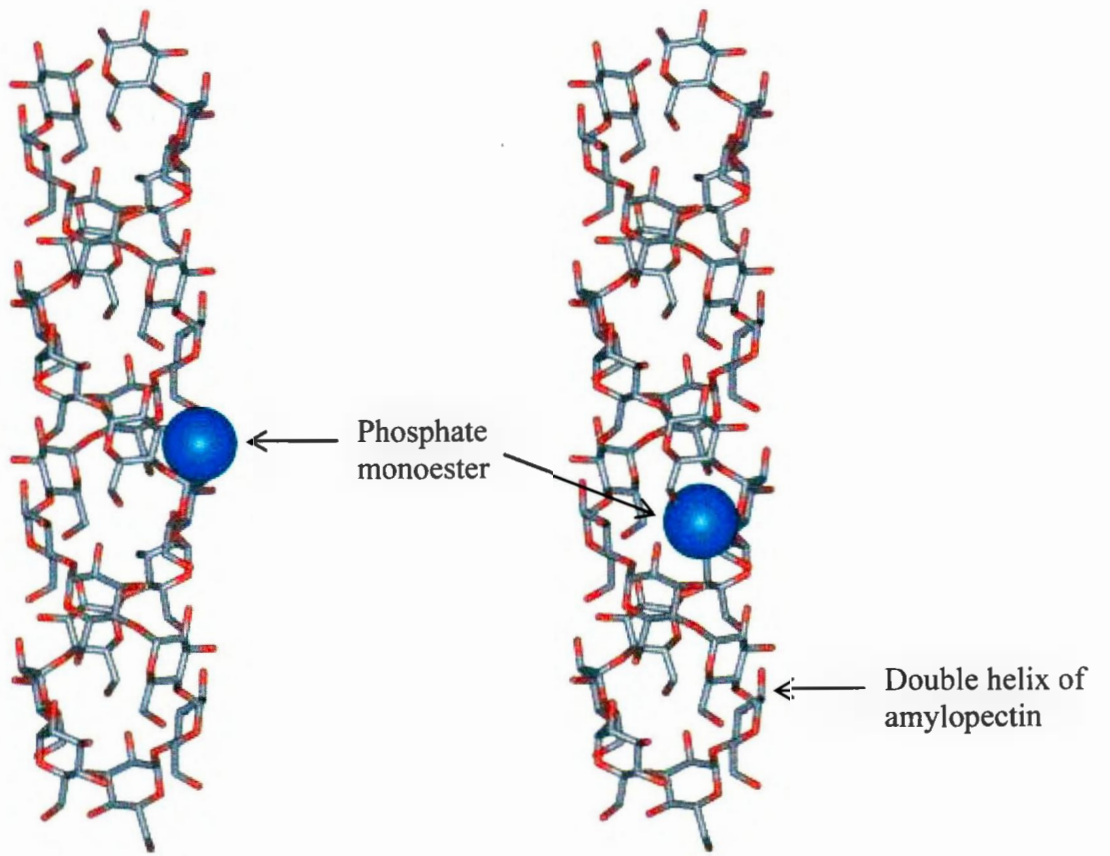
cereal starches are found in the form of lysophospholipids (LPL) and free fatty acids (FFA) whereas, the surface contaminants comprise triacylglycerols, glycolipids, phospholipids and free fatty acids derived from the amyloplast membrane and non-starch sources (Morrison, 1981). Surface and internal lipids differ in extractability from granules with common lipid solvents. Surface lipids are extractable with cold solvents (chloroform and ether), whereas internal lipids can be extracted with hot aqueous alcohol (propanol-water 3:1 [v/v]) (Vasanthan and Hoover, 1992). LPL and FFA are positively correlated with the amylose fraction (section 2.5.1.4) and the LPL may account for up to ~2% of starch weight (in high amylose cereal starches) (Tester, Karkalas and Qi, 2004). Linoleic (18:2) and palmitic (16:0) acids are the major components of cereal starches (Morrison, 1988). Stearic (18:0), oleic (18:1) and linolenic (18:3) acids could be present in trace amounts (Morrison, 1988).

2.5.5 Phosphorus

Phosphorus is present as phosphate monoesters and phospholipids in various starches, which varies considerably with the botanical origin of starch. Tuber starches (potato) have been shown to have a higher phosphate monoester content (~ 0.09%) than cereal starches (Hizukuri, Tabata and Nikuni, 1970; Lim, Kasemsuwan and Jane, 1994; Blennow et al., 1998; McPherson and Jane, 1999), and one in 200–500 glucose residues on average being phosphorylated in potato starch. Takeda and Hizukuri (1982) have studied the location of phosphate groups in potato amylopectin and showed that one

phosphate monoester group per 317 glucose residues, equivalent to one phosphate group per 13 branch chains. Studies have shown that most of the phosphate groups in the tuber starches are covalently bound to amylopectin but not to amylose (Blennow et al. 2002). The enzyme α -glucan water dikinase (GWD) is responsible for the starch phosphorylation. GWD catalyzes the formation of starch phosphate esters from β -phosphate group of ATP to the C-6 or C-3 positions of the glucose residues (Blennow et al., 2002). Blennow et al. (2002) reported that the C-6 position aligns well in one of the double-helix surface interior and will not severely affect double-helix formation or the crystal packing. Whereas, C-3 hydroxyl groups protrude from the double-helical surface, which will probably have greater effects on starch double-helix packing (Fig. 2.17). Consequently, this will have an influence on the crystallinity of starch and hence starch properties. Studies have shown that phosphate monoesters and phospholipids have different effects on starch pasting properties. For instance, phosphate monoester increase paste clarity and paste viscosity in potato starch whereas phospholipids found in normal cereal starches (e.g. wheat, rice and maize) decrease paste clarity and viscosity (Morrison, 1988; Jane, 2009).

Figure 2.17 A molecular model of phosphorylated starch (crystalline domain). The helices are phosphorylated on the same glucose residue, at the C-3 (a) and C-6 (b) positions (Adapted from Blennow et al., 2002).



(a)



(b)

2.6 Starch properties

2.6.1 Granular swelling and amylose leaching

Native starches are insoluble in cold water, but they can absorb up to 30% of moisture by weight into the amorphous region of the starch granule (Jane, 2004). However, when starch granules are heated in presence of water granular swelling occurs. This process requires the prior loss of at least some of the ordered structures within the native granule (Debet and Gidley, 2006). Crystalline structures of starch molecules are disrupted by increased hydrogen bonding between water molecules and hydroxyl groups (Srichuwong et al., 2005b). Granular swelling is also accompanied by leaching of starch molecules from the granules. This material is mainly amylose, while amylopectin may also solubilize depending on the nature of the starch and the severity of heat-shear conditions employed (Eliasson, 1986; Biliaderis, 2009). Leaching of amylose molecules out of the swollen starch granules is referred to as amylose leaching (Whistler and BeMiller, 1997). Thus, granular swelling and amylose leaching reflects the extent of starch chain interactions (amylose-amylose and/or amylose/amylopectin) within a starch granule.

Granular swelling and solubilization of macromolecules have an influence on the rheological behavior of the starch gel (Lopez, Rolee and Meste, 2004). Tester and Morrison (1990) reported that swelling is a property of amylopectin. Granular swelling has been shown to increase with higher proportions of long amylopectin chains ($DP > 35$) and to decrease linearly with an increase in amylose content (Sasaki and Matsuki, 1998). However, Gomand et al. (2010) have shown that longer amylopectin chains ($DP > 18$)

inhibit swelling while short chains ($DP < 14$) favour swelling in potato and cassava starches. The extent of granular swelling and amylose leaching has been shown to be influenced by: 1) the extent of interaction between starch chains (amylose - amylose and/or between amylose and outer branches of amylopectin) (Gomand et al., 2010; Hoover et al., 2010; Jayakody et al., 2007; Karim et al., 2007; Zhou, Hoover and Liu, 2004), 2) the amount of lipid complexed with amylose chains (Morrison et al., 1993b; Ratnayake et al., 2001; Gunaratne and Hoover, 2002; Nakazawa and Wang, 2004), 3) phosphate content (Gunaratne and Hoover, 2002), 4) protein content (Wang and Seib, 1996), and 4) granular size (Lindeboom, Chang and Tylera, 2004).

Pulse starches have been shown to exhibit a single stage restricted swelling and low extent of amylose leaching (Hoover and Sosulski, 1985 and Schoch and Maywald, 1968), whereas normal cereal starches exhibit a two-stage swelling (Langton and Hermansson, 1989; Doublier, Llamas and LeMeur, 1987; Leach, McCowen and Schoch, 1959). Tuber starches (potato) have a higher swelling power than other starches due to the presence of higher amount of phosphate ester groups on potato amylopectin (Swinkels, 1985; Vandeputte et al., 2003a).

Granular swelling has been studied by different methods. The classical swelling power (SP) technique proposed by Leach et al. (1959) cannot distinguish intragranular water from intergranular water. However that blue dextran dye exclusion method proposed by Tester and Morrison (1990) to determine granule swelling (known as swelling factor) measures only intragranular water. In the blue dextran method, the volume of the starch

particles is determined from changes in the concentration of blue dextran dye, which by virtue of its high molecular weight (2×10^6) is excluded from the swollen starch granules.

2.6.2 Gelatinization

When starch granules are heated in excess water, a point is reached where the birefringence pattern (radial orientation of starch crystallites) starts to disappear and the granules begin to swell irreversibly. These phenomena, associated with the disruption of granular structure, are called gelatinization (Biliaderis, 2009). Jenkins and Donald (1998) proposed that the first stage of gelatinization in excess water is the uptake of water by the amorphous background region of the starch granules followed by their subsequent rapid expansion, which exerts a strong destabilizing effect on the crystallites contained within the crystalline lamellae. Thus, gelatinization of starch is disruption of molecular order revealed in irreversible changes in swelling, crystallite melting, loss of birefringence, unravelling and dissociation of the double helices and solubility (Stevens and Elton, 1971; Cooke and Gidley, 1992; Jenkins and Donald, 1998). Colonna and Buléon, (2009) postulated that gelatinization appears as the result of four processes: (1) cleavage of existing starch-starch-OH bonds (endothermic), (2) formation of starch-solvent-OH bonds (exothermic), (3) the unwinding helix-coil transition of amylopectin helices (endothermic) and (4) the formation of amylose lipid complexes.

Waigh et al. (2000) proposed a liquid-crystalline model for gelatinization (Fig 2.18). In this model, depending on the heating rate and water content, gelatinization results from

helix-coil transitions and transformations from a glassy nematic phase to a plasticized smectic phase of amylopectin helices. In the nematic state, helices are not aligned into lamellae, whereas in the smectic state (as in the granules at native conditions), the mesogens (rigid units corresponding to double helices) are aligned which leads to a 9 nm repeat between the lamellar lengths (Waigh et al., 2000). At low water content (< 5%, w/w), the amylopectin helices are in a glassy nematic state (mesogens are somewhat disordered) and the single peak corresponds to a helix-coil transition, whereas at intermediate water content (5 - 40%, w/w), biphasic peak corresponds to dislocations between double helices (leading to a smectic–nematic transition) and helix-coil transition with irreversible disentanglement of double helices, respectively. Since free disassociated helices are unstable at excess water content (>40%), lamellar break-up and disentanglement of double helices occur simultaneously (Waigh et al., 2000).

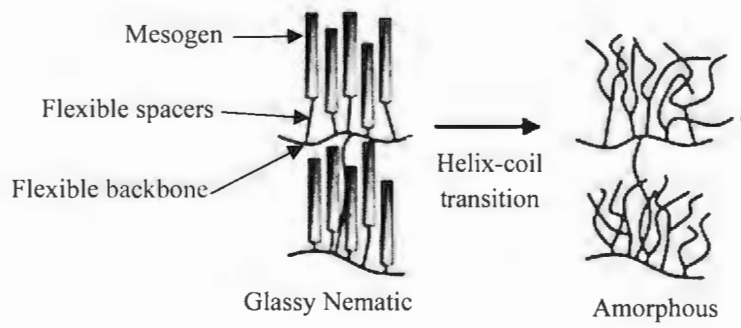
Starch gelatinization has been studied using wide variety of techniques (Swinkles, 1985; Galliard and Bowler, 1987). These include light microscopy (Biliaderis, 1982; Liu and Zhou, 1990), electron microscopy (Leach, McCowen and Schoch, 1959; Ziegler, Thompson and Casasnovas, 1993; Valetudie et al., 1995), light transmission (Hill and Dronzek, 1973), viscometry (Okechukwu and Rao, 1996b), swelling and solubility determinations (Lansky, Kooi and Schoch, 1949), particle size analysis with laser light scattering (Whistler and Doane, 1961), ¹H-NMR (Jaska, 1971), ¹³C CP/MAS NMR (Biliaderis, 1992), FTIR (Jane et al., 1992), WAXS (Biliaderis, 1982; Morrison, Law and Snape, 1993), SAXS (Carlson et al., 1979; Morrison et al., 1993) and DSC (LeMeste et al., 1992).

The most common and reliable method used for analysis of starch gelatinization temperatures (T_o , onset; T_p , peak; T_c , conclusion) and enthalpy of gelatinization (ΔH) is by a differential scanning calorimetry (Jane, 2004). T_o and T_c represent the melting of the weakest crystallites and melting of highly stable crystallites, respectively (Jacobs et al., 1998; Nakazawa and Wang, 2004). Tester and Morrison (1990) postulated that ΔH reflects the overall crystallinity (quality and amount of starch crystallites) of amylopectin. However, Cooke and Gidley (1992) suggested that the ΔH primarily reflects loss of double helical order (melting of double helices) rather than loss of crystalline order. Recently, Lopez-Rubio et al. (2008) have shown that ΔH reflects melting of imperfect amylopectin-based crystals with potential contribution from both crystal packing and helix melting. Gelatinization properties of starches have been shown to vary substantially. T_o varies from 47.8 (sugary-2 maize starch) to 71.5°C (ae-waxy maize starch), $T_c - T_o$ varies from 6.6 (barley starch) to 58.8°C (high amylose maize VII starch) and ΔH varies between 10 (barley starch) to 22 J/g (ae-waxy maize starch) (Jane et al., 1999).

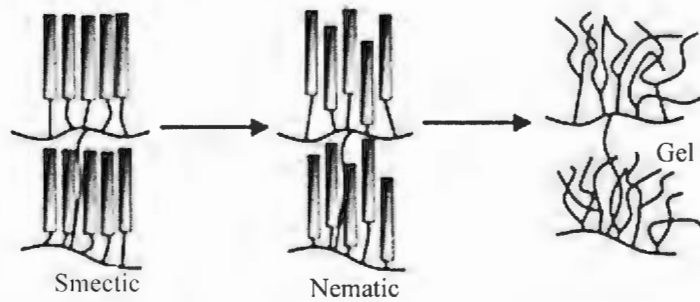
Figure 2.18 Liquid-crystalline model of starch gelatinization

- a) The single stage process in the gelatinization of starch at low water contents.
- b) The two stage process involved in the gelatinization of starch in limiting water.
- c) The two stage process involved in the gelatinization of starch in excess water. The first stage involves a slow dissociation of the helices side by-side. Immediately a helix-coil transition occurs as a secondary effect (Waigh et al., 2000, Copyright Elsevier, reproduced with permission).

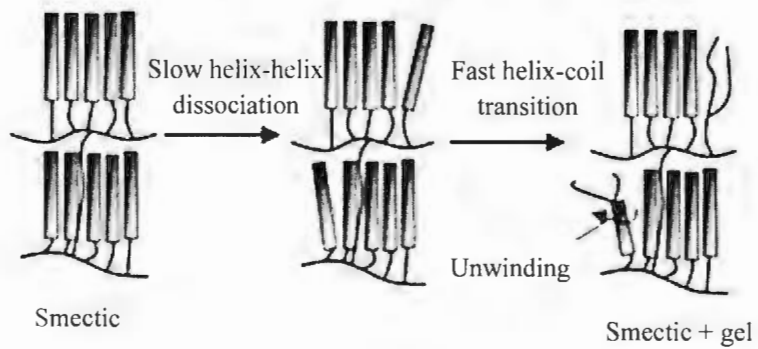
a) Limited water content



b) Intermediate water content



c) Excess water content



Starch gelatinization has been shown to be influenced by starch source, amylose to amylopectin ratio, amylopectin structure, water content, lipid content, starch damage and presence of salts (Donovan, 1979; Tester, Morrison and Schulman, 1993; Eliasson and Gudmundsson, 1996; Hoover and Ratnayake, 2002). Starch gelatinization is an endothermic reaction and requires the presence of water or other plasticizers such as glycerol (Jane, 2004). Donovan (1979) reported that under insufficient water content, starch gelatinization temperature increased and the range of gelatinization temperature also broadened and observed a biphasic endotherm. It has been suggested that in the presence of less water, the endothermic transition is characterized as a solvent-aided melting of crystallites in the starch granules (Donovan, 1979). The gelatinization temperature of starch is highly correlated to the branch chain length of amylopectin (Shi and Seib, 1992; Yuan, Thompson and Boyer, 1993; Franco et al., 2002). Noda et al. (1996) reported that gelatinization transition parameters are influenced by molecular architecture of the crystalline region, which is related to the distribution of amylopectin short chains (DP 6-11) and not by the proportion of crystalline region (corresponds to amylose to amylopectin ratio). They also observed a negative correlation between the amount of amylopectin short chains and transition temperatures. Short chains are known to be located on the external part of the crystalline structure and form a less stable double helical structure and consequently get disrupted by heat at lower temperatures (Hizukuri, 1986; Jane, 2004). Studies have shown that the melting temperature of B-type crystallite is about 20°C lower than that of A-type crystallite at constant water content (Gidley, 1987; Gidley and Bulphin, 1987). This suggests that the A-type polymorphic structure is the more stable of the two polymorphs.

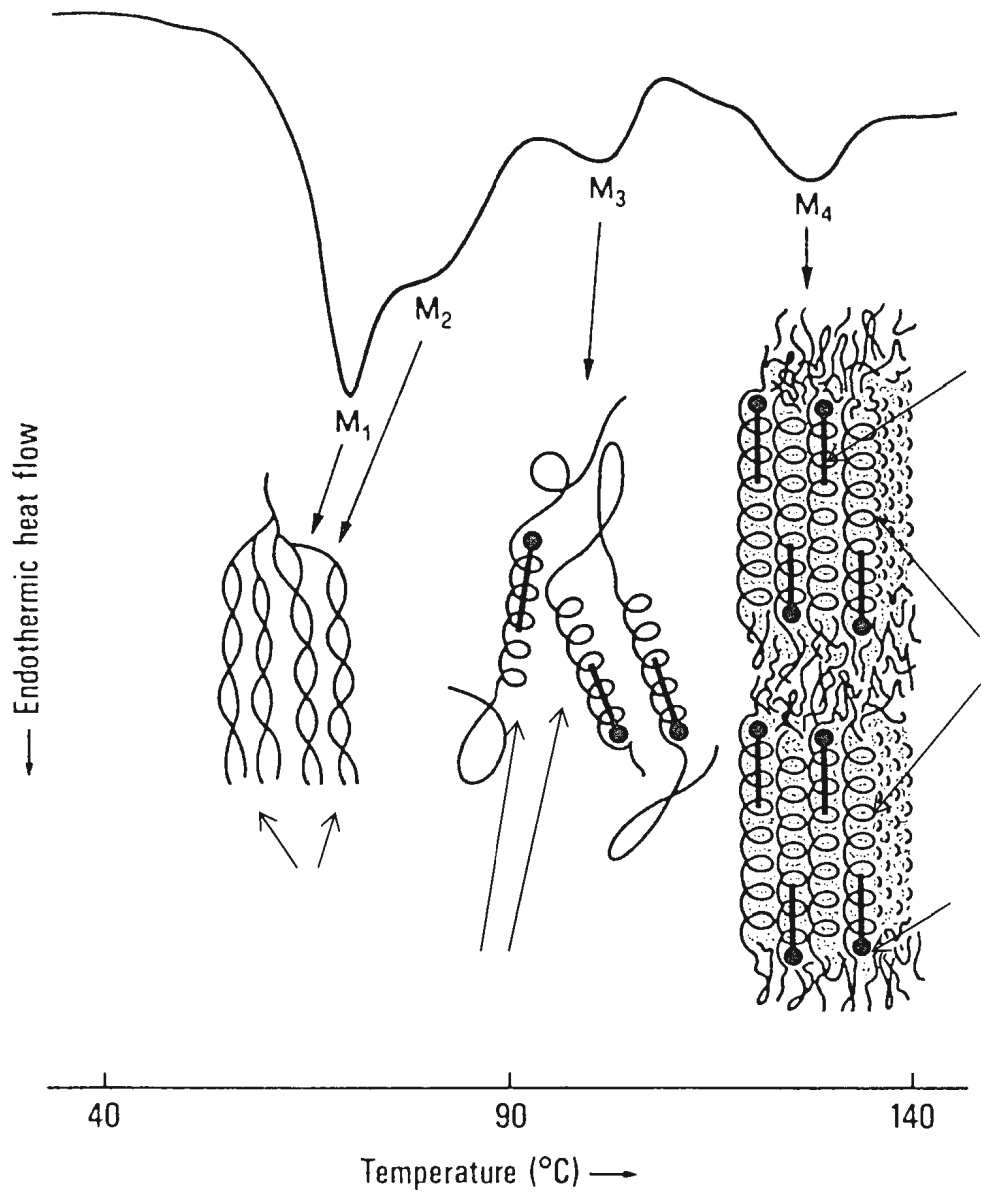
Gelatinization of starch also has been studied using aqueous alkaline solutions (e.g. NaOH, KOH), $(\text{CH}_3)_2\text{SO}$ and various neutral salt solutions such as CaCl_2 , LiCl, KI and KSCN (Evans and Haisman, 1982; Jane, 1993). Donavon and Mapes (1980) and Kugimiya and Donavon (1981) have observed an additional thermal transition peak at high temperature in DSC thermograms (Fig. 2.19) of normal cereal starches (e.g. maize and wheat). This peak has been attributed to the melting of the amylose lipid complex (Donavon and Mapes, 1980; Hoover and Hadziyev, 1981; Kugimiya and Donavan, 1981; Bulpin, Welsh and Morris, 1982; Biliaderis et al., 1985; Eliasson and Krog, 1985). The melting temperature of the amylose-lipid complexes have been shown to increase with the chain length of the fatty acid (Karkalas et al., 1995; Raphaelides and Karkalas, 1988).

Figure 2.19 A typical DSC thermal curve (50%) solid of a cereal starch showing the different melting transitions and the corresponding structural domains undergoing a phase change.

M₁, M₂: melting of amylopectin crystallites at intermediate moisture content

M₃: melting of type 1 amylose-lipid complex

M₄: melting of type II amylose-lipid complex (adapted from Billiaderis, 1998; Biliaderis and Galloway, 1989).



2.6.3 Pasting

Pasting is an important function for many applications of starch, such as thickening and sizing agent (Jane, 2004). It is the phenomenon following gelatinization in the dissolution of starch (Atwell et al., 1988), involves granular swelling, leaching of molecular components from the granule and eventually, total disruption of the granules. The paste is a viscous mass consisting of a continuous phase (a molecular dispersion) of solubilized amylose and/or amylopectin and a discontinuous phase of granule remnants (granule ghosts and fragments) (Whistler and BeMiller, 1997).

The Brabender Visco Amylograph was traditionally used worldwide in the characterization of the pasting behavior of starches (Okechukwu and Rao, 1996a). Later, the Brabender Visco Amylograph was largely replaced by the Rapid Visco Analyzer (RVA) for routine analyses (Doublier, Llamas and LeMeur, 1987). In both techniques, changes in viscosity (consistency) of starch – water dispersions are monitored continuously under constant stirring and following a programmed heating and cooling cycle. Pasting property of a starch is determined based on parameters including pasting temperature (initiation of paste formation); peak viscosity (the highest apparent viscosity obtained); breakdown viscosity (the degree of breakdown in viscosity during holding period) and setback viscosity (the viscosity after cooling at 50°C).

Normal cereal starches display a higher pasting temperature and less peak viscosity and less shear thinning than their waxy counterparts due to the presence of amylose and lipid (Jane et al., 1999). Yoo and Jane (2002) showed that normal wheat starch with 0.06% of phospholipid content showed an extremely high pasting temperature and low peak viscosity. Phospholipids form a helical complex with amylose and long branch chains of amylopectin, which entangles with amylopectin molecules and prohibits swelling of starch granules (Yoo and Jane, 2002). Root and tuber starches (e.g. Potato, tapioca) consist of little lipid display lower pasting temperatures and greater peak viscosities (McPherson and Jane, 1999). Exceptional low pasting temperature and high peak viscosity of potato has been attributed to its large content of phosphate monoesters (~0.08 %) and large granule size. Pasting properties have been shown to be influenced by several factors such as botanical source, granule rigidity and granule size, extent of granular swelling and amylose leaching, heat, shear and stirring rate, heating temperature, starch concentration, the presence of solutes, friction between swollen granules, phosphate monoester content and the proportion of long amylopectin branch chains (Evans and Haisman, 1979; Ziegler, Thompson and Casasnovas, 1993; Hoover and Vasanthan, 1994b; Eerlingen et al., 1996; Jane et al., 1999; Hagenimana and Ding, 2005).

2.6.4 Retrogradation

The formation of an elastic gel when a heated starch suspension is cooled is called retrogradation. Retrogradation profoundly influences quality, acceptability and shelf life

of starch containing foods. Retrogradation of amylose and amylopectin involve chain entanglements, short range molecular order and crystallization of double helical aggregates. Short term development of gel structure and crystallinity in starch gels during retrogradation is dominated by irreversible ($T < 100\text{ }^{\circ}\text{C}$) gelation and crystallization (within gelatinized granules) involving amylopectin (Hoover et al., 2010). Starch retrogradation is a non-equilibrium thermo reversible recrystallization process, which takes place in three consecutive steps: nucleation, propagation, and maturation (Silverio et al., 2000). Studies (Perera and Hoover, 1999) have shown that storage of starch pastes at 4°C for 1 day followed by 25°C would facilitate nucleation (formation of crystal nuclei) and propagation (growth crystallites from the nuclei formed), respectively. Retrogradation is accompanied by increase in crystallinity, gel firmness, exudation of water (syneresis), gel network formation and in the appearance of a “B” type X-ray pattern (Hoover, 1995).

Starch retrogradation has been shown to be influenced by amylopectin chain length distribution (Lu, Chen and Lii, 1997; Klucinec and Thompson, 1999; Vandeputte et al., 2003b; Chung et al., 2008), amylose content (Fan and Marks, 1998; Klucinec and Thompson, 1999; Thygesen, Blennow and Engelsen 2003; Vandeputte et al., 2003b), phosphorus content (Thygesen et al., 2003), co-crystallization of amylose with amylopectin (Gomand et al., 2010) and presence of nonstarch components such as lipids (Biliaderis and Tonogai, 1991), proteins (Appelqvist and Debet, 2000) and oligosaccharides (Biliaderis and Prokopowich, 1994), storage conditions (Mua and

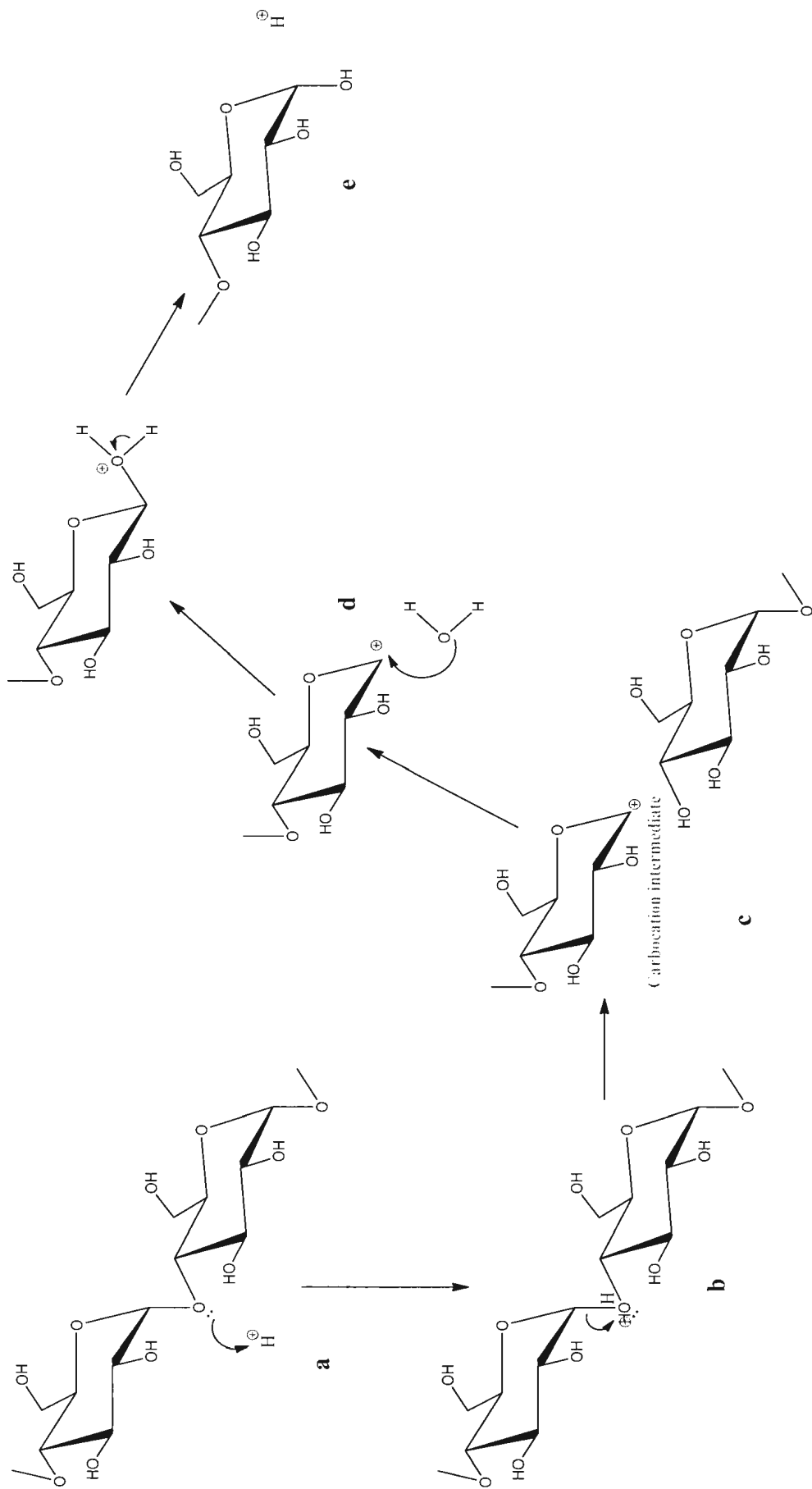
Jackson, 1998) and sample concentration (Jouppila, Kansikas and Roos, 1998). Retrogradation of cereal and tuber starches has been determined by measurement of: 1) syneresis (Yuan and Thompson, 1998; Zheng and Sosulski, 1998), 2) turbidity (Jacobson, Obanni and BeMiller, 1997; Klucinec and Thompson, 1999; Perera and Hoover, 1999), 3) crystallinity (Bello-Pérez et al., 2005; Lionetto et al., 2005), 4) conformational changes (van Soest et al., 1994; Bello-Pérez et al., 2005; Ottenhoff, Hill and Farhat, 2005), 5) molecular mobility of carbon chains (Gidley et al., 1995; Florez-Morales, Jiménez-Estrada and Mora-Escobedo, 2012), 6) enthalpy (Fisher and Thompson, 1997; Vandeputte et al., 2003b; Gomand et al., 2010), 7) and polymer network formation (Biliaderis and Zawistowski, 1990; Klucinec and Thompson, 1999; Matalanis, Campanella and Hamaker, 2009). Measurements 1, 2, 3, 4, 5, 6 and 7 have been determined by centrifugation, spectrophotometry, wide angle X-ray diffraction (WAXS), fourier transform infra-red spectrophotometry (FTIR), ^{13}C cross polarization magic angle spinning NMR (^{13}C CP/MAS NMR), differential scanning calorimetry (DSC) and oscillatory rheometry, respectively. Each of these techniques not only measures a different property of a retrograded starch gel at different levels of order (short and long range), but also reflect the contribution made by amylose and/or amylopectin to the observed property of the retrograded gel. However, the extent of the contribution will depend on the storage time, chain length of amylose and amylopectin, amylose content, extent of amylose leaching during gelatinization, amount of lipid complexed amylose chains and on the technique used.

2.6.5 Acid hydrolysis of starch

Acid hydrolysis is a chemical modification that alters the starch structure without disrupting the starch granule, depending on the parameters (temperature, time, type of acid and concentration) used in the modification (Palma-Rodriguez et al., 2012). Starch granules treated with dilute acids (HCl, H₂SO₄, or H₃PO₄) either at room temperature (for a period of several days) or at elevated temperature below the gelatinization point (for several hours) and has been used to modify starch granule structure (Singh and Ali, 2000). In the presence of acid and heat, the glycosidic bond between monosaccharide units in a polysaccharide is cleaved (Hoover, 2000). Initially, the hydronium ion (H₃O⁺) carries out an electrophilic attack on the oxygen atom of the α(1→4) glycosidic bond (Fig. 2.20a) and then the electrons in one of the carbon-oxygen bonds move onto the oxygen atom (Fig. 2.20b) to create an carbocation intermediate (Fig. 2.20c). The high energy, unstable carbocation subsequently reacts with water (Fig. 2.20d) and leading to regeneration of a hydroxyl group (Fig. 2.20e).

Figure 2.20 Mechanism of acid hydrolysis (Adapted from Hoover, 2000)

- a. Electrophilic attack of H^+ on the oxygen atom of the α (1 \rightarrow 4) glycosidic linkage
- b. Electrons in one of the $C=O$ bonds moves to the oxygen atom
- c. Unstable, high-energy carbocation intermediate
- d. Reaction with water
- e. Regeneration of OH group



The most traditional acid hydrolysis procedures used for modification of starch include those reported by Nageli and Lintner (Robin et al., 1974). Treatment of starch with sulfuric acid (15%) at room temperature produces Nageli amyloextrins (a low molecular weight acid-resistant fraction), whereas with hydrochloric acid (2.2N) at elevated temperatures (30-40°C) lintnerized starch is formed (a higher molecular weight acid resistant fraction) (Hoover, 2000). Nageli amyloextrin has been shown to be a mixture of low molecular, linear and branched dextrans, with an average degree of polymerization (DP) of 25-30 (Ratnayake et al., 2001). Several researchers have shown that lintnerized starches consist of linear AM chains with a DP between 13-15, singly branched AM chains (DP 25), multiple branched chains, and retrograded AM and AM-lipid complexes (Robin et al., 1974; Biliaderis, Grant and Vose, 1981; Morrison et al., 1993a). The molecular weight and viscosity of acid-modified starches vary with the conditions (acid concentration, temperature and time) used during modification, however, their yield decreases consistently with increasing acid concentration and hydrolysis time (Xia et al., 2010). Singh and Ali (2000) have studied the influence of various acids (HCl, HNO₃, H₂SO₄ and H₃PO₄) on acid degradation of many starches and found variations in molecular weight distribution (HCl > HNO₃ > H₂SO₄ > H₃PO₄).

Acid preferentially attacks the amorphous regions first and then the crystalline regions of starch granules, giving a two-stage hydrolysis pattern (Robin et al., 1974; Biliaderis, Grant and Vose, 1998). The slower hydrolysis rate of the crystalline region is attributed to the dense packing of starch chains within the crystallites which hinders rapid penetration of H₃O⁺ and also restricts the conformational change (chair to half chair)

required for the electrophilic attack of H_3O^+ on the glycosidic oxygen (Jayakody and Hoover, 2002). AM has been shown to retard the rate of lintnerization and decrease the amount of acid resistant double helices (Bertoft, 2004). Jane et al. (Jane, Wong and McPherson, 1997) found that high AM maize starch was solubilized slowly in comparison with normal and waxy maize starches. Bertoft and Wiik (2004) reported that the presence of AM (at least in B-type starch) could affect the organization of the starch granules, making both the amorphous and crystalline parts more acid stable. Jenkins and Donald (1995) have shown that the AM disrupts the packing of AP double helices within the crystalline lamella, thereby increasing the relative length of the crystalline lamella and decreasing the size of amorphous lamella. Morrison et al. (1993) reported that the lipid-complexed segments of single V_6 - AM helices in barley starches are resistant to acid hydrolysis. A study on maize starches with varying AM contents revealed that susceptibility towards acid hydrolysis is influenced by the extent of interaction between starch chains within the amorphous domains of the granule (Hoover and Manuel, 1996b). Biliaderis et al. (1981) hypothesized that AM is hydrolyzed more rapidly than AP due to the presence of AM in amorphous regions. However, direct evidence for the mode of degradation of AM and AP is limited (Wang et al., 2012).

Acid hydrolysis has been shown to increase the gelatinization temperatures, the breadth of gelatinization endotherms, retrogradation rate, water solubility, gel strength and decrease the viscosity of starches (Hoover, 2000). Many studies have shown that acid hydrolysis increases gelatinization enthalpy (ΔH). However, recently Gao et al. (2012) observed a decrease in ΔH on acid treatment of high AM and waxy starches. They

postulated that hydrolysis of α (1 \rightarrow 6) branch points in amorphous lamella would increase helical mobility, resulting in better alignment and perfection between adjacent double helices. Consequently, the number of double helices that unravel and melt (indicated by ΔH) would decrease (due to stronger interaction between adjacent double helices) after acid treatment.

2.6.6 Enzyme hydrolysis of starch

Native starches differ in their susceptibility to enzyme hydrolysis, depending on starch source and the type of amylase (Hoover and Sosulski, 1985). α -amylases hydrolyze α (1 \rightarrow 4) linkages, but are able to bypass the (1 \rightarrow 6) branch points without hydrolyzing them (Hoover and Zhou, 2003). However, β -amylase is an inverting exo-amylase which hydrolyze the α (1 \rightarrow 4) linkages from the non-reducing ends of starch molecules. The hydrolysis mechanism of α -amylase and β -amylase is illustrated in Fig. 2.21. α -amylases work according to the double displacement mechanism (Fig. 2.21a) (Robyt and French, 1970; MacGregor, Janeček and Svensson, 2001). Carboxylate base initiates cleavage of the bond via nucleophilic attack at C-1 of the glucopyranosyl unit. Simultaneously, the glycosidic oxygen is displaced and protonated by the carboxylic acid group. The attacking carboxylate group forms a covalent β -linked acetal ester, giving a glucopyranosyl-enzyme intermediate. This high energy intermediate subsequently reacts with water giving retention of the configuration of the product at its reducing end (Robyt, 2009). In contrast, β -amylases work through the single displacement mechanism (Fig. 2.21b) (Robyt and French, 1970). The hydrolysis reaction proceeds through an

oxocarbenium ion-like transition state (O-anomeric C bond has partial double bond character) (Withers and Aebersold, 1995).

α -amylases from different sources (*pig pancreas*, *Bacillus sp* and *Aspergillus fumigatus*) have been shown to have different profiles of hydrolysis (Fig 2.22) (Planchot et al. 1995). Porcine pancreatic α -amylase (PPA) hydrolytic products are mainly maltose, maltotriose and maltotetrose while α -amylase from *Bacillus amyloliquefaciens* produces mainly maltotriose, maltohexaose and maltoheptaose (Robyt and French, 1970; Yook and Robyt, 2002). Maltose acts as an inhibitor, which can bind to the active sites of α -amylase (Whitaker, 1994). Franco and Ciacco (1987) reported that elimination of soluble hydrolysis products by dialysis increased the degree of hydrolysis. When amyloglucosidase is used in combination with α -amylase, the amyloglucosidase hydrolyses the maltose into glucose and increased the rate of α -amylolysis (Colonna, Leloup and Buléon , 1992).

α -amylase hydrolyzes starch by a multiple attack mechanism from the reducing end towards the non-reducing end and form maltodextrins (Robyt and French, 1970). However, the mechanism involved in the hydrolysis of the crystalline domain is not well-known. Enzyme hydrolysis has been shown to be influenced by granule size, surface porosity, extent of starch chain interactions within the amorphous and crystalline regions, AM/AP ratio, degree of crystallinity, difference in type and proportion of polymorphic (A, B, C) forms, amount of α (1 \rightarrow 6) linkages, extent of distribution of α (1 \rightarrow 6) linkages

between the amorphous and crystalline domains, chemical composition (presence of phosphorus, granule bound proteins, lipids) and enzyme inhibitors (Hoover and Sosulski, 1985; Colonna, Buléon and Lemarié, 1988; Jane, Wong and McPherson, 1997; Hoover and Zhou, 2003; Blazek and Copeland, 2010). Controversy still exists with respect to the hydrolysis mechanism of enzyme hydrolysis. In some starches (wheat, barley), the amorphous and crystalline regions have been shown to be digested at the same rate (Colonna, Buléon and Lemarié, 1988). This was based on the observation there was no significant increase in crystallinity level, as indicated by constant diffracted intensities and scattering background (Hoover and Zhou, 2003). Whereas, in other starches, the amorphous regions are hydrolyzed first (Zhou, Hoover and Liu, 2004). No satisfactory explanation has been put forward to explain this difference.

Enzyme hydrolysis of starch occurs via three successive phases: 1) diffusion of the enzyme molecule towards the surface of solid phase and then inside the granules, 2) adsorption of enzymes on the substrate and 3) catalytic reaction (Gallant et al., 1992; Sujka and Jamroz, 2007; Bird et al., 2009). Colonna et al. (1992) have shown that smaller granules, by virtue of their higher available surface area per unit mass, facilitate diffusion and adsorption of enzymes, and thus are catalyzed more rapidly compared to larger granules. Oates (1997) postulated that the enzyme-catalyzed hydrolysis of α -(1 \rightarrow 4) glucosidic bonds involves the enzyme-induced ring distortion of one of the D-glucosyl residues from the 4C_1 -chair conformation to a 'half chair' conformation. Ring distortion decreases the enthalpy of activation and increase the susceptibility of the

glycosyl residues. Consequently, chains with restricted mobility, either complexed or crystallized will be hydrolyzed less readily (Oates, 1997).

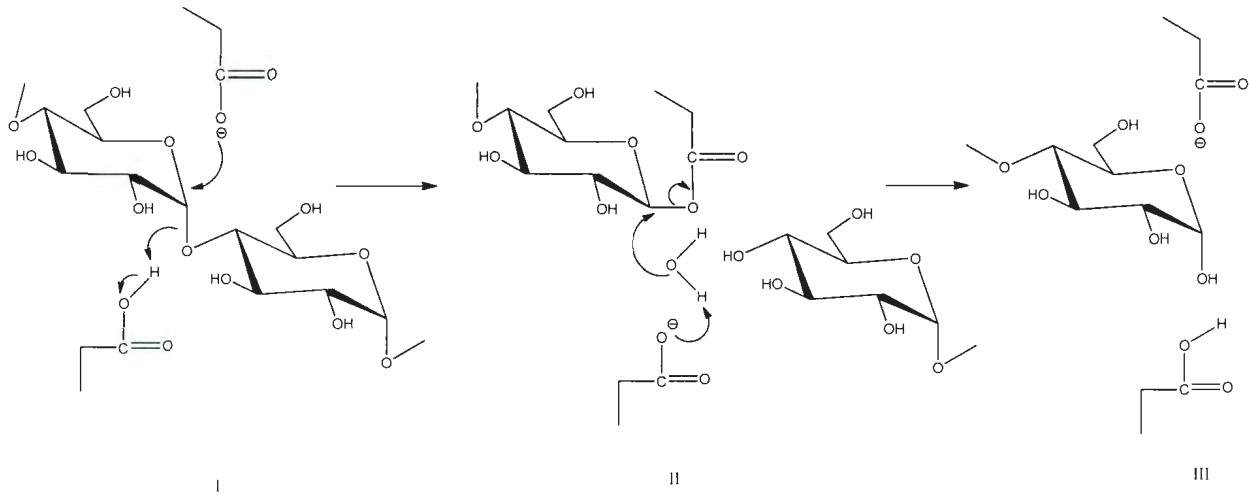
Crystalline material is considered to be an important factor in defining the rate and extent of enzymatic hydrolysis. The susceptibility of different crystalline polymorphs (A-, B- and C-type) towards hydrolysis continues to be a matter of debate. Several studies have shown that B-type starches are usually less susceptible to enzyme hydrolysis than A-type starches (Robyt, 2009). Susceptibilities and hydrolytic patterns of various starches towards PPA, bacterial α -amylase, fungal α -amylase, amyloglucosidase and isoamylase and have shown that A-type starches are more susceptible to PPA than B- and C- type starches (Gallant et al., 1992). Tester, Qi and Karkalas (2006) have shown that the amount of native starch hydrolyzed by α -amylases is inversely related to the AM content (waxy maize > normal maize > high AM maize). Jane, Wong and McPherson (1997) have shown that the presence of an inferior crystalline structure containing α (1 \rightarrow 6) linked branched points and short double helices results in weak points in A-type starches and makes them more susceptible to α -amylolysis. However, in B-type starches location of more α (1 \rightarrow 6) linkages in the amorphous region and fewer short branch chains makes the crystalline structure superior to that of the A-type starches, and hence render B-type starches more resistant to α -amylolysis (Zhou, Hoover and Liu, 2004). Ratnayake et al. (2001) have shown by studies on starches from different cultivars of field peas (C-type starch) that resistance to α -amylase increases with increase in B-polymorph content. Jinglin et al. (2009) have shown that the B-type polymorph present in the C-type starch granules are preferentially degraded or degraded faster than the A-type polymorph.

Figure 2.21 Proposed mechanisms involved in the hydrolysis of glycosidic linkages
(adapted from Robyt and French, 1970).

- a) Double displacement, S_N2 , mechanism, giving retention of configuration (α -amylases)
 - I. Attack on C-1 by a carboxylate group and donation of a proton to the leaving oxygen atom by a carboxyl group
 - II. Attack on water on the covalent β -acetal-carboxyl-ester to give product III with retained configuration at the anomeric end

- b) Direct displacement, S_N1 , mechanism, giving inversion of configuration (β -amylases)
 - I. Direct attack on C-1 by water, assisted by a carboxylate group and donation of a proton to the leaving oxygen atom by a carboxyl group.
 - II. Product with inverted configuration
 - III. Regeneration of the catalytic groups at the active-site by proton exchange between the two carboxyl groups

a) Double displacement, S_N2 , mechanism (α -amylases)



b) Direct displacement, S_N1 , mechanism (β -amylases)

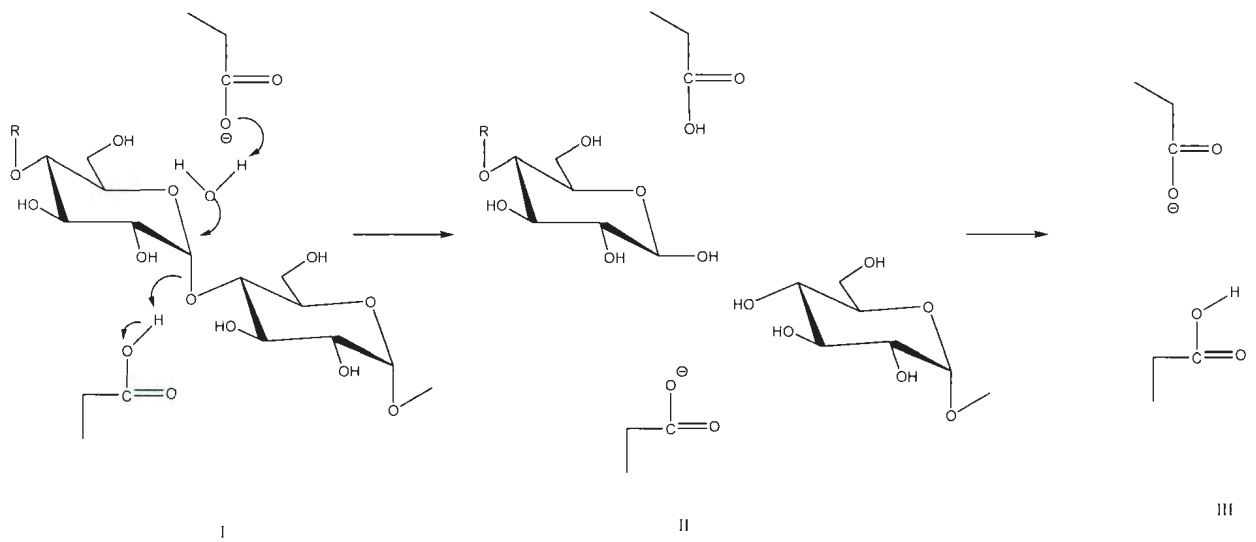


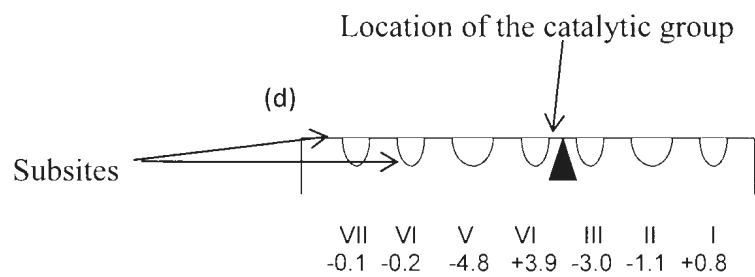
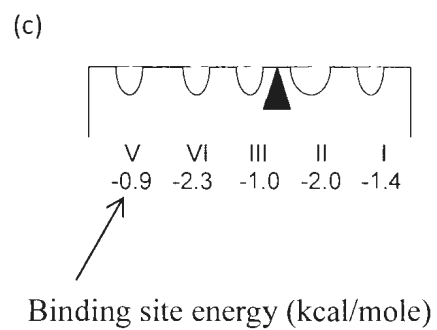
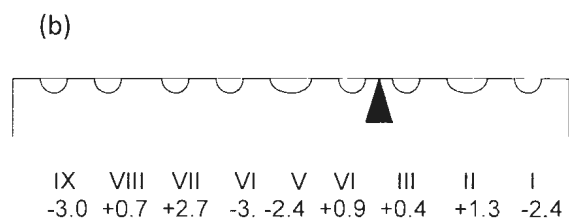
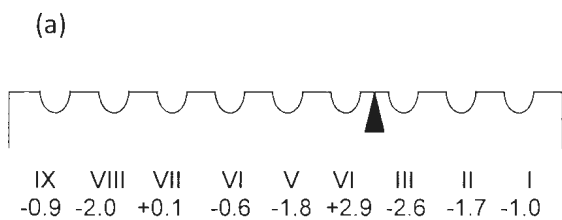
Figure 2.22 Glucose-binding subsites at the active-site of four endo-acting α -amylases (adapted from Robyt, 2009) (Subsites for endo-acting amylases are numbered with Roman numerals for subsite beginning with the subsite that would bind the reducing-end glucosyl unit; Arabic numbers indicate binding energies (kcal/mole), with increasing negative values indicating the strongest binding; \blacktriangle represents the location of the catalytic groups in relation to the glucose-binding sites).

(a) *Bacillus amyloliquefaciens* α -amylase – Nine subsites (Robyt and French, 1970; Thoma et al., 1971)

(b) Barley malt α -amylase – Nine subsites (MacGregor and MacGregor, 1985)

(c) Porcine pancreatic α -amylase – Five subsites (Robyt and French, 1970; Seigner et al., 1987)

(d) *Aspergillus oryzae* α -amylase - Seven subsites (Suganuma et al., 1978)



2.6.7 Nutritional fractions

Carbohydrates are one of the major sources of energy (4 kcal/g) in the human diet and account for 40-75% of total energy intake (FAO/WHO, 1998). Glucose released from carbohydrates have been shown to affect blood glucose and insulin levels, cholesterol and triglyceride metabolism, as well as influence satiety, and exert prebiotic effects in the large intestine (Holt et al., 1995; Saltiel and Kahn, 2001; Eckel et al., 2005; Englyst, Liu and Englyst, 2007; Venn and Green, 2007). Depending on the rate and extent of digestion, starches are generally classified into rapidly digestible starch (RDS), slowly digestible starch (SDS) and resistant starch (RS). RDS reflects starch that is rapidly and completely digested in the small intestine (associated with a rapid elevation of postprandial plasma glucose). SDS reflects starch that is more slowly digested in the small intestine (alternates post prandial plasma glucose and insulin levels) and RS reflects the sum of starch and the product of starch degradation not absorbed in the small intestine but is fermented in the large intestine. Consequently, high levels of SDS and RS levels have been shown to reduce the risk of cardiovascular disease (CVD), diabetes, colon cancer and obesity (Jenkins et al., 1983; Abeysekara et al., 2012). The term glycemic index (GI) was first introduced in 1981 by Jenkins et al. (1981) as a physiological (*in vivo*) way of classifying foods rich in carbohydrates based on their blood glucose-raising potential (Ek, Miller and Copeland, 2012). GI is defined as the incremental post prandial glucose area after injection of the test product, as a percentage of the corresponding area after injection of an equicarbohydrate portion of the reference product (Jenkins et al., 1983). Foods with a GI value of above 70 are classified as high GI, foods that have a GI

of 55 and less as low GI, and GI between 56–69 are classified as medium GI foods (ISO Standard, 2010).

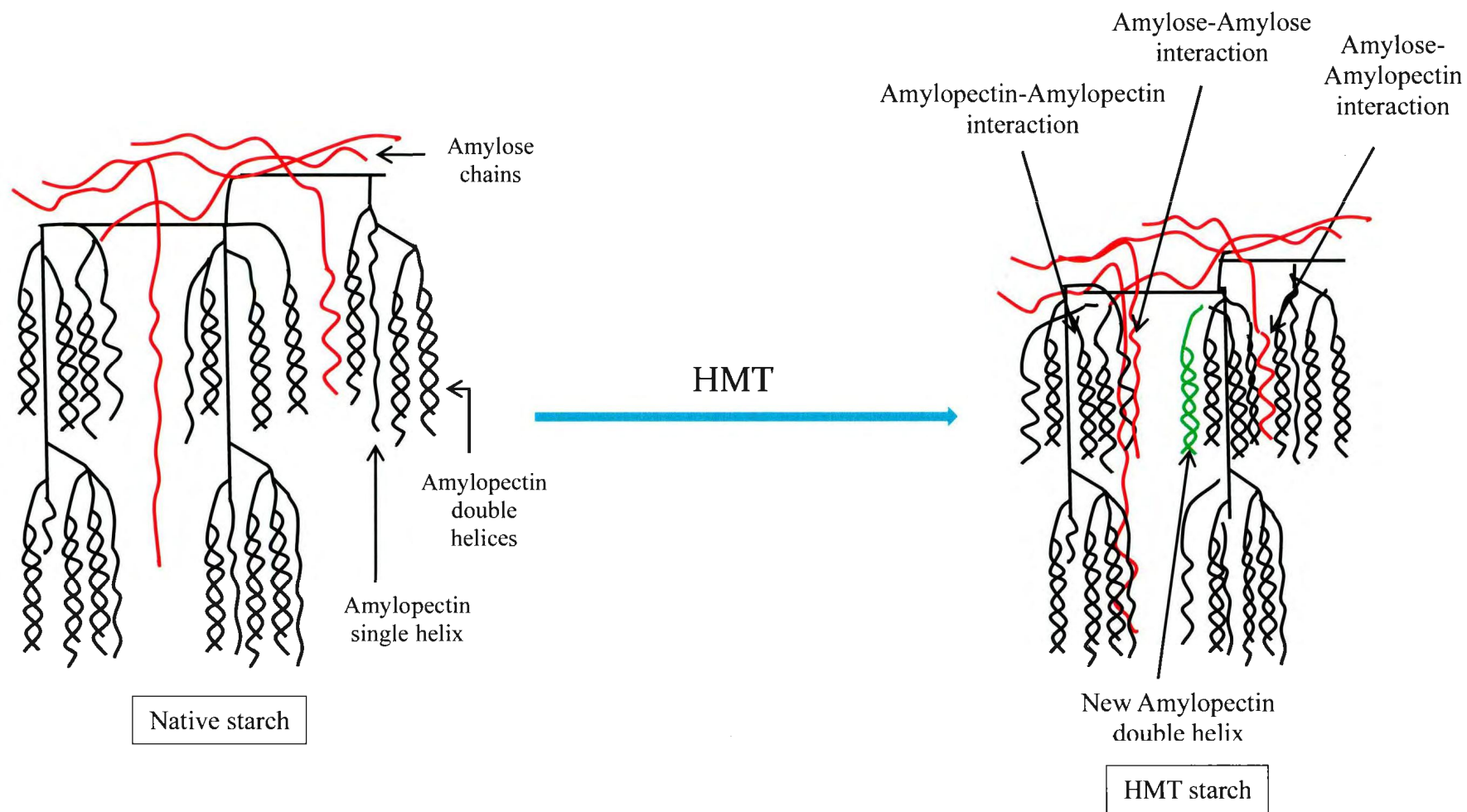
RS has been classified into four different groups, 1) physically inaccessible starch within (e.g. intact plant tissues or dense food matrices) (RS I), 2) Intact granular starches that have slow digestion rates (raw potatoes, green bananas, some legumes, high-amylose starches) (RS II), 3) Starch that has been processed and partially retrograded (cooked and cooled potatoes, bread, cornflakes) (RS III), and 4) Chemically modified starch that slows α -amylase attack (RS IV) (Nugent, 2005; Bird et al., 2009). Studies have shown that in many foods, a small proportion of the starch present will be RS (~ 0–5% of starch in most cereal products) although for some foods such as legumes this is higher (~10–20% of starch for some beans) (Englyst, Liu and Englyst, 2007). The amounts of RS in foods is largely dependent on the degree of food processing, which could result either an increase or a decrease in the RS content from those found in the raw product (Englyst, Liu and Englyst, 2007). RS has been shown to behave more like soluble dietary fibre. The most common results include increased fecal bulk and lower colonic pH and improvements in glycemic control, bowel health, and cardiovascular disease risk factors (Lunn and Buttriss, 2007). RS also shows promising physiological impact in the prevention of gall stone formation (Patindol et al., 2010). Fuentes-Zaragoza et al. (2011) reported that similar to soluble fibre, a minimum intake of RS (5–6 g) appears to be needed in order for beneficial reductions in insulin response to be observed (Kay et al., 2006). The fermentation of RS by anaerobic bacteria yields short chain fatty acids, primarily composed of acetic, propionic, and butyric acids, which can lower the lumen pH, creating

an environment less prone to the formation of cancerous tumours (Yao, Paez and White, 2009).

2.7 Heat-moisture treatment

Native pulse starches have poor functional properties such as low shear and acid resistance, low thermal stability and high retrogradation tendency. Therefore modification of pulse starches is needed to meet industrial demands. In this respect, chemical modifications are commonly used to produce pulse starches with desirable properties. However, at the present time, there is a great interest in the use of physical modification techniques, such as heat-moisture treatment (HMT), which changes the physicochemical properties of starches by facilitating starch chain interactions within the amorphous and crystalline domains. HMT involves treatment of starch granules at low moisture levels (< 35 % moisture w/w) during a certain time period (15 min - 16 h) and at a temperature (80 – 130 °C) above the glass transition temperature (T_g) but below the gelatinization temperature (Hoover, 2010; Jacobs and Delcour, 1998; Kulp and Lorenz, 1981; Sair, 1967). HMT facilitates starch chain interactions within the amorphous and crystalline domains without disrupting its granular structure. Some possible changes of starch chains that could occur during HMT are presented in Fig 2.23.

Figure 2.23 A schematic representation of some possible changes during HMT



Several studies have shown that HMT influence morphology, X-ray diffraction pattern, gelatinization parameters, crystallinity, granule swelling, amylose leaching, viscosity, retrogradation and susceptibility towards acid and α -amylase hydrolysis of starch granules (Hoover and Vasanthan, 1994a; Gunaratne and Hoover, 2002; Chung, Liu and Hoover, 2009; Varatharajan et al., 2010). However, the type and extent of change varies with botanical origin (cereal, tuber, root and legume), starch composition (amylose-amylopectin ratio and lipid) and treatment conditions (temperature, starch to moisture ratio and duration of heating). There are several studies on HMT of cereal and tuber starches at varying temperature and moisture conditions (Jacobs and Declour, 1998; Hoover, 2010; Zavareze and Dias, 2011). However, studies on HMT of pulse starches are limited. Previous studies on HMT of pulse starches are presented in Table 2.4.

Table. 2.4 HMT parameters of pulse starches

Starch Source	Temp. (°C)	Time (h)	Moisture (%)	Reference
Black bean	100	16	30	Hoover and Manuel (1996a)
Borlotti bean	100	16	22	Guzel and Sayar (2010)
Green gram	120	2	14	Sekine et al. (2000)*
Jack bean	100	16	18–27	Lawal and Adebawale (2005a)
Lentil	100	16	10–30	Hoover et al. (1994)
	120	2	30	Chung et al. (2009)
	120	24	30	Chung, Liu and Hoover (2010)
Mucuna bean	100	16	18–27	Adebawale and Lawal (2003)
Navy bean	120	24	30	Chung, Liu and Hoover (2010)
Pea	120	2	30	Chung et al. (2009)
	120	24	30	Chung, Liu and Hoover (2010)
Pigeon pea	100	16	30	Hoover, Swamidas and Vasanthan (1993)
Pinto bean	100	16	30	Hoover and Manuel (1996a)
Smooth pea	100	16	30	Hoover and Manuel (1996a)
Wrinkle pea	100	16	30	Hoover and Manuel (1996a)

*heating under pressure

2.7.1 Impact of HMT on granule morphology

Studies have shown that HMT does not alter the size or shape of cereal (maize, wheat, finger millet, rice) tuber and root (potato, sweet potato, yam, cassava, canna) and pulse (lentil) starch granules (Kulp and Lorenz, 1981; Stute, 1992; Hoover and Vasanthan, 1994a; Franco et al., 1995; Hoover and Manuel, 1996a; Gunaratne and Hoover, 2002; Adebowale, Afolabi and Olu-Owolabi, 2005; Tattiyakul et al., 2006; Khunae, Tran and Sirivongpaisal, 2007; Watcharatewinkul et al., 2009). However, Kawabata et al. (1994) observed formation of cracks on the surface of HMT maize and potato starches, together with a hollow inside the granule. Recently, Zavareze et al. (2011) observed an irregular surface morphology of high (32%) and medium amylose (23%) rice starches and signs of loss of physical integrity with distension of the granular surface in low amylose (7%) rice starch after HMT at 110°C (25% moisture, 1 h). They postulated that this change in granular morphology of low-amylose rice starch by HMT is probably due to the high moisture content prevailing during hydrothermal treatment, which may have caused partial gelatinization and morphological changes (Zavareze and Dias, 2011).

Vermeulen et al. (2006) and Varatharajan et al. (2011) observed that birefringence at the granular center (hilum region) disappeared with increasing HMT temperature (90–130 °C; 17–26% moisture) in normal and waxy potato starches. Chung et al. (2009) have also observed a decrease in birefringence intensity and loss of birefringence at the granular centre during HMT of corn, pea and lentil starches (100-120 °C; 30% moisture). However, in the above studies, birefringence intensity at the granule periphery remained

unchanged with HMT. The disappearance of birefringence at the granular centre of potato starch has been attributed to the formation of voids surrounding the hilum (Vermeulen et al., 2006). This was confirmed by confocal laser scanning microscopy studies on HMT normal and waxy potato starches (Vartharajan et al. 2010).

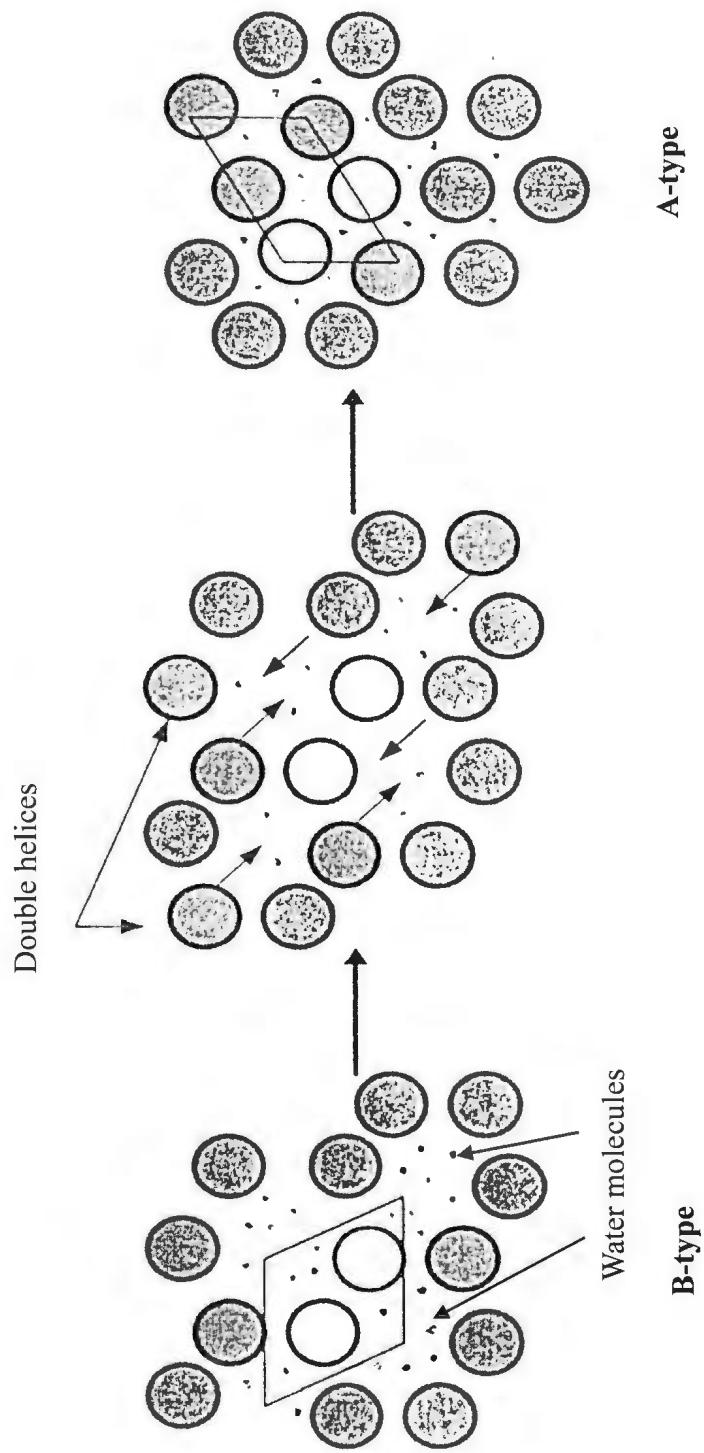
2.7.2 Impact of HMT on granule structure

2.7.2.1 Starch polymorphism and X-ray diffraction pattern

Change in polymorphism from B-type (tuber and high amylose) starches either to a pure A-type (characteristic of cereal starches) or to a mixed A + B type (characteristic of legumes and some tuber and root starches) pattern during HMT has been shown by many studies (Sair, 1967; Kulp and Lorenz, 1981; Lorenz and Kulp, 1982; Donovan, Lorenz and Kulp, 1983; Stute, 1992; Lim, Chang and Chung, 2001; Miyoshi, 2002; Gunaratne and Hoover, 2002; Vermeulen et al., 2006; Tattiyakul et al., 2006; Vieira and Sarmiento, 2008; Varatharajan et al., 2010). Gidley and Bociek (1985) confirmed this polymorphic transformation by ^{13}C CP/MAS NMR based on variations in C-1 multiplicity. In contrast, taro, cassava (Gunaratne and Hoover, 2002) and cereal starches (Jacobs and Delcour, 1998) did not exhibit an altered X-ray diffraction pattern after HMT. Jacobs and Delcour (1998) suggested that not all temperature and moisture conditions induce a change from B- to A-type crystallinity in potato starch.

Transformation of the less thermodynamically stable B-polymorphic structure (with hexagonal packing of double helices and about 36 water molecules inside each cell) into a more stable monoclinic structure of A-type polymorphs (with about six water molecules inside the helices) is attributed to dehydration of water molecules in the central channel of B polymorph as well as to movement of a pair of double helices into the central channel (Fig. 2.24) (Hoover, 2010). Gunaratne and Hoover (2002) suggested that this movement during HMT could disrupt starch crystallites and/or change the crystalline orientation.

Figure 2.24 A proposed model of the polymorphic transformation from B-type to A-type unit cell in the solid state (adapted from Imberty et al., 1991).



2.7.2.2 Peak intensity and relative crystallinity

Studies have shown that the A-type diffraction pattern and peak intensities of cereal starches remain unchanged with HMT (Sair, 1967; Fukui and Nikuni, 1969; Donovan, Lorenz and Kulp, 1983; Radosta et al., 1992; Hoover and Vasanthan, 1994a; Franco et al., 1995; Hoover and Manuel, 1996a, b). Vieira and Sarmiento (2008) observed an increase in peak intensity with HMT of sweet potato starch. Zavareze and Dias (2011) postulated that the increase in the X-ray intensity with HMT of sweet potato and corn starches is due to the displacement of the double helical chains within the starch crystals, resulting in a crystalline matrix that is more orderly than in native starch. However, triticale (Lorenz and Kulp, 1982), cassava (Abraham, 1993), yam (Hoover and Vasanthan, 1994a), maize (Franco et al., 1995), pea (Hoover and Manuel, 1996a), mucuna bean (Adebowale and Lawal, 2003), barley (Singh et al., 2005), potato (Hoover and Vasanthan, 1994a; Lim, Chang and Chung, 2001; Miyoshi, 2002; Vermeulen et al., 2006) and Peruvian carrot (Vieira and Sarmiento, 2008) starches exhibited a decrease in peak intensities on HMT. Reduction in X-ray intensity on HMT reflects reduced crystallinity or an increase in the amount of amorphous area within the semi-crystalline lamella (Zavareze and Dias, 2011). Changes in X-ray patterns and intensities with HMT have been shown to be influenced by HMT conditions such as temperature and moisture content (Hoover and Vasanthan, 1994a; Vermeulen et al., 2006; Tattiyakul et al., 2006). Hoover and Vasanthan (1994a) suggested that in A-type starches the thermal energy and moisture during HMT causes double helices to realign within the crystallites resulting in an increase in the number of direct hydrogen-bonds linking adjacent helices than in the native starch. Whereas, in

native B-type starches, adjacent double helices are mainly linked by hydrate water bridges and to a limited extent by direct hydrogen bonding (Leach, McCowen and Schoch, 1959). Consequently, in B-type starches, rupture of hydrate water bridges (causes the adjacent double helices to move apart and assume orientations that are not in perfect parallel crystalline array) on HMT result in decreased X-ray intensities (Hoover and Vasanthan, 1994a).

Relative crystallinity has been shown to remain unchanged with HMT of A-type tuber (new coco yam, cassava, taro) starches and to decrease in B-type tuber (true yam, potato), C-type pulse (pea, lentil, navy bean) and A-type cereal (rice starches) (Gunaratne and Hoover, 2002; Vermeulen et al., 2006; Khunae et al., 2007; Vieira and Sarmento, 2008; Chung, Liu and Hoover, 2010). The decrease in crystallinity has been attributed to disruption of amylopectin crystallites, which has been confirmed by HPAEC-PAD studies (Hoover and Vasanthan, 1994a; Gunaratne and Hoover, 2002; Vermeulen et al., 2006). However, Vermeulen et al. (2006) observed an increase in crystallinity in potato starch subjected to HMT 130°C (17-26 % moisture content, 24 h) and suggested that disruption of covalent linkages at 130°C results in decoupling of double helices from the amylopectin backbone which renders the double helices sufficiently mobile to become organized in a more perfect crystalline array.

2.7.2.3 Molecular order at the granular surface

Molecular order at the granular surface ($1048/1016\text{ cm}^{-1}$) has been shown to decrease with HMT of navy bean, corn, pea and lentil starches (Chung, Liu and Hoover, 2010). They suggested that crystallite disruption on HMT would have a greater impact on crystallites that are highly organized at the granule surface. Varatharajan et al. (2010) have shown that both the $1048/1016\text{ cm}^{-1}$ and $995/1016\text{ cm}^{-1}$ ratios decreased with HMT of normal and waxy potato starches and suggested that removal of water during HMT would have changed the alignment of double helices at the granular surface. They postulated that the $995/1016\text{ cm}^{-1}$ ratio is more sensitive than the $1048/1016\text{ cm}^{-1}$ ratio in determining changes to the alignment of double helices at short-range order on HMT. However, Watcharatewinkul et al. (2009) reported no change in the FTIR spectrum on HMT of canna starch (100°C , moisture content of 25%, 16 h). Khunae et al. (2007) reported by studies on rice starches of varying amylose content (1-20%) that short-range molecular order remained unchanged in Chiang rice starch (20.2% amylose) but decreased in glutinous (1.4%) and Jasmine (15%) rice starches. They attributed the decrease to an increase in amylose-lipid complex formation in the Chiang rice starch.

2.7.2.4 Lamellar organization

Vermeylen et al. (2006) have shown by small angle X-ray scattering (SAXS) studies that 0.6 nm^{-1} scattering maximum [corresponds to the wide angle X-ray (WAXS) diffraction peak at $5.6^\circ 2\theta$ (characteristic peak of B-type starches)] disappears with HMT of potato starch. They suggested that during the polymorphic transformation ($B \rightarrow A + B$), double

helices move laterally within the high density lamella, and also along their helical axis and concluded that HMT disturbs the lamellar stacked system (Vermeulen et al., 2006).

2.7.2.5 Amylose-lipid complex formation

Fukui and Nikuni, (1969) and Kawabata et al. (1994) observed the development of a V-type X-ray diffraction pattern [Fig. 2.16] (attributed to crystalline amylose–lipid complexes) on HMT of cereal starches. Shih et al. (2007) and Khunae et al. (2007) also observed a V-amylose lipid peak ($20^\circ 2\theta$) in rice starches with HMT (100-110°C, 18-40% moisture content). The intensity of the V-amylose lipid peak ($20^\circ 2\theta$) was shown to increase with increase in moisture content. This was attributed to increased mobility of V-amylose-lipid complex chains in cereal starches due to the presence of lipids. However, starches with trace quantities of lipid (potato) have been shown to exhibit a decrease in apparent amylose content with HMT (Hoover and Vasanthan, 1994a; Hoover and Manuel, 1996b) due to interaction of amylose chains among and between amylopectin chains.

2.7.3 Impact of HMT on starch properties

2.7.3.1 Granular swelling

Several researchers have observed that granular swelling decreases with HMT of many cereals (Kulp and Lorenz, 1981; Hoover and Vasanthan, 1994a; Hoover et al., 1994; Hoover and Manuel, 1996a, b; Hormdok and Noomhorm, 2007; Olayinka et al., 2008;

Sun et al., 2013), tuber (Sair, 1967; Hoover and Vasanthan, 1994a; Hoover et al., 1994; Gunaratne and Hoover, 2002; Lawal, 2005; Tattiyakul et al., 2006; Varatharajan et al., 2010) and pulse (Hoover and Vasanthan, 1994a; Hoover, Swamidas and Vasanthan, 1993; Hoover et al., 1994; Chung, Liu and Hoover, 2009) starches. This reduction in granular swelling has been attributed to increased crystallinity, reduction of available hydroxyl groups for hydration, increased interactions between amylose and amylopectin molecules, strengthened intramolecular hydrogen bonds, the formation of amylose–lipid complexes and changes in the arrangements of the crystalline regions of starch (Hoover and Vasanthan, 1994a; Hoover and Manuel, 1996a; Jacobs et al., 1995; Waduge et al., 2006).

2.7.3.2 Amylose leaching

Several studies have shown that amylose leaching decreases with HMT of cereal, tuber and pulse starches (Sair, 1967; Kulp and Lorenz, 1981; Hoover and Vasanthan, 1994a; Lawal, 2005; Tattiyakul et al., 2006; Hormdok and Noomhorm, 2007; Olayinka et al., 2008; Chung, Liu and Hoover, 2009; Varatharajan et al., 2010; Sun et al., 2013). However, in some cereal starches, (rye, barley, triticale, finger millet, wheat) amylose leaching, has been shown to increase with HMT, in spite of reduced granular swelling (Kulp and Lorenz, 1981; Radosta et al., 1992; Adebawale et al., 2005). Hormdok and Noomhorm (2007) observed no significant difference in the amylose leaching of hydrothermally treated rice and native rice starch. The effect of HMT on amylose leaching has been attributed to crystallite disruption (mainly in tuber starches), increase in

crystallinity, amylose-lipid interactions, interaction between amylose-amylose and/or amylopectin-amylopectin chains, and change in polymorphic form ($B \rightarrow A+B$) (Hoover and Vasanthan, 1994a; Hoover and Manuel, 1996a, b; Shin et al., 2005, Hoover, 2010).

2.7.3.3 Gelatinization

HMT has been shown to influence onset temperature (T_o), peak temperature (T_p), conclusion temperature (T_c), and gelatinization enthalpy (ΔH) of starch. Studies have shown that HMT increases the gelatinization temperatures, and broadens the temperature range (T_c-T_o) (Sair, 1967; Kulp and Lorenz, 1981; Donovan et al., 1983; Radosta et al., 1992; Stute, 1992; Hoover et al., 1993, 1994; Hoover and Vasanthan, 1994a; Eerlingen et al., 1996; Hoover and Manuel, 1996; Chung et al., 2009; Watcharatewinkul et al., 2009) or remains unchanged (Eerlingen et al., 1996; Hoover and Manuel, 1996) after HMT. Increase in gelatinization temperatures on HMT have been attributed to the newly formed starch chain interactions (amylose-amylose, amylose-amylopectin and/or amylose-lipid), which would suppress the mobility of starch chains in the amorphous regions. Consequently, the amorphous regions would require a higher thermal energy to incur swelling that could contribute to the disruption of the crystalline regions (Kulp and Lorenz, 1981; Hoover et al., 1993; Hoover and Vasanthan, 1994a; Hoover and Manuel, 1996a,b; Eerlingen et al., 1996; Gunaratne and Hoover, 2002; Hoover, 2010). The extent of starch chain interactions has been shown to be mainly influenced by starch source, amylose chain length, and the moisture content and temperature during heat-moisture treatment (Hoover and Vasanthan, 1994a).

However, the enthalpy of gelatinization (ΔH) has been shown to either decrease (Kulp and Lorenz, 1981; Donovan et al., 1983; Radosta et al., 1992; Hoover and Vasanthan, 1994a; Eerlingen et al., 1996; Kweon et al., 2000; Adebowale et al., 2005; Pukkahut and Varavinit, 2007; Pukkahuta et al., 2008; Chung et al., 2009) or remain unchanged (Hoover and Vasanthan, 1994a; Eerlingen et al., 1996; Collado and Corke, 1999) on HMT. Recently, Pucha-arnon and Uttapap (2013) observed an increase in the gelatinization enthalpy after HMT of rice starch. In some studies researchers have observed a biphasic endotherm (in excess water) during HMT of wheat, potato and rye starches (Donovan et al., 1983; Radosta et al., 1992; Pucha-arnon and Uttapap, 2013). The decrease in ΔH due to HMT has been suggested as a result of the disruption of double helices present in the crystalline and non-crystalline regions of the granules (Gunaratne and Hoover, 2002). Horndok and Noomhorm (2007) argued that the reduction in ΔH after hydrothermal treatment may be due to the partial gelatinization of amylose and amylopectin molecules that are less stable during heating. Studies have shown that the decrease in ΔH on HMT was more pronounced in tuber starches than in cereal starches due to the greater susceptibility of double helices for disruption in tuber starches. This was attributed to: 1) difference in the packing arrangement of double helices [in B-type starches helical packing is less compact than in A-type starches], and higher phosphate monoester content in tuber starches (Hizukuri, Tabata and Nikuni, 1970; Wu and Sarko, 1978a,b; Gunaratne and Hoover, 2002). The higher water content, less compact arrangement of starch chains and higher phosphate content in B-type starches would facilitate greater chain flexibility during HMT resulting in crystalline disruption which is manifested by a decrease in ΔH (Hoover, 2010). However, studies on

amylomaize starch (Hylon V) (B-type) showed that ΔH remains same before and after HMT (Hoover and Manuel, 1996a, b). This suggests that the disruptive effect of HMT on amylopectin double helices is mainly influenced by phosphate monoester content [Hylon V (110 ppm), potato (840 ppm) (Takeda et al., 1993)] rather than by the unit cell structure (Hoover, 2010).

2.7.3.4 Pasting

Several studies have shown that HMT increases thermal stability of starch paste (Kulp and Lorenz, 1981; Stute, 1992; Hoover and Vasanthan, 1994a). HMT has been shown to increase pasting temperature, decrease peak viscosity, increase thermal stability, and increase or decrease set-back of potato (Kulp and Lorenz, 1981; Stute, 1992; Hoover and Vasanthan, 1994a; Svegmak et al., 2002; Purwani et al., 2006; Gunaratne and Corke, 2007; Varatharajan et al., 2010), cassava (Lorenz and Kulp, 1981; Abraham, 1993), yam (Hoover and Vasanthan, 1994a; Moorthy, 1999; Lawal, 2005), sweet potato (Collado and Corke, 1999; Singh et al., 2005), lentil (Hoover and Vasanthan, 1994a), mucuna bean (Adebowale and Lawal, 2003), pigeon pea (Hoover et al., 1993), wheat (Lorenz and Kulp, 1983; Kulp and Lorenz, 1981; Hoover and Vasanthan, 1994a), amaranth (Gunaratne and Corke, 2007), rice (Anderson and Guraya, 2006; Horndok and Noomhorm, 2007; Shih et al., 2007; Zavareze et al., 2010; Pancha-arnon and Uttapap, 2013), sorghum (Olayinka et al., 2008), maize (Schierbaum and Kettlitz, 1994; Franco et al., 1995; Hoover and Manuel, 1996b; Loisel et al., 2006) and oat (Hoover and Vasanthan, 1994a) starches. The extent of these changes have been shown to be

influenced by starch source, HMT condition and the instrument (RVA, BVA) used for determination of pasting properties (Hoover, 2010). Hoover and Vasanthan (1994a) reported that the above changes in pasting properties on HMT is due to decreased granular swelling and amylose leaching, increased interaction between starch chains and to an increase in granule rigidity.

2.7.3.5 Acid hydrolysis

Susceptibility of HMT starches towards acid hydrolysis has been shown to vary widely among starch sources. HMT was shown to decrease acid hydrolysis in wheat (Hoover and Vasanthan, 1994a), maize (Hoover and Manuel, 1996b), pea (Hoover et al., 1993), potato (Hoover and Vasanthan, 1994a; Varatharajan et al., 2010), oat, and yam (Hoover and Vasanthan, 1994a) starches, and to increase hydrolysis in cassava and taro starches (Gunaratne and Hoover, 2002 and Hoover and Vasanthan, 1994). Hoover and Manuel (1996a) showed that pulse starches (field pea, wrinkled pea, lentil pinto bean, black bean) were hydrolyzed to a greater extent (11 to 17%) than their native counterparts with HMT. Gunaratne and Hoover (2002) postulated that the changes in acid hydrolysis with HMT may be due to the interplay of structural changes that occur during HMT including amylose-amylose, and/or amylose-amylopectin interactions, crystallite disruption, crystallite reorientation, changes in polymorphic composition, formation of new crystallites and development of cracks on the granule surface.

2.7.3.6 Enzyme hydrolysis

Susceptibility of starches towards α -amylase on HMT has been shown to be influenced by starch botanical origin and HMT condition (moisture content, temperature and duration of heating) (Hoover, 2010). HMT has been shown to increase susceptibility towards porcine pancreatic α -amylase (PPA) in pulse starches (field pea, wrinkle pea, pigeon pea, black bean, lentil) (Hoover and Manuel, 1996a), and in tuber and root starches (potato, taro, new cocoyam, cassava, yam) (Kawabata et al., 1994; Hoover and Vasanthan, 1994a; Perera and Hoover, 1998; Gunaratne and Hoover, 2002). Lorenz and Kulp (1983) have shown that HMT (100°C, 16 h) at 18% and 27% moisture content increased potato starch digestibility (after 24 h) by 0.05 and 0.3%, respectively. In cereal starches, the digestibility of normal and waxy maize starches by a mixture of PPA and amyloglucosidase was shown to decrease with HMT (100°C, 16 h) at 18% moisture content but increase with HMT at 27% moisture (100°C, 16 h) (Franco et al., 1995). Thus, digestibility has been shown to be influenced by moisture content prevailing during HMT. Kweon et al. (2000) also showed that the extent of hydrolysis of HMT (100°C, 16 h) Hylon V (57% amylose) and Hylon VII (71% amylose) maize starches at 100°C by heat-stable α -amylase progressively decreased with increasing moisture levels (15 to 27%). However, starch digestibility increased with HMT (110°C, 16 h) at moisture contents in the range 24–27% in normal and Hylon V starches, and at 27% moisture in waxy and Hylon VII starches. A similar trend has been shown by Zavareze et al. (2010) on HMT (110°C, 1h, at 15, 20, and 25% moisture content) of high, medium and low amylose rice starches hydrolyzed by bacterial α -amylase. All of the above studies

suggested that rearrangement of starch molecules strengthens the bonds within the granules, while HMT at a moisture level of 27% led to the disruption and subsequent rearrangement of bonds within the granules, causing starch degradation and thus increasing the number of regions accessible to enzymatic hydrolysis (Zavareze and Dias, 2011). Thus, HMT on PPA hydrolysis is influenced by starch moisture content, and by structural (crystallite disruption, change in polymorphic form, crystallite reorientation, amylose-lipid interaction, starch chain interaction), and morphological (formation of fissures and cracks on the granule surface) changes with HMT (Hoover, 2010).

2.7.3.7 Nutritional fractions

There are very few studies on the impact of HMT on starch nutritional fractions such as RDS, SDS, RS and GI. Some researchers have used HMT to modify the amount of RDS, SDS, and RS in various native starches (Brumovsky and Thompson, 2001; Shin et al., 2005; Sang and Seib, 2006). A comparison of the effect of HMT (30% moisture at 100–140°C, 80 min) on RS formation in normal and high amylose (ae-VII) maize starches has shown that HMT of ae-VII maize starch increases the amount of boiling-stable RS (43.9%) compared to native counterparts (18.4%) (Brumovsky and Thompson, 2001; Jacobasch et al., 2006). Brumovsky and Thompson (2001) also showed that partial acid hydrolysis (78 h) followed by HMT at 120°C, increased the yield (~63.2%) of boiling-stable granular RS. The authors suggested that preferential attack of the amorphous portions of the granule by acid would provide potential freedom for chain ends to form

double helices, and for double helices to associate. Consequently, the HMT would then allow the potential mobility of the chains to be realized and form highly ordered structures that hinder the action of α -amylase (Hoover, 2012).

Niba (2003) investigated the effect of HMT on digestibility of maize, potato, cocoyam, yam, plantain, and rice flours and reported that the SDS content for all flours were increased compared to the native flours. Shin et al. (2005) investigated the formation and structural characteristics of RDS, SDS and RS in sweet potato starch under various hydrothermal treatments (40, 55 and 100°C at 20, 50, and 90% moisture for 12 h) and reported that depending on the temperature and the moisture content of the hydrothermal treatment, the SDS content could be doubled compared to the native starch. The above authors (Shin et al., 2005) attributed changes in the extent and rate of enzymatic hydrolysis with HMT to structural alteration within the amorphous and crystalline regions. Chung et al. (2009b) observed that HMT of corn, pea and lentil starches at 120°C (30% moisture), decreased RDS levels and increased SDS and RS levels. The increase was attributed to the interactions formed during hydrothermal treatments, which may have partly restricted the accessibility of starch chains towards the hydrolyzing enzymes.

2.7.4 Applications of HMT starch

HMT starches are used in infant foods, processing of potato starch to replace corn starch in times of shortage, production of starches with increased freeze–thaw stability, and to improve the baking quality of potato starch (Collado and Corke, 1999). Jayakody and Hoover (2008) reported that HMT starches could be utilized in canned food and frozen food industries due to increased thermal stability and decreased rate of retrogradation on HMT. HMT starches are widely used in noodle manufacture due to the decreased swelling power and amylose leaching and the elevation in heat and shear stability (Horndok and Noomhorm, 2007). Horndok and Noomhorm (2007) investigated the quality of noodles by substituting HMT rice flour and showed an improvement in the texture (adhesiveness, chewiness, and tensile strength) of the noodles. Purwani et al. (2006) investigated the noodles prepared from HMT (25% moisture, 110°C, 16 h) sago starch and observed higher firmness and elasticity, and lower stickiness compared to those prepared from native starch. They also reported less cooking loss, increased cooking time, and lower rehydration weight.

Several researchers have investigated the bread making potential of HMT starches. Lorenz and Kulp (1981) evaluated the bread and cake baking potential and the thickening power of wheat and potato starches subjected to HMT at varying moisture contents (18–27% moisture, 100°C, 16 h) and reported that the bread baking quality and bread volume of wheat starch decreased with HMT. In contrast, baking potential, grain texture, and bread volume of potato starch increased with HMT. Decrease in bread and cake making

potential of wheat starch on HMT was attributed to starch damage, while the improvement in the baking and cake making potential of potato starch on HMT was attributed to changes in swelling power, solubility and paste stability on HMT (Lorenz and Kulp, 1981). Furthermore, Miyazaki and Morita (2005) have shown that replacement of wheat flour with HMT corn starch improved bread quality. HMT starches could be used as an alternative to chemical modification in retort foods, dressings, batter products, fillings and confections (Hoover et al., 2010; Zavareze and Dias, 2011).

Chapter 3

Materials and Methods

3.1 Materials

Faba bean (*Vicia faba*) cultivars (CDC Fatima, FB 9-4, F 18-20, SSNS-1) and Black bean (*Phaseolus vulgaris*) cultivars (BYT 03 Espresso, BRT CDC Jet, BRT 1519-10, BYT 01 1681a-b) were obtained from the Crop Development Centre, University of Saskatchewan, Canada. Pinto bean (*Phaseolus vulgaris*) cultivars (AC Pintoba, AC Ole, Pecos, HR 119) were obtained from the Greenhouse and Processing Crops Research Center, Agriculture and Agri-Food, Canada. Porcine pancreatic α -amylase (EC 3.2.1.1, type 1A) and pancreatin from porcine pancreas (cat. no. P-1625, activity 3 \times USP/g) was purchased from Sigma Chemical (St. Louis, MO). Amyloglucosidase (EC 3.2.1.3., 3,300 U/mL), isoamylase from *pseudomonas* sp and glucose oxidase-peroxidase assay kit (cat. no. K-GLUC) were purchased from Megazyme International Ireland Ltd. (Bray, Ireland). APTS (8-aminopyrene-1, 3, 6-trisulfonic acid, trisodium salt), sodium cyanoborohydride was purchased from Molecular Probes, Eugene, OR. All chemicals and solvents were of ACS certified grade.

3.2 Methods

3.2.1 Starch isolation

Three lots of faba bean, black bean and pinto bean seeds were taken, representing whole samples from the experimental plots of each cultivar. Each lot was further subdivided into three parts and starch was extracted by the procedure of Hoover and Sosulski (1985) with some modifications. 50 g of beans were steeped in 250 mL of deionized water containing 0.01% (w/v) sodium metabisulfite for 36 h at 40°C. The swollen seeds were dehulled by pressing the endosperm out of the soften hull and thoroughly rinsed with water. The softened seeds were wet milled (1:3) with sufficient water using waring commercial blender (Dynamics corporation of America, USA) for 3 min and screened through cheese cloth. This step was repeated three times and pooled the filtrates. The filtrate was passed through 210 µm polypropylene sieve followed by 70 µm nylon sieve and allowed to sediment at room temperature for 18 h. The supernatant was decanted and the sediment was suspended in excess 0.2% sodium hydroxide solution at room temperature. This step was repeated several times until a white starch was obtained. The resulting starch was washed with deionized water, passed through 70 µm nylon sieve, neutralized to pH 7.0 with 0.2% hydrochloric acid, filtered on a Buchner funnel using Whatman No. 4 filter paper and thoroughly washed on the filter with distilled water. The filter cake was oven dried overnight at 40°C. The dried starch cake was ground and passed through a 60-mesh screen.

3.2.2 Heat moisture treatment

Starch samples were equilibrated at room temperature in a desiccator using a saturated salt solution of K_2SO_4 (water activity 0.97) for up to two months. Following equilibration, the moisture content (~23%) of the samples was determined by the standard AACC (2000) method (Section 3.2.4.1). The starch samples were sealed and then heated at 80°, 100° and 120°C for 12 h in a forced air oven (Fisher scientific, model Fisher Isotemp® 615G, Pittsburgh, PA, USA). The HMT starches were subsequently air dried to uniform moisture content (~10%).

3.2.3 Starch damage

Starch damage was determined by enzyme digestion procedure according to the AACC (2000) method. The starch sample (1 g, db) was weighed into a 125 mL Erlenmeyer flask and 50 mg fungal amylase from *Aspergillus oryzae* (157 units/mg protein) was added. Acetate buffer (45 mL) was brought down to 30°C in a water bath and added into the Erlenmeyer flask. The contents were mixed using glass rod to obtain a uniform suspension before incubating into the water bath at 30°C. At the end of 15 min of incubation the enzyme action was terminated by the addition of 3 mL H_2SO_4 and 2 mL sodium tungstate solution. Contents were mixed thoroughly and allowed to stand for 2 min. Solution was filtered through Whatman No 4 filter paper and first 8-10 drops of filtrate were discarded. Reducing sugar determination was conducted according to the

procedure described in Bruner's method (1964) (section 3.2.6.6.1). Reagent blank also was prepared by the same procedure, omitting only flour sample.

3.2.4 Chemical composition

3.2.4.1 Moisture content

The moisture content of the starch samples were quantitatively analyzed according to the AACC (2000) method. Empty moisture pans and lids were dried in an oven for 1 h at 130°C, and cooled in a desiccator before the analysis. 5 g of starch samples were weighed into the pre-weighed moisture pans and dried in an air forced oven (Fisher scientific, model Fisher Isotemp® 615G, Pittsburgh, PA, USA) at 130°C for 1 h. Moisture pans were placed in oven without covering and the lids were placed under the pans. The samples were then removed and covered rapidly with lids and transferred to a desiccator. Samples were weighed after they reached room temperature. Three replicates were used in each determination and the moisture content was determined as the percentage weight loss of sample using following equation,

$$\text{Moisture (\%)} = \frac{W_1 - W_2}{W_1 - W_0} \times 100$$

Where,

W_0 - Weight of the moisture pan and lid (g)

W_1 - Weight of sample, moisture pan and lid before drying (g)

W_2 - Weight of sample, moisture pan and lid after drying (g)

3.2.4.2 Ash content

The ash content of native starches was determined according to AACC (2000) method. Pre-weighed (5 g) samples were transferred into clean, dry porcelain crucibles, charred using a flame and then placed in a pre-heated (550°C) muffle furnace (Lab Heat, Blue Island, IL, USA) and left overnight until a grey ash was obtained. The samples were then cooled to room temperature in a desiccator and weighed. The ash content was calculated as percentage weight of the remaining material using following formula,

$$Ash (\%) = \frac{W_2 - W_1}{W_1 - W_0} \times 100$$

Where,

W_0 - Weight of empty crucible and lid (g)

W_1 - Weight of sample, crucible and lid (g)

W_2 - Weight of ash, crucible and lid (g)

3.2.4.3 Nitrogen content

The nitrogen content of native starches was determined by the Micro Kjeldahl method (AACC, 2000). The samples (0.3 g, db) were weighed on nitrogen-free papers and placed in the digestion tubes of Büchi 430 (Büchi Laboratoriums-Technik AG, Flawill/Schweiz) digester. The catalyst (2 Kjeltabs M pellets [Fisher Scientific, Fair Lawn, NJ, USA]) and 20 mL of concentrated H₂SO₄ acid were added and the samples were digested until a

clear yellow solution was obtained. The digested samples were then cooled, diluted with 50 mL of distilled water, 100 mL of 40% (w/w) NaOH were added, and the released ammonia was steam distilled into 50 mL of 4% H₃BO₃ containing 12 drops of end point indicator (N-point indicator, Sigma Chemical Co., St. Louis, MO, USA) using a Büchi 321 distillation unit until 150 mL of distillate was collected. The amount of ammonia in the distillate was determined by titrating it against 0.05 N H₂SO₄. The nitrogen content was determined using following equation,

$$\text{Nitrogen (\%)} = \frac{(V_1 - V_2) \times N \times 14.0067}{w} \times 100$$

Where;

V₁ - Volume (mL) of H₂SO₄ to titrate sample

V₂- Volume (mL) of H₂SO₄ to titrate blank

N - Normality of H₂SO₄

W- Sample weight (g/db)

3.2.4.4 Phosphorus content

The phosphorus content of native starches was determined according to the procedure described by Morrison (1964). Starch (5 mg, db) was placed in a hard glass test tube (15-20 mL capacity) accurately calibrated at the 5 mL level. Concentrated sulphuric acid (0.3 mL, 98%) was added and the contents were gently heated over a small micro burner

flame until charring was completed, and the climbing film of acid on the walls of the tubes was no longer viscous with partially charred organic matter. One drop of hydrogen peroxide (30%, w/v) was then added to hit the walls of the tubes, just above the acid and the tubes were well shaken. Clarity of the acid was checked and the process was repeated using one drop of peroxide at a time till a clear solution is obtained. When clear, the tubes were gently boiled for 1 min, and allowed to cool. The contents were diluted to about 4 mL with deionized water and the walls of the tubes were washed. Sulphite ($\text{Na}_2\text{SO}_3 \cdot 7\text{H}_2\text{O}$, 33% w/v) solution (0.1 mL) was then added and the tubes shaken to acidify the lower walls of the tube. Molybdate [$(\text{NH}_4)_6\text{Mo}_7\text{O}_{24} \cdot 4\text{H}_2\text{O}$, 2%, w/v] solution (1 mL) was added directly into the acid, (taking care not to touch the walls of the tube) followed by the addition of ascorbic acid (0.001 g). The tubes were then heated at 100°C for 10 min and cooled. The final volume of the solution was adjusted to 5 mL, the tube stoppered, shaken and the absorbance at 822 nm measured against water. Absorbance of the blank reading was taken at 822 nm for corrections. A standard curve (Appendix I) was developed using standard phosphorus solution (1.0068 g $\text{NaH}_2\text{PO}_4 \cdot 2\text{H}_2\text{O}$ /litre contains 200 $\mu\text{g}/\text{mL}$) to calculate the phosphorus content of the samples.

3.2.4.5 Apparent amylose content

Amylose content was determined by high performance size exclusion chromatography (HPSEC) and by a colorimetric method.

3.2.4.5.1 High performance size exclusion chromatography (HPSEC)

Apparent amylose content was determined using high performance size exclusion chromatography (HPSEC) (Demeke et al., 1999). Starch (5 mg) was suspended in distilled water (5 mL) in a glass tube and incubated at 130°C for 30 min. To 1 mL of vortex mixed starch solution, 55 µL of 1 M sodium acetate (pH 4) was added. The solution was vigorously mixed and 4 units of isoamylase (200 units/ml of stock solution) were added to debranch the starch. After 4 h of incubation at 40°C, the reaction mixture was boiled for 20 min to inactivate the enzyme, and the starch solution was freeze-dried. The freeze-dried sample was dissolved in 200 µL of 99% dimethyl sulfoxide (DMSO) and centrifuged in a microfuge at 15,000 × g for 10 min. A 40 µL of the supernatant was injected into a PLgel 5 µM MiniMix-C guard column attached to a PLgel Minimix 4.6 mm i.d. column (Polymer Laboratories, Inc., Amherst, MA, USA) to separate amylose and amylopectin using a high-performance liquid chromatography (HPLC) system comprising a Waters 600 controller, Waters 610 fluid unit, Waters 717 Plus auto sampler and Waters 410 differential refractometer (Waters Corporation, Milford, MA, USA). The data were collected and analyzed using Empower software (Waters Corporation). Starch samples, column, and detector were maintained at 40, 100 and 45°C respectively. DMSO (99%) was used as an eluent at a flow rate of 0.2 mL/min. The amylose content was

calculated by integration of the peak area corresponding to both amylose and amylopectin.

3.2.4.5.2 Colorimetry

Amylose content (section 3.2.5.1) of starches was also determined by the colorimetric method of Hoover and Ratnayake (2004). Starch (20 mg/db) was weighed into a round bottom screw cap tube and solubilized by adding dimethylsulfoxide (90% DMSO, 8 mL). The contents were vigorously vortexed for 2 min and heated for 15 min in a water bath at 85°C with intermittent mixing. The tubes were then allowed to cool to room temperature and diluted to 25 mL in volumetric flask. 1 mL of the diluted solution was mixed with water (40 mL) and I₂/KI solution (5 mL, [0.0025 M I₂ and 0.0065 M KI mixture]) and vortexed. The final volume was adjusted to 50 mL in a volumetric flask and the contents were allowed to stand in the dark for 15 min at room temperature. The absorbance measurements were taken at 600 nm using a UV-visible spectrophotometer and the amylose content of the tested samples was calculated from the standard curve obtained with the pure amylose and amylopectin mixtures, over the range 0 to 100% (Appendix II).

3.2.4.6 Lipid content

3.2.4.6.1 Surface lipid

Surface lipids of the native starch samples were determined according to the procedure described by Vasanthan and Hoover (1992). The surface lipids were extracted at ambient temperature (25-27°C) by mixing a starch sample (5 g, db) with 100 mL of

chloroform/methanol (2:1, v/v). The contents were mixed thoroughly for 1 h and the solution was filtered carefully using Whatman No 4 filter paper into a 250 mL round bottom flask. The residue was thoroughly washed out with chloroform/methanol solution. The lipid solvent mixture was evaporated to dryness using a rotary evaporator (Rotovapor-R110, Büchi Laboratorimus-Technik AG, Flawill/Schweiz, Switzerland). The crude lipid extracts were purified by the method of Bligh and Dyer (1959) before quantification (section 3.2.4.6.3).

3.2.4.6.2 Bound lipid

Bound lipid content of starch samples was determined according to the method of Vasanthan and Hoover (1992b). The residues from the chloroform/methanol extractions were refluxed with n-propanol water (3:1, v/v) in a Soxhlet apparatus at 85°C for 7 h. The solvent was evaporated to dryness using a rotary evaporator and the crude lipid residue was purified by the method of Bligh and Dyer (1959) before quantification (section 3.2.4.6.3).

3.2.4.6.3 Crude lipid purification

The crude lipid extracts were purified according to the method of Bligh and Dyer (1959) using a separatory funnel with chloroform /methanol/water. The round bottom flask with crude lipid extract was washed by with a chloroform/methanol/water mixture in the ratio of 1:2:0.8 (v/v/v) respectively. After mixing the contents were transferred to separatory

funnel and chloroform and water were added further to form the biphasic layer. The heavy chloroform layer in the bottom of the separatory funnel which contained the purified lipid was withdrawn into the pre-weighted round bottom flask and evaporated to dryness in the rotary evaporator. The round bottom flask with purified lipid was then removed and dried at 60°C in an air forced oven. The dried lipids were cooled to room temperature in a desiccator and weighed. Lipid content was calculated using following formula,

$$\text{Lipid (\%)} = \frac{W_2 - W_1}{W_0} \times 100$$

Where;

W_0 - Sample weight (g/db)

W_1 - Weight of round bottom flask (g)

W_2 - Weight of round bottom flask and lipid after drying (g)

3.2.5 Granule morphology and particle size distribution

3.2.5.1 Starch granule size distribution

Starch granule size distribution was determined by a Malvern Mastersizer-2000 laser-diffraction analyzer (Malvern Instruments Ltd, Malvern, UK). Refractive indices of 1.31 for water and 1.52 for starch were used as standard. Starch (40 mg) was suspended in 1 mL water and dispersed (1,700 rpm) in a sample holder attached to the instrument. Each

sample (volume %) was analyzed three times. Laser obscuration was maintained between 12-14% during sample addition as recommended by the manufacturers.

3.2.5.2 Polarized light microscopy

Starch suspensions (water-glycerol 50:50, v/v) were observed under bright field light and crossed polarized light (magnification 200×) using a binocular microscope (Nikon Microscope, Eclipse 80i, Nikon INC, Melville, NY, USA) equipped with real time viewing (Q-capture Pro™, Surrey, BC, Canada). A QImaging digital camera (QICAM fast 1394, Surrey, BC, Canada) was used for image capture.

3.2.5.3 Scanning electron microscopy

Granule morphologies of pulse starches were analyzed using a Hitachi (S570, Nissei Sangyo Inc., Rexdale, ON, Canada) scanning electron microscope at an accelerating potential of 10 kV. Dry starch samples were brushed onto the surface of double-sided carbon adhesive tape mounted on an aluminum stub and then coated with a thin film (20 nm) of gold in an argon atmosphere.

3.2.5.4 Confocal laser scanning microscopy

Distribution of AM and AP were visualized by staining with APTS according to the method described by Blennow et al. (2003). Starch samples (10-15 mg) were stained in 10 µL of freshly made APTS solution (20 mM APTS in 15% acetic acid) and 10 µL of

1M sodium cyanoborohydride at 30°C for 15 h (Appendix III). After thoroughly washing five times with deionized water, the stained starch granules were then suspended in 0.5 mL of 50% glycerol and then visualized by a confocal laser scanning microscope (NIKON microscope, ECLIPSE 80i, Nikon INC, Melville, NY, USA) equipped with a 40x/1.3 oil objective lens. The excitation wavelength achieved with a diode laser was 488 nm. Laser power capacity and master gain were adjusted to maximum saturation. Images of starch granules were recorded with EZ-C1 3.8 software (Nikon Corporation, Nikon INC, Melville, NY, USA). For each starch sample, a population of granules was examined with 15-20 images and about 10-15 granules in each image.

3.2.6 Starch structure

3.2.6.1 Determination of amylopectin chain length distribution by high-performance anion-exchange chromatography with pulsed amperometric detection (HPAEC-PAD)

Isoamylase debranching of whole starch accompanied by high performance anion exchange chromatography with pulsed amperometric detection (HPAEC-PAD) was used to determine the amylopectin branch chain length distribution of the starches (Liu et al., 2007). Starch was dispersed in 2 mL of 90% DMSO (5 mg/mL) by stirring in a boiling water bath for 20 min. After cooling, 6 mL of methanol was added with vortexing, and the tube was placed in an ice bath for 30 min. The pellet, which was recovered by centrifugation (1000 ×g for 12 min), was dispersed in 2 mL of 50 mM sodium acetate buffer (pH 3.5) by stirring in a boiling water bath for 20 min. Following equilibration of

the tube at 37°C, isoamylase (5 µL) was added (EN102, 68,000 U/mg protein, Hayashibara Biochemicals Laboratories Inc., Okayama, Japan). The sample was incubated at 37°C with slow stirring for 22 h. The enzyme was inactivated by boiling for 10 min. An aliquot (200 µL) of the cooled debranched sample was diluted with 2 mL of 150 mM NaOH. The sample was filtered in a 0.45 µm nylon syringe filter and injected into the HPAEC-PAD system using 50 µL loop. The HPAEC-PAD system consisted of a Dionex DX 600 equipped with an ED50 electrochemical detector with a gold working electrode, GP50 gradient pump, LC30 chromatography oven and AS40 automated sampler (Dionex Corporation, Sunnyvale, CA). The standard triple potential waveform was employed, with the following periods and pulse potentials: T1= 0.40 s, with 0.20 s sampling time, E1 = 0.05 V; T2 = 0.20 s, E2 = 0.75 V; T3 = 0.40 s, E3 = -0.15 V. Data were collected using Chromeleon software, version 6.50 (Dionex corporation, Sunnyvale, CA). The weight fraction of DP 6-12, 13-24, 25-36 and 37-58 was measured based on the area of peaks. The average chain length was also calculated. Eluents were prepared in distilled deionized water with helium sparging; eluent A was 500 mM sodium acetate in 150 mM NaOH, and eluent B was 150 mM NaOH. Linear components were separated on a Dionex CarboPac™ PA1 column (4-mm i.d.× 25 cm) with gradient elution (0 min, 40% eluent A; 5 min, 60% eluent A; 45 min, 80% eluent A) at a column temperature of 26°C and a flow rate of 1 mL/min. A CarboPac™ PA1 guard column (4-mm i.d.× 5 cm) was installed in front of the analytical column.

3.2.6.2 Determination of short range molecular order by attenuated total reflectance fourier transform infrared spectroscopy (ATR-FTIR)

ATR-FTIR spectra were recorded on a Digilab FTS 7000 spectrometer (Digilab USA, Randolph, MA, USA) equipped with a thermoelectrically cooled deuterated triglycine sulphate (DIGS) detector using an attenuated total reflectance (ATR) accessory at a resolution of 4 cm^{-1} by 128 scans. Starch samples were placed on the crystal in the sample compartment, which had a hinged cover to seal it from the environment. A spectrum of the empty cell was used as the background. Spectra were base line-corrected and then deconvoluted by drawing a straight line between 1200 and 800 cm^{-1} using Win-IR Pro software (Bio-Rad, Mississauga, ON, Canada). A half-band width of 15 cm^{-1} and a resolution enhancement factor of 1.5 with Bessel apodization were employed. Intensity measurements were performed on the deconvoluted spectra by recording the peak heights of the absorbance bands from the base line.

3.2.6.3 Wide angle X-ray diffraction (WAXS)

3.2.5.6.1 X-ray pattern and relative crystallinity

WAXS were obtained with a Rigaku Ultima IV X-ray diffractometer (Rigaku Americas, TX, USA) with operating conditions of target voltage 40 kV; current 44 mA; scanning range $3\text{--}35^\circ$; scan speed $1.00^\circ/\text{min}$; step time 0.95; divergence slit width 0.5° ; scatter slit width 0.5° ; sampling width 0.03° and receiving slit width 0.3 mm. Relative crystallinity of the starches was quantitatively estimated following the method of Lopez-Rubio et al. (2008) using a software package IGOR pro 6.1 software (Wave Metrics Inc. OR, USA).

A Gaussian function was used for curve fitting (Appendix IV). The moisture content of all starch samples for X-ray diffraction was adjusted to ~23% by being kept in a desiccator over saturated K₂SO₄ solution (25 °C, $a_w = 0.98$) for 14 days.

3.2.5.6.2 Determination of 'A' and 'B' polymorphic composition by X-ray diffraction

The proportion of 'A' and 'B' polymorphic compositions of the starches were calculated using the method outlined by Zhou, Hoover and Liu (2004). The 'B' polymorph content was calculated by determining the ratio of the area under the diffraction peak at 5.6° 2 θ to the total crystalline area (as described in 2.3.3.1) together with a calibration curve (Appendix V) derived from mixtures of pure 'B' type (0–100% potato starch) and pure 'A' type (100–0% waxy corn starch).

3.2.6.3 Determination of double helical content by ¹³C cross polarization magic angle spinning nuclear magnetic resonance spectroscopy (¹³C CP/MAS NMR)

¹³CCP/MAS NMR) spectroscopy was performed using a Bruker AVANCE II 600 operating at frequencies of 600.33 MHz for ¹H and 150.96 MHz for ¹³C. All experiments were carried out using a Bruker 3.2 mm MAS triple-tuned probe (H/C/N/D). The moisture content of all starch samples was adjusted to ~23% by being kept in a desiccator over saturated K₂SO₄ solution (25 °C, $a_w = 0.98$) for 14 days. The samples were spun at 20 kHz and the temperature was maintained constant at 298 K. The contact time was 2 ms for all experiments and the Hartmann-Hahn condition was set at 62.5 kHz.

1024 scans were collected with a 3 s recycling delay. ^{13}C chemical shifts were referenced to TMS with adamantane as an external secondary reference. The ^{13}C CP/MAS NMR spectra were peak fitted by using DMfit #20110512 software (Dominique Massiot). The spectra were interpreted in terms of a combination of amorphous (single chain) and the ordered double helical components. The ordered sub spectrum was obtained by subtracting the sub spectrum due to the amorphous content from the native starch spectrum (Appendix VI). The percentage of double helix content was calculated by the equation shown below (Tan et al. 2007).

$$\text{Double helix \%} = \frac{\text{Area for the C1 signals in the ordered subspectrum}}{\text{Area for the C1 signals in the native spectrum}} * 100$$

3.2.6 Starch properties

3.2.5.1 Amylose leaching (AML)

Starches (20 mg/db) in water (10 mL) were heated at 60–95°C in volume calibrated sealed tubes for 30 min (tubes were shaken by hand every 5 min to suspend the starch slurry). The tubes were then cooled to room temperature and centrifuged at 2000 × g for 10 min. The supernatant liquid (1 mL) was withdrawn and amylose content determined as described by Hoover and Ratnayake (2004) (section 3.2.3.5.1). AML was expressed as percentage of amylose leached per 100 g of dry starch. Three replicate samples were used in the determination.

3.2.6.2 Swelling factor (SF)

The SF of the starches when heated to 60–95°C in an excess of water was measured according to the method of Tester and Morrison (1990). This method measures only intragranular water and hence the true SF at a given temperature. Starch samples (50 mg, db) were weighed into screw cap tubes; 5 mL water was added and heated in a shaking water bath at appropriate temperature for 30 min. The tubes were then cooled rapidly to 20°C in an ice water bath and 0.5 mL of Blue Dextran (Pharmacia MW 2×10^6 , 5 mg/mL) was added and the contents mixed by inverting the closed tubes several times. The tubes were centrifuged at $1500 \times g$ for 10 min and the absorbance of the supernatant was measured at 620 nm. The absorbance of the reference tube that contained no starch was also measured. Three replicate samples were used in this determination. The SF is reported as the ratio of the volume of swollen starch granules to the volume of the dry starch using following equation,

Calculation of SF was based on starch weight corrected to moisture content, assuming a density of 1.4 g/mL.

Free or interstitial-plus-supernatant water (FW) is given by:

$$FW \text{ (mL)} = 5.5(A_R / A_S) - 0.5 \quad 1$$

The initial volume of the starch (V_0) of weight W (mg) is

$$V_0 \text{ (mL)} = W/1400 \quad 2$$

And the volume of absorbed intragranular water (V_1) is thus

$$V_1 = 5.0 - FW \quad 3$$

Hence the volume of the swollen starch granules (V_2) is

$$V_2 = V_0 + V_1 \quad 4$$

$$SF = V_2/V_0 \quad 5$$

This can be expressed by the single equation

$$SF = 1 + \{(7700/w) \times [(A_s - A_r)/A_s]\}$$

3.2.6.3 Differential scanning calorimetry (DSC)

Gelatinization parameters of native and HMT starches were measured using a Mettler Toledo differential scanning calorimeter (DSC1/700/630/GC200) equipped with a thermal analysis data station and data recording software (STAR@ SW 9.20). Water (11 μ L) was added with a micro syringe to starch (3.0 mg, db) in the DSC pans, which were then sealed, reweighed and allowed to stand overnight at room temperature before DSC analysis. The scanning temperature range and the heating rates were 30–110°C and 10°C/min, respectively. In all measurements, the thermogram was recorded with an empty aluminum pan as a reference. During the scans, the space surrounding the sample chamber was flushed with dry nitrogen to avoid condensation. The transition temperatures reported are the onset (T_o), peak (T_p) and conclusion (T_c). The enthalpy of

gelatinization (ΔH) was estimated by integrating the area between the thermogram and a base line under the peak and was expressed in terms of Joules per gram of dry starch.

3.2.6.4 Rapid Visco Analyzer (RVA)

A Rapid Visco Analyzer RVA-4 (Newport Scientific Pty. Ltd., Warriewood, NSW, Australia) was employed to measure the pasting properties of native and HMT starches (5% db, 25 g total weight). The samples were equilibrated at 50°C for 1 min, heated at 6°C/min at 95°C, held at 95°C for 5 min, cooled at 6°C/min at 50°C, and held at 50°C for 2 min. The speed was 960 rpm for the first 10 s, then 160 rpm for the remainder of the experiment.

3.2.6.5 α -amylase hydrolysis

α -amylase hydrolysis of starches was conducted using a crystalline suspension of porcine pancreatic α -amylase (PPA) in 2.9 M NaCl containing 3 mM CaCl₂ (Sigma Chemical Co; St. Louis, MO, USA) in which the concentration of α -amylase was 26 mg protein/mL and the specific activity was 1333 units/mg protein. The procedure was essentially that of Knutson et al. (1982) with a slight modification. Starch (20 mg) was added with 5 mL distilled water and 4 mL of 0.1 M phosphate buffer (pH 6.9), containing 0.006 M NaCl. The slurry was pre-warmed for 30 min at 37°C and gently stirred before adding PPA suspension (12 units/mg starch). The samples were analyzed after 3, 24 and 72 h of incubation at 37°C in a constant temperature water bath (New Brunswick Scientific,

G76D, Edison, NJ, USA). Samples were taken at specific time intervals and enzyme reaction was terminated by adding 2 mL of 95% ethanol. The mixture was centrifuged ($1500 \times g$, for 5 min) and aliquots of the supernatant were analyzed for soluble carbohydrate (Bruner, 1964) (section 3.2.5.6). The degree of hydrolysis was defined as the reducing sugars generated in the supernatant, expressed as mg maltose equivalents released per 100 mg dry starch.

3.2.6.6 Acid hydrolysis

Starches were hydrolyzed in triplicate with 2.2 M HCl (1 g, db, starch/40 mL) at 35°C in a water bath (New Brunswick Scientific, G76D, Edison, NJ, USA) for periods ranging from 0 to 15 days. Starch slurries were vortexed daily to re-suspend the deposited starch granules. Aliquots taken at specific time intervals were neutralized with 2.2 M NaOH and centrifuged ($2000 \times g/10$ min). The extent of hydrolysis was determined by expressing the solubilized carbohydrates (Jane and Robyt, 1984) as a percentage of the initial starch using the method of Bruner (1964).

3.2.6.6.1 Determination of reducing value

Soluble carbohydrates were determined according to the method of Bruner (1963). 2 mL of 3,5-dinitrosalicylic acid (DNS) were taken into a glass tube and placed in an ice-water bath to chill for 5 min. An aliquot of the sample (1 mL) was pipetted into 2 mL of the chilled 3, 5-DNS and the reaction mixture was then diluted to 4 mL with distilled water.

The contents were mixed by rapid swirling and returned to an ice-water bath until thoroughly chilled and then the contents were heated in a boiling water bath for exactly 5 min for color development. After that, contents were returned in an ice-water bath prior to the color measurement. After chilling, the final volume was adjusted to 8 mL with distilled water at room temperature. Contents were mixed by rapid swirling before taking the absorbance measurement at 540 nm. If the sample relative absorbance exceeds 1.5 at 540 nm, the spectrophotometer was reset to 590 nm without delay, and the relative absorbance was measured at that wave length. The apparent sugar content of the sample was determined by calculation from the appropriate regression equation of the standard curves (Appendix VII).

$$\text{Enzyme Hydrolysis (\%)} = \frac{\text{Reducing sugar (as maltose)} \times 0.95 \times 100}{\text{Initial starch weight (g/db)}}$$

3.2.6.7 *In-vitro* starch digestibility and expected glycemic index (eGI)

In-vitro starch digestibility was determined by the AACC approved method 32-40 (AACC International, 2000). Pulse starches (100 mg) were incubated with pancreatin (10 mg) and amyloglucosidase (12 U) in 4 mL of 0.1 M sodium maleate buffer (pH 6.0) at 37°C with continuous shaking (200 strokes/min) for 0.5–16 h. After incubation, 4 mL of ethanol (95%) were added to inactivate the enzyme and the sample was centrifuged at 2000 × g for 10 min. Glucose content of the supernatant was measured by a glucose oxidase-peroxidase assay (section 3.2.5.7.1) kit (Megazyme International Ireland Ltd., Bray, Ireland). Starch classification (Chung, et al., 2008) based on the rate of hydrolysis

were: rapidly digestible starch (digested within 0.5 h; RDS), slowly digestible starch (digested between 0.5 and 16 h; SDS) and resistant starch (undigested after 16 h; RS), which was starch not hydrolyzed even after 16 h. The hydrolysis index (HI) was calculated by dividing the area under the hydrolysis curve of each starch sample by the corresponding area obtained from a standard material (white bread). The eGI was calculated using the equation (Granfeldt et al., 1992) shown below:

$$\text{eGI} = 8.198 + 0.862 \text{ HI}$$

3.2.6.7.1 Determination of glucose content by Megazyme Glucose method

Glucose oxidase/oxidase (GOPD) reagent buffer [1 M, pH 7.4, *p*-hydroxybenzoic acid and sodium azide (0.4% w/v)] was diluted to 1:1 with distilled water. Then the GOPOD reagent enzyme (>12000 U) was dissolved in 20 mL of freshly prepared GOPOD buffer (this glucose determination reagent is only stable for 3 months at 2-5°C or > 12 months at -20°C). GOPOD reagent (3 mL) was added to 0.1 mL of sample solution containing glucose and incubated at 50°C for 20 min. Finally, the absorbance (ΔA) of sample was measured at 510 nm against reagent blank. Glucose content was determined using following formula,

$$\text{Glucose } (\mu\text{g}/0.1 \text{ mL}) = \frac{\Delta A \text{ sample}}{\Delta A \text{ glucose standard } (100 \mu\text{g})} \times 100$$

3.2.7 Retrogradation

3.2.7.1 Turbidity

A 2% aqueous suspension (200 mL) of starch was heated in a boiling water bath for 1 h under continuous gentle stirring, and then cooled for 20 min at 25°C. Triplicate paste samples were placed in cuvettes and turbidity was determined by measuring transmittance at 640 nm against water blank with a Milton Roy UV-visible spectrophotometer (Spectronic 601, Milton Roy Company, USA). The development of turbidity was followed by storing the remaining starch pastes for 1 day at 4°C followed by 2-25 days at 25°C.

3.2.7.2 Gel preparation

Gels were prepared by heating native starch suspensions (50% (w/v)) at 95°C in a shaking water bath for 1 h (Roulet et al. 1988). The samples were then cooled rapidly to room temperature (25°C). After cooling, the gels formed were stored at 4°C for 1 day followed by 25 days at 25°C. The procedure (with minor modifications) of Roulet et al. (1988) was used to convert freshly gelatinized and stored gels to a powder prior to examination by X-ray diffraction. The gels were rinsed with water, cut into small pieces and mixed with 100 mL acetone. After homogenization using a polytron, the mixture was left to decant for 5 min. The liquid was discarded and the rest was transferred to screw cap tubes. Acetone was again added, the mixture centrifuged (3000 ×g) and the supernatant

discarded. The procedure was repeated three times and the remaining mass was then freeze dried.

3.2.8 Statistical analysis

Statistical analysis was performed among species and among cultivars of each species. All determinations were replicated three times and mean values and standard deviations reported. Analysis of variance (one-way ANOVA) was performed and the mean separations were compared using Tukey's HSD test ($P < 0.05$) using SPSS 16.0 for Windows (SPSS Inc., Chicago, IL, USA).

Chapter 4

Results and Discussion

4.1 STRUCTURE OF FABA BEAN, BLACK BEAN AND PINTO BEAN STARCHES AT DIFFERENT LEVELS OF GRANULE ORGANIZATION AND THEIR PHYSICOCHEMICAL PROPERTIES

4.1.1 Composition

Data on the yield and composition of faba bean (FB), black bean (BB) and pinto bean (PB) starches are presented in Table 4.1. The yield (on a total seed basis) of starch from the pulse seeds ranged from 27.4 to 36.3% (FB > BB ~ PB). Apparent amylose content ranged from 25.85 to 33.62%. There was no significant difference ($P < 0.05$) in apparent amylose content among FB cultivars. However, cultivars of BB and PB exhibited significant differences ($P < 0.05$) in apparent amylose content (PB > BB). The ash content ranged from 0.03 – 0.08%. The low ash content indicates that the starches were relatively free of hydrating fine fibers, which are derived from the cell wall enclosing the starch granule. The nitrogen content (0.02 – 0.09%) was low in all starches indicating the absence of non-starch lipids (lipids associated with endosperm proteins [Morrison, 1981]). In all starches, the free lipid (obtained by extraction with chloroform-methanol 2:1 v/v at 25°C), bound lipid (obtained by extraction of the chloroform-methanol residue with 1-propanol-water 3:1 v/v for 7 h) and phosphorus (in the form of phosphate monoesters) contents ranged from 0.04 – 0.05%, 0.13 – 0.15% and 0.04 – 0.09%,

respectively. Differences in phosphate content were significant ($P < 0.05$) among cultivars of FB, BB and PB (Table 4.1) starches. The above values for nitrogen, ash, and lipids were in the range reported for other pulse starches (Hoover et al., 2010). There are no data available in the literature for the phosphorus content of other pulse starches. The purity of the starches was judged on the basis of composition (low nitrogen and ash contents) and by microscopic observation of a large number of granules which demonstrated the absence of any adhering protein (Fig. 4.1 g, h, i) on the granule surface (due to the high magnification needed to clearly visualize the granule surface only a few granules are shown in the above figures). None of the starches exhibited granule damage during isolation and purification.

Table 4.1

Chemical composition (%) of faba, black and pinto bean starches *¹

Starch source	Yield	Moisture	Ash	Nitrogen	Phosphorus	Apparent amylose content ⁴	Lipid	
							Surface lipid ²	Bound lipid ²
Faba bean								
Fatima	32.94±0.23 ^a	9.26±0.06 ^{ab}	0.03±0.02 ^a	0.05±0.02 ^a	0.007±0.00 ^a	31.86±1.84 ^a	0.05±0.03 ^a	0.13±0.01 ^a
FB 9-4	34.56±1.22 ^a	8.95±0.06 ^a	0.08±0.05 ^b	0.06±0.03 ^a	0.006±0.00 ^b	32.23±0.56 ^a	0.05±0.02 ^a	0.14±0.13 ^a
F 18-20	36.34±1.18 ^a	9.52±0.11 ^{ab}	0.10±0.01 ^b	0.04±0.01 ^a	0.005±0.00 ^c	31.38±0.55 ^a	0.04±0.00 ^a	0.13±0.01 ^a
SSNS 1	34.44±0.24 ^a	9.71±0.25 ^b	0.14±0.06 ^c	0.07±0.01 ^a	0.005±0.00 ^c	31.63±0.34 ^a	0.05±0.02 ^a	0.14±0.01 ^a
Mean	34.57±1.44^a	9.36±0.33^a	0.09±0.05^{ab}	0.06±0.02^a	0.006±0.001^a	31.78±0.92^a	0.05±0.02^a	0.13±0.01^a
Black bean								
BYT 03 Espresso	27.53±1.14 ^b	9.15±0.14 ^c	0.15±0.00 ^d	0.02±0.01 ^b	0.008±0.00 ^d	30.74±0.95 ^b	0.04±0.01 ^b	0.13±0.00 ^b
CDC Jet	28.61±0.36 ^b	8.15±0.21 ^d	0.07±0.00 ^c	0.05±0.02 ^b	0.007±0.00 ^c	32.71±0.95 ^c	0.05±0.01 ^b	0.13±0.01 ^b
BRT1519-10	29.89±0.02 ^b	11.00±0.04 ^c	0.18±0.00 ^f	0.07±0.03 ^b	0.006±0.00 ^f	33.62±0.18 ^d	0.04±0.00 ^b	0.13±0.01 ^b
BYT 01 1681a-b	29.55±0.57 ^b	11.57±0.11 ^f	0.14±0.00 ^d	0.09±0.02 ^b	0.008±0.00 ^d	31.30±0.33 ^{bc}	0.05±0.00 ^b	0.13±0.00 ^b
Mean	28.89±1.10^a	9.97±1.59^a	0.14±0.04^a	0.06±0.03^a	0.007±0.001^a	31.95±1.32^a	0.05±0.01^a	0.13±0.00^a
Pinto bean								
AC Pintoba	29.77±0.13 ^c	7.76±0.13 ^g	0.05±0.00 ^g	0.03±0.01 ^c	0.004±0.00 ^g	25.85±0.20 ^e	0.05±0.01 ^c	0.13±0.00 ^c
AC Ole	27.41±0.16 ^d	7.99±0.00 ^g	0.06±0.03 ^g	0.04±0.02 ^c	0.006±0.00 ^h	31.75±0.05 ^f	0.05±0.02 ^c	0.15±0.00 ^c
Pecos	31.16±0.37 ^c	8.63±0.43 ^{gi}	0.07±0.01 ^g	0.06±0.03 ^c	0.009±0.00 ⁱ	32.53±0.11 ^g	0.05±0.01 ^c	0.13±0.01 ^c
HR 119	30.62±0.39 ^{ce}	9.41±0.11 ^{hi}	0.05±0.00 ^g	0.02±0.00 ^c	0.005±0.00 ^j	29.72±0.50 ^h	0.05±0.00 ^c	0.14±0.00 ^c
Mean	29.74±1.55^a	8.48±0.74^a	0.06±0.02^b	0.04±0.02^a	0.006±0.002^a	29.97±2.72^a	0.05±0.01^a	0.14±0.01^a

*Statistical analysis was performed among cultivars within each starch source and also among the means for each starch source.

¹ All data reported on dry basis and represents the mean of three determinations. Values followed by different superscript in each column are significantly different ($P < 0.05$).² Lipid extracted from the starch by chloroform–methanol (CM) 2:1(v/v) at 25°C (mainly free lipids).³ Lipid extracted by hot 1-propanol–water (PW) 3:1(v/v) from the residue left over CM extraction (mainly bound lipids).⁴ Determined by high-performance size exclusion chromatography.

4.1.2. Granule characteristics

The birefringence patterns of FB, BB and PB starches are presented in Figs. 1a-c. The birefringence patterns (interference cross known as “maltese cross”) under polarized light indicates that amylopectin crystallites are arranged radially within the granule at right angles to the surface with their single reducing end group towards the hilum (Sivak and Preiss, 1998). All granules of BB (Fig. 4.1 b) and PB (Fig. 4.1 c) starches exhibited strong birefringence patterns. However, granules of FB starches exhibited both strong (Fig. 4.1 a, arrow 3) and weak (Fig. 4.1 a, arrow 4) birefringence patterns. Weaker birefringence patterns are indicative of disorganized amylopectin double helices within the crystalline lamella of these granules. Bright field microscopy (BFM) [Fig. 1d], scanning electron microscopy (SEM) [Fig 1g] and confocal laser scanning microscopy (CLSM) [Fig. 4.1 j] showed the presence of numerous cracks in granules of FB. The nature and extent of cracking varied among granules of FB. However, cracked granules were not seen in BB (Fig. 4.1 e, h, k) and PB (Fig. 4.1 f, i, l) starches. Cracks have also been reported in corn (normal, waxy, high amylose), sorghum, potato, kidney bean and mung bean starches (Hoover and Sosulski, 1985; Huber and BeMiller, 2000; van de Velde, van Riel and Tromp, 2002; Glaring, Koch and Blennow, 2006. Glaring et al. (2006) postulated based on studies on normal, high amylose and high amylopectin starches, that cracking may reflect low granule integrity (due to weak interaction between radially arranged amylopectin chains) resulting in an increase in strain as the granule grows. Blennow et al. (2003) have also postulated by studies on antisense SBE and antisense GWD potato starches, that cracks could reflect sub-optimal packing of starch

chains within the granules. CLSM image (Fig. 4.1 j) of FB starch showed that the outer regions of the granule were stained non-uniformly with APTS. Whereas, the cracked region was stain free. The hilum (crossing point of the maltese cross which generally appears as a bright fluorescence dot or as an elongated structure in starch granules stained with APTS) and the growth rings layered around the hilum were not visible in the CLSM image of FB (Fig. 4.1 j). However, the hilum and growth rings were clearly visible in granules of BB (Fig. 4.1 k) and PB (Fig. 4.1 l) starches. In both BB and PB starches, the hilum region was elongated and more intensely stained with APTS than the growth rings. Bright fluorescence near the hilum region is an indication of a high concentration of amylose (since amylose has been shown to be more heavily labelled with APTS than amylopectin [since it contains a much higher molar ratio of reducing ends per glucose residue than amylopectin (Blennow et al., 2003)]). The above authors have also shown by studies on amylopectin rich starches, that bright fluorescence in the hilum region could also reflect the presence of a higher concentration of amylopectin reducing ends. The data suggest that disorganized amylopectin crystallites in FB may have lowered granule integrity. Consequently, FB granules may have been fragile and thus prone to cracking during granule development. It is likely, that during granule development, cracking may have resulted in redistribution of amylose and/or amylopectin reducing ends to the outer regions of the granule (Fig. 4.1 j). This seems plausible due to non-uniform APTS staining in the outer regions of the granules (Fig. 4.1 d). Distribution of different size granule fractions of FB, BB and PB starches are presented in Fig. 4.2. The granule size range of 8 – 15 μm , 16 – 30 μm , 31 – 60 μm and > 60 μm followed the order: FB ~ BB >

PB, FB ~ PB > BB, BB ~ PB > FB, respectively. Granule size > 60 μm were present only in two cultivars of BB (Fig. 4.2). SEM images showed that the shape of all three starches varied from oval to round to irregular (Figs. 4.1 g, h, i).

Figure 4.1 a, b and c represent polarized light microscopy ($\times 200$) of faba bean (Fatima), black bean (BYT 03 Espresso) and pinto bean (AC Pintoba) starches, respectively. Arrows 1 (weak birefringence pattern) and 2 (strong birefringence pattern) indicates maltese cross pattern of faba bean (Fig. 1a). Arrow 3 represents the well-defined maltese cross pattern in black bean (Fig. 4.1 b) and pinto bean (Fig. 4.1 c) starches.

d, e and f represent bright field microscopy ($\times 200$) of faba bean (Fatima), black bean (BYT 03 Espresso) and pinto bean (AC Pintoba) starches, respectively. Arrow 4 (Fig. 4.1 d) indicates different types of cracked granules in faba bean starch.

g, h and i represent the scanning electron microscopy ($\times 5400$) of faba bean (Fatima), black bean (BYT 03 Espresso) and pinto bean (AC Pintoba) starches, respectively (due to the high magnification needed to clearly visualize the granule surface only a few granules are shown in the above figures). Arrow 4 (Fig. 4.1 g) indicates cracked region on the granule surface of faba bean (scale bars: $5 \mu\text{m}$).

j, k and l represent confocal laser scanning microscopy ($\times 600$ oil) of APTS stained faba bean (Fatima), black bean (BYT 03 Espresso) and pinto bean (AC Pintoba) starches, respectively. Arrow 4 (Fig. 4.1 g) points to the dark central cracked region of faba bean granule and arrows 5 and 6 indicate that the region surrounding the dark region are stained differently with APTS. Arrows 7 and 8 indicate the elongated hilum region and the growth rings in black bean (Fig. 4.1 k) and pinto bean (Fig. 4.1 l) starches, respectively (scale bars: $0.5 \mu\text{m}$).

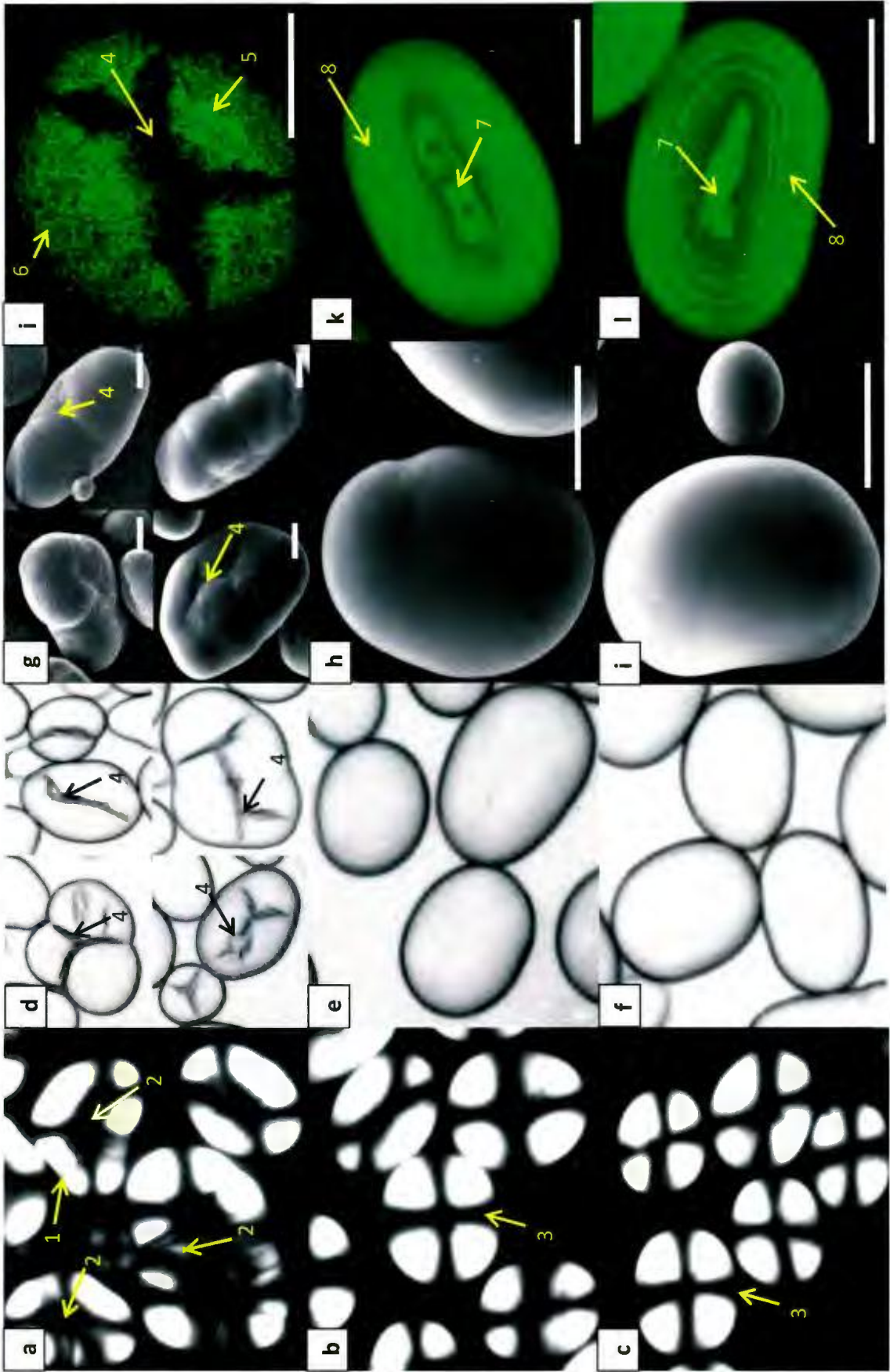
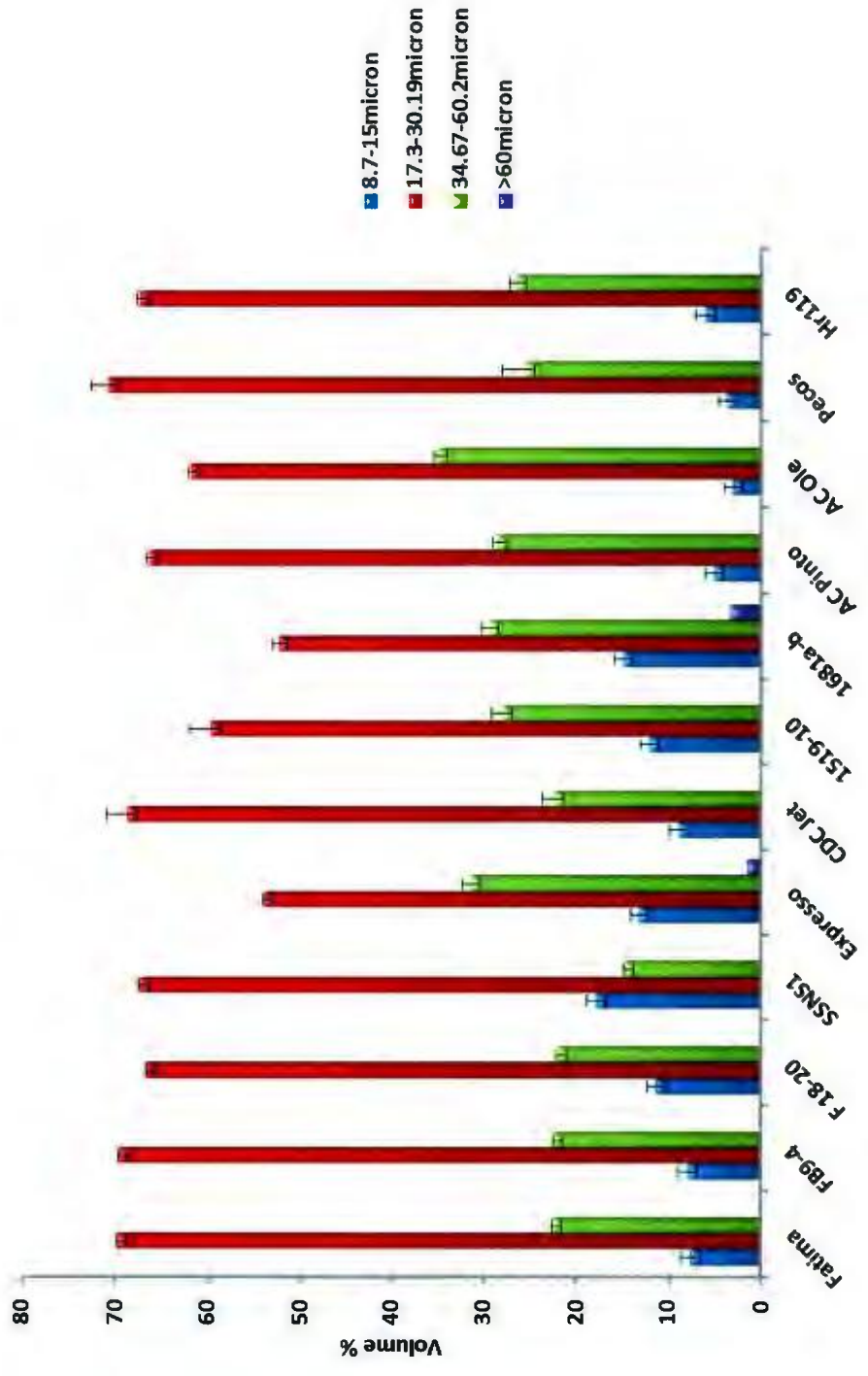


Figure 4.2 Starch granule size distribution of faba, black and pinto bean starches



4.1.3. Amylopectin chain length distribution

The chain length distribution of FB, BB and PB starches are presented in Table 4.2.

There was no significant difference ($P < 0.05$) in the proportion of DP 6–12, DP 13–24,

DP 37–50 among starch sources and between cultivars of each starch source.

Table 4.2

Amylopectin chain length distribution of faba, black and pinto bean starches determined by high performance anion exchange chromatography with pulsed amperometric detection.*¹

Starch source	Degree of Polymerization ² (DP) %			
	6-12	13-24	25-36	37-50
Faba bean				
Fatima	21.69±1.83 ^a	53.30±0.67 ^a	13.74±1.84 ^a	11.27±0.68 ^a
FB 9-4	20.07±2.58 ^a	53.13±2.63 ^a	15.00±3.64 ^a	11.80±1.56 ^a
F 18-20	19.33±2.02 ^a	53.06±1.01 ^a	15.50±2.92 ^a	12.10±0.12 ^a
SSNS 1	20.43±1.78 ^a	54.07±3.07 ^a	15.10±3.54 ^a	10.41±1.31 ^a
Mean	20.38±1.81^a	53.39±1.65^a	14.83±2.42^a	11.40±1.07^a
Black bean				
BYT 03 Espresso	19.85±0.94 ^b	53.62±0.74 ^b	16.48±0.25 ^b	10.06±0.05 ^b
BRT CDC Jet	19.79±1.82 ^b	54.71±2.99 ^b	14.83±3.72 ^b	10.68±1.09 ^b
BRT 1519-10	18.05±0.65 ^b	51.64±1.26 ^b	18.18±0.02 ^b	12.12±0.63 ^b
BYT01 1681a-b	20.78±1.95 ^b	55.27±0.40 ^b	14.57±2.06 ^b	9.38±0.29 ^b
Mean	19.62±1.42^a	53.81±1.82^a	16.01±2.09^a	10.56±1.11^a
Pinto bean				
AC Pintoba	22.54±2.53 ^c	54.05±0.03 ^c	14.46±0.49 ^c	8.95±2.01 ^c
AC Ole	21.39±2.47 ^c	54.00±1.24 ^c	15.48±2.45 ^c	9.12±1.26 ^c
Pecos	20.06±2.02 ^c	54.40±1.46 ^c	15.10±3.45 ^c	10.44±0.03 ^c
HR 119	21.00±2.25 ^c	55.77±1.76 ^c	13.76±3.49 ^c	9.48±0.52 ^c
Mean	21.25±2.00^a	54.56±1.25^a	14.70±2.20^a	9.49±1.10^a

*Statistical analysis was performed among cultivars within each starch source and also among the means for each starch source.

¹All data represent the mean of triplicates. Values followed by the same superscript in each column for each starch source are not significantly different ($P < 0.05$) by ANOVA and Tukey's HSD test.

²DP_n: indicates degree of polymerization. Total relative area was used to calculate the percent distribution.

4.1.4. Attenuated total reflectance Fourier transform infrared spectroscopy (ATR-FTIR)

In ATR-FTIR spectroscopy, the vibrational modes influencing absorption bands at 1105, 1125 and 1155 cm^{-1} (C – OH, C – C and C – O stretching), 928, 995, 1016, 1048, 1080 cm^{-1} (C – OH bending and CH_2 vibrational modes), and 860 cm^{-1} (C – O – C symmetrical stretching and C – H deformation) reflect conformational and crystalline order in starch (van Soest, et al., 1995). The ATR-FTIR spectrum is sensitive to short range order, defined as the double helical order, as opposed to long range order related to the packing of double helices (detected by X-ray diffraction). The IR beam penetrates only to a depth of a few micrometers (2 μm) of the sample (Sevnou et al., 2002). Hence, the IR spectra mainly reflect short range order near the granule surface. The ATR-FTIR data of FB, BB and PB starches are presented in Table 4.3. The absorbance bands at 1016 and 1048 cm^{-1} are characteristic of amorphous and crystalline structures in starch, respectively (van Soest et al., 1995). Thus the ratio of 1048/1016 cm^{-1} has been used to express the amount of ordered crystalline domains to amorphous domains in starches (Capron et al., 2007; van Soest et al., 1995). FB starches exhibited a lower 1048/1016 cm^{-1} ratio (0.872 – 0.890) than did BB (0.910 – 0.971) and PB (0.895 – 0.946) starches. The mean of the 1048/1016 cm^{-1} ratio for each starch source [FB (0.886 \pm 0.016), BB (0.938 \pm 0.028) and PB (0.922 \pm 0.023)] was significantly different ($P < 0.05$) only between FB and the other two starches. The lower 1048/1016 cm^{-1} ratio for FB starches suggests that although the amount of ordered crystalline domains are higher (based on the higher intensity of the 1048 cm^{-1} peak), the crystallites of FB starch are probably smaller and/or the double

helices forming the crystallites are weakly associated within the crystalline lamella. This seems plausible, since the peak attributed to the amorphous domains (1016 cm^{-1}) was also of a higher intensity in FB starches. The $995/1016\text{ cm}^{-1}$ ratio has been shown to reflect helical organization (alignment of helices at short range order) within the crystalline lamella (Capron et al., 2007). The mean $995/1016\text{ cm}^{-1}$ ratio's for FB (1.135 ± 0.021), BB (1.125 ± 0.019) and PB (1.125 ± 0.038) starches were not significantly ($P < 0.05$) different. However, with the exception of FB cultivars, the $995/1016\text{ cm}^{-1}$ ratio was significantly different ($P < 0.05$) among cultivars of BB (BRT CDC Jet $>$ BYT 01 1681a-b $>$ BRT 1519-10 $>$ BYT 03 Espresso) and PB (Pecos \sim AC Ole \sim HR 119 $>$ AC Pintoba). This suggests that among cultivars of BB and PB, differences exist with regard to helical organization within the crystalline lamella.

Table 4.3

Short-range molecular order of faba, black and pinto bean starches measured by attenuated total reflectance–Fourier-transform infrared spectroscopy.*¹

Starch source	Intensity Ratio	
	R (1048/1016 cm ⁻¹) ²	R (995/1016 cm ⁻¹) ³
Faba bean		
Fatima	0.872±0.012 ^a	1.140±0.005 ^a
FB 9-4	0.889±0.032 ^a	1.127±0.030 ^a
F 18-20	0.889±0.016 ^a	1.151±0.012 ^a
SSNS 1	0.892±0.004 ^a	1.124±0.033 ^a
Mean	0.886±0.016^a	1.135±0.021^a
Black bean		
BYT 03 Espresso	0.946±0.025 ^b	1.107±0.000 ^b
BRT CDC Jet	0.910±0.018 ^b	1.154±0.000 ^c
BRT 1519-10	0.971±0.000 ^b	1.118±0.000 ^d
BYT01 1681a-b	0.924±0.021 ^b	1.121±0.000 ^c
Mean	0.938±0.028^b	1.125±0.019^a
Pinto bean		
AC Pintoba	0.895±0.003 ^c	1.070±0.001 ^f
AC Ole	0.946±0.024 ^c	1.145±0.003 ^{gh}
Pecos	0.925±0.000 ^c	1.162±0.017 ^h
HR 119	0.924±0.021 ^c	1.121±0.000 ^g
Mean	0.922±0.023^b	1.125±0.038^a

*Statistical analysis was performed among cultivars within each starch source and also among the means for each starch source.

¹All data represent the mean of triplicates. Values followed by the same superscript in each column for each starch source are not significantly different ($P < 0.05$) by ANOVA and Tukey's HSD test.

²Amount of ordered crystalline domain to amorphous domains in starch.

³Reflects helical organization within the crystalline lamella.

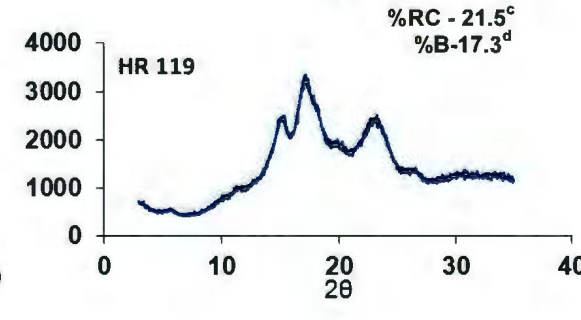
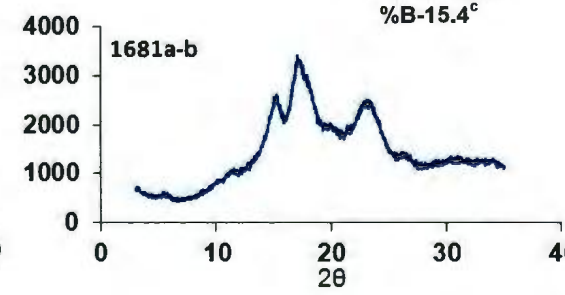
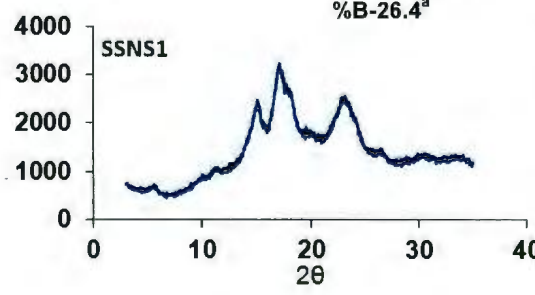
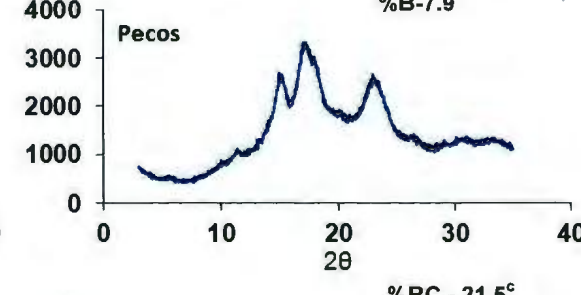
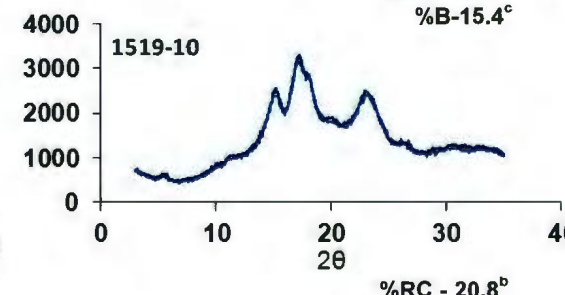
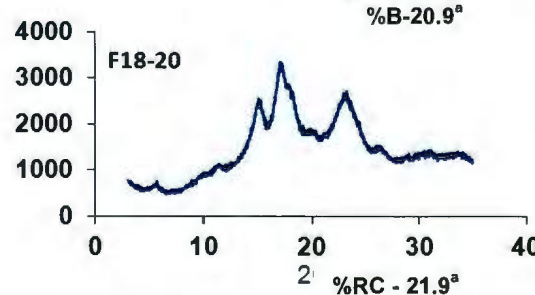
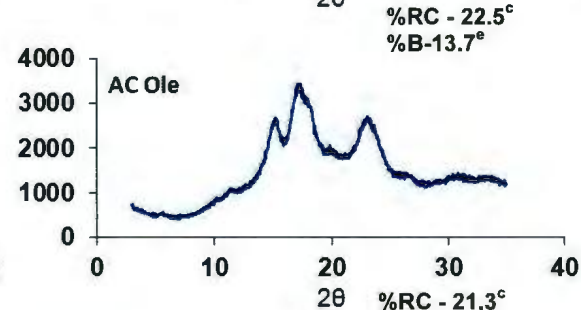
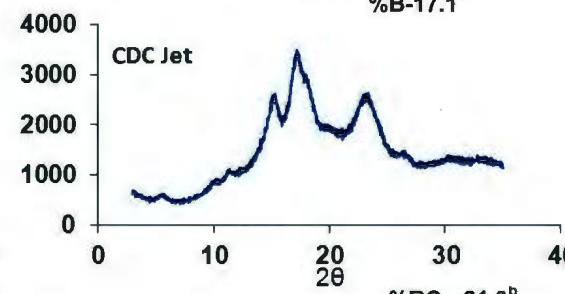
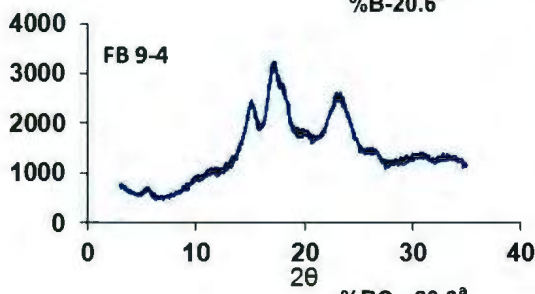
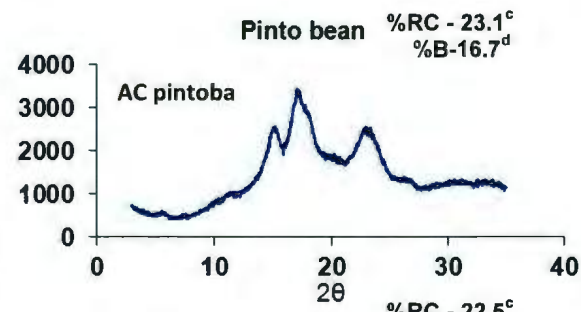
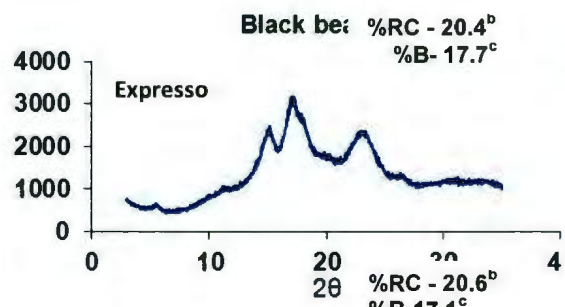
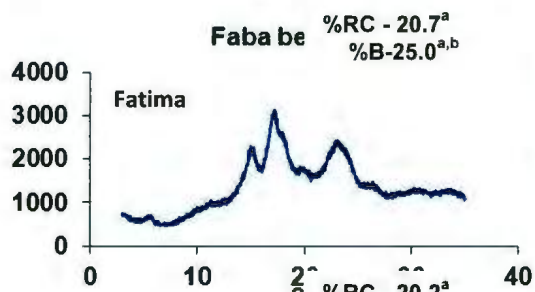
4.1.5. X-ray Diffraction

All pulse starches exhibited the characteristic “C-type” X-ray pattern (Hoover and Ratnayake, 2002). Gernat et al. (1990) have shown that the “C” pattern is a mixture of ‘A’ and ‘B’ unit cells in varying proportions. The intensity of the peak characteristic of the “B” polymorphic form (centered at $5.2^{\circ} 2\theta$) followed the order: FB > BB > PB (Fig. 4.3). The “B” polymorphic content in FB, BB and PB starches ranged from 20.6 – 26.3%, 15.4 – 17.7%, 7.9 – 17.3%, respectively. Among cultivars of FB, BB and PB starches, the ‘B’ polymorph content followed the order: Fatima ~ SSNS1 > FB 9-4 ~ F 18-20, BYT 03 Espresso ~ CDC Jet ~ BRT 1519-10 ~ BYT 01 1681a-b and HR 119 ~ AC Pintoba > AC Ole > Pecos, respectively. The B polymorphic content of FB was in the range reported for other pulse starches (22.1 – 38.6%) (Hoover et al., 2010). However, those of BB and PB were lower. The relative crystallinity (RC) of FB, BB and PB starches was in the range 20.2 – 21.9%, 20.4 – 21.3% and 21.5 – 23.1%, respectively. These values were within the range (17.0 – 34.0%) reported for other pulse starches (Hoover et al., 2010). The mean RC of PB cultivars (22.3%) was significantly ($P < 0.05$) higher than those of BB (20.8%) and FB (20.8%) cultivars. Generally, differences in RC between starches could be attributed to differences in crystal size, amount of crystallite regions (influenced by amylopectin content and amylopectin chain length), orientation of the double helices within the crystalline domains and the extent of interaction between double helices. The difference in RC between PB and the other two starches cannot be attributed to differences in crystallite size (since the sharpness in X-ray pattern was identical in FB, BB and PB [Fig. 3]), amylopectin content (differences among PB, FB and

BB was marginal [Table 4.1]), or to amylopectin chain length distribution (no significant difference ($P < 0.05$) among FB, BB and PB [Table 4.2]). Therefore, the higher RC of PB starches probably reflects stronger interaction between double helices within the crystalline lamellae and/or better orientation of crystallites to the X-ray beam.

As shown earlier (Fig. 4.1, Table 4.3), crystallites in BB and PB starches were better organized within the crystalline lamella than those of FB starches. Consequently, the intensity of the X-ray pattern and relative crystallinity of FB starches (Fig. 4.3) should have been theoretically much lower than those of BB and PB starches. This suggests that the higher content of B-type crystallites (Fig. 4.3) in FB starches may have negated the influence of crystalline packing ($BB \sim PB > FB$) on X-ray intensities and relative crystallinity. This seems plausible, since B-type crystallites have been shown (Cairns et al. 1997) to be larger (14.0 nm) than those of A-type crystallites (10.0 nm), and an increase in crystallite size has been shown (Rocha et al. 2011) to increase X-ray crystallinity.

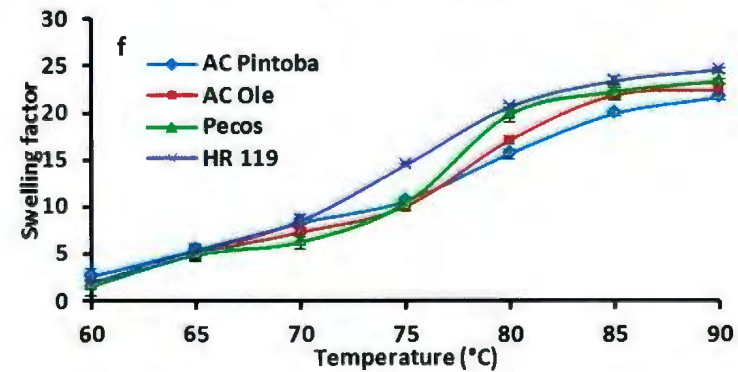
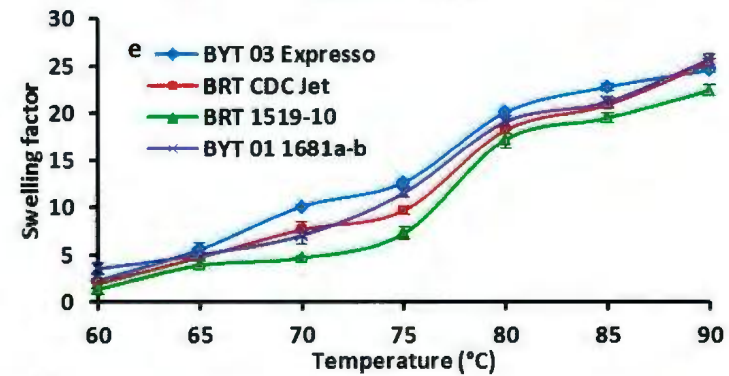
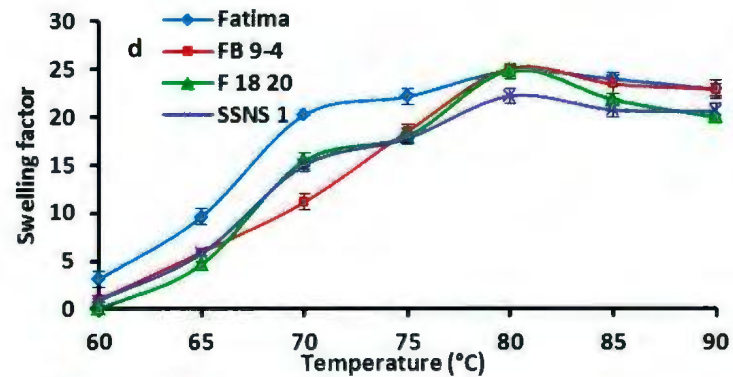
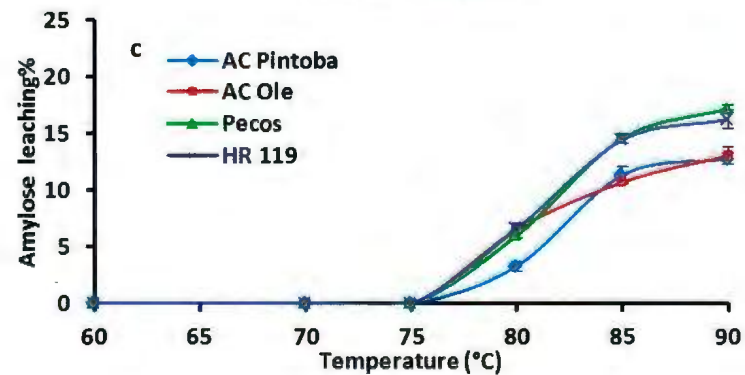
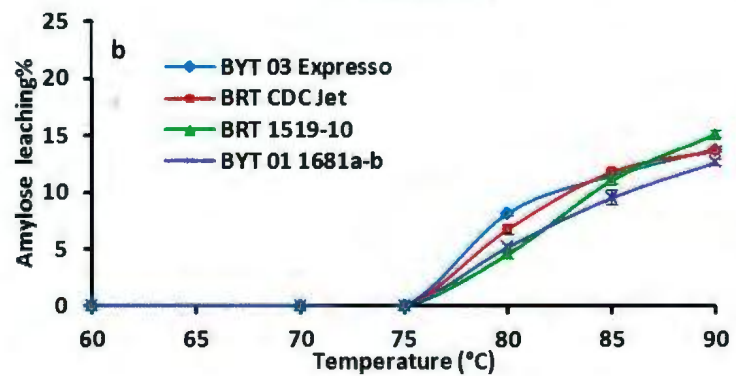
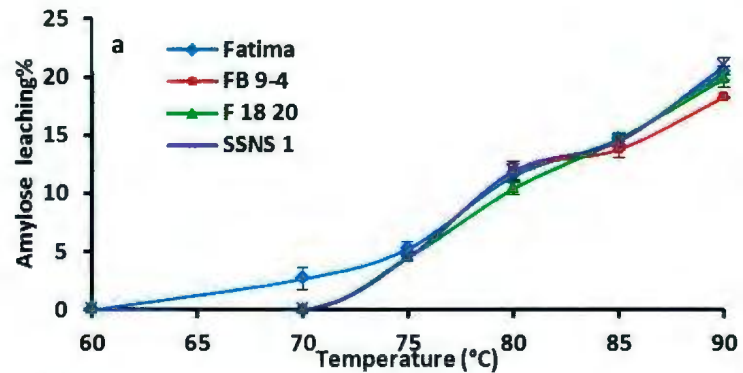
Figure 4.3 X-ray diffraction patterns (y axis: Intensity, x axis: 2θ), relative crystallinity (RC) and B-polymorphic content of faba, black and pinto bean starches^a.
(^aValues followed by the same superscript for RC and B-polymorphic content data for each starch source are not significantly different ($P < 0.05$) by ANOVA and Tukey's HSD test).



4.1.6. Amylose leaching (AML) and Swelling factor (SF)

AML and SF of FB, BB and PB starches over the temperature range 60 to 90°C are presented in Fig. 4.4. The extent of AML at all temperatures followed the order: FB > BB ~ PB (Fig. 4.4 a, b, c). There was no significant difference in AML among cultivars of FB starches. However, difference in AML among cultivars of BB and PB starches was significant ($P < 0.05$). In all cultivars of BB and PB starches, AML was detectable only at temperatures exceeding 80°C, whereas, AML among FB cultivars was detectable at 70°C in Fatima and at 75°C in the other three cultivars. AML has been shown to be influenced by the extent of interaction between amylose – amylose (AM-AM), and/or amylose – amylopectin (AM-AP) chains, apparent amylose content and lipids bound to amylose chains (Chung, Hoover and Liu, 2009). The extent of AML cannot be attributed to differences in apparent amylose content since cultivars of FB, BB and PB starches that differed significantly ($P < 0.05$) in their apparent amylose content (Table 4.1) did not exhibit significant differences ($P < 0.05$) in AML (Fig. 4.4 a, b, c). Furthermore, the absence of any significant differences ($P < 0.05$) in bound lipid content among cultivars of FB, BB and PB starches (Table 4.1) make their influence on AML highly improbable. This suggests that in FB starches, the higher extent of AML and AML at temperatures below 80°C (Fig. 4.4 a) reflect weaker interactions between AM-AM and/or AM-AP chains and/or to the presence of cracked granules (Fig. 4.1 d, g, j). The SF in the temperature range 60 to 85°C and at 90°C followed the order: FB > BB ~ PB and BB ~ PB > FB (Fig. 4.4 d, e, f), respectively. Differences in SF among cultivars of FB and BB starches were significant ($P < 0.05$) at temperatures below 80°C, whereas in PB starches,

Figure 4.4 Amylose leaching (a, b, c) and swelling factor (d, e, f) of faba (a, d), black (b, e) and pinto (c, f) bean starches over the temperature range 60-90°C.



SF differences among cultivars more significant ($P < 0.05$) at temperatures above 80°C (Fig. 4.4 d, e, f). In BB and PB starches, SF increased with increase in temperature. However, SF decreased in FB starches at temperatures beyond 80°C (Fig. 4.4 d). SF has been shown to be influenced by: 1) amylopectin structure (Tester, Morrison and Schulman, 1993), 2) lipids bound to amylose chains (Hoover and Manuel, 1996), 3) crystallinity (Chung et al., 2009) and 4) amylopectin content (Varatharajan et al., 2010). As shown earlier, there were no significant differences ($P < 0.05$) in factors 1 to 4 among FB, BB and PB starches. This suggests that the higher SF of FB starches in the temperature range 60 – 85°C reflect the interplay of the following factors: 1) cracked granules, 2) poorly ordered amylopectin crystallites and 3) weaker interaction between AM-AM and/or AM-AP chains. Factor 1 would facilitate rapid entry of water into the amorphous domains of the granule, whereas factors 2 and 3 will expose hydroxyl groups for hydration. The decrease in SF shown by FB starches at temperatures beyond 85°C, reflects loss of granule integrity due to cracked granules and/or to amylopectin crystallites in FB starches being less well ordered than in BB and PB starches.

4.1.7. Pasting properties

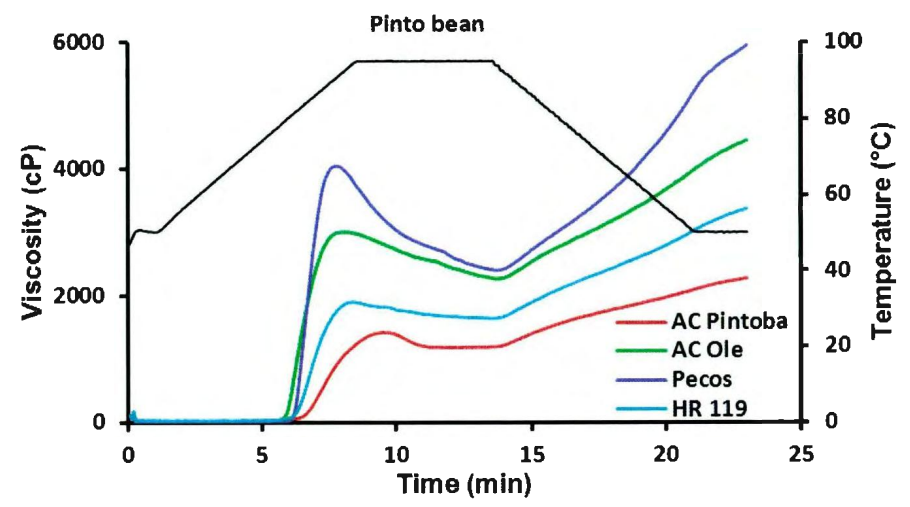
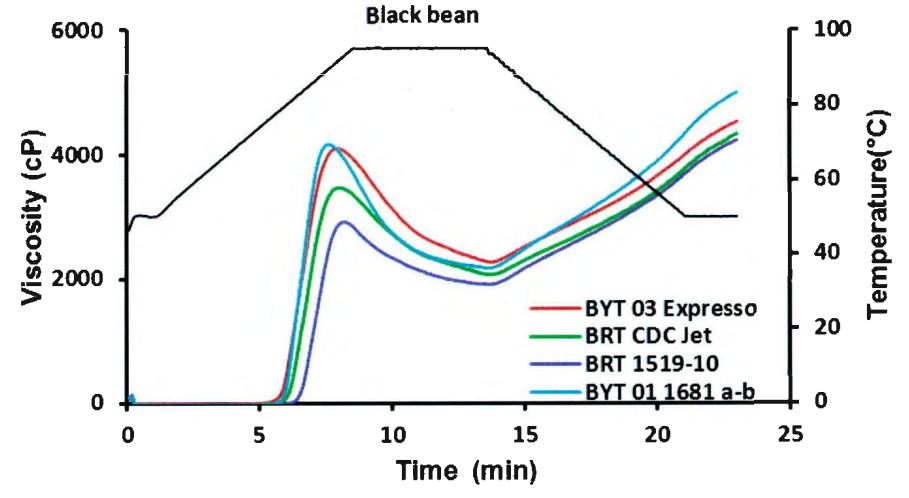
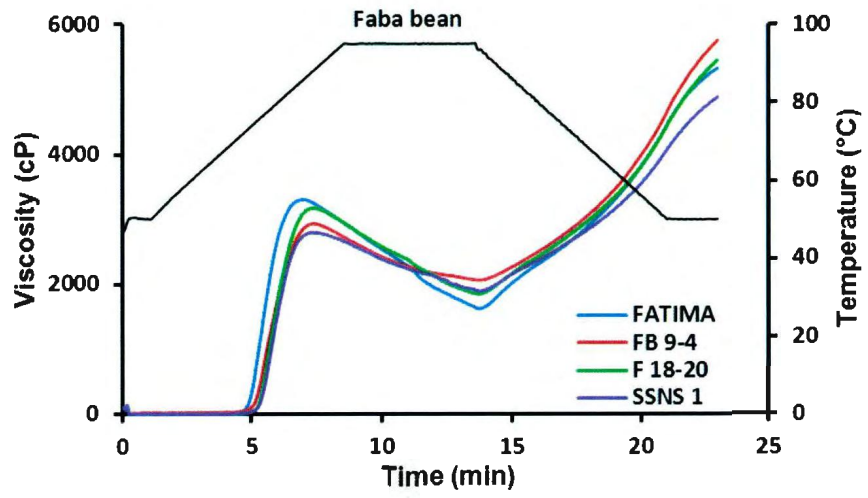
Pasting is the phenomenon following gelatinization in the dissolution of starch. The granules become increasingly susceptible to shear disintegration as they swell and release soluble material as they disintegrate. The paste that is obtained on gelatinization is a viscous mass consisting of a continuous phase of solubilized amylose and /or amylopectin and a discontinuous phase of granule remnants. The pasting properties of FB, BB and PB starches are presented in Fig. 4.5. The peak viscosity and shear stability have been shown to be influenced by amylose content, proportion of amylopectin chain lengths of DP 13–24 and DP > 37 and phosphorus content (Han and Hamaker, 2001; Karim et al., 2009). The extent of set-back has been shown to be influenced by amylose content (Lu et al., 2011), by the absence or presence of unfragmented rigid swollen granules embedded in the leached amylose network (Chung et al., 2008) and by rapid retrogradation of leached amylose in the starch paste. Among FB cultivars, the peak viscosity (PV), breakdown viscosity (BV), set-back viscosity (SB) followed the order: Fatima ~ F 18-20 ~ FB 9-4 ~ SSNS1, Fatima > F 18-20 > FB 9-4 ~ SSNS1 and Fatima ~ F18-20 ~ FB 9-4 > SSNS1, respectively. Among BB cultivars, PV, BV and SB followed the order: BYT 03 Espresso ~ BYT 01 1681a-b > BRT CDC Jet > BRT 1519-10, BYT 03 Espresso ~ BYT 01 1681a-b > BRT CDC Jet ~ BRT 1519-10 and BYT 03 Espresso ~ BYT 01 1681a-b ~ BRT CDC Jet ~ BRT 1519-10, respectively. Among PB cultivars PV, BV and SB followed the order: Pecos > AC ole > HR 119 > AC pintoba, Pecos > AC ole > HR 119 > AC pintoba and Pecos > AC ole > HR 119 > AC pintoba, respectively. As shown in Table 4.1, there was no significant difference in amylopectin chain length distribution

among cultivars of FB, BB and PB. Therefore, differences in PV among cultivars of each starch are likely influenced by differences in phosphorus and amylose content.

Nutting (1952) reported that when potato starch is pasted its phosphate groups ionize, leaving the starch with a negative charge. The resulting slight coulombic repulsion weakens the bonding forces between amylopectin clusters enabling increased solvation. Compared with an electrically neutral starch, this increased solvation results in larger pasted granules and a higher starch paste viscosity. This might explain the following observations: 1) among each starch source, the highest PV was seen in cultivars with the highest P content (Fatima [FB], BYT 01 1681a-b, BYT 03 Espresso [BB], Pecos [PB]), 2) PV decreased with decrease in P content, and 3) PB starches with the largest variations in their P content exhibited more pronounced differences in PV. The BV was also strongly influenced by variations in P content, since among each starch source, the cultivars (Fatima, BYT 01 1681a-b, Pecos) with the highest P content (Table 4.1) exhibited the highest BV (Fig. 4.5). This could be attributed to a weakened amylopectin structure (due to repulsion between ionized phosphate groups), which increases granule susceptibility towards shear. It is highly unlikely that leached amylose contributes significantly to the viscosity rise during the heating cycle in FB and BB cultivars, since the difference in apparent amylose content and the extent of AML (Fig. 4.4) among cultivars of FB and BB are marginal. However, in PB cultivars, AML may have been partly responsible for the PV of Pecos and AC ole (Pecos > AC ole) being higher than those of AC pintoba and HR 119 (HR 119 > AC pintoba) due to significant differences ($P < 0.05$) in their apparent amylose content (Pecos > AC ole > HR 119 > AC pintoba).

Difference in the extent of SB among PB cultivars (Fig. 4.5) could be attributed to wide variations in extent of AML (due to significant differences [$P < 0.05$] in their apparent amylose content [Table 4.1]) and extent of granule breakdown during the holding period (Pecos < AC ole < HR 119 < AC pintoba) (Fig. 4.5). Differences in SB among cultivars of FB and BB are less pronounced than in PB starches (Fig. 4.5), due to differences in apparent amylose content (Table 4.1) and extent of granule breakdown (Fig. 4.5) among FB and BB cultivars being less significant ($P < 0.05$) than among cultivars of PB (Fig. 4.5).

Figure 4.5 Pasting (Rapid Visco Analyzer) profiles of faba, black and pinto bean starches.



4.1.8. Gelatinization characteristics

The gelatinization transition temperatures (T_o [onset temperature], T_p [peak temperature], T_c [conclusion temperature]) and the enthalpies of gelatinization (ΔH) of the pulse starches are presented in Table 4.4. T_o , T_p , T_c and ΔH followed the order: BB ~ PB > FB. DSC parameters have been shown to be influenced by the molecular architecture of the crystalline region, which corresponds to the amylose to amylopectin ratio (Noda et al., 1996). The above authors showed, in studies on cereal starches, that low T_o , T_p , T_c reflect the presence of abundant short amylopectin chains. Jayakody et al. (2005) and Chung et al. (2008) showed in studies on tuber and pulse starches, respectively, that T_o , T_p and T_c are influenced by granule crystallinity. Protserov et al. (2000) and Lan et al. (2008) have shown by studies on potato and barley starches, respectively, that gelatinization parameters decrease progressively with an increase in the amount of crystalline defects. The ΔH values have been shown to represent the number of double helices that unravel and melt during gelatinization (Cooke and Gidley, 1992). As shown earlier, FB, BB and PB starches did not exhibit any significant difference ($P < 0.05$) with regard to amylopectin chain length distribution (Table 4.2), amylose/amylopectin ratio (Table 4.1) or crystallinity (Fig. 4.3). Therefore, the above cannot be considered as factors influencing T_o , T_p , T_c and ΔH . Ratnayake et al. (2001) showed that field pea starches varying in B-polymorphic content did not exhibit any significant difference ($P < 0.05$) in T_o , T_p , T_c and ΔH . Therefore, the difference in B-polymorphic content among the starches (FB > BB ~ PB) also cannot be considered as a factor influencing T_o , T_p , T_c and ΔH .

Nutting (1952) postulated that coulombic repulsion between ionized phosphate groups on adjacent amylopectin chains would open up the branched amylopectin molecules and increase their solvation. On that basis, among PB cultivars, Pecos with a higher phosphorus content (Table 4.1) should have exhibited a lower T_o , T_p , T_c and ΔH (increased solvation due to a higher extent of coulombic repulsion between ionized phosphate groups would lower the thermal energy required for crystallite melting). This suggests that differences in phosphorus content among cultivars of FB, BB and PB starches (Table 4.1) and among FB, BB and PB (Table 4.1) starches cannot be considered a factor influencing T_o , T_p , T_c and ΔH . Birefringence (Fig. 4.1a-c) and FTIR data (Table 4.3) showed that amylopectin crystallites are less well ordered in FB than in BB and PB starches. This suggests that interactions between adjacent double helices within the crystalline domains are much weaker in FB starch. Consequently, less thermal energy will be required to dissociate, unravel and melt amylopectin double helices of FB starch during gelatinization. This would then explain differences in T_o , T_p , T_c and ΔH between FB and other pulse (BB and PB) starches.

Table 4.4

Gelatinization parameters of faba, black and pinto bean starches as determined by differential scanning calorimetry. *¹

Starch Source	Gelatinization transition parameters			
	To (°C) ²	Tp (°C) ²	Tc (°C) ²	Enthalpy ³ (J/g)
Faba bean				
FATIMA	62.00±0.73 ^a	67.45±1.10 ^a	73.62±1.27 ^a	10.25±0.02 ^a
FB 9-4	64.94±0.37 ^b	70.20±0.50 ^b	75.79±0.02 ^a	8.15±0.21 ^b
FB 18-20	65.22±0.00 ^b	70.59±0.14 ^b	76.46±0.74 ^a	8.21±0.22 ^b
SSNS 1	64.98±0.08 ^b	69.93±0.36 ^{ab}	75.40±0.29 ^a	7.84±0.13 ^b
Mean	64.28±1.45^a	69.54±1.40^a	75.31±1.26^a	8.61±1.03^a
Black bean				
BYT 03 Espresso	64.11±0.30 ^c	72.17±0.60 ^c	80.43±0.31 ^b	13.53±1.53 ^c
BRT CDC Jet	64.06±0.13 ^c	74.00±0.13 ^d	82.68±0.09 ^b	13.87±1.08 ^c
BYT 01 1681a-b	67.10±0.29 ^d	76.64±0.14 ^c	82.07±1.24 ^b	13.69±0.00 ^c
BRT 1519-10	64.77±0.38 ^c	71.30±0.36 ^c	80.39±0.24 ^b	13.96±0.65 ^c
Mean	65.00±1.34^a	73.52±2.21^b	81.39±1.18^b	13.76±0.77^b
Pinto bean				
AC Pintoba	66.34±0.08 ^c	73.71±0.01 ^f	80.03±1.45 ^c	14.51±0.15 ^c
AC Ole	69.07±0.64 ^f	75.11±0.35 ^g	80.80±0.52 ^c	13.87±2.73 ^c
Pecos	69.89±0.00 ^f	75.91±0.23 ^g	82.61±1.07 ^c	14.58±0.05 ^c
HR 119	64.40±0.37 ^g	71.73±0.01 ^h	79.98±0.26 ^c	15.12±1.70 ^c
Mean	67.42±2.36^b	74.11±1.70^b	80.85±1.34^b	14.51±1.31^b

*Statistical analysis was performed among cultivars within each starch source and also among the means for each starch source.

¹All data represent the mean of triplicates. Values followed by the same superscript in each column for each starch source are not significantly different ($P < 0.05$) by ANOVA and Tukey's HSD test.

²To, Tp, Tc represents the onset, peak and end temperature, respectively.

³Gelatinization enthalpy of starch expressed in J/g of dry starch.

4.1.9. *In-vitro* digestibility

Rapidly digestible starch (RDS), slowly digestible starch (SDS), resistant starch (RS), hydrolysis index (HI) and expected glycemic index (eGI) determined by *in vitro* digestibility of FB, BB and PB starches by a mixture of pancreatin and amyloglucosidase are presented in Table 4.5 and Fig. 4.6. The above nutritional classification reflects both the kinetic component and the completeness of digestibility. RDS reflects starch that is rapidly and completely digested in the small intestine (associated with a rapid elevation of postprandial plasma glucose). SDS reflects starch that is more slowly digested in the small intestine (alternates post prandial plasma glucose and insulin levels) and RS reflects the sum of starch and the product of starch degradation not absorbed in the small intestine but is fermented in the large intestine. The HI expresses the digestibility of the starch in foods in relation to the digestibility of starch in a reference material such as white bread. eGI is calculated from HI and defined as the incremental post prandial glucose area after injection of the test product, as a percentage of the corresponding area after injection of an equicarbohydrate portion of the reference product (Jenkins et al., 1983). The levels of RDS, SDS and RS followed the order: FB (2.5%) > BB (1.6%) ~ PB (1.6%), FB (76.3%) > BB (44.0%) ~ PB (42.0%) and BB (43.1%) ~ PB (45.0%) > FB (11.0%), respectively. Variations in RDS, SDS and RS levels among cultivars of each starch species were marginal in FB, but were significant ($P < 0.05$) in BB and FB (Table 4.5) starches. RDS levels in FB, BB and PB (Table 4.5) starches were much lower than those reported (using the same methodology and definition for RDS, SDS and RS) by Chung et al. (2008) and Hughes et al. (2009) for pea (19.2%), lentil (14.8%), navy bean (8.2%) and chickpea

(12.4%) starches. The SDS level in FB (Table 4.5) was much higher than that reported by Chung et al. (2008) and Hughes et al. (2009) for pea (40.3%), lentil (41.5%), navy bean (32.3%) and chickpea (52.0%) starches. However, SDS levels in BB and PB (Table 4.5) were comparable to those of pea, lentil and navy bean starches, but were lower than in chickpea. The RS level in FB (Table 4.5) was much lower than that reported by Chung et al. (2008) and Hughes et al. (2009) for pea (40.5%), lentil (43.7%), navy bean (59.4%) and chickpea (35.0%) starches. However, RS levels in BB and PB (Table 4.5) starches were lower than that of navy bean, but higher than that of chickpea. The hydrolysis index (HI) calculated using the hydrolysis curve (Fig. 4.5) and the expected glycemic index (eGI) calculated using the HI followed the order: FB (65.2%) > BB (38.4%) > PB (35.5%) and FB (64.4%) > BB (41.3%) > PB (38.8%), respectively (Table 4.5). The above HI and eGI values for FB starches are comparable with those reported for other pulse starches (Chung et al., 2008). However, HI and eGI values for BB and PB starches were much lower than those reported for pea (~70%), lentil (~66%), chickpea (~70%) starches (Chung et al., 2008).

Differences in digestibility among and within species of native starches have been attributed to the interplay of several factors such as starch source (Ring et al. 1988), granule size (Snow and O'Dea, 1981), extent of molecular association between starch chains (Blazek and Gilbert, 2010), amylose content (Hoover and Sosulski, 1985), branch chain length distribution of amylopectin (Srichuwong et al. 2005a), degree of crystallinity (Hoover and Sosulski, 1985), polymorphic composition (Zhang, Venkatachalam and Hamaker, 2006; Bogracheva et al., 1998; Gerard et al., 2001; Wang, Yu and Yu, 2008),

granular pores, fissures and channels within the granule (Blazek and Gilbert, 2010; Dhital, Shrestha and Gidley, 2010).

Jane, Wong and McPherson (1997) have shown that in A-type starches, the branch points are scattered in both amorphous and crystalline regions. Consequently, there are many short A chains derived from branch linkages located inside the crystalline regions which produces an inferior crystalline structure containing branch α (1 \rightarrow 6) linkages and short double helices. However, in B-type starches, the branch points are clustered in the amorphous regions and there are fewer short branch chains. Thus, the crystalline structure of A-type starches is more readily hydrolyzed than those of B-type starches. Gerard et al. (2001) have shown by studies on maize mutant starches that regardless of amylose content or crystallinity level, starches with a predominant B-crystalline type were more resistant to amylolysis than others and initial rates of hydrolysis were lower for B-type than A-type starches. The above authors showed that final hydrolysis extents followed the order: A-type (>70%) > C-type (60%) > B-type (35%). However, in this study variation in B polymorphic content (Fig. 4.3) among the starches (FB > BB > PB) cannot be considered as a factor influencing RDS, SDS and RS levels for the following reasons: 1) among FB cultivars, Fatima and SSNS1 exhibited significant differences ($P < 0.05$) in their B-polymorphic content (Fig. 4.3). However, their RDS, SDS and RS levels (Table 4.5) did not differ significantly ($P < 0.05$), 2) among BB cultivars, BRT 1519-10 and BYT 01 1681a-b with identical B-polymorphic contents (Fig. 4.3) exhibited significantly different ($P < 0.05$) levels of RDS, SDS and RS (Table 4.5) and 3) among PB cultivars, Pecos with a significantly lower ($P < 0.05$) level of B-polymorphic content

(Fig. 4.3) exhibited significantly ($P < 0.05$) lower SDS and higher RS levels (Table 4.5). The lower SDS and higher RS levels in BRT 1519-10 (among BB cultivars) and Pecos (among PB cultivars) seems to suggest higher amounts of crystallites near the granular surface in these cultivars. This would decrease the rate and extent of hydrolysis by hindering the accessibility of the glycosidic oxygens (present in the starch chains forming the crystalline structure) towards amylolysis. Relative crystallinity (Fig. 4.3) and apparent amylose content (Table 4.1) cannot be considered as factors influencing RDS, SDS and RS levels, since variations in relative crystallinity and amylose content among FB, BB and PB were not large enough to account for the large differences in RDS, SDS and RS levels among cultivars of each starch source. Zhang et al. (2006) postulated that a high amount of short A-chains of DP 5-10 cannot form stable double helices (since chains with DP 5-10 would disrupt the formation of an ordered crystalline structure and thus negatively affect the perfection of amylopectin crystalline structure) and are thus likely to be attacked by enzymes leading to a significant correlation with RDS. Salmon et al. (2009) have also shown by studies on wheat starches that starches with a higher proportion of DP 6–12 chains were hydrolyzed faster. Furthermore, Srichuwong et al. (2005a) and Mutungi et al. (2011) have shown in studies on starches from different botanical origins, that very long amylopectin chains ($DP > 36$) retard amylolysis. This was attributed to strengthening of hydrogen bonds between chains spanning the entire crystalline region. As shown in Table 4.2 there was no significant ($P < 0.05$) differences in amylopectin chain length distribution among FB, BB and PB starches. Consequently, differences in RDS levels among FB, BB and PB starches cannot be attributed to

amylopectin chain length distribution. Blazek and Gilbert (2010) have shown in studies on waxy potato, high amylose maize, tapioca, normal rice and normal maize starches, that the mechanism of amylolysis involves both the preferential disruption of amorphous regions (amorphous growth rings) as well as side-by-side hydrolysis of amorphous and crystalline regions (of the semicrystalline growth ring). The above authors postulated that the preferential disruption of the amorphous growth rings in cereal starches is due to the ability of the enzymes to penetrate into the interior through the surface pores, which is not possible for potato starch. The influence of granule surface on amylolysis was also shown by Dhital et al. (2010), who observed that fissures on granule surface would influence enzyme diffusivity inside granules as obstacles (such as longer blocklets) on the surface are minimized. As shown earlier (Fig. 4.1), cracks on granule surfaces were present only on the surface of FB starches (Fig. 4.1 d, g, j). The presence of cracks on the granule surface of FB starches would enable the enzymes to rapidly penetrate the granule interior and hydrolyze starch chains near the granule surface. This would then explain the higher RDS levels in FB starches during the first 30 min of hydrolysis. Birefringence (Fig. 4.1a-c) and DSC (Table 4.4) data showed that compared to BB and PB starches, AP double helices are less well ordered within the lamella structure of FB starches. Consequently, the degree of accessibility of the glycosidic oxygens of starch chains in the crystalline region of FB starches to enzymic attack would be much greater than in BB and PB starches. This could then explain not only the higher SDS level in FB starches, but also their lower RS levels (Table 4.5). The above data suggest that RDS levels are influenced by granule surface characteristics. In contrast, SDS and RS levels are influenced by the interplay between the extent of double helical organization within the

crystalline lamella and by crystallite distribution within the granule interior. Based on the above data, BB and PB starches with their lower eGI and higher RS content would be more suitable than FB starches for control of blood glucose levels.

Table 4.5

Nutritional fractions, hydrolysis index and expected glycemic index of native faba, black and pinto bean starches determined by *in vitro* hydrolysis.*¹

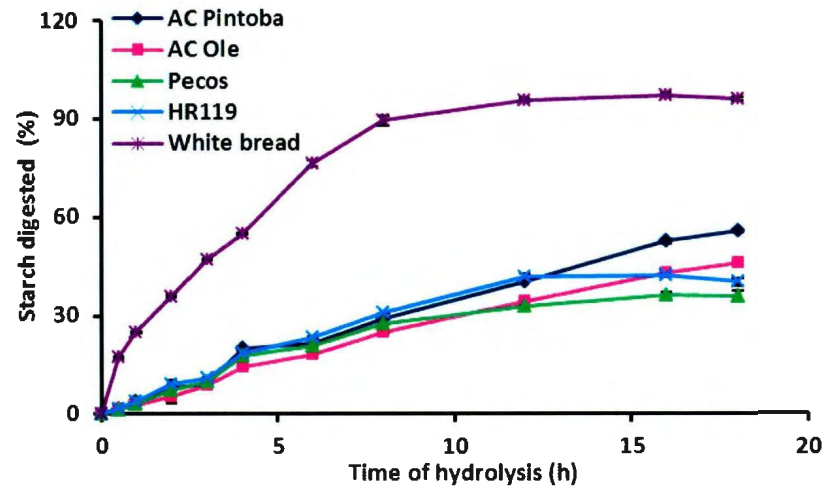
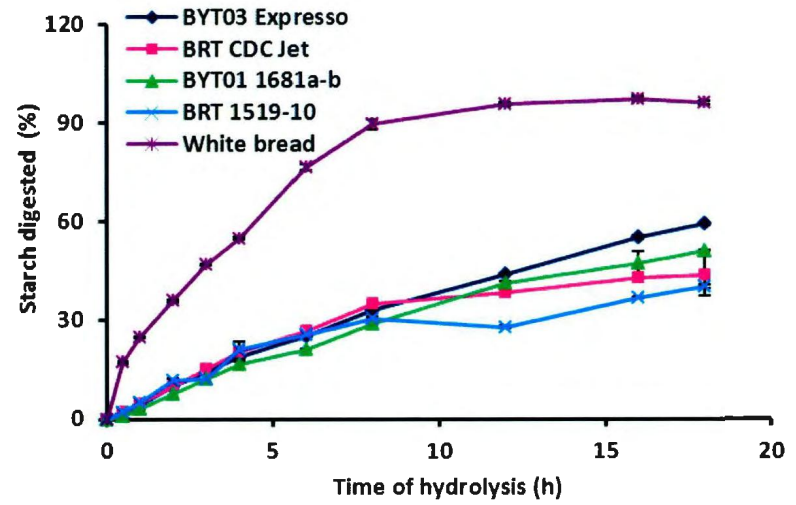
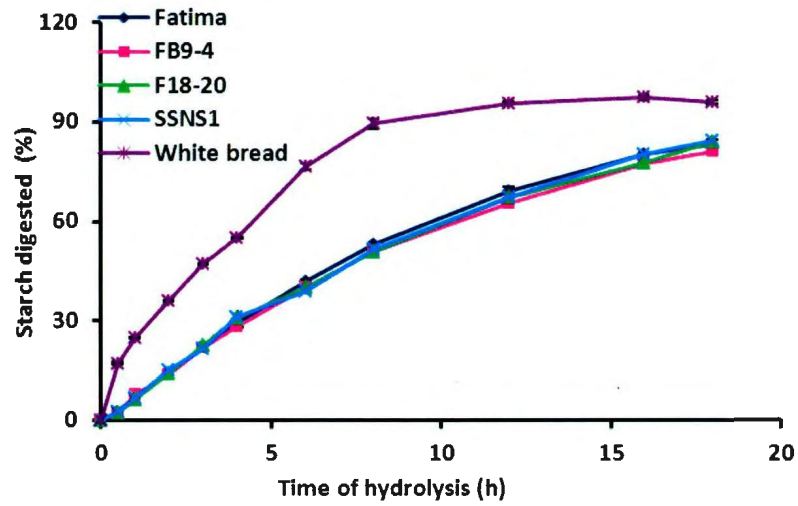
Starch source	RDS ²	SDS ²	RS ²	HI ²	eGI ²
Faba bean					
Fatima	2.80±0.35 ^a	77.29±0.98 ^a	10.00±0.70 ^a	67.20±0.60 ^a	66.20±0.50 ^a
FB 9-4	2.29±0.06 ^b	74.99±0.75 ^a	10.95±0.70 ^a	61.60±3.50 ^b	61.30±3.00 ^b
F 18-20	2.40±0.14 ^{ab}	75.34±2.99 ^a	15.03±2.86 ^b	65.60±0.40 ^a	64.80±0.30 ^a
SSNS 1	2.44±0.06 ^{ab}	77.64±0.37 ^a	8.14±0.34 ^a	66.20±0.40 ^a	65.20±0.30 ^a
Mean	2.48±0.26^a	76.32±1.88^a	11.03±2.94^a	65.16±2.72^a	64.37±2.35^a
Black bean					
BYT 03 Espresso	1.57±0.12 ^c	53.62±0.55 ^b	33.46±0.59 ^c	43.90±0.30 ^c	46.00±0.30 ^c
BRT CDC Jet	2.12±0.27 ^d	40.58±1.30 ^c	45.53±1.18 ^d	39.30±0.30 ^d	42.10±0.30 ^d
BRT 1519-10	2.05±0.23 ^d	34.90±0.15 ^e	51.67±0.22 ^c	33.80±0.40 ^e	37.30±0.30 ^e
BYT01 1681a-b	0.87±0.20 ^c	46.44±3.67 ^d	41.79±3.52 ^d	36.90±2.70 ^d	40.00±2.40 ^d
Mean	1.65±0.55^b	43.88±7.39^b	43.11±7.02^b	38.46±4.02^b	41.35±3.46^b
Pinto bean					
AC Pintoba	1.72±0.13 ^f	50.90±0.73 ^f	36.57±0.64 ^f	38.20±2.70 ^f	41.10±2.30 ^f
AC Ole	1.59±0.26 ^f	41.51±0.32 ^g	44.89±0.09 ^g	33.50±0.30 ^g	37.1±0.30 ^g
Pecos	1.41±0.30 ^f	34.94±1.01 ^h	52.84±0.72 ^h	32.40±0.20 ^g	36.10±0.10 ^g
HR 119	1.59±0.26 ^f	40.63±0.84 ^g	47.12±0.50 ⁱ	37.90±0.20 ^f	40.90±0.20 ^f
Mean	1.58±0.30^b	42.00±5.95^b	45.36±6.05^b	35.50±2.95^c	38.79±2.55^c

*Statistical analysis was performed among cultivars within each starch source and also among the means for each starch source.

¹All data represent the mean of triplicates. Values followed by the same superscript in each column for particular bean starches are not significantly different ($P > 0.05$) by ANOVA and Tukey's HSD test.

²RDS: rapidly digestible starch; SDS: slowly digestible starch; RS: resistant starch; HI: hydrolysis index, eGI: expected glycemic index.

Figure 4. 6 Digestibility profile of faba, black and pinto bean starches.

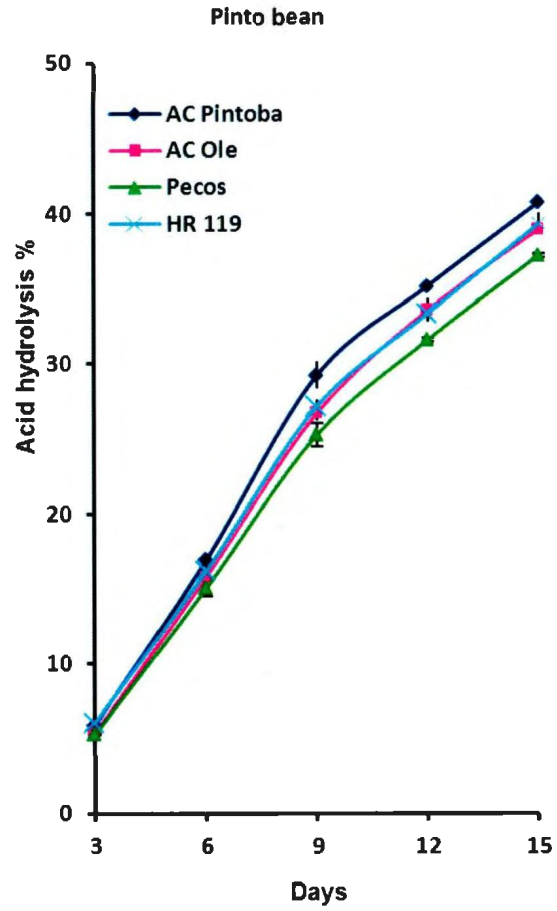
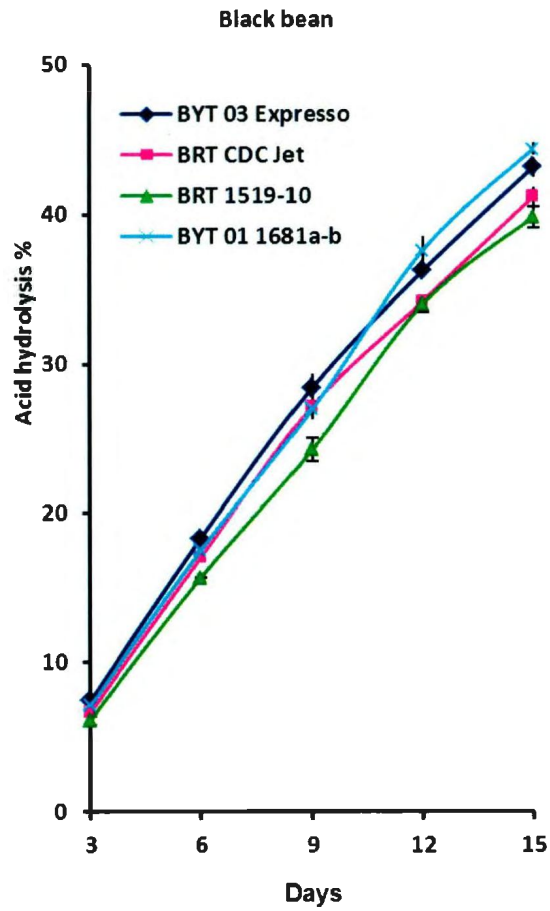
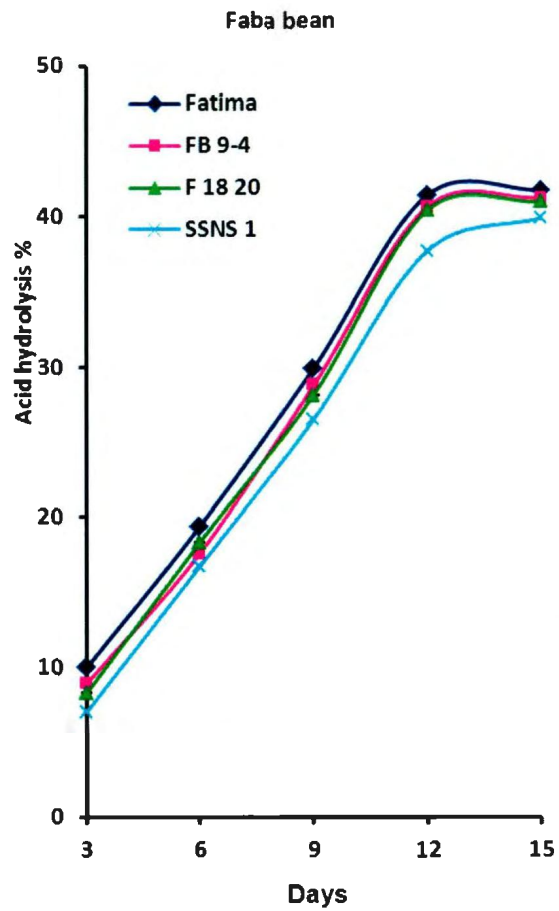


4.1.10. Acid hydrolysis

The extent of acid hydrolysis of FB, BB and PB starches are presented in Fig. 4.7. At the end of the 15th day the extent of hydrolysis followed the order: FB ~ BB > PB. The difference in hydrolysis among cultivars of FB, BB and PB was marginal. Beyond the 12th day, the hydrolysis curve reached a plateau in FB starches (indicating that most of the starch chains in the crystalline region were degraded at the end of this time period), but continued to increase in PB and BB starches. It has been suggested that heterogeneous acid hydrolysis preferably attacks the more amorphous regions of the granule, whether they be at the surface or interior. In contrast, crystalline regions are less accessible to attack by hydrated protons (H_3O^+) and are attacked only after a period of 9-12 days (Hoover, 2000). Differences in the extent of acid hydrolysis among starches has been attributed to differences in granule size, amount of lipids bound to amylose chains, amylopectin chain length distribution and proportion of 'B' type unit cells (Vasanthan and Bhatta, 1996; Morrison, Tester and Gidley, 1993; Srichuwong et al., 2005a; Gerard et al., 2002). In this study, variations in granule size (Table 4.2), bound lipid content and amylopectin chain length distribution among cultivars of FB, BB and PB starches were not significant ($P < 0.05$). The faster rate of hydrolysis between the 9th and 12th day observed with FB starches can be attributed to rapid entry of H_3O^+ via the cracks on the granule surface (Fig. 4.1) and/or to the presence of less well ordered double helical organization (Fig. 4.1a, Table 4.4) within the crystalline lamella. This would render the α (1→4) and α (1→6) linkages in FB starches more accessible to attack by H_3O^+ . As discussed earlier, 'A' type crystallites are inferior (less perfect) than those of 'B' type

crystallites due to the presence of α (1 \rightarrow 6) branch points within the crystalline lamella in the former. This suggests that 'A' type crystallites would be more susceptible than 'B' type crystallites to hydrolysis by H_3O^+ . On this basis, differences in hydrolysis among cultivars of FB, BB and PB starches should have been influenced by differences in their proportion of 'B' type (Fig. 4.3) crystallites (for instance, among cultivars of FB, BB and PB starches, the extent of hydrolysis based on B-polymorphic content should have followed the order: SSNS1 ~ Fatima > F 18-20 ~ FB 9-4, 1519-10 ~ 1681a,b > CDC Jet ~ Espresso and Pecos > AC ole > AC pintoba ~ HR 119, respectively). However, among cultivars of FB SSNS1 having a much higher B-polymorphic content (26.4%) was hydrolyzed only to a slightly higher extent than FB 9-4 and F 18-20 cultivars in which the B-polymorphic content was in the range 20.6 – 20.9% (Fig. 4.6). Furthermore, among cultivars of PB, Pecos having a very low B-polymorphic content (7.9%) was hydrolyzed only to a slightly lower extent than the other cultivars in which the B-polymorphic content ranged from 13.7 to 17.3% (Fig. 4.6). This suggests that differences in acid hydrolysis among starch sources reflect the interplay between differences in granule surface characteristics and extent of double helical order within the crystalline lamella.

Figure 4.7 Acid hydrolysis (2.2 M HCl) profile of faba, black and pinto bean starches.



4.1.11. Retrogradation studies on pulse starches

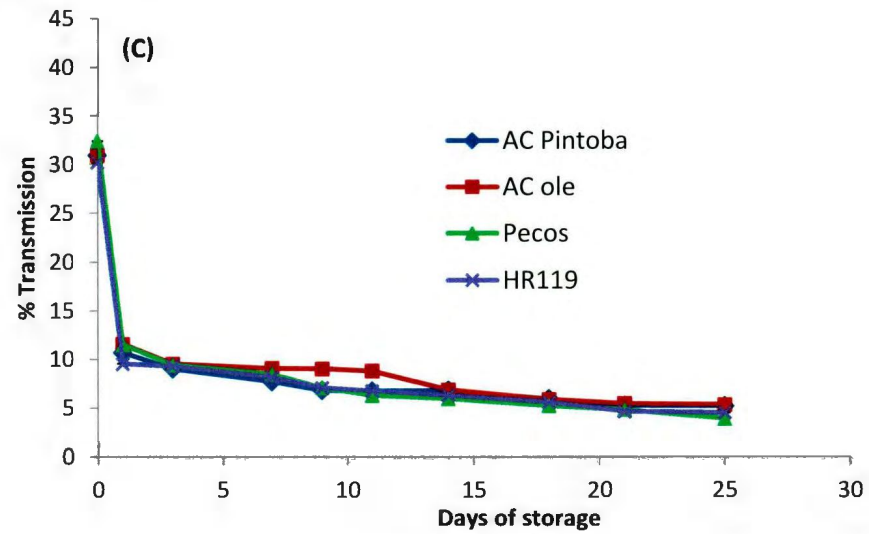
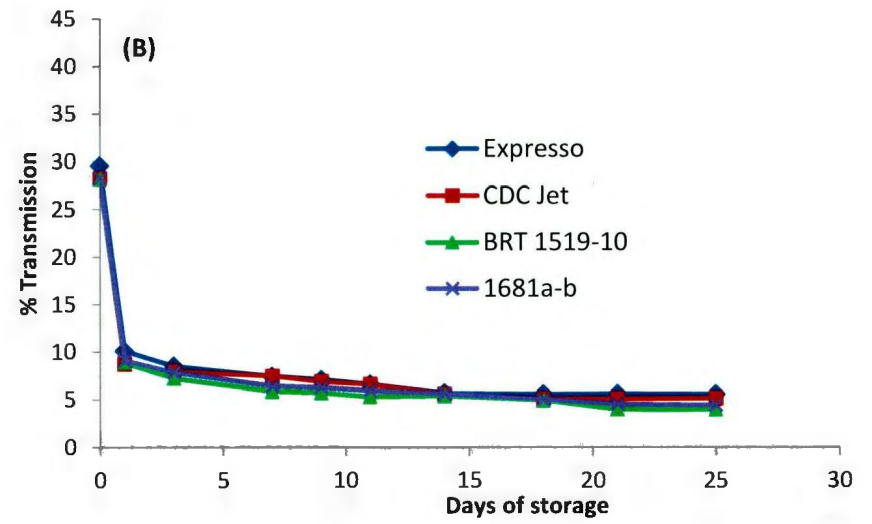
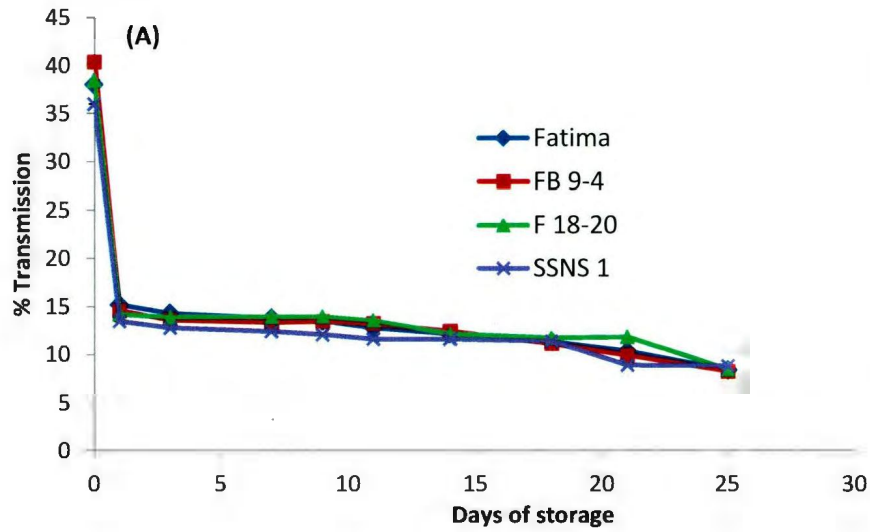
4.1.11. 1 Turbidity measurements

Turbidity effects have their origin in refractive index fluctuations over a distance scale comparable to the wavelength of observation (Gidley and Bulpin, 1989). In a polymer-solvent system this is caused by density fluctuations over the same distance scale and is most likely due to extensive polymer-polymer aggregation. The first stage of retrogradation has been shown to involve mainly interaction between amylose (AM) chains leading to crystallization, which is completed within the first few hours of storage, whereas, the second stage that occurs over longer periods (days) involves primarily interaction between amylopectin (AP) chains leading to crystallization (Silveiro et al., 1996). As illustrated in Fig. 4.8, the extent of light transmittance decreased rapidly in all starches during the first 24 h of storage (BB [17.70%] ~ PB [19.96%] > FB [15.20%]). Thereafter, light transmittance decreased gradually to about the same extent in all starches. At the end of the 25th day, the extent of decrease (not significant at $P < 0.05$) in light transmittance in FB, BB and PB starches were 23.90, 26.21 and 25.66%, respectively. No significant difference ($P < 0.05$) in light transmittance was also observed among cultivars of each starch source. The rapid decrease in light transmittance during the first 24 h (Fig. 4.8) reflects network formation (Lewen et al., 2003) resulting mainly from interaction between AM chains (AM-AM) that were leached out of the granules during gelatinization. This seems plausible, since interactions involving AP chains would be much slower due to its highly branched nature and would not be reflected during the time period. Orford et al. (1987) have shown by studies on gels (10-

40% w/w) from pulse, cereal and tuber starches, that the development of gel stiffness during the progress of retrogradation is related to the amylose solubilized during gelatinization. In all starches, the gradual decrease in transmittance between the 2nd and 25th day of storage (Fig. 4.8) reflects interactions among and between leached AM and AP chains. On the basis of AM leaching (FB > BB ~ PB [Fig. 4.4]), the extent of decrease in light transmittance (Fig. 4.8) should have also followed the same order as AM leaching, since polymer network formation between leached AM chains (Hoover and Hadziyev, 1981) during retrogradation would be more extensive in FB (due to higher amounts of leached AM) resulting in a greater decrease in light transmittance. However the observed order of decrease in transmittance (PB ~ BB > FB) suggests, that interaction between AP chains (AP-AP) during the progress of retrogradation may have been much weaker and/or slower in FB than in BB and PB, due to a higher increase in suspension viscosity (decreases AP chain mobility and enhances entanglement of AP chains within the AM network) resulting from the higher extent of leached AM during gelatinization (Fig. 4.4). Consequently, the contribution made by double helical associations of AP branches and the subsequent intermolecular crystallization of the outer branches of AP towards light transmittance would be lower in FB than in BB and PB. This would then explain why the extent of decrease in transmittance at the end of the 25th day of storage is lower in FB, in spite of higher extent of leached AM. It has been reported that light transmittance is influenced by large granules (Singh and Singh, 2003) and phosphate monoester content (Lim and Seib, 1993). However, FB, BB and PB starches were shown to exhibit only minor variations in large granule size distribution and no significant differences in their phosphate monoester content (Section 4.1.1). This suggests, the order

of decrease in % T (Fig. 4.8) among the starches, mainly reflects the interplay between the rate and extent of AM network formation ($FB > BB \sim PB$) and AP recrystallization ($BB \sim PB > FB$) during the storage period. Thus, based on turbidity measurements, the rate and extent of retrogradation follows the order: $PB \sim BB > FB$.

Figure 4.8 Turbidity profiles of faba bean (A), black bean (B) and pinto bean (C) starches stored at 25°C.



4.1.11. 2 Differential scanning calorimetry (DSC)

The retrogradation transition temperatures of the starch gels stored at 25°C for periods ranging from 2-25 days is presented in Table 4.6. DSC measurements were carried out at 50% starch concentration, since the maximum extent of starch recrystallization occurrence has been shown to be between 50 – 60% starch concentration (Longton and LeGrys, 1981; Gudmundsson and Eliasson, 1991). In all starches, the retrogradation endotherm appeared only after 2 days storage. T_o , T_p and T_c , which represents the onset, mid-point and conclusion of melting of crystallized amylopectin, respectively, were much lower (due to improper alignment of starch chains during association) than those of the native gelatinization endotherm (Section 4.1.8). However, $T_c - T_o$ was much broader (due to differences in size, stability and perfection of the crystallites formed during retrogradation) than that of the gelatinization endotherm (Section 4.1.8). Differences and the extent of changes in T_o , T_p and T_c (represents changes in crystalline stability) and $T_c - T_o$ (represents changes in crystalline perfection) within and among cultivars of FB, BB and PB starches were marginal (Table 4.6). The DSC data suggest that crystallites formed in FB, BB and PB starches during storage are similar in size, perfection and stability. This was not surprising since there was no significant difference in AP chain length distribution (Section 4.1.3) among the starches and their cultivars. The enthalpy (ΔH_r) of retrogradation, which reflects the thermal energy, associated with crystalline melting and dissociation and unravelling (resulting from disruption of inter and intra helical hydrogen bonds) of double helices increased on storage (Fig. 4.9). The mean increase in ΔH_r between the 2nd and 25th day in FB, BB and PB starches was 1.63, 3.18

and 3.14 J/g, respectively. During the first 2 days differences in ΔH_r values (significant at $P < 0.05$) among the starches followed the order: FB > BB > PB. Thereafter, ΔH_r values differed only marginally among FB, BB and PB starches. At the end of the storage period there was no significant difference ($P < 0.05$) in ΔH_r values among FB, BB and PB starches. As shown in Fig. 4.4, AM leaching is more extensive in FB than in the other starches. This suggests that AM-AP interactions during storage are probably more pronounced in FB than in BB and PB starches. Disruption of double helices formed between AM-AP interactions would require a higher input of thermal energy due to linearity of AM chains. This would then explain the ΔH_r value for FB starches being much higher than those of BB and PB starches at the initial (first 2 days) stage of retrogradation (Fig. 4.9). The slower rate of retrogradation shown by FB starches, reflects decreased AP chain mobility. FB starches exhibited a limiting value for ΔH_r on the 10th day, whereas in both BB and PB starches, limiting ΔH_r values were reached only on the 25th day. Cultivars of FB and BB starches exhibited nearly similar ΔH_r values throughout the storage period. As shown in Fig.4.4 the extent of AM leaching among PB cultivars was lower in AC pintoba. However, AC pintoba exhibited higher ΔH_r values than the other cultivars (AC pintoba > AC ole ~ Pecos ~ HR119) from day 6 onwards (Fig. 4.4). Since ΔH_r reflects the overall enthalpy change involved in: 1) melting of crystallites (formed due to associations between AM-AP and AP-AP chains) and 2) the dissociation of AP double helices (which may or may not have been involved in crystallite formation), the higher ΔH_r of AC pintoba could be attributed to its amylopectin content (74.1%) being higher than that of other PB (68.2 – 70.3%) cultivars (Section 4.1.1). This seems plausible, since the double helical content determined by ¹³C CP/MAS

NMR (Table 4.8) was much higher in AC pintoba (21.6%) than in the other PB cultivars (15.53 – 16.87%). Differences in ΔH_r among starches have been explained on the basis of differences in amylopectin chain length distribution (Shi and Seib, 1992; Silverio et al. 2000) and degree of phosphorylation (Thygesen et al. 2003). Silverio et al. (2000) have shown by studies on cereal, tuber and pea starches, that differences in AP chain length distribution have a significant impact on DSC parameters of retrograded starches. The above authors showed that AP chains with DP 6 and the population of chains of DP 18–19 were positively correlated to ΔH , whereas the correlation to the population of chains of DP 8–11 was negative. Thygesen et al. (2003) have shown by low field ^1H NMR relaxometry studies on A, B and C-type starches, that high phosphate content suppress retrogradation. However, starches used in this study did not exhibit any significant difference in amylopectin chain length distribution or phosphate monoester content (Section 4.1.1). Therefore, the marginal differences in the rate and extent of retrogradation among FB, BB and PB starches is mainly influenced by the interplay between the extent of AML (FB > BB ~ PB) and amylopectin content.

Table 4.6

Retrogradation transition temperatures of faba bean, black bean and pinto bean starches. *^{ab}

Starch Source	Days of storage at 25°C	Retrogradation transition temperatures (°C)			
		To ^c	Tp ^c	Tc ^c	Tc-To ^c
Faba bean	2	46.54±0.89 ^a	59.59±0.64 ^a	76.54±0.37 ^a	30.00±0.66 ^a
	6	46.96±0.59 ^a	60.16±0.47 ^{ab}	77.30±1.58 ^{ab}	30.35±1.86 ^a
	10	48.21±0.56 ^b	60.23±0.72 ^{ab}	77.33±0.83 ^{ab}	29.12±0.98 ^{ab}
	18	47.52±0.29 ^{ab}	60.95±0.38 ^{ab}	77.25±0.84 ^{ab}	29.73±0.75 ^{ab}
	25	50.12±0.57 ^c	61.65±0.40 ^b	78.21±1.28 ^b	28.09±1.07 ^b
Black bean	2	47.25±0.93 ^d	60.07±0.83 ^c	77.19±1.01 ^c	29.94±0.47 ^c
	6	48.00±0.71 ^d	60.17±0.57 ^c	77.10±0.98 ^c	29.09±0.56 ^c
	10	48.49±0.80 ^{de}	60.99±0.57 ^c	77.15±0.20 ^c	28.66±0.89 ^c
	18	50.14±0.40 ^e	61.19±0.60 ^c	79.64±0.52 ^d	29.50±0.70 ^c
	25	50.81±0.28 ^e	64.13±1.87 ^d	77.62±1.31 ^c	26.80±1.32 ^d
Pinto bean	2	47.22±1.05 ^f	59.96±0.71 ^e	77.17±0.78 ^c	29.95±0.63 ^{cg}
	6	49.26±0.51 ^g	60.10±0.72 ^e	76.88±0.58 ^e	27.63±0.70 ^f
	10	49.56±0.68 ^g	60.85±0.61 ^e	77.33±0.66 ^e	27.77±0.98 ^f
	18	49.13±1.00 ^g	60.84±0.68 ^e	79.20±1.37 ^f	30.08±0.69 ^g
	25	50.70±0.25 ^g	61.84±0.42 ^e	79.55±1.16 ^f	28.86±0.98 ^{ef}

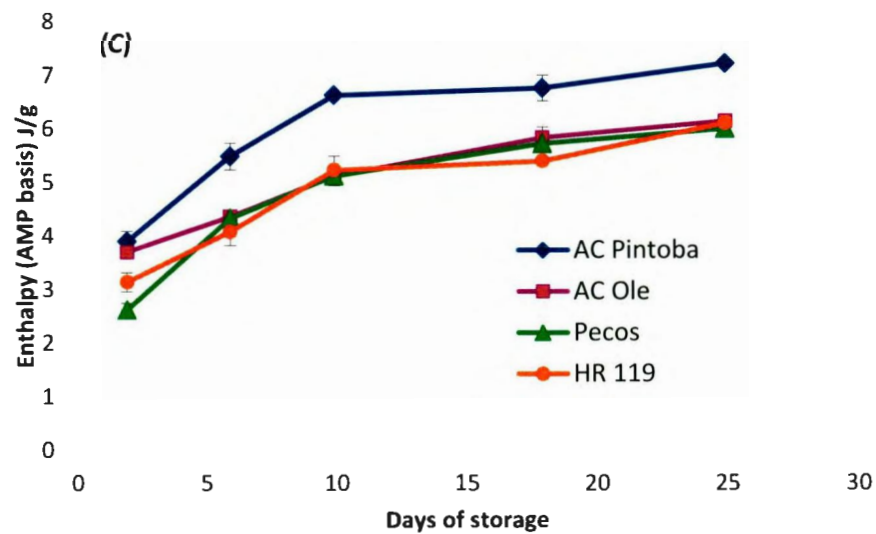
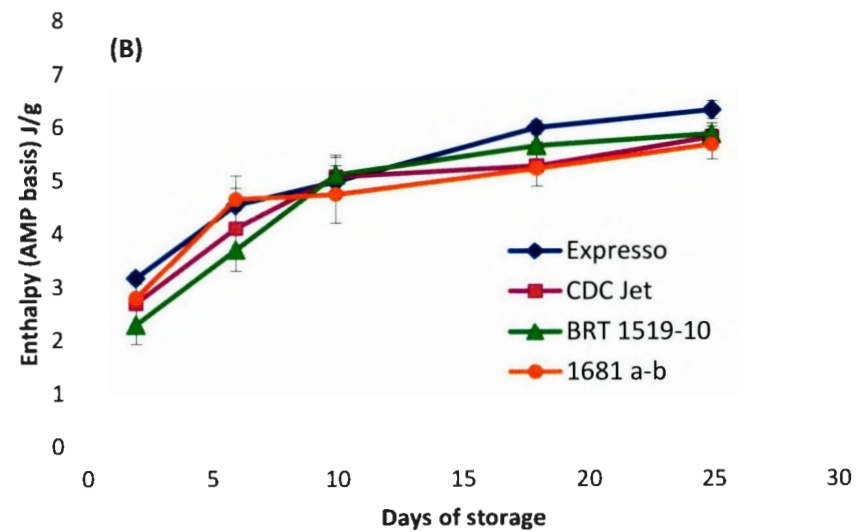
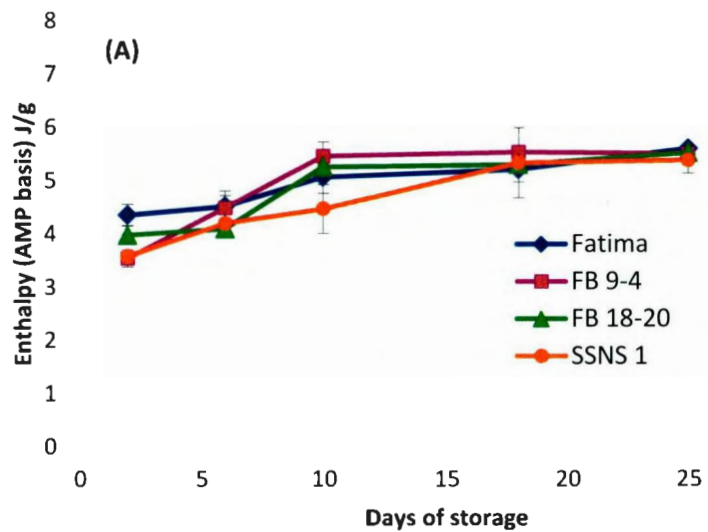
*Statistical analysis was performed among days of storage within each starch source

^a All data represent the mean of cultivars of each starch source. Values followed by the same superscript in each column for each starch source are not significantly different ($P > 0.05$) by ANOVA and Tukey's HSD test.

^b To, Tp, Tc and Tc-To among cultivars of each starch source was not significantly ($P > 0.05$) different.

^c To, Tp, Tc represents the onset, peak and end temperature, respectively.

Figure 4.9 Enthalpy profile of retrograded faba bean (A), black bean (B) and pinto bean (C) starches stored at 25°C.



4.1.11. 3 Attenuated total reflectance Fourier transform infrared spectroscopy (ATR-FTIR)

FTIR spectra of the retrograded starches in the range 800-1300 cm^{-1} are presented in Table 4.7. This region mainly reflects C-O and C-C stretching vibrations and is sensitive to changes in polymer conformation and starch hydration (Htoon et al., 2009). The bands at 1048 cm^{-1} and 1016 cm^{-1} reflect the amounts of ordered and amorphous regions, respectively. The band at 995 cm^{-1} is very sensitive to water content (van Soest et al., 1994). The ratio 995/1016 cm^{-1} represents the state of organization of the double helices localized inside crystallites. Capron et al. (2007) have shown in studies on lintners (highly crystalline material) obtained from mild acid hydrolysis of maize starches varying in amylose content, that the 995/1016 cm^{-1} ratio increases with hydration to a greater extent than under anhydrous conditions. This was interpreted as mesogenic units sliding over each other arranging helices localized inside the crystallites, into a flat-layered smectic structure. The author's concluded that the 995/1016 cm^{-1} ratio is sensitive to the nematic-smectic transition according to the side-chain liquid crystalline polymer model (Waigh et al., 2000). In all starches, the 1048/1016 cm^{-1} ratio and the 995/1016 cm^{-1} ratio increased on storage (Table 4.7). The increase in both ratios between the 2nd and 25th day followed the same order: PB > BB > FB. The extent of increase in the 1048/1016 cm^{-1} on storage varied significantly among cultivars of FB, BB and PB. However, variations in the above changes among cultivars of each starch source were marginal. In starches containing B-type crystallites, adjacent double helices are mainly linked by hydrate water bridges and to a limited extent by hydrogen bonding (Leach, McCowen and Schoch,

1959). This suggests that the water molecules released (syneresis) when double helices begin to aggregate together during the progress of retrogradation would increase chain mobility, thereby enabling better alignment of starch chains (nematic – smectic transition) at short range order. The increase in the 1048/1016 cm^{-1} and 995/1016 cm^{-1} ratios during the storage period, suggests improved helical alignment resulting in stronger aggregation between aligned helices. As discussed earlier, AM-AP interactions during retrogradation decrease AP chain mobility and their alignment within the crystalline lamella to a greater extent in FB than in BB and PB starches. This would then explain the lower extent of molecular order increase seen with FB starches (Table 4.7) at the end of the 25 days of storage. The difference in molecular order between retrograded PB and BB (PB > BB) can be explained as follows: as seen in Table 4.7, the improvement in helical alignment on storage was slightly higher in PB than in BB. This was reflected in the mean increase in the 995/1016 cm^{-1} ratio being higher in PB. The higher increase in molecular order (1048/1016 cm^{-1}) seen with PB is a reflection of stronger aggregation between helices. This seems plausible, since the increase in the 995/1016 cm^{-1} ratio among PB cultivars (Pecos > HR119 ~ AC pintoba > AC ole) followed the same order of increase in the 1048/1016 ratio (Pecos > HR119 ~ AC pintoba > AC ole). The FTIR data showed that the extent of retrogradation followed the order: PB > BB > FB. The discrepancy between the order of retrogradation assessed by DSC (PB ~ BB ~ FB) and FTIR could be attributed to the fact that ΔH_r values obtained by DSC measurements reflects mainly melting of recrystallized AP crystallites and disruption and dissociation of double helices formed during retrogradation, whereas FTIR measures the conformational change observed by measuring intensity changes in the conformational sensitivity bands in the

range 1300-800 cm^{-1} . The FTIR data show the extent to which the range of conformations present at the time of gelatinization is reduced during the progress of retrogradation due to the development of short range molecular order (helical order) developed as a result of interaction between AM-AM, AM-AP and AP-AP chains. This would then explain the observed discrepancies. A similar discrepancy between DSC and FTIR data was also reported by Ottenhof et al. (2005) on retrograded wheat, maize and waxy maize starches at intermediate water contents.

Table 4.7

Short range molecular order of retrograded faba, black and pinto bean starches measured by attenuated total reflectance–Fourier-transform infrared spectroscopy.*^a

Starch source	Intensity ratios (cm ⁻¹)			
	1048/1016 ^b		995/1016 ^c	
	2 days	25 days	2 days	25 days
Faba bean				
Fatima	0.624±0.003 ^a	0.750±0.000 ^a	1.08±0.005 ^a	1.12±0.005 ^a
FB 9-4	0.643±0.010 ^a	0.770±0.007 ^b	1.07±0.007 ^a	1.12±0.008 ^a
F 18-20	0.657±0.004 ^b	0.769±0.004 ^{ab}	1.11±0.001 ^b	1.12±0.008 ^a
SSNS 1	0.652±0.005 ^b	0.773±0.005 ^b	1.08±0.004 ^a	1.13±0.001 ^a
Mean	0.644±0.015^a	0.766±0.010^a	1.08±0.015^a	1.12±0.005^a
Black bean				
Expresso	0.658±0.003 ^c	0.772±0.007 ^c	1.12±0.000 ^c	1.14±0.005 ^b
CDC Jet	0.678±0.002 ^d	0.794±0.000 ^d	1.09±0.000 ^d	1.16±0.000 ^b
BRT 1519-10	0.641±0.004 ^c	0.799±0.004 ^d	1.09±0.003 ^d	1.16±0.010 ^b
1681 a-b	0.624±0.001 ^f	0.784±0.000 ^{cd}	1.05±0.000 ^e	1.13±0.006 ^b
Mean	0.650±0.023^b	0.787±0.012^b	1.09±0.023^a	1.15±0.011^b
Pinto bean				
AC Pintoba	0.666±0.005 ^e	0.827±0.005 ^e	1.09±0.001 ^f	1.16±0.005 ^c
AC Ole	0.649±0.002 ^h	0.789±0.005 ^f	1.10±0.002 ^f	1.14±0.001 ^c
Pecos	0.631±0.002 ⁱ	0.813±0.007 ^{ce}	1.05±0.000 ^h	1.15±0.000 ^c
HR 119	0.645±0.002 ^h	0.805±0.001 ^{fg}	1.08±0.000 ^f	1.15±0.006 ^c
Mean	0.648±0.014^b	0.809±0.015^c	1.08±0.022^a	1.15±0.004^b

*Statistical analysis was performed among cultivars within each starch source and also among the means for each starch source.

^aAll data represent the mean of triplicates. Values followed by the same superscript in each column for each starch source are not significantly different ($P > 0.05$) by ANOVA and Tukey's HSD test.

^bAmount of ordered crystalline domain to amorphous domains in starch.

^cReflects helical organization within the crystalline lamella.

4.1.11.4 Solid state ^{13}C cross-polarization / magic angle spinning nuclear magnetic spectroscopy (^{13}C CP/MAS NMR)

^{13}C CP/MAS NMR has been used to investigate both amorphous and crystalline starch (Gidley and Boceik, 1988; Morgan, Furneaux and Stanley, 1992). The development of rigid amorphous and crystalline starch components during aging of bread has been monitored using this technique (Morgan et al., 1992). The ^{13}C CP/MAS NMR spectrum has been shown to exhibit a significant loss in signal intensity during gelatinization, as more mobile, liquid like starch components are formed. However, during retrogradation, some of the mobile amorphous starch becomes more rigid and some recrystallized, resulting in an increased NMR signal intensity (Morgan et al., 1992). This increase in intensity reflects a decrease in segmental mobility resulting in more efficient cross-polarization from ^{13}C to the protons connected to it (Dickinson et al., 1998). ^{13}C CP/MAS NMR measures structural organization of starch at a shorter distance scale than X-ray diffraction and gives characteristic spectra for ordered helices and non-ordered chains. The ^{13}C CP/MAS NMR spectrum of native, gelatinized and retrograded FB, BB and PB starches stored at 4°C for 1 day and then at 25°C for 2 and 25 days are shown in Fig. 4.10. Cultivars of each starch source exhibited similar spectra (not shown). Therefore, only one cultivar from each source [Fababean (fatima), Blackbean (expresso), Pintobean (AC pintoba)] is illustrated in the Fig. 4. The intensity of the C-4 resonance (exhibits a broad signal at 82.0 ppm) and the proportion of double helical content in native, gelatinized and retrograded starches are presented in Table 4.8. The multiplicity of C-1 resonance has been shown to yield information on the type of unit cell (A or B).

An A-type crystal exhibits three peaks at 102, 101, and 100 ppm, whereas in a B-type crystal, the C-1 resonance exhibits two peaks at 101 and 100 ppm (Primo-Martin et al., 2007). This is due to the fact that in A-type and B-type crystals, the repeat unit is maltotriose and maltose, respectively. As shown in Fig. 4.10 it was difficult to ascertain the nature of the C-1 splitting (doublet or triplet) in native, gelatinized and retrograded starches. It is likely that this may have been due to the presence of both A and B-type crystals being present in different proportions in the native starch granules (Section 4.1.5). In all starches, C-1, C-2,3,5 and C-6 resonance intensities changed only marginally on retrogradation. However, C-4 resonance (at 82 ppm) whose intensity is solely due to amorphous contribution (Tan et al., 2007) increased on gelatinization (reflects loss of crystalline structure) but decreased on retrogradation (reflects development of rigid structures due to interaction between starch chains). The extent of this decrease at the end of 25th day followed the order: PB ~ BB > FB (Table 4.8). The double helical content increased nearly to the same extent BB and PB starches but was lower in FB (Table 4.8). Cultivars of FB, BB and PB exhibited significant variations with respect to change in amorphous and double helical content during the storage period. The above data showed that the rate and extent of retrogradation followed the order: PB ~ BB ~ FB.

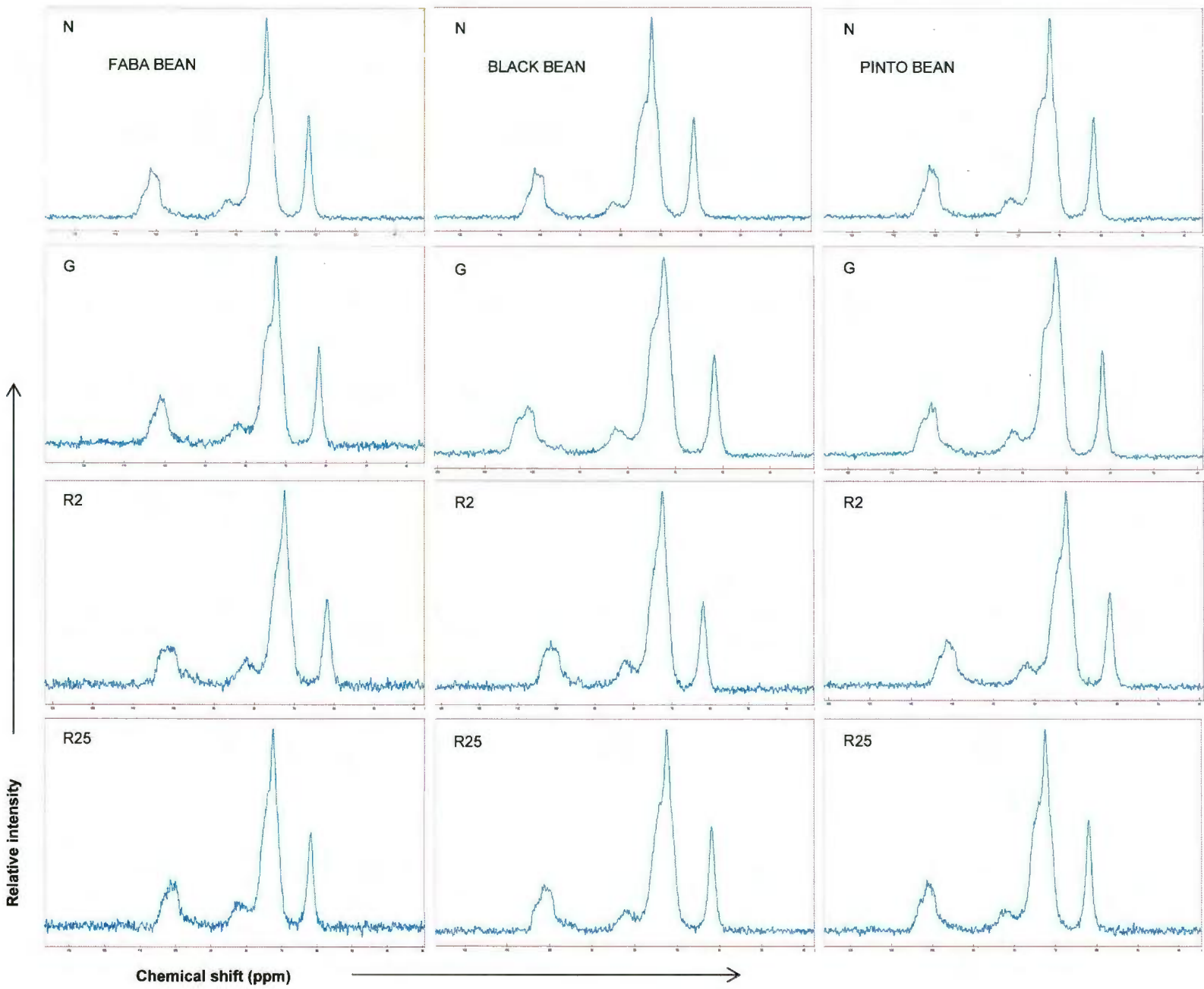
Table 4.8

¹³C CP/MAS NMR C-4 peak intensity of native, gelatinized, 2 days retrograded and 25 days retrograded faba bean, black bean and pinto bean starches^a

Starch source	C-4 peak intensity (ppm)				Double helix (%)		
	Native	Gelatinized	Retrograded		Native	Retrograded	
			2 days	25 days		2 days	25 days
Faba bean							
Fatima	38.19	78.26	51.02	45.67	24.63	6.93	15.47
FB 9-4	20.46	83.29	54.37	39.47	26.85	4.48	15.65
F 18-20	32.63	77.88	58.56	58.56	36.65	6.35	16.02
SSNS 1	39.25	98.75	60.91	58.92	33.33	3.79	15.21
Mean	32.63±8.62^a	84.55±9.79^a	56.22±4.39^a	50.66±9.67^a	30.37±5.58^a	5.38±1.49^a	15.59±0.34^a
Black bean							
Espresso	33.11	84.48	81.71	59.83	46.77	6.41	16.73
CDC Jet	72.53	75.2	72.53	51.63	49.69	5.95	15.83
1519-10	60.75	100.29	63.71	47.87	47.61	6.98	16.31
1681a-b	64.71	102.96	100.15	55.93	43.93	5.44	15.54
Mean	57.78±17.16^b	90.73±13.18^a	79.53±15.59^b	53.82±5.19^a	47.00±2.39^b	6.20±0.66^a	16.10±0.53^{ab}
Pinto bean							
AC pintoba	75.28	99.7	68.94	47.6	30.11	7.32	21.6
AC ole	58.55	92.82	74.74	66.36	38.93	6.42	16.51
Pecos	67.82	79.63	57.61	47.88	40.8	5.96	16.87
HR 119	68.02	84.56	59.6	51.71	32.23	7.22	15.53
Mean	67.42±6.86^b	89.18±8.88^a	65.23±8.04^b	53.39±8.85^a	35.52±5.15^c	6.73±0.65^a	17.63±2.71^b

^aThe maximum standard deviation for the ¹³C NMR analysis calculation was 2.8%

Figure 4.10 ^{13}C CP/MAS NMR spectra of native (N), gelatinized (G), 2 days retrograded (R2) and 25 days retrograded (R25) faba bean, black bean and pinto bean starches.



4.11.5 Wide angle X-ray diffraction (WAXS)

WAXS was used to assess changes in X-ray pattern, B-polymorph content and relative crystallinity (RC) of FB, BB and PB starches throughout the storage period (Table 4.9, Fig. 4.11). X-ray reflections correspond to the contributions of irregularly packed crystallites, small chain aggregates and isolated single helices (Lopez Rubio et al. 2008). The type of polymorph formed as a result of recrystallization is influenced by the storage temperature, water content and amylopectin chain length (Hizukuri, 1961). The diffractograms acquired immediately after gelatinization showed a diffuse X-ray pattern, which is typical of an amorphous material. This indicated that all crystallites were destroyed on gelatinization. All starches exhibited well-defined X-ray spectra on storage (characteristic of crystallinity development). In FB, all cultivars exhibited an A-type polymorph pattern on day 2 (characterized by peaks at 15° , 17° , 17.9° , 23° and 30° 2θ) and a mixed (A + B) – type polymorph pattern (characterized by peaks at 5.4° , 15° , 17° , 23° , 26° and 30° 2θ) on days 10 and 25 (Fig. 4.12). The presence of peaks at 5.4° , two peaks at 23° and 26° and the absence of a shoulder peak at 18.0° 2θ are characteristic of pure B-type crystalline polymorphs. However, none of the starches exhibited the two peaks at 23° and 26° 2θ). In all cultivars of FB, the intensity of the 5.4° 2θ peak increased, whereas those of the other peaks decreased with storage time (Fig. 4.12). In BB and PB starches, all cultivars exhibited mixed (A + B) polymorph patterns throughout the storage period. As in FB, the intensities of the peaks centered at 15° , 17° , 23° and 30° 2θ decreased in both BB and PB starches (PB > BB).

However, the intensity of the peak centered at $5.4^\circ 2\theta$ increased only marginally in BB and PB starches. The extent of this increase was much lower than in FB. At the end of the storage period, the mean B-polymorph content followed the order: FB > BB > PB (Table 4.9). The extent of increase in mean B-polymorph content between the 10th and 25th day was more pronounced in FB than in BB and PB starches. The absence of B-type unit cells in FB starches on day 2 (Table 4.9) is difficult to explain. Among cultivars of FB, BB and PB starches, the B-polymorph content on day 25 followed the order: SSNS-1 > FB 18-20 ~ FB 9-4 > Fatima, Expresso ~ 1519-10 > 1681a-b ~ CDC Jet, AC pintoba > HR 119 > Pecos ~ AC ole, respectively. It was interesting to observe that not only did retrograded FB, BB and PB starches revert to their native starch polymorphic composition (A + B), but also variations (significant at $P < 0.05$) in B-polymorphic content (FB > BB > PB) followed the same trend in both native and retrograded starches. RC of all starches increased with storage time (Table 4.9). On day 25, the mean RC differed only marginally among FB, BB and PB starches and their cultivars. The rate of increase in RC during storage was similar in FB, BB and PB starches. In this study, the increase in RC on storage in FB, BB and PB starches mainly reflects organization of double helices into A-type crystallites. This seems plausible for the following reasons: 1) on the 2nd day of storage, the mean RC of FB (16.60%) (lacking B-type crystallites) [Table 4] was nearly similar to that of BB (17.68%) and PB (17.12%) starches, and 2) on the 25th day of storage, the mean RC of FB (20.19%) was also similar to those of BB (21.33%) and PB (21.67%) starches, although the mean B-polymorphic content at the above time period was more pronounced in FB (33.76%) than in BB (26.38%) and PB

(21.86%) starches. This suggests that B-type unit cells formed during retrogradation are less well aligned to the X-ray beam and/or are smaller in size than A-type unit cells. The X-ray data suggest that FB, BB and PB starches retrograde to the same extent.

Table 4.9

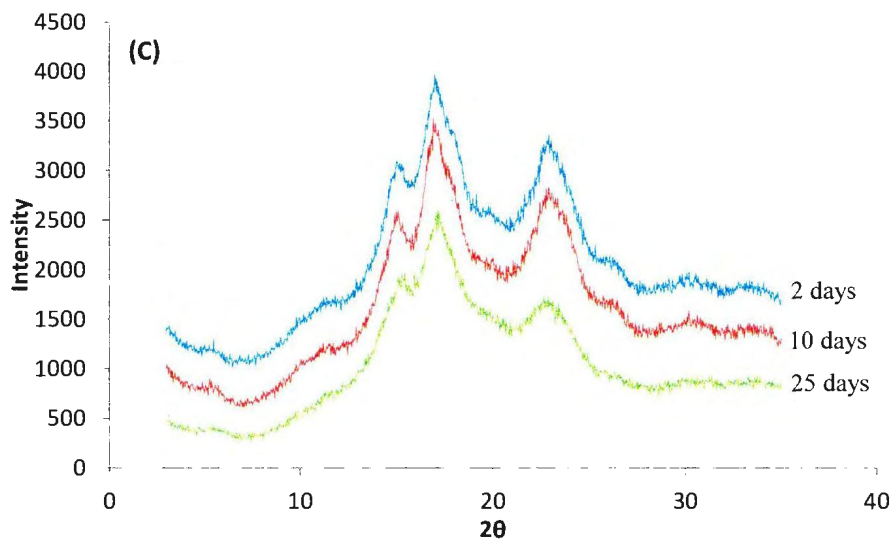
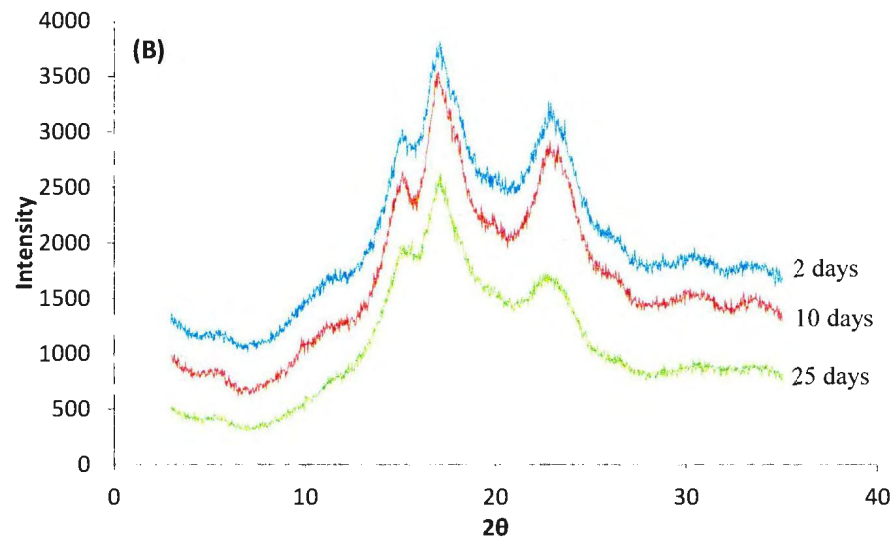
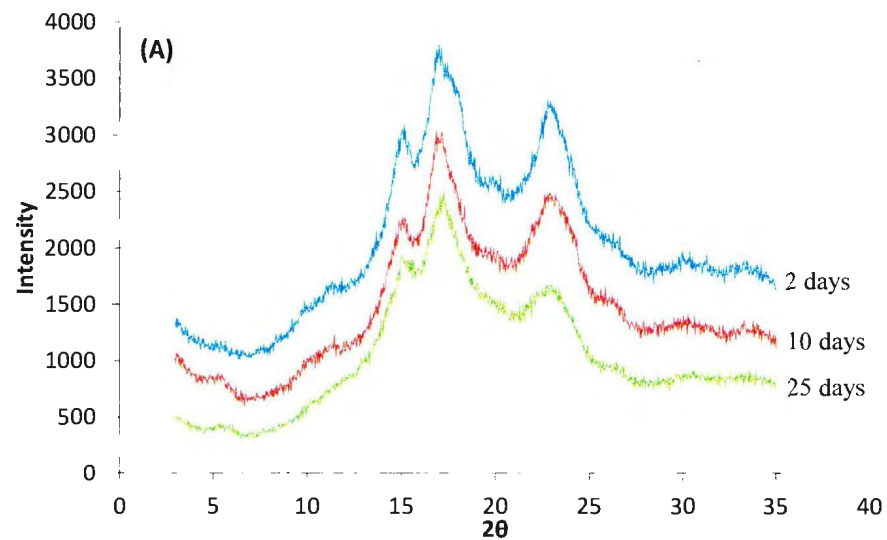
Relative crystallinity and B polymorphic content of retrograded faba, black and pinto bean starches measured by wide angle X-ray diffraction.*^a

Starch source	Crystallinity %			B polymorph %		
	2 days	10 days	25 days	2 days	10 days	25 days
Faba bean						
Fatima	16.55±1.02 ^a	18.00±0.96 ^a	20.34±0.08 ^a	0.00±0.00 ^a	28.42±0.27 ^a	29.31±0.46 ^a
FB 9-4	17.51±1.47 ^a	21.59±0.21 ^a	20.39±0.66 ^a	0.00±0.00 ^a	17.73±0.22 ^b	33.16±0.11 ^b
F 18-20	18.61±0.26 ^a	19.25±0.90 ^a	19.62±0.12 ^a	0.00±0.00 ^a	23.28±0.53 ^c	33.08±0.37 ^b
SSNS 1	13.72±0.01 ^b	18.47±0.40 ^a	20.42±0.40 ^a	0.00±0.00 ^a	28.07±0.11 ^a	39.50±0.53 ^c
Mean	16.60±2.09^a	19.33±1.59^a	20.19±0.38^a	0.00±0.00^a	24.38±5.01^a	33.76±4.22^a
Black bean						
Expresso	18.55±0.37 ^c	20.25±0.67 ^b	20.54±0.46 ^b	19.60±1.43 ^b	20.25±0.67 ^d	27.81±1.71 ^d
CDC Jet	18.23±0.37 ^c	18.72±0.84 ^b	20.06±0.12 ^b	16.35±1.30 ^{bd}	24.28±0.41 ^e	23.93±0.14 ^e
BRT 1519-10	15.70±0.39 ^d	20.18±0.49 ^b	21.64±0.27 ^{bc}	21.64±0.27 ^c	26.23±0.25 ^e	28.65±0.05 ^d
1681 a-b	18.22±0.79 ^c	20.69±0.89 ^b	23.11±0.47 ^c	14.46±0.52 ^d	18.80±0.00 ^d	24.40±0.11 ^e
Mean	17.68±1.15^a	19.96±0.86^a	21.33±1.35^a	18.01±3.22^b	22.39±3.45^{ab}	26.38±2.38^b
Pinto bean						
AC Pintoba	16.92±0.96 ^c	20.84±0.50 ^c	21.41±0.03 ^d	11.96±0.00 ^c	21.94±0.17 ^f	24.29±0.58 ^f
AC Ole	16.55±0.41 ^c	21.91±0.12 ^c	23.44±0.16 ^d	15.33±0.96 ^f	17.25±0.44 ^g	18.76±0.08 ^g
Pecos	17.54±0.38 ^c	20.40±0.24 ^c	21.33±0.87 ^d	16.72±0.00 ^g	17.98±0.00 ^g	19.01±0.81 ^g
HR 119	17.48±0.27 ^c	19.53±0.99 ^c	20.48±0.79 ^d	17.16±0.28 ^h	20.55±0.17 ^f	25.39±0.08 ^f
Mean	17.12±0.41^a	20.67±0.99^a	21.67±1.26^a	15.29±2.35^c	19.43±2.19^b	21.86±3.47^c

*Statistical analysis was performed among cultivars within each starch source and also among the means for each starch source.

^aAll data represent the mean of triplicates. Values followed by the same superscript in each column for each starch source are not significantly different (P < 0.05) by ANOVA and Tukey's HSD test.

Figure 4.11 X-ray diffraction patterns of retrograded faba bean (A), black bean (B) and pinto bean (C) starches stored at 25°C.



4.11.6 Enzyme hydrolysis of retrograded starches

The susceptibility of the retrograded starches (25 days) towards porcine pancreatic α -amylase at different time intervals of hydrolysis is presented in Table 4.10. At all-time intervals, the extent of hydrolysis followed the order: FB > BB > PB. The greatest difference in hydrolysis among the starches was seen after 3 h, where FB was hydrolyzed to a much greater extent (54.6%) than BB (40.91%) and PB (37.8%). The enzyme catalyzed hydrolysis of α -D (1 \rightarrow 4) glucosidic linkages has been shown to involve enzyme-induced ring distortion of one of the D-glucosyl residues from the 4C_1 chair conformation to a "half chair" conformation (Thoma, 1968). This ring distortion decreases the enthalpy of activation and increases the susceptibility of the glucosyl residues to nucleophilic attack by the functional groups on PPA and water. László et al. (1978) have shown that ring distortions or a "half chair" conformation is involved in the transition state of PPA. As shown in Fig. 4.4, AM leaching during gelatinization was more extensive in FB than in BB and PB (PB \sim BB). Consequently, interaction between AM-AM chains during storage would be more extensive in FB. Therefore, theoretically, FB should have been more resistant to PPA than PB and BB. This is based on the premise that interaction between linear AM chains would be very strong, thereby hindering the conformational transformation (${}^4C_1 \rightarrow$ half chair) required for accessibility of PPA towards the glycosidic oxygen. We speculate that the higher susceptibility of retrograded FB starches towards PPA may have resulted from interactions of leached AM with AP. AM-AP interactions during retrogradation have been reported by several researchers (Russell, 1987). It is likely, that AM-AP interactions may have partially

disrupted the crystalline structure of FB resulting in a crystalline structure that is less compactly packed in FB than in BB and PB starches. This decrease in chain packing density in the crystalline lattice would not only increase accessibility of PPA into the crystalline lattice, but would also facilitate the conformational transformation. The probability of AM-AP interaction would be greater in FB, due to greater extent of AM leaching (Fig. 4.4) during gelatinization. The presence of loosely packed crystallites in FB is also supported by FTIR data (Table 4.7), which showed that the molecular order in FB was much lower than in BB and PB. It was interesting to observe that the extent of PPA hydrolysis (FB > BB > PB) closely paralleled the difference in molecular order PB > BB > FB (Table 4.7).

Table 4.10

Amylase hydrolysis of 25 days retrograded faba bean, black bean and pinto bean starches.*^a

Starch Source	Time (hours)		
	3	24	72
Faba bean			
Fatima	57.34±0.15 ^a	69.15±0.19 ^a	71.43±0.36 ^a
FB 9-4	53.23±0.46 ^b	69.26±0.64 ^a	71.20±0.27 ^a
F 18-20	54.82±0.07 ^b	69.67±0.56 ^a	70.93±0.64 ^a
SSNS 1	53.03±0.18 ^b	69.47±0.65 ^a	70.39±0.84 ^a
Mean	54.61±1.99^a	69.39±0.23^a	70.99±0.44^a
Black bean			
Expresso	41.36±0.91 ^c	64.00±0.68 ^b	66.20±0.51 ^b
CDC Jet	40.93±0.64 ^c	63.34±0.50 ^b	65.41±0.23 ^b
BRT 1519-10	40.17±0.39 ^c	63.62±0.20 ^b	65.61±0.23 ^b
1681 a-b	41.18±0.17 ^c	63.10±0.28 ^b	65.91±0.57 ^b
Mean	40.91±0.52^b	63.52±0.39^b	65.78±0.35^b
Pinto bean			
AC Pintoba	38.48±0.63 ^d	60.83±0.00 ^c	63.12±0.70 ^c
AC Ole	38.86±0.27 ^d	60.05±0.61 ^c	63.94±0.62 ^c
Pecos	35.98±0.78 ^e	59.65±0.36 ^c	61.42±0.28 ^c
HR 119	38.06±0.68 ^d	59.05±0.78 ^c	62.93±0.86 ^c
Mean	37.84±1.29^c	59.89±0.75^c	62.85±1.05^c

*Statistical analysis was performed among cultivars within each starch source and also among the means for each starch source.

^aAll data represent the mean of triplicates. Values followed by the same superscript in each column for each starch source are not significantly different ($P > 0.05$) by ANOVA and Tukey's HSD test.

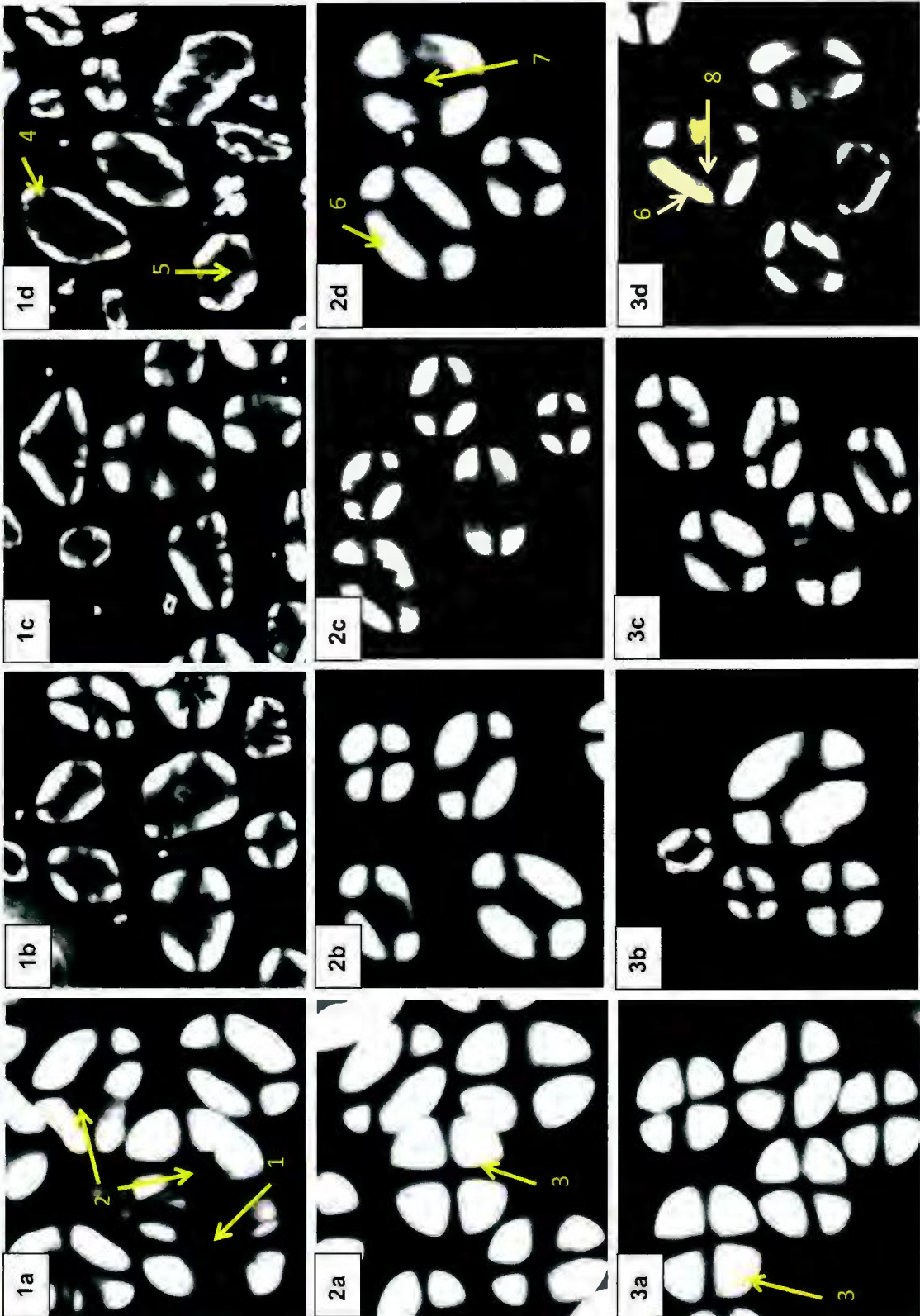
4.2. IMPACT OF HEAT-MOISTURE TREATMENT ON PULSE STARCH STRUCTURE AND PROPERTIES

4.2.1 Birefringence

The birefringence patterns (maltese cross) viewed under polarized light reflects radial arrangement of AP crystallites within the granules at right angles to the surface with their single reducing end group towards the hilum (Sivak and Preiss, 1998). All granules of both cultivars of native BB (Fig.4.12.2a) and PB (Fig.4.12.3a) exhibited strong birefringence patterns with a well-defined quadrant, (Fig.4.12; arrow 3). However, granules of both cultivars of FB exhibited weaker birefringence (Fig. 4.12.1a) with less well-defined quadrants and voids (Fig. 4.12.1a; arrow 2). The weaker birefringence pattern of native FB is indicative that the degree of order in molecular orientation is lower than in BB and PB. The impact of HMT on granule birefringence was more pronounced in FB (Figs. 4.12.1b, c, d) than in BB (Figs. 4.12.2b, c, d) and PB (Figs. 4.12.3b, c, d). On HMT, all starches [FB (Figs. 4.12.1b, c, d), BB (Figs. 4.12.2b, c, d) and PB (Figs. 4.12.3b, c, d)] exhibited decreased birefringence intensity at the granule periphery and development of voids at the granule center. Similar observations (Chung et al., 2009; 2010; Kawabata et al., 1994; Vermeylen, Goderis and Delcour, 2006) have also been reported on potato, corn, pea, lentil and navy bean starches during HMT (90–130°C; 17–30% moisture). The extent of the above changes increased with HMT temperature and followed the order: FB > BB ~ PB. For instance, at HMT120, the decrease in birefringence intensity in FB (Fig. 4.12.1d; arrow 4) was more pronounced than in BB (Fig. 4.12.2d; arrow 6) and PB (Fig. 4.12.3d; arrow 6), and occupied only a smaller area

around the peripheral regions of the granules. Furthermore, voids at the granule center (Fig. 4.12.1d; arrow 5) in FB were much larger than in BB (Fig. 4.12.2d; arrow 7) and PB (Fig. 4.12.3d; arrow 8). The decrease in birefringence intensity on HMT is indicative of a change in radial orientation of AP crystallites due to increased AP chain flexibility. This change is more pronounced in FB, due to weaker organization of AP crystallites within the crystalline domains, which facilitates greater chain flexibility during HMT.

Figure 4.12 Polarized light microscopy ($\times 200$) images of native (a), HMT80 (b), HMT100 (c), HMT120 (d) FB (Fatima; 1), BB (Expresso; 2) and PB (AC Pintoba; 3) starches, respectively. Arrows 1 (weak birefringence pattern); 2, 5, 7 (voids at the granular center); 3 (well defined birefringence pattern); 4, 6 (birefringence intensity at the granular periphery).



4.2.2 Amylopectin chain length distribution (HPAEC-PAD)

Our previous study (section 4.1.3) showed no significant difference in amylopectin chain length distribution (dp6-12 [19-21%], dp13-24 [53-55%], dp25-36 [13-15%], dp37-50 [8-11%]) and average chain length (19-20%) between and among genotypes of native FB, BB and PB. The above parameters remained unchanged in FB, BB and PB at all HMT temperatures (Table 4.11). This implies that covalent bonds linking glucose units in starch chains forming the AP crystallites were not degraded under the HMT conditions (MC 23%; 80, 100, 120°C; 12 h). Varatharajan et al. (2010) have also observed constancy in amylopectin chain length distribution on HMT of normal and waxy potato starches at 100°C (24% moisture).

Table 4.11

Amylopectin chain length distribution of native and HMT faba bean, black bean and pinto bean starches determined by HPAEC.¹

Starch source	Degree of Polymerization ² (DP) %				CL ³
	6-12	13-24	25-36	37-50	
Faba bean					
Fatima native	21.69±1.83 ^a	53.30±0.67 ^a	13.74±1.84 ^a	11.27±0.68 ^a	20.52±0.60 ^a
Fatima 80	21.14±1.71 ^a	56.27±0.79 ^b	13.96±1.21 ^a	8.63±0.29 ^b	19.87±0.24 ^a
Fatima 100	22.73±1.53 ^a	55.65±0.16 ^b	13.02±1.90 ^a	8.60±0.21 ^b	19.63±0.31 ^a
Fatima 120	21.62±1.71 ^a	55.83±0.30 ^b	13.89±1.49 ^a	8.65±0.09 ^b	19.82±0.30 ^a
FB 9-4 native	20.07±2.58 ^a	53.13±2.63 ^a	15.00±3.64 ^a	11.80±1.56 ^a	20.96±1.08 ^a
FB 9-4 80	20.37±1.67 ^a	55.73±2.10 ^a	14.90±0.03 ^a	9.00±0.40 ^b	20.13±0.01 ^a
FB 9-4 100	21.83±1.14 ^a	54.61±1.05 ^a	14.39±0.52 ^a	9.17±0.43 ^b	20.01±0.06 ^a
FB 9-4 120	21.80±1.79 ^a	55.78±0.54 ^a	13.28±2.16 ^a	9.13±0.17 ^b	19.86±0.46 ^a
Black bean					
Expresso native	19.85±0.94 ^a	53.62±0.74 ^a	16.48±0.25 ^a	10.06±0.05 ^a	20.71±0.07 ^a
Expresso 80	20.40±1.89 ^a	55.44±0.20 ^a	15.10±1.42 ^a	9.07±0.27 ^a	20.23±0.37 ^a
Expresso 100	22.50±2.60 ^a	53.27±0.67 ^a	14.14±2.72 ^a	10.09±0.79 ^a	20.30±0.18 ^a
Expresso 120	21.42±2.15 ^a	55.98±1.37 ^a	13.43±2.99 ^a	9.18±0.53 ^a	20.06±0.52 ^a
BRT 1519-10 native	18.05±0.65 ^a	51.64±1.26 ^a	18.18±0.02 ^a	12.12±0.63 ^a	21.67±0.13 ^a
BRT 1519-10 80	20.53±2.15 ^a	56.76±1.00 ^b	14.64±2.44 ^a	8.08±0.70 ^b	19.95±0.60 ^b
BRT 1519-10 100	19.07±0.67 ^a	54.34±0.69 ^{ab}	16.80±0.08 ^a	9.79±0.10 ^b	20.76±0.04 ^{ab}
BRT 1519-10 120	21.09±2.13 ^a	54.45±0.67 ^{ab}	14.82±2.12 ^a	9.64±0.66 ^b	20.35±0.19 ^b
Pinto bean					
AC Pintoba native	22.54±2.53 ^a	54.05±0.03 ^a	14.46±0.49 ^a	8.95±2.01 ^a	19.86±0.88 ^a
AC Pintoba 80	20.36±2.00 ^a	54.88±0.34 ^a	15.23±2.39 ^a	9.53±0.05 ^a	20.39±0.45 ^a
AC Pintoba 100	21.82±2.29 ^a	54.16±0.83 ^a	14.72±2.77 ^a	9.30±0.35 ^a	20.21±0.58 ^a
AC Pintoba 120	20.90±2.11 ^a	55.24±1.06 ^a	14.26±3.61 ^a	9.60±0.43 ^a	20.36±0.41 ^a
Pecos native	20.06±2.02 ^a	54.40±1.46 ^a	15.10±3.45 ^a	10.44±0.03 ^a	20.73±0.50 ^a
Pecos 80	19.18±2.27 ^a	55.55±1.09 ^a	15.48±2.85 ^a	9.78±0.51 ^a	20.61±0.66 ^a
Pecos 100	17.93±0.80 ^a	54.99±1.27 ^a	17.21±0.08 ^a	9.86±0.39 ^a	20.97±0.06 ^a
Pecos 120	17.96±0.69 ^a	53.96±0.95 ^a	17.67±0.01 ^a	10.41±0.25 ^a	21.16±0.01 ^a

¹All data represent the mean of triplicates. Values followed by the same superscript in each column for each starch source are not significantly different ($P > 0.05$) by ANOVA and Tukey's HSD test.

²DP_n: indicates degree of polymerization. Total relative area was used to calculate the percent distribution.

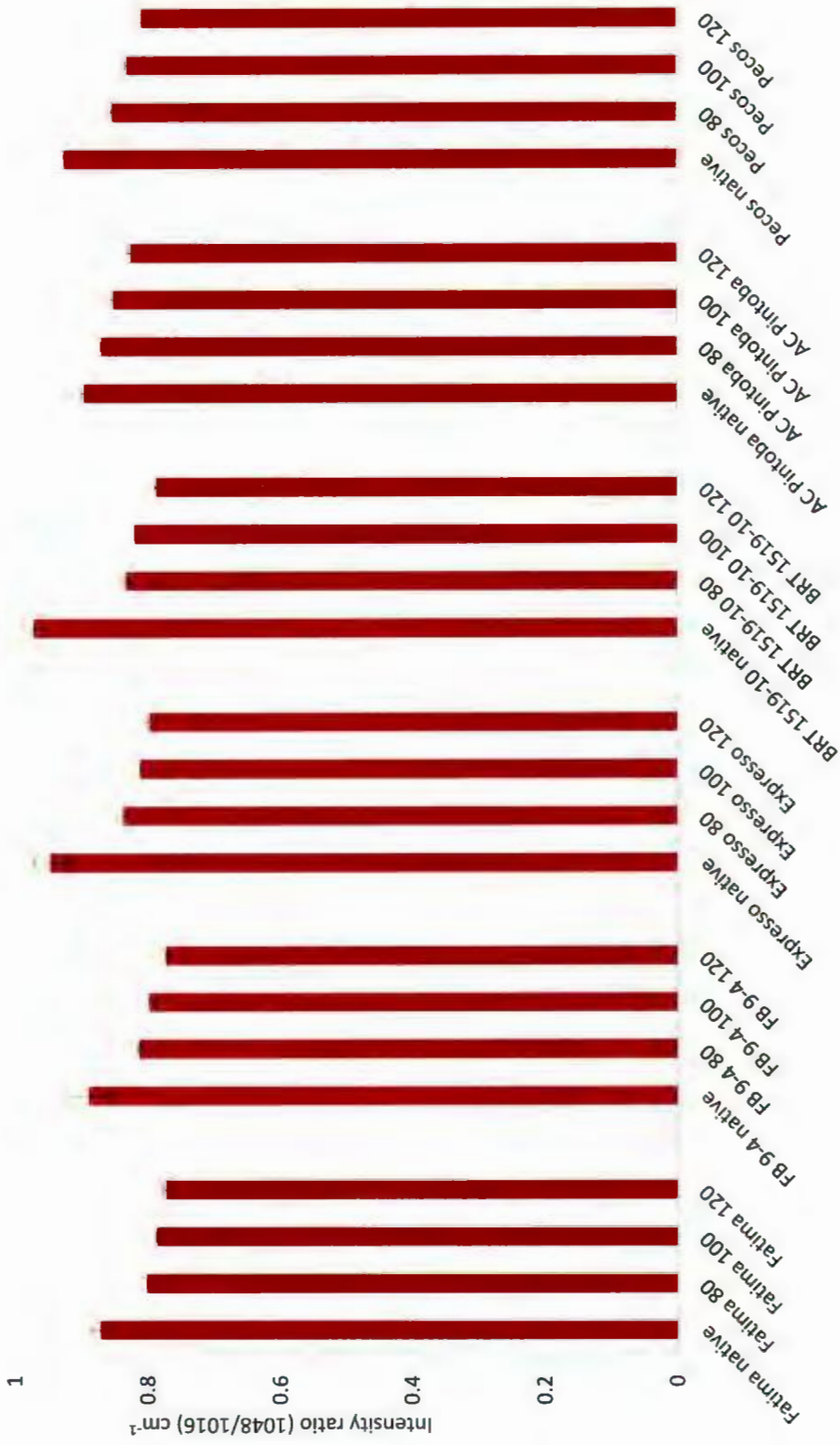
³Average chain length (CL) calculated by $\sum(DP_n \times \text{peak area}) / \sum(\text{peak area}_n)$.

4.2.3 Attenuated total reflectance Fourier transform Infra-red Spectroscopy (ATR-FTIR)

ATR-FTIR spectrum of starch has been shown to be sensitive to changes in structure on a molecular level (short range order) (Sevenou et al., 2002). Short range order reflects double helical order as opposed to long range order related to packing of double helices (detected by X-ray diffraction). The penetration depth of the IR beam in the ATR-FTIR system is about 2 μm . Thus, organization investigated by ATR-FTIR is limited to the regions near the granule surface. The ATR-FTIR absorbance at 1048 cm^{-1} is related to crystallinity [since this band increases with crystallinity]. In contrast, the band at 1016 cm^{-1} has been attributed to vibrational modes within the amorphous domains of starch granules [since this band has been observed to decrease with increase in crystallinity (van Soest, Tournois, de Wit and Vliegthart, 1995)]. Thus, the ratio $1048/1016\text{ cm}^{-1}$ has been used to express the amount of ordered crystalline domains to amorphous domains in starches (van Soest et al., 1995). HMT decreased the $1048/1016\text{ cm}^{-1}$ ratio (HMT120 > HMT100 > HMT80) in FB, BB and PB (Fig. 4.13). The extent of this decrease at all HMT temperatures, varied significantly among cultivars of each starch source. For instance, at HMT120, the above decrease, between cultivars of FB, BB and PB ranged from 11.3 – 13.2%, 15.7 – 19.0% and 7.8 – 12.6%, respectively. The decrease in molecular order is indicative of reorientation of double helices. The variation in molecular order decrease between cultivars of FB, BB and PB suggests, that double helical packing density (compact or loose) near the vicinity of the granule surface may

have been different. A decrease in the molecular order has also been observed in pea and lentil starches subjected to HMT (100° and 120°C) at 30% moisture for 2 h (Chung et al., 2009).

Figure 4.13 Degree of molecular order at the granular surface ($1048/1016\text{ cm}^{-1}$) of native and HMT FB, BB and PB starches determined by ATR-FTIR spectroscopy.



4.2.4 X-ray diffraction, patterns and crystallinity

X-ray patterns are illustrated only for genotypes of FB (fatima), BB (expresso) and PB (AC pintoba) [Fig.4.14], since the X-ray pattern of the other genotype of FB, BB and PB exhibited similar trend and differences in relative crystallinity (RC) between genotypes (section 4.1.5) of native FB (20.2–20.7%), BB (20.4–21.3%) and PB (22.1–23.1%) was not significant ($P>0.05$). Native FB, BB and PB starches showed a mixed A+B type X-ray pattern with reflections centered at 5.5° , 15.0° , 17.0° , 23.2° , 26.2° , 30.4° and $34^\circ 2\theta$ (Fig. 4.14). HMT80 increased RC of FB, BB and PB cultivars in the range 8.3 – 8.5%, 4.9 – 8.0% and 4.4 – 5.3%, respectively. However, the RC of all starches at HMT100 and HMT120 (HMT100 ~ HMT120) were lower than that at HMT80, but higher than that of their native counterparts (Table 4.12). The amount of B-type unit cells (indicative of a peak at $5.5^\circ 2\theta$) decreased significantly ($P<0.05$) in genotypes of FB (25.05 to 10.17%), BB (17.73 to 3.33%) and PB (16.72 to 5.34%) at HMT80 (Fig. 4.14, Table 4.12). However, this peak was not seen among the cultivars of FB, BB and PB at HMT100 and HMT120 (Fig. 4.14). HMT changed the X-ray pattern of FB, BB and PB (Fig.4.14) from A+B to a pure A-type pattern (this transformation was fully complete at HMT100). In all starches amorphous area (area between the experimental data and base line – area under the crystalline peak [Fig. 4.14]) decreased with increase in HMT temperature [X-ray patterns are illustrated only for cultivars of FB [fatima], BB [expresso] and PB [AC pintoba] [Fig. 4.14], since other cultivars of FB, BB and PB exhibited similar trends]. Gunaratne and Hoover (2002) have suggested that changes in X-ray pattern on HMT of

starches containing the B-type unit cells is due to dehydration of the 36 water molecules in the central channel of the B-type unit cell and to the movement of a pair of double helices into the central channel. Vermeulen et al. (2006) have suggested that double helical movement during HMT could occur laterally and/or along the vertical axis. The movement of double helices has been shown to cause disruption of crystallites in starches containing pure B-type unit cells (Hoover, 2010). However, in this study, the increase in RC (Table 4.12), and constancy in amylopectin chain length distribution (Table 4.11) and enthalpy of gelatinization (Table 4.13) at all HMT temperatures, suggest that crystalline structure was not disrupted on HMT (crystallite disruption on HMT would have resulted in general broadening of all X-ray reflections). Singh et al. (1995) have shown that the crystal size of B-type starches, and the number of crystal lattice planes perpendicular to the observed X-ray reflection is larger and higher than in cereal (A-type) and pulse (C-type) starches, respectively. On this basis, the transformation of B-type unit cells in FB, BB and PB to A-type unit cells on HMT may have been accompanied by a decrease in crystal size. The increase in RC on HMT (Table 4.12) suggests that the transformation of B to A-type crystals may have resulted in the newly formed smaller A-type crystals being able to pack together in a crystalline array more closely than the larger B-type crystals present in the native starch. Differences in RC (HMT80 > HMT100 > HMT120) (Table 4.12) suggest that due to the increased kinetic energy imparted to starch chains at the higher temperatures of HMT (> 100°C), double helical alignment within the crystalline lamellae and crystallite orientation to the incoming X-ray beam may have been less well organized than at HMT80.

Figure 4.14 X-ray pattern of native and HMT cultivars of FB (Fatima), BB (Expresso) and PB (AC pintoba). The arrow depicts the amorphous area (area between the experimental data and base line – area under the crystalline peak).

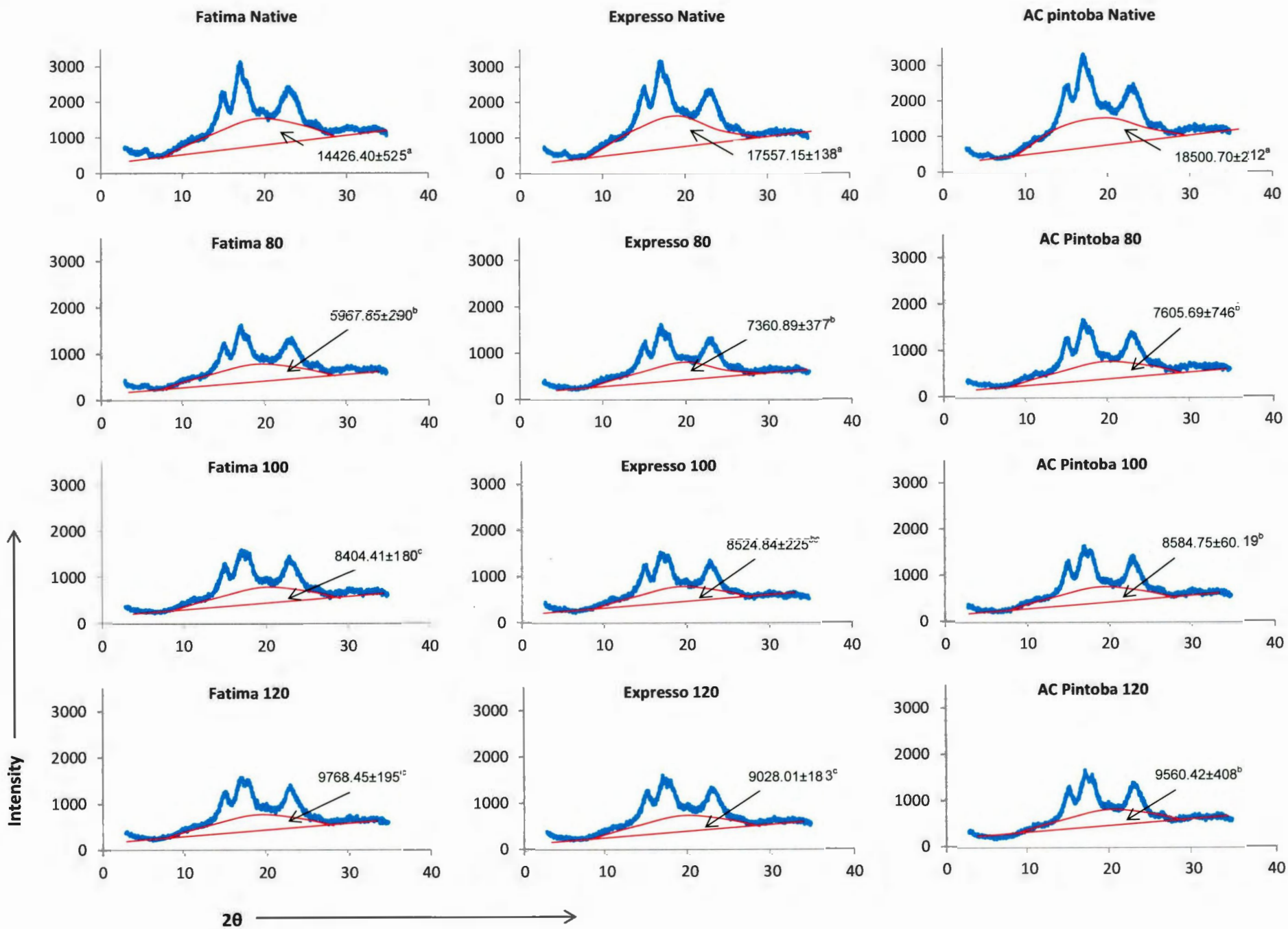


Table 4.12

Relative crystallinity and B polymorphic content of native and heat moisture treated faba, black and pinto bean starches.¹

Starch source	Crystallinity %	B polymorph%
Faba bean		
Fatima native	20.71±0.05 ^a	25.05±1.32 ^a
Fatima 80	29.01±0.41 ^b	10.17±1.03 ^b
Fatima 100	26.49±1.16 ^c	0.00±0.00 ^c
Fatima 120	25.99±0.77 ^c	0.00±0.00 ^c
FB 9-4 native	20.21±0.55 ^a	20.62±1.00 ^a
FB 9-4 80	28.68±0.08 ^b	9.68±0.02 ^b
FB 9-4 100	25.14±1.04 ^c	0.00±0.00 ^c
FB 9-4 120	26.22±0.32 ^c	0.00±0.00 ^c
Black bean		
Expresso native	20.44±0.56 ^a	17.73±0.11 ^a
Expresso 80	28.47±0.12 ^b	3.33±0.01 ^b
Expresso 100	24.56±0.94 ^c	0.00±0.00 ^c
Expresso 120	24.57±0.21 ^c	0.00±0.00 ^c
BRT 1519-10 native	21.31±0.69 ^a	15.42±1.55 ^a
BRT 1519-10 80	26.17±0.15 ^b	6.40±0.06 ^b
BRT 1519-10 100	24.34±1.26 ^c	0.00±0.00 ^c
BRT 1519-10 120	23.22±1.55 ^c	0.00±0.00 ^c
Pinto bean		
AC Pintoba native	23.14±0.11 ^a	16.72±0.91 ^a
AC Pintoba 80	27.56±0.79 ^b	5.34±0.77 ^b
AC Pintoba 100	24.33±0.44 ^c	0.00±0.00 ^c
AC Pintoba 120	23.51±0.95 ^{ac}	0.00±0.00 ^c
Pecos native	22.09±0.01 ^a	7.91±0.32 ^a
Pecos 80	27.43±0.18 ^b	5.44±0.22 ^b
Pecos 100	25.04±0.66 ^c	0.00±0.00 ^c
Pecos 120	24.88±0.87 ^c	0.00±0.00 ^c

¹All data represent the mean of triplicates. Values followed by the same superscript in each column for a particular bean are not significantly different ($P < 0.05$) by ANOVA and Tukey's HSD test.

4.2.5 Differential scanning calorimetry (DSC)

The gelatinization temperatures ([To-onset], [Tp-midpoint] and [Tc-conclusion]), gelatinization temperature range (Tc-To) and enthalpy of gelatinization (ΔH) of native and HMT starches are presented in Table 4.13. To, Tp and Tc represent crystalline stability, whereas, ΔH reflects the melting of AP based crystals with potential contributions from both crystal packing and helix melting enthalpies (Lopez-Rubio et al., 2008). In all genotypes of FB, BB and PB, To, Tp and Tc increased with increase in HMT temperature (HMT120 > HMT100 > HMT80; Table 4.13). Furthermore, in all genotypes, the extent of increase in To, Tp and Tc between HMT80 and HMT100 was more pronounced than between HMT100 and HMT120. In most genotypes, there was no significant difference in To, Tp and Tc at HMT100 and HMT120. BRT 1519-10 behaved differently from other genotypes in exhibiting no significant difference ($P > 0.05$) in Tp at HMT80. Increases in To, Tp and Tc have also been observed on HMT (120°C; 30%MC) of pea, lentil and navy bean starches (Chung et al., 2010). This increase represents melting of A-type crystallites (A-type crystallites being more compact have been shown to melt at a higher temperature than B-type crystallites [Jenkins, Cameron & Donald, 1993]) formed during the polymorphic transformation (A+B→A) and those formed due to interaction between AM-AP and AP-AP chains during HMT. These interactions can be explained as follows: the increase in thermal energy imparted to starch chains on HMT would increase flexibility in AM chains and in the spacers (segments that link AP double helices to the backbone [Fig. 4.15]). Increased spacer flexibility would impart sufficient mobility to adjacent double helices to interact with each other via hydrogen bonding.

Increase in AP chain mobility would also favor interactions with AM chains that may be interspersed among amylopectin clusters in the amorphous and crystalline regions (Fig. 4.15). The above interactions increases crystalline stability and also decreases starch chain flexibility in the bulk and intercrystalline amorphous regions during granular swelling. Consequently, the amorphous regions would require a higher input of thermal energy to incur swelling that could contribute to the disruption of the crystalline region during gelatinization. Increases in T_o , T_p and T_c on HMT were nearly similar between genotypes of FB, but were significantly different between genotypes of BB (expresso > BRT 1519-10) and PB (AC pintoba > pecos). Since AP chain length distribution was not significantly different among genotypes, the extent of increase in T_o , T_p and T_c among genotypes of FB, BB and PB mainly reflects the extent to which AM and AP chains within native granules are able to interact during HMT. This in turn would depend on the organization (compact vs loose packing) of AM and AP chains within the granule interior. At HMT80, T_c - T_o increased marginally among genotypes of FB, but decreased significantly ($P < 0.05$) in BB (expresso ~ BRT 1519-10) and PB (AC pintoba ~ pecos). However, T_c - T_o increased significantly ($P < 0.05$) at HMT100 and HMT120 (FB > BB ~ PB [Table 4.13]). The wider increase in T_c - T_o among the genotypes of FB reflects greater variation in crystalline stability. Amylose leaching data (Table 4.13) showed that AM chains in FB genotypes were more loosely organized than in genotypes of BB and PB. Consequently, AM-AP interaction during HMT would be more pronounced in FB. Thus, the wider range (T_c - T_o) of crystallite melting with FB genotypes (Table 4.13) reflects melting of both AP-AP and AM-AP crystallites. In contrast, in genotypes of BB and PB, T_c - T_o represents mainly melting of AP-AP crystallites. The ΔH of FB

genotypes, BB (BRT 1519-10) and PB (AC pintoba) remained unchanged at all HMT temperatures. This is indicative that the breakage of covalent bonds and/or double helical dissociation (due to breakage of inter and intra helical hydrogen bonds) and helical unravelling did not occur on HMT. However, at HMT100 and HMT120, genotypes of BB (expresso) and PB (pecos) exhibited a slight decrease in ΔH (Table 2). This may have been due to a breakage of a few inter and intra helical hydrogen bonds, rather than breakage of covalent bonds, since at HMT100 and HMT120, the RC (Fig.4.14) of both expresso (24%) and pecos (24-25%) were significantly ($P < 0.05$) higher than their native counterparts (expresso [20%], pecos [22%]), and their amylopectin chain length distribution remained unaltered at the above temperatures. However, decreased ΔH following HMT (100-120°C; at 30%MC) has been reported in pea, lentil and navy bean starches (Chung et al., 2009; 2010). It is likely, that this discrepancy with respect to the direction (increase or decrease) of change in ΔH on HMT, may have been due to differences with respect to starch source, moisture content, starch: water ratio (during gelatinization) and organization of AM and AP (compactly or loosely packed) within the granule interior.

Figure 4.15 The diagram illustrates changes to AM and AP chain flexibility and interactions between and among AM and AP chains during the progress of heat-moisture treatment. **○** - The circled section illustrates the movement of the spacers (during HMT) bringing the adjoining double helices closer together.

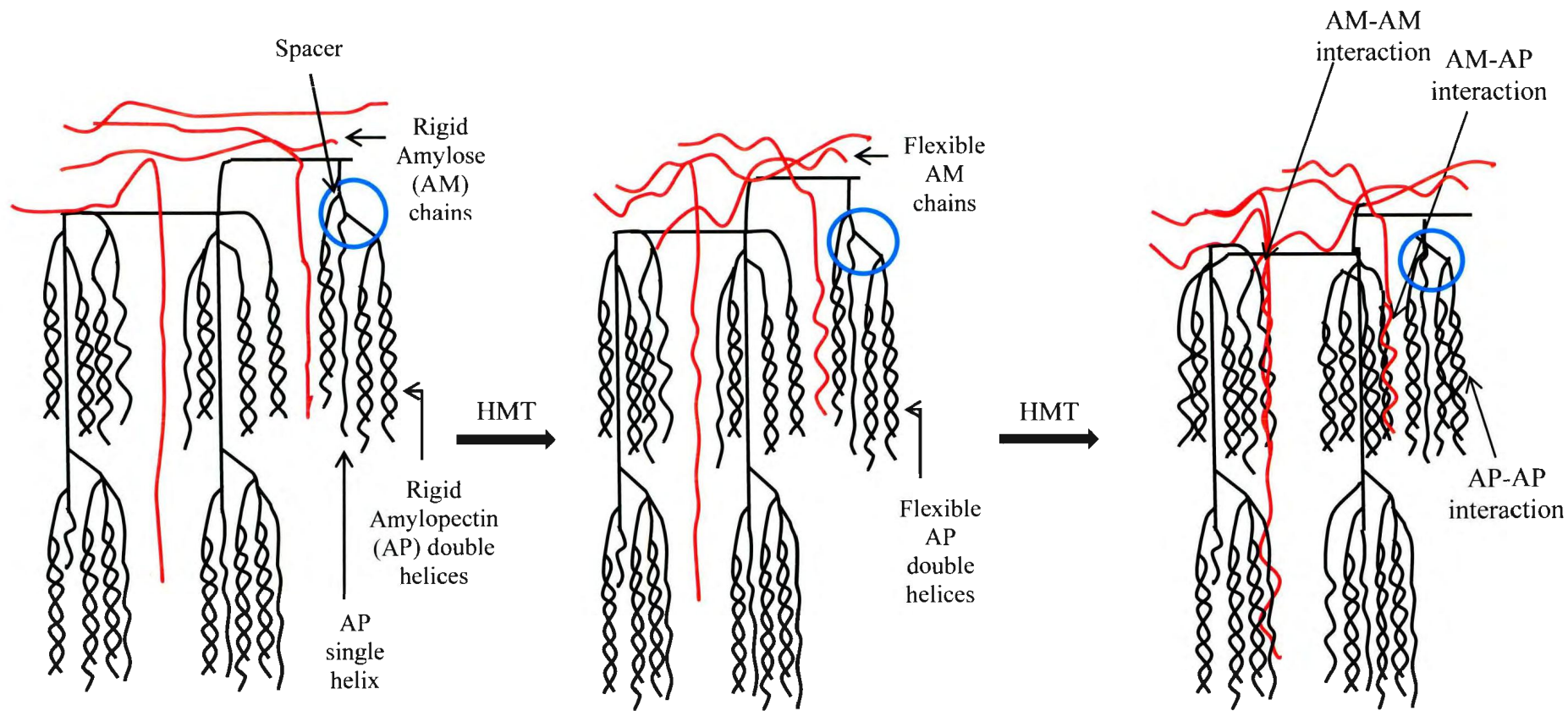


Table 4.13 Gelatinization transition parameters of native and HMT faba bean, black bean and pinto bean starches. ¹

Starch source	Gelatinization transition parameters				
	Onset Temp (°C)	Peak Temp (°C)	End Temp (°C)	T _c -T _o (°C)	Enthalpy (J/g)
Faba bean					
Fatima native	62.55±0.05 ^a	66.67±0.00 ^a	74.47±0.08 ^a	11.92±0.13 ^a	10.25±0.02 ^a
Fatima 80	66.14±0.02 ^b	71.93±0.12 ^b	78.41±0.42 ^b	12.28±0.45 ^a	10.48±0.46 ^a
Fatima 100	65.28±0.01 ^b	78.32±0.01 ^c	84.31±0.33 ^c	19.03±0.34 ^b	10.67±0.01 ^a
Fatima 120	65.55±0.30 ^b	80.51±0.02 ^c	85.19±0.13 ^c	19.64±0.16 ^b	10.26±0.42 ^a
FB 9-4 native	62.25±0.23 ^a	66.95±0.13 ^a	73.34±0.61 ^a	11.10±0.44 ^a	12.34±0.08 ^a
FB 9-4 80	65.01±0.25 ^b	71.79±0.11 ^b	77.54±0.16 ^b	12.54±0.40 ^a	12.39±0.42 ^a
FB 9-4 100	67.16±0.43 ^b	74.83±0.04 ^c	82.38±0.89 ^c	15.23±0.46 ^b	12.51±0.35 ^a
FB 9-4 120	66.06±0.01 ^b	76.25±0.11 ^d	83.83±0.16 ^c	17.77±0.16 ^c	11.96±0.01 ^a
Black bean					
Espresso native	64.54±0.30 ^a	71.62±0.18 ^a	80.64±0.01 ^a	16.11±0.29 ^a	13.53±0.53 ^a
Espresso 80	69.77±0.06 ^b	75.68±0.01 ^b	83.88±0.88 ^b	14.11±0.82 ^b	13.30±0.23 ^a
Espresso 100	70.23±0.08 ^b	79.48±0.23 ^c	87.19±0.11 ^c	16.96±0.19 ^{ac}	12.45±0.16 ^b
Espresso 120	70.59±0.13 ^b	82.15±0.01 ^d	88.13±0.11 ^c	17.54±0.24 ^c	12.51±0.57 ^b
BRT 1519-10 native	67.10±0.29 ^a	76.64±0.14 ^a	82.96±0.01 ^a	15.86±0.28 ^a	13.07±0.03 ^a
BRT 1519-10 80	69.71±0.13 ^b	75.53±0.01 ^a	83.44±0.09 ^a	13.73±0.04 ^b	12.15±0.85 ^a
BRT 1519-10 100	70.21±0.21 ^b	80.18±0.01 ^b	87.92±0.08 ^b	17.71±0.34 ^c	12.81±0.46 ^a
BRT 1519-10 120	70.59±0.13 ^b	82.15±0.01 ^c	88.13±0.11 ^b	17.54±0.24 ^c	12.51±0.57 ^a
Pinto bean					
AC Pintoba native	66.64±0.08 ^a	73.71±0.01 ^a	80.53±0.74 ^a	14.19±0.82 ^a	14.51±0.15 ^a
AC Pintoba 80	73.37±0.29 ^b	78.82±0.00 ^b	85.71±0.01 ^b	12.34±0.30 ^b	14.42±0.05 ^a
AC Pintoba 100	75.32±0.25 ^c	86.39±0.15 ^c	92.93±0.13 ^c	17.61±0.13 ^c	14.47±0.11 ^a
AC Pintoba 120	75.66±0.04 ^c	87.41±0.36 ^c	92.78±0.05 ^c	17.12±0.01 ^c	14.05±0.37 ^a
Pecos native	69.89±0.00 ^a	75.91±0.23 ^a	83.11±0.36 ^a	13.22±0.36 ^a	14.58±0.05 ^a
Pecos 80	74.09±0.21 ^b	78.74±0.11 ^b	85.17±0.57 ^b	11.08±0.78 ^b	14.42±0.05 ^a
Pecos 100	75.27±0.27 ^b	83.55±0.30 ^c	90.40±0.01 ^c	15.13±0.28 ^c	13.83±0.06 ^b
Pecos 120	75.59±0.18 ^b	83.24±0.14 ^c	90.68±0.20 ^c	15.10±0.37 ^c	13.70±0.12 ^b

¹All data represent the mean of triplicates. Values followed by the same superscript in each column for each starch source are not significantly different ($P < 0.05$) by ANOVA and Tukey's HSD test.

² ($T_c - T_o$) represents the gelatinization temperature range.

³ Gelatinization enthalpy of starch expressed in J/g of dry starch.

4.2.6 Swelling factor (SF) and amylose leaching (AML)

HMT decreased SF (HMT120 < HMT100 < HMT80) and AML (HMT120 ~ HMT100 < HMT80) in all starches (Table 4.14). The decrease in SF at all HMT temperatures followed the order: FB > BB ~ PB. There was no variation in the extent of SF reduction among cultivars of FB. However, among cultivars of BB and PB, SF was reduced to a greater extent in *expresso* and *pecos*, respectively. FB, BB and PB exhibited extensive reduction in AML on HMT (BB ~ PB > FB). AML was not detected at all HMT temperatures in cultivars of PB (*AC pintoba* and *pecos*) and BB (*BRT 1519-10*). However, AML was detectable in FB (*Fatima*, FB9-4) and in BB (*expresso*) at HMT120 and HMT100, respectively (Table 4.14). Similar reductions in SF and AML have been reported in cereal, tuber and other pulse starches (Hoover, 2010). The reduction in SF on HMT has been attributed to the interplay of: 1) crystalline disruption (mainly in tuber starches) 2) increase in crystallinity, 3) amylose-lipid interactions, 4) interaction between AM-AM, AM-AP and AP-AP chains, and 5) change in polymorphic form (Hoover, 2010). In this study, only the factors 2, 4 and 5 are plausible, since there was no evidence of crystalline disruption (Fig. 4.14) or AM-lipid complex formation [absence of a DSC endothermic peak centered at 104°C (diagram not shown)] and the absence of V-AM-lipid complex peak at 20°2θ [Fig. 4.14] on HMT. The reduction in AML on HMT indicates stronger and/or additional interactions between AM-AM and/or AM-AP chains. The SF reduction on HMT could be partly attributed to a reduction in the amount of free hydroxyl groups available for hydration due to interaction between and among AM and AP chains. It is also likely, that the polymorphic transformation (A+B→A) on HMT (Fig. 4.14), which is fully completed at HMT100 in all starches, may have also contributed to the SF decrease. This seems plausible, since A-type crystallites being

more compactly packed than B-type crystallites (Varatharajan et al., 2010) could decrease the ingress of water into the amorphous and crystalline domains during SF measurements. Thus, the SF decrease between genotypes of FB, BB and PB on HMT reflects the interplay of: 1) extent of increase in RC, 2) extent of interactions between and among AM and AP chains and 3) amount of A-type crystallites formed during the polymorphic transformation.

Table 4.14

Swelling factor and amylose leaching at 80°C for native and HMT faba bean, black bean and pinto bean starches. ¹

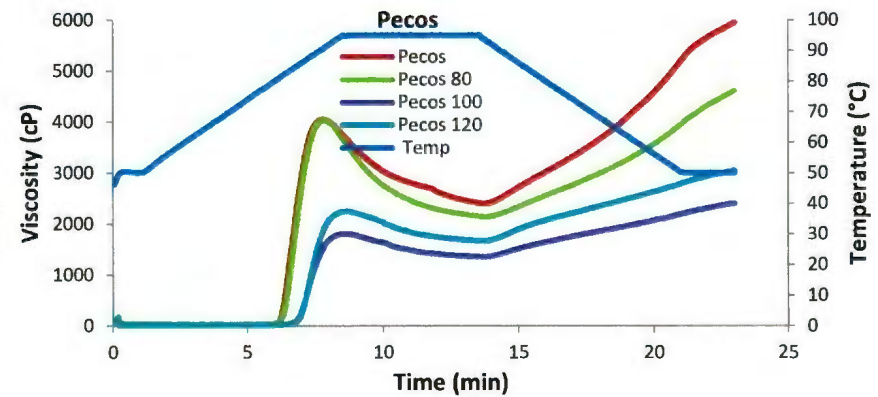
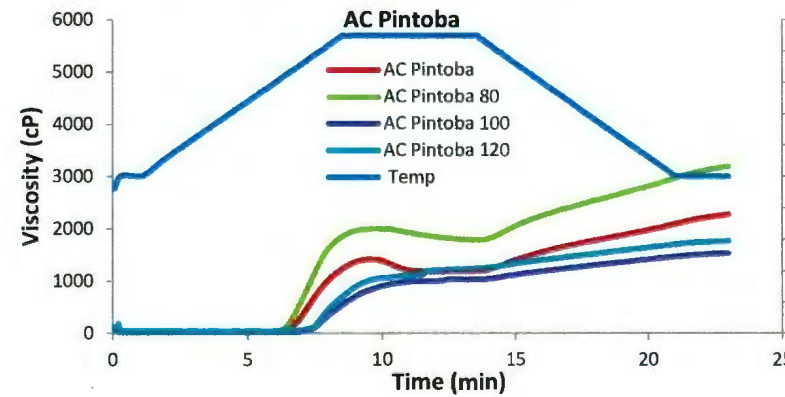
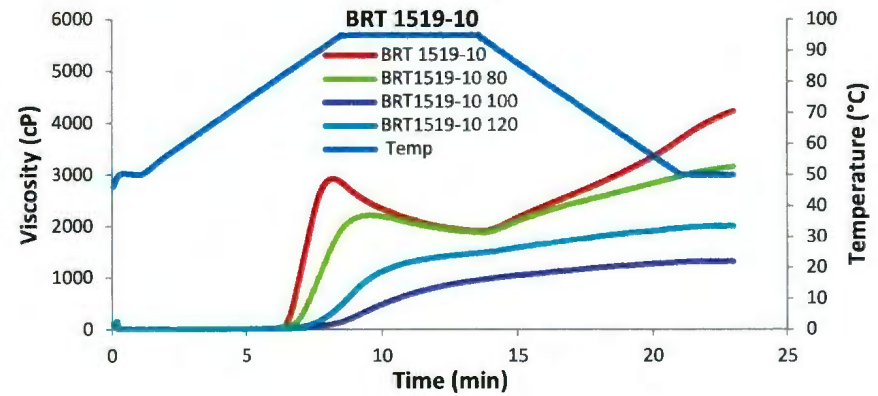
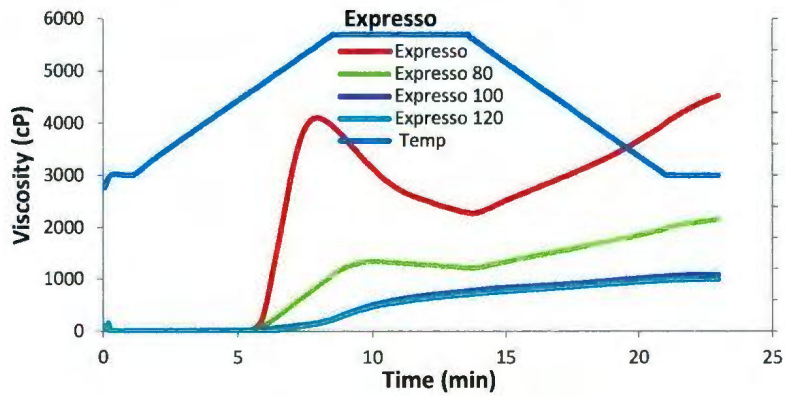
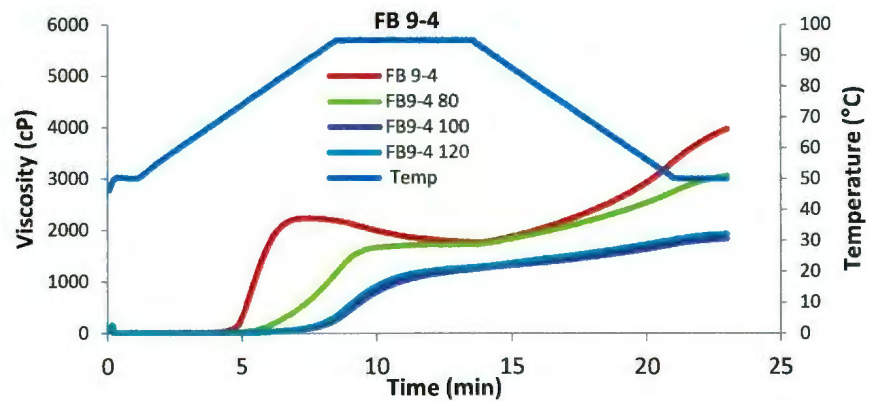
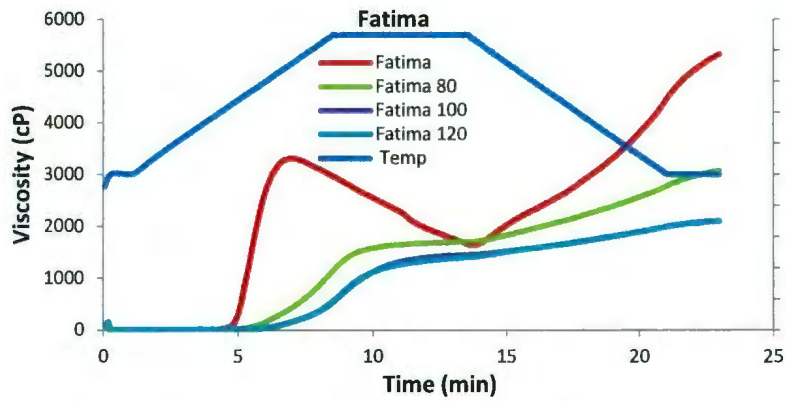
Starch source	Swelling Factor	Amylose Leaching
Faba bean		
Fatima native	24.37±0.36 ^a	11.47±0.41 ^a
Fatima 80	17.36±0.07 ^b	4.24±0.18 ^b
Fatima 100	14.17±0.52 ^c	0.44±0.14 ^c
Fatima 120	10.22±0.47 ^d	0.52±0.00 ^c
FB 9-4 native	25.08±0.17 ^a	11.86±0.65 ^a
FB 9-4 80	16.48±0.10 ^b	4.40±0.42 ^b
FB 9-4 100	14.89±0.60 ^c	0.83±0.27 ^c
FB 9-4 120	11.78±0.67 ^d	1.38±0.65 ^c
Black bean		
Expresso native	20.13±0.36 ^a	8.16±0.20 ^a
Expresso 80	17.13±0.60 ^b	1.30±0.65 ^b
Expresso 100	15.69±0.32 ^c	0.56±0.07 ^{cb}
Expresso 120	11.53±0.24 ^d	0.00±0.00 ^c
BRT 1519-10 native	16.66±0.17 ^a	4.56±0.38 ^a
BRT 1519-10 80	16.61±0.61 ^a	0.00±0.00 ^b
BRT 1519-10 100	12.46±0.51 ^b	0.00±0.00 ^b
BRT 1519-10 120	10.40±0.06 ^c	0.00±0.00 ^b
Pinto bean		
AC Pintoba native	15.94±0.02 ^a	3.30±0.45 ^a
AC Pintoba 80	15.13±0.47 ^a	0.00±0.00 ^b
AC Pintoba 100	12.13±0.51 ^b	0.00±0.00 ^b
AC Pintoba 120	8.62±0.40 ^c	0.00±0.00 ^b
Pecos native	19.40±0.26 ^a	6.01±0.27 ^a
Pecos 80	15.37±0.40 ^b	0.00±0.00 ^b
Pecos 100	12.63±0.55 ^c	0.00±0.00 ^b
Pecos 120	9.88±0.20 ^d	0.00±0.00 ^b

¹All data represent the mean of triplicates. Values followed by the same superscript in each column for each starch source are not significantly different ($P > 0.05$) by ANOVA and Tukey's HSD test.

4.2.7 Pasting characteristics

The pasting properties of native and HMT starches measured using a Rapid visco analyzer are presented in Fig. 4.16. Differences in RVA parameters (peak viscosity [PV], pasting temperature [PT], breakdown viscosity [BDV], set-back [SB]) among cultivars of native FB, BB and PB were discussed in section 4.1.7. In all starches, HMT decreased PV, BDV and SB and increased the PT (Fig. 4.16). These changes varied significantly between cultivars of FB, BB and PB and were more pronounced between cultivars (Fig. 4.16). The reduction in PV, BDV (reflects thermal stability during the holding period at 95°C) and SB (reflects the extent of retrogradation during the cooling cycle), and the increase in PT on HMT could be attributed to decreased granular swelling (Table. 4.14) and AML (Table. 4.14) as a result of enhanced interaction between AM-AM, AM-AP and AP-AP chains during HMT.

Figure 4.16 Pasting profiles of native and HMT FB, BB and PB starches determined by Rapid Visco Analyzer.

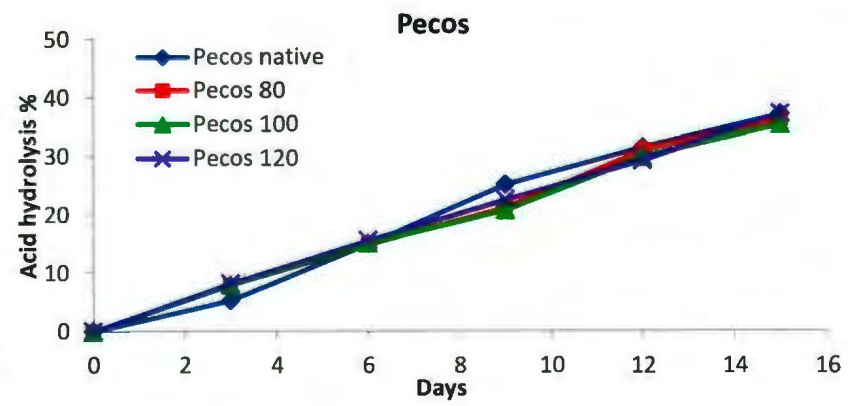
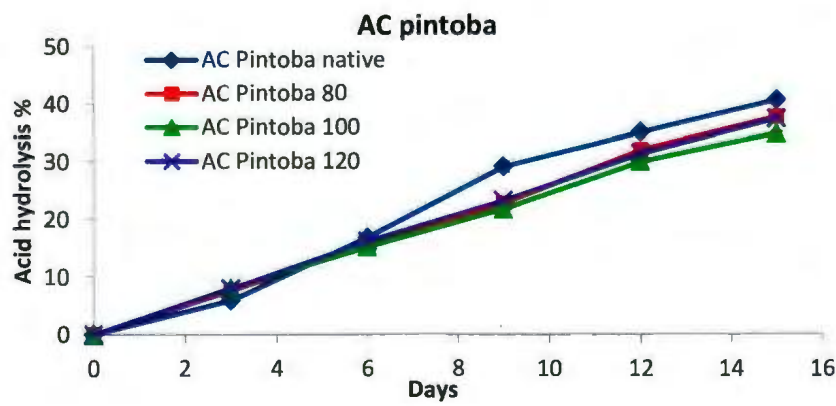
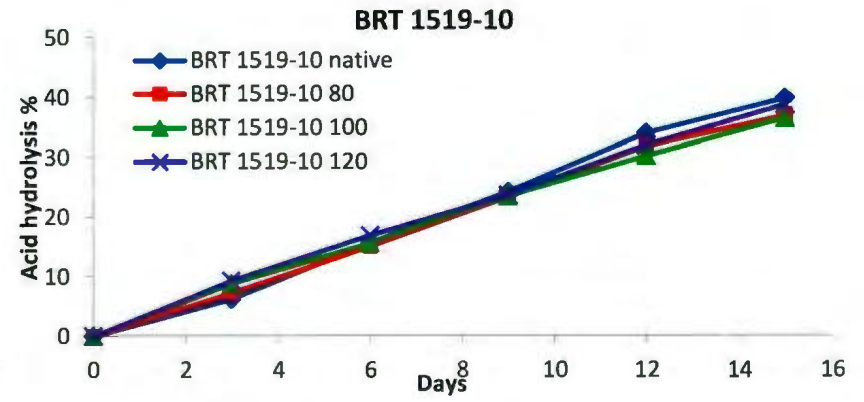
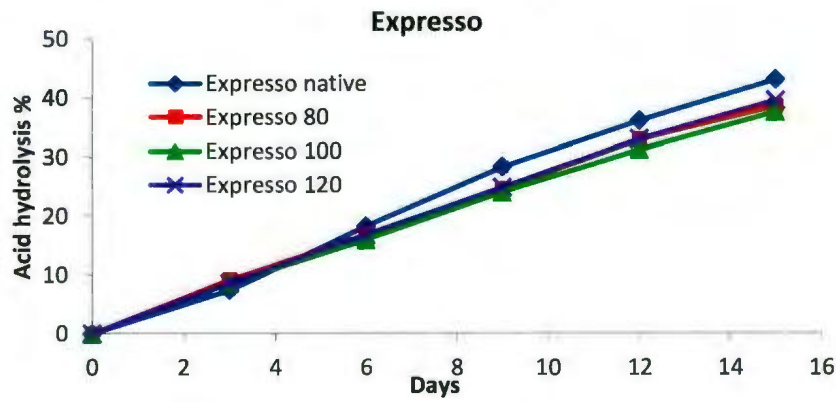
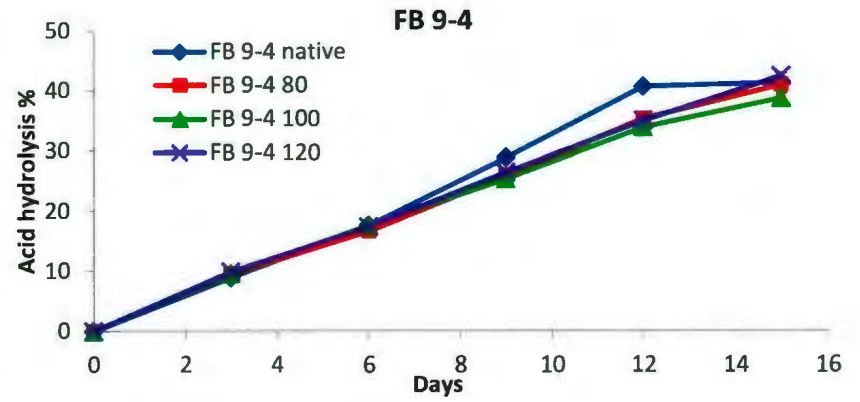
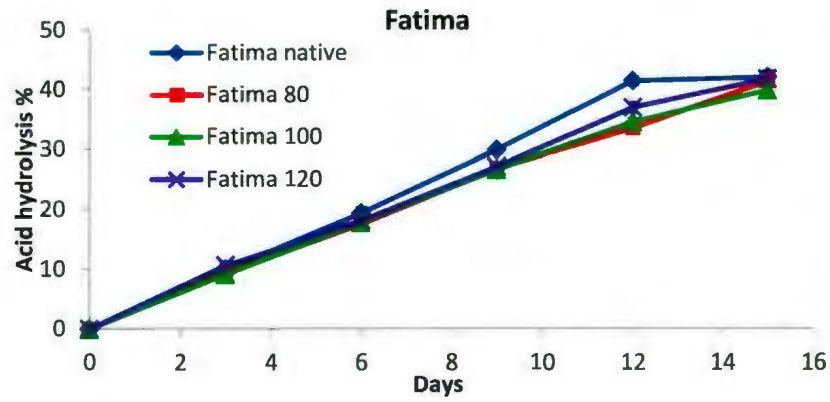


4.2.8 Acid Hydrolysis

It has generally been accepted that heterogeneous acid hydrolysis preferably attacks the bulk and inter-crystalline amorphous regions of the granule. In contrast, crystalline regions are less accessible to attack by hydrolytic protons and are attacked only after a period of 10-12 days (Hoover, 2000). To account for the slower hydrolysis of the crystalline domains, two hypotheses have been proposed (Hoover, 2000). First, the dense packing of starch chains within the starch crystallites hinders penetration of H_3O^+ . Second, acid hydrolysis of a glucosidic bond requires a conformational change (chair \rightarrow half chair) of the D-glucopyranosyl unit. Immobilization of the sugar conformation due to dense packing of amylopectin double helices in the crystalline domains would render the conformational transition difficult. HMT has been shown to decrease acid hydrolysis marginally in cereal (Hoover and Manuel, 1996b) and tuber (Varatharajan et al. 2010) starches. Gunaratne and Hoover (2002) have shown that changes in the extent of acid hydrolysis on HMT of tuber starches is influenced by the interplay of structural changes (crystalline reorientation, polymorphic changes, interactions between starch chains [AM-AM, AM-AP, AP-AP], crystallite disruption, formation of new crystallites and development of cracks on the granule surface) on HMT. The impact of HMT on the extent of acid hydrolysis is presented in Fig. 4.17. In all starches, hydrolysis decreased marginally on HMT. Hydrolysis, during the first 9 days, mainly reflects hydrolysis within the amorphous regions of the granule. The extent of decrease in hydrolysis at all HMT temperatures during this time period was marginal and not significant ($P < 0.05$) in cultivars of all starches. This suggests that the extent of starch chain interactions (AM-

AM, AM-AP) on HMT within the amorphous domain was not strong enough to hinder the accessibility of H_3O^+ into the amorphous domains. However, beyond the 9th day (reflects hydrolysis of starch crystallites), hydrolysis decreased significantly ($P < 0.05$) in all starches on HMT (HMT80 > HMT100 ~ HMT120). The above changes were more pronounced in FB. The extent of reduction in acid hydrolysis among cultivars of FB, BB and PB during this time period was not significant ($P < 0.05$) (Fig. 4.17). Decrease in hydrolysis beyond the 9th day probably reflects interplay among changes to crystallite orientation, crystal size and double helical realignment.

Figure 4.17 Acid hydrolysis (2.2 M HCl) profiles of native and HMT FB, BB and PB starches.



4.2.9 Nutritional Fractions

Rapidly digestible starch (RDS), slowly digestible starch (SDS), resistant starch (RS) and expected glycemic index (eGI) of native and HMT starches determined by *in-vitro* digestibility by a mixture of pancreatin and α -amylglucosidase are presented in Table 4.15. The above classification reflects both the kinetic component and the completeness of digestibility. In this *in-vitro* study, RDS, SDS and RS are defined as the amount of starch digested within the first 30min, between 30 min to 16 h and starch remaining undigested after 16 h, respectively (Jenkins et al., 1983). Among native starches, FB exhibited higher levels of RDS, SDS and eGI and lower RS levels (Table 4.15). Between genotypes, differences in the above parameters followed the order: PB>BB>FB. RDS mainly reflects hydrolysis of starch chains at or near the vicinity of the granule surface, since the time period (30 min) at which RDS levels were determined was not sufficient for all of the added enzymes to enter the granule interior (since diffusion to the substrate followed by adsorption on the granule surface must occur prior to the hydrolytic event). The difference in RDS levels among the starches reflects the interplay between surface characteristics and the extent of molecular order at the granule surface. RDS levels are much higher in FB starches, due to their lower extent of molecular order at the granular surface (Table 4.15) and to the presence of cracked granules with weak birefringence (Fig. 4.12.1a) patterns compared to BB and PB. Both of the above factors may have facilitated diffusion of the amylolytic enzymes into the granule interior. This seems plausible, since both BB and PB starches, with intact granules (Fig. 4.12.1b, c) and nearly similar extent of molecular order (Fig. 4.13) exhibited RDS levels that were much lower

than those seen with FB genotypes (Table 4.15). The SDS levels in native starches varied significantly among genotypes of FB (Fatima > FB 9-4), BB (expresso > BRT 1519-10) and PB (AC pintoba > pecos) (Table 4.15). The SDS levels in FB, BB and PB ranged from 74.99–77.29, 46.44–53.62 and 34.94–50.90%, respectively. The difference in SDS levels among the native starches reflects the interplay between crystalline stability (reflects double helical organization within the granule interior) and the extent to which hydrolyzed starch chains interact during the progress of hydrolysis. The high SDS levels in FB starches reflect their weaker amylopectin architecture (Fig. 4.12.1a), which facilitates easier access of the amylolytic enzymes to the glycosidic linkages. It is highly unlikely that SDS levels are influenced by amylopectin chain length distribution (APCLD), relative crystallinity (RC), amylose content (AM) and/or B-polymorphic content, since difference in the above parameters among the starches was marginal, and pecos (PB genotypes) with a much lower B-polymorph (7.91%) content (Table 4.11) was hydrolyzed to a lesser extent than the other genotypes (Table 4.15), where the B-polymorph contents (Table 4.11) ranged from 15.42–25.05%. B-type polymorphs have been shown to be less susceptible than A-type polymorphs towards amylolysis [Jane, Wong and McPherson (1997)]. DSC data showed that among genotypes of FB, BB and PB, gelatinization transition temperatures (especially T_0) and the enthalpy of gelatinization (ΔH) were higher in pecos (Table 4.13). This suggests that the low SDS levels with pecos (Table 4.15) reflect higher crystalline stability (Table 4.13) and denser packing of double helices within the crystalline domains (both of which would restrict accessibility of the amylolytic enzymes towards the glycosidic linkages). The RS and

eGI levels also varied between genotypes of FB, BB and PB (Table 4.15). Variation in RS content between genotypes of FB was marginal (10.00–10.95%), but were significant between genotypes of BB (33.46–41.79%) and PB (36.57–52.84%). The factors influencing difference in RS content among the starches is the same as that discussed for SDS variations. In all starches, RDS levels increased on HMT. The extent of this increase at HMT120 (FB > BB ~ PB) was in the range 8.22–10.7% (FB), 5.74–6.32% (BB) and 5.63–6.41% (PB). The increase in RDS on HMT reflects the change in AP chain realignment at the granular surface on HMT (Fig. 4.13, section 4.2.3). If a decrease in molecular order at HMT120 (BB > FB > PB) was the sole factor influencing increased RDS levels in FB, BB and PB, then increased RDS levels at HMT120 should have also followed the above trend in molecular order. Several studies (Jane et al., 1997; Gerard, Colonna, Buléon & Planchot, 2001) have shown that A-type crystallites are weaker (due to $\alpha(1\rightarrow6)$ branch points being present in the crystalline region) than B-type crystallites (due to $\alpha(1\rightarrow6)$ branch points being present solely in the amorphous regions) and hence more susceptible to attack by amyolytic enzymes. This suggests that, since the amount of B-type crystallites that were transformed into A-type crystallites at HMT120 (Table 4.11), followed the order: FB (Fatima > FB 9-4) > BB (expresso) > PB (AC pintoba) > BB (BRT1519-10) > PB (pecos), theoretically, the extent of increase in RDS content at HMT120 should also have followed the same trend. Thus, the observed trend in RDS increase (FB > BB ~ PB) at HMT120 suggests an interplay between: 1) the influence of decrease in molecular order, and 2) the amount of A-type crystallites formed at HMT120. In all starches, SDS levels decreased significantly ($P < 0.05$) on HMT. The extent of this

decrease in SDS at HMT80 was more pronounced than at HMT100 and HMT120 of genotypes of all starch sources (Table 4.15), whereas, RS levels in all starches increased at HMT80 but decreased at HMT100 and HMT120. The extent of SDS decrease at HMT80 followed the order: FB (Fatima ~ FB 9-4) > PB (AC pintoba) > BB (expresso > BRT 1519-10) > PB (pecos). The higher decrease in SDS levels at HMT80 in FB genotypes could be attributed to the higher increase in RC (similar in both genotypes [Table 4.11]). In BB genotypes, the decrease in SDS at HMT80 is higher in expresso than in BRT 1519-10 due to the increase in RC in expresso (20.44 to 28.47%) being higher than in BRT 1519-10 (21.31 to 26.17%) (Table 4.11). It was interesting to observe that although the increase in RC at HMT80 was higher in pecos (22.09 to 27.43%) than in AC pintoba (23.14 to 27.56%) (Table 4.11), the extent of decrease in SDS at HMT80 was much smaller in pecos (34.94 to 21.57%) (Table 4.15). As discussed earlier, starch chains in pecos are more densely packed than in AC pintoba. Therefore, an increase in RC (which reflects better alignment of crystallites and/or more closely packed crystallites) on HMT of pecos would not make a significant impact on SDS levels as in AC pintoba. This would then explain why the decrease in SDS is lower in pecos in spite of increased crystallinity. The difference in the extent of increase in SDS levels at HMT100 and HMT120 in genotypes of FB (Fatima ~ FB9-4), BB (BRT 1519-10 > expresso) and PB (AC pintoba ~ pecos) reflects the interplay between: 1) the amount of A-type crystallites present at HMT100 and HMT120 (Fatima > FB 9-4 > AC pintoba > BRT 1519-10 > pecos) and 2) the extent of decrease in RC (Fatima > FB 9-4 > expresso ~ AC pintoba > pecos > BRT 1519-10). Both factors 1 and 2 could facilitate the extent of diffusion into the granule interior and the hydrolytic event within the crystalline domains.

At HMT80, RS levels in FB, BB and PB were higher than their native counterparts (HMT80 > HMT100). However, in all starches, the RS levels at HMT120 were lower than their native counterparts. The increase in RS content at HMT80 (Fatima ~ FB 9-4 > expresso > AC pintoba > BRT 1519-10 > pecos) is higher than at HMT100 (Fatima ~ FB 9-4 > expresso > AC pintoba > BRT 1519-10 > pecos) due to higher increase in RC (Table 4.11) and the presence of B-type crystallites (Table 4.11). The large decrease in RS content at HMT120 seems to suggest that the A-type crystallites that were formed on HMT may have been organized differently (due to higher temperature prevailing during HMT) to that in HMT100 starches, rendering these crystallites more accessible to attack by the amylolytic enzymes. Chung, Liu and Hoover (2010) observed a higher RDS levels (21-25%) and low RS content (~29%) on HMT (30% MC, 24h at 120°C) of pea and lentil (21.7%) starches. In contrast, they observed a low RDS (7.6%) and high RS (49.9%) content for navy bean starches under the same HMT conditions. Li et al. (2011) have shown that RS content in mung bean starch increased from 11.2% to 45.2% on HMT at 120°C (20% MC, 12h). Kojima et al. (2006) also showed an increase in RS content during HMT (MC 20%, 100°, 120° and 130°C autoclaved for 30 min) of adzuki bean (~2.5% increase) and kidney bean (~4% increase) starches. As seen above, increase or decrease in RS content may be influenced by HMT conditions (moisture content, temperature during HMT, duration of heating, methodology [oven vs. autoclaving]), amylose content, proportion of A+B type crystallites and extent to which AM and AP chains are co-crystallized within the native granule). The high resistance of pecos towards hydrolysis is also reflected in the hydrolysis profile (Fig. 4.18) which showed a

plateau only after 8h of hydrolysis, whereas the genotypes of the other starches exhibited plateau's only after 12–14h of hydrolysis.

Jenkins et al. (2012) reported that pulses (beans, chickpeas, and lentils) with low GI are effective in controlling blood glucose level and reducing risk of coronary heart disease in individuals with diabetes. Studies also have shown that RS intake would decrease postprandial glycemic and insulinemic responses, lower plasma cholesterol and triacylglycerol concentrations, improve whole body insulin sensitivity, increase satiety and reduce fat storage (Higgins, 2004). Based on the above data, among genotypes, pecos with its higher RS content and lower GI may have greater beneficial effects for protection against metabolic syndrome, including insulin resistance, obesity and diabetes.

Table 4.15

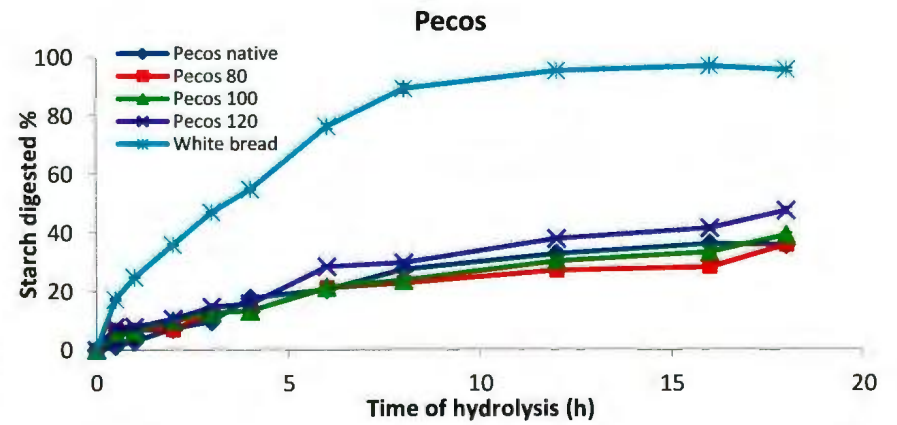
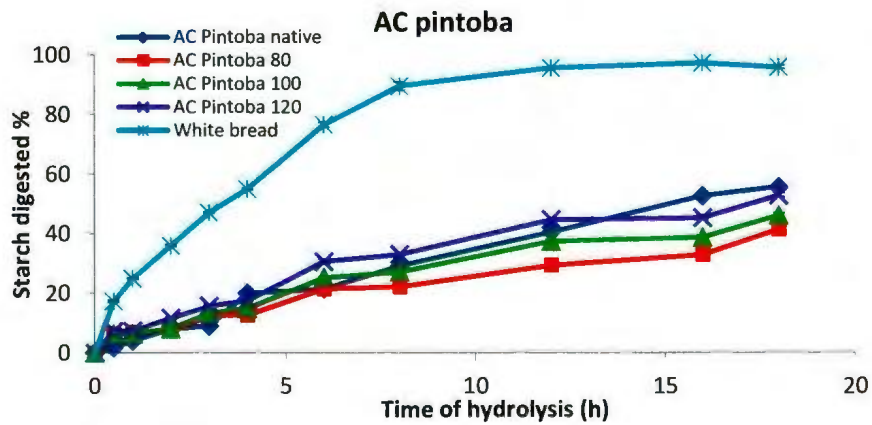
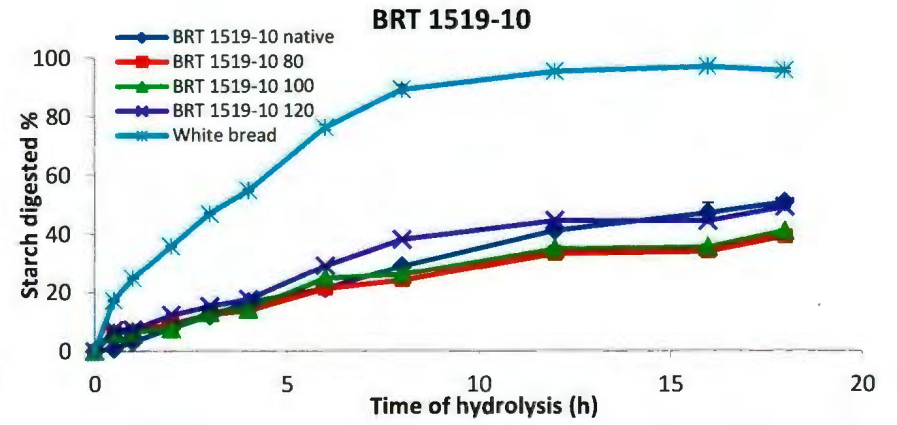
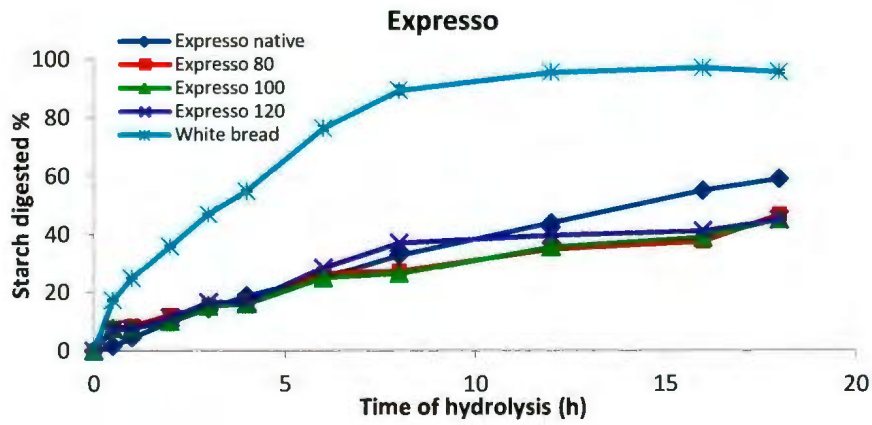
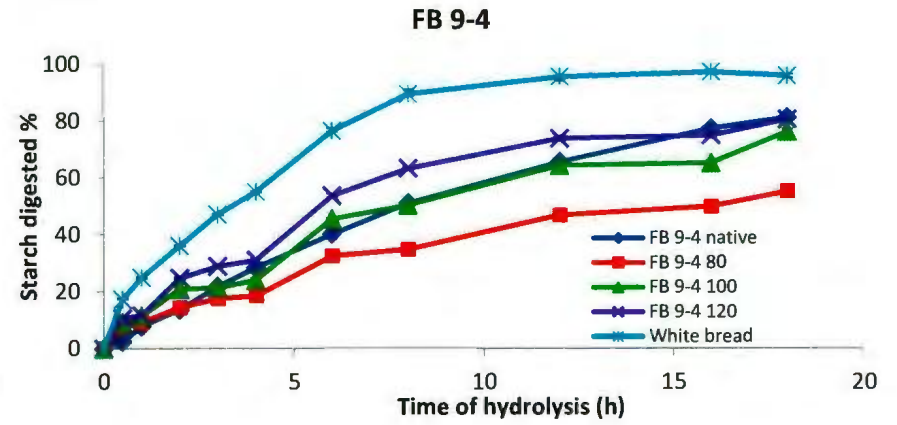
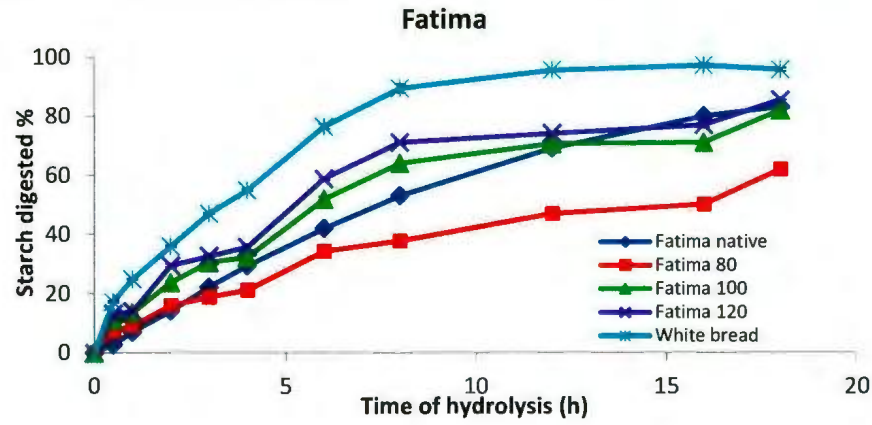
Nutritional fractions, hydrolysis index and expected glycemic index of native and HMT faba bean, black bean and pinto bean starches determined by *in vitro* hydrolysis.¹

Starch source	RDS ²	SDS ²	RS ²	eGI ²
Faba bean				
Fatima native	2.80±0.35 ^a	77.29±0.98 ^a	10.00±0.70 ^a	66.20±0.50 ^a
Fatima 80	7.17±0.33 ^b	43.05±0.46 ^b	32.75±0.79 ^b	49.30±0.30 ^b
Fatima 100	11.11±0.55 ^c	60.00±1.00 ^c	11.39±0.45 ^a	70.00±0.10 ^c
Fatima 120	13.15±0.74 ^d	63.86±0.15 ^d	2.21±0.89 ^c	75.30±0.30 ^d
FB 9-4 native	2.29±0.06 ^a	74.99±0.75 ^a	10.95±0.70 ^a	61.30±3.0 ^a
FB 9-4 80	7.65±0.24 ^b	42.16±1.10 ^b	33.53±0.86 ^b	47.60±0.30 ^b
FB 9-4 100	9.02±0.16 ^c	56.49±0.20 ^c	14.66±0.05 ^c	61.90±0.30 ^a
FB 9-4 120	10.52±0.77 ^d	64.31±0.21 ^d	4.17±0.98 ^d	71.20±0.20 ^c
Black bean				
Expresso native	1.57±0.12 ^a	53.62±0.55 ^a	33.46±0.59 ^a	46.00±0.30 ^a
Expresso 80	7.71±0.68 ^b	30.05±0.33 ^b	44.90±0.36 ^b	39.20±0.30 ^b
Expresso 100	7.70±0.25 ^b	31.40±0.09 ^c	41.91±0.17 ^c	39.10±0.10 ^b
Expresso 120	7.31±0.17 ^b	34.09±0.59 ^d	39.23±0.58 ^d	43.00±0.20 ^c
BRT 1519-10 native	0.87±0.20 ^a	46.44±3.67 ^a	41.79±3.52 ^a	40.00±2.40 ^a
BRT 1519-10 80	6.35±0.50 ^b	27.86±0.85 ^b	47.02±0.35 ^b	35.70±0.30 ^b
BRT 1519-10 100	6.28±0.25 ^b	29.46±0.72 ^b	46.86±0.47 ^b	37.40±0.10 ^b
BRT 1519-10 120	7.19±0.69 ^b	37.49±0.69 ^c	32.47±0.00 ^c	45.50±0.01 ^c
Pinto bean				
AC Pintoba native	1.72±0.13 ^a	50.90±0.73 ^a	36.57±0.64 ^a	41.10±2.30 ^a
AC Pintoba 80	6.32±0.09 ^b	26.65±0.92 ^b	44.14±0.83 ^b	34.00±0.10 ^b
AC Pintoba 100	6.34±0.24 ^b	32.37±0.46 ^c	41.34±0.70 ^c	39.00±0.10 ^c
AC Pintoba 120	7.30±0.10 ^a	37.94±0.97 ^d	25.54±0.87 ^d	44.90±0.40 ^d
Pecos native	1.41±0.30 ^a	34.94±1.01 ^a	52.84±0.72 ^a	36.10±0.10 ^a
Pecos 80	6.81±0.51 ^b	21.57±0.31 ^b	54.09±0.81 ^b	32.50±0.50 ^b
Pecos 100	6.03±0.25 ^b	27.45±0.03 ^c	46.99±0.28 ^c	34.80±0.10 ^c
Pecos 120	7.81±0.39 ^a	33.90±1.29 ^a	27.94±0.90 ^d	41.30±0.20 ^d

¹All data represent the mean of triplicates. Values followed by the same superscript in each column for each starch source are not significantly different ($P > 0.05$) by ANOVA and Tukey's HSD test.

²RDS: rapidly digestible starch; SDS: slowly digestible starch; RS: resistant starch; eGI: expected glycemic index.

Figure 4.18 *In-vitro* digestibility profiles of native and HMT FB, BB and PB starches subjected to hydrolysis by mixture of pancreatin and amyloglucosidase.



4.2.9.1 Granule morphology of native and HMT80 starches before and after amylolysis

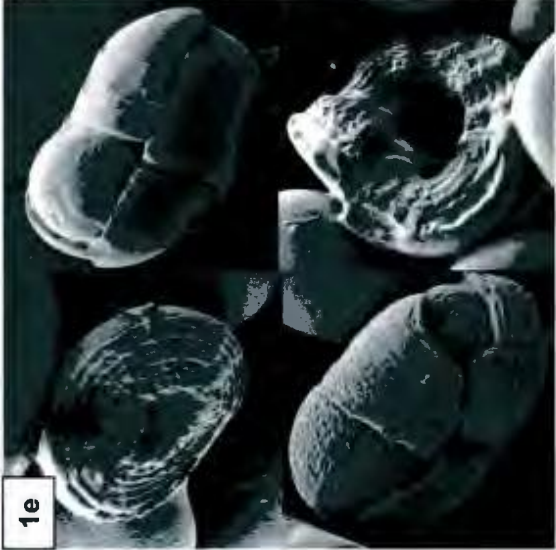
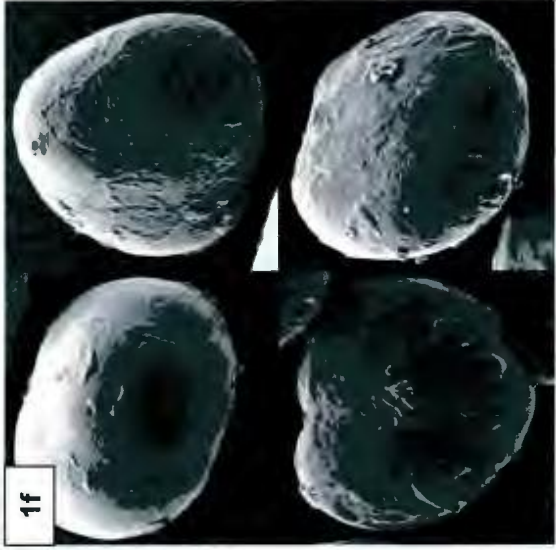
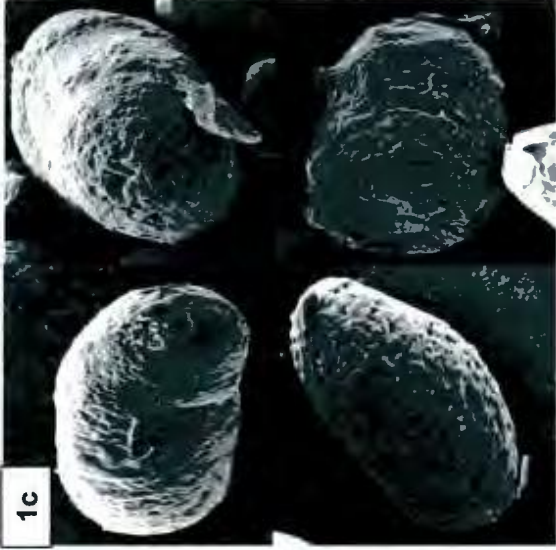
In this discussion, the following abbreviations FB-RDS, FB-RS, BB-RDS, BB-RS, PBAC-RDS, PBAC-RS, PBPE-RDS and PBPE-RS will be used to denote native FB (fatima) after 30 min hydrolysis, native FB (fatima) after 16 h hydrolysis, native BB (expresso) after 30 min hydrolysis, native BB (expresso) after 16 h hydrolysis, native PB (AC pintoba) after 30 min hydrolysis, native PB (AC pintoba) after 16 h hydrolysis, native PB (pecos) after 30 min hydrolysis and native PB (pecos) after 16 h hydrolysis, respectively.

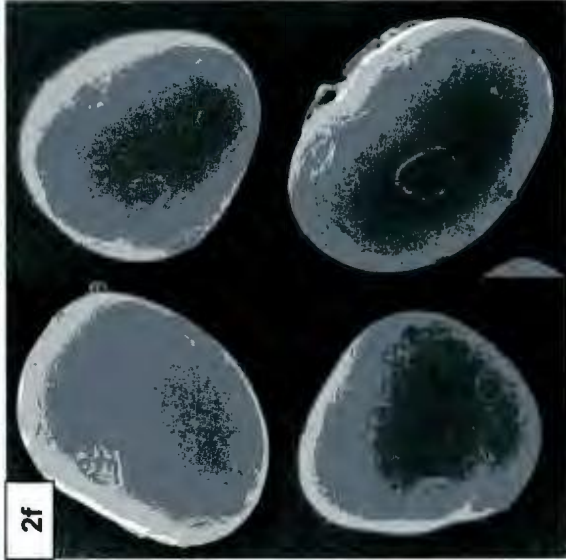
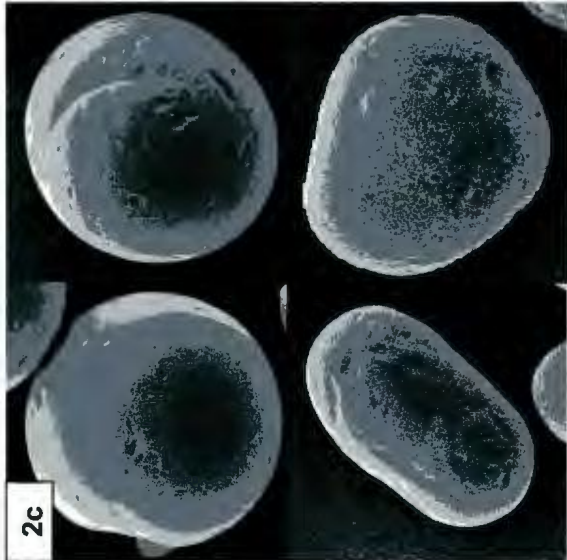
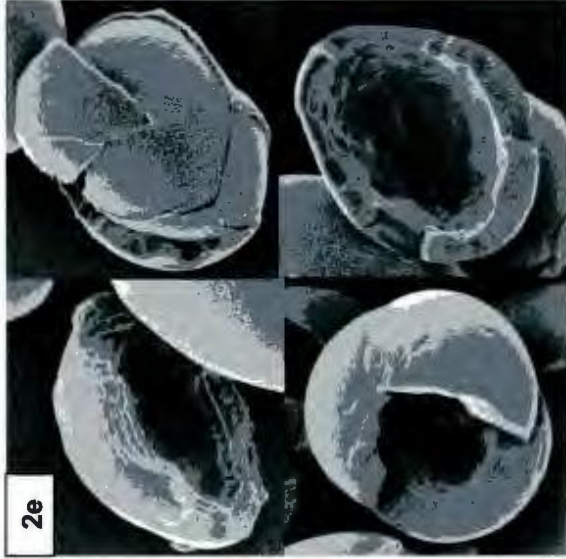
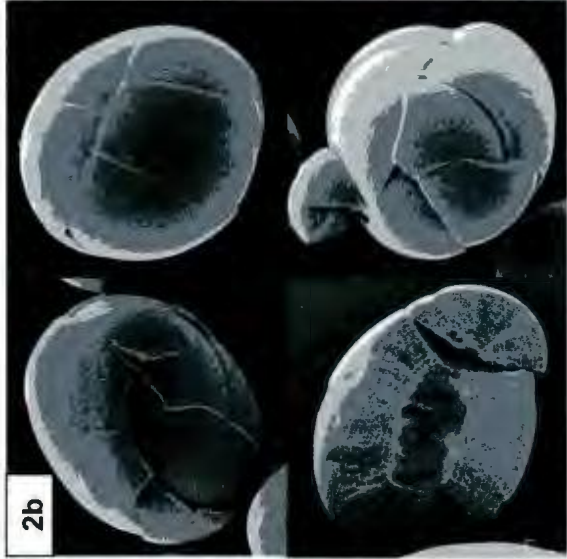
Scanning electron micrographs of FB (fatima), BB (expresso) and PB (AC pintoba and pecos) starches subjected to HMT80, and amylolysis for 30 min (RDS) and 16 h (RS) using a mixture of α -amylase and amyloglucosidase are shown in Figs. 4.19.1-4.19.4. Native FB (Fig. 4.19.1a) showed the presence of numerous cracks on the granule surface. The extent of cracking varied among the granules. Cracks have also been reported in other pulses (kidney bean, mung bean [Hoover and Sosulski, 1985]). Glaring, Koch and Blennow (2006) postulated, that cracking may reflect low granule integrity (due to weak interaction between radially arranged amylopectin chains) resulting in an increase in strain as the granule grows. The native granule morphology of FB (Fig. 4.19.1a) remained unchanged on HMT (Fig. 4.19.1d). After 30 min hydrolysis, many native FB-RDS granules exhibited extensive splitting (nature of the splitting varied among the granules) with some hollow granules. The layered structure was visible in some FB-RDS granules (Fig. 4.19.1b). After 16 h hydrolysis, all granules of FB-RS were extensively

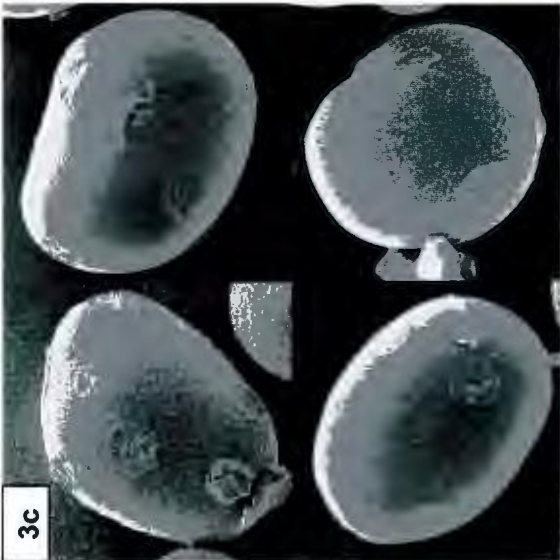
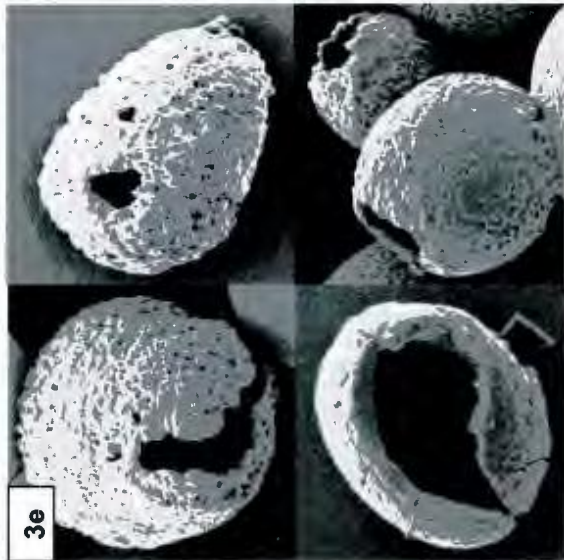
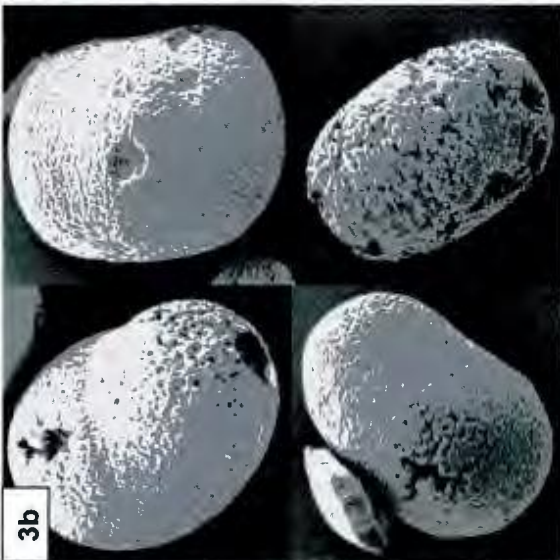
corroded with numerous pits on the granule surface (Fig. 4.19.1c). Splitting was not visible in any of the FB-RS granules (Fig. 4.19.1c). HMT80-FB-RDS granules showed more extensive splitting (Fig. 4.19.1d) after 30 min hydrolysis than FB-RDS granules. The layered structure was also seen among HMT80-FB-RDS (Fig. 4.19.1e) granules. In comparison to FB-RS granules (Fig. 4.19.1c), HMT80-FB-RS granules exhibited mainly surface indentations and a rugged granular appearance (Fig. 4.19.1f) after 16 h hydrolysis. Native BB (Fig. 4.19.2a) and HMT80 BB (Fig. 4.19.2d) granules exhibited similar granule morphology (smooth surfaces with no cracks). After 30 min hydrolysis, BB-RDS granules exhibited similar type of splitting (Fig. 4.19.2b) as seen with FB-RDS granules (Fig. 4.19.1b). Layered structure was also visible in BB-RDS granules (Fig. 4.19.2b). In comparison to FB-RS (Fig. 4.19.1c) granules, BB-RS exhibited only surface indentations and some granules showed small cracks on the granule surface. HMT80-BB-RDS was more extensively eroded (Fig. 4.19.2e) than BB-RDS (Fig. 4.19.2b). HMT80-BB-RS (Fig. 4.19.2f) exhibited less corrosion (Fig. 4.19.2f) than HMT80-BB-RDS (Fig. 4.19.2c) granules. Among the PB cultivars, both AC pintoba (PBAC [Fig. 4.19.3a]) and pecos (PBPE [Fig. 4.19.4a]) exhibited similar granular morphologies before (Fig. 4.19.3a,b) and after HMT80 (Fig. 4.19.3b, 4.19.4d). The granule surface of PBAC-RDS was extensively eroded over the entire granule surface (Fig. 4.19.3b). However, none of the granules were split or cracked. The outer surface appeared spongy as a result of surface erosion over the entire surface. Similar observations have been reported in other pulses (lentil, mung bean, kidney bean) hydrolyzed by porcine pancreatic α -amylase (Hoover and Sosulski, 1985; Hoover and Manuel, 1995). After 16 h of hydrolysis, PBAC-RS showed

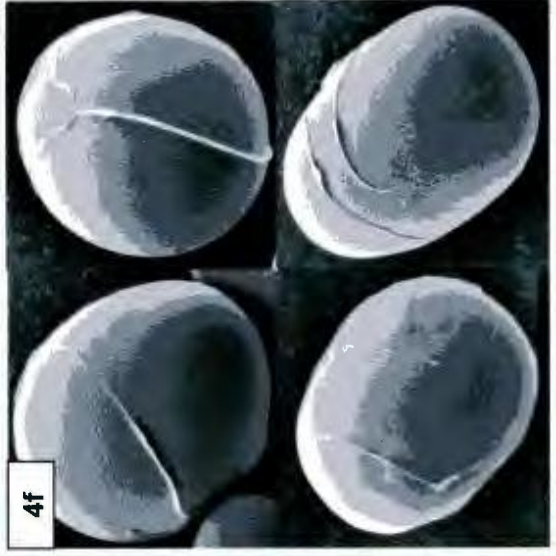
minor corrosion with surface indentations and small pits scattered over the entire surface (Fig. 4.19.3c). After 30 min hydrolysis, the extent of granule degradation (splitting and presence of pits) was more extensive in HMT80-PBAC-RDS (Fig. 4.19.3e) than in PBAC-RDS (Fig. 4.19.3b) granules. However, after 16 h hydrolysis, HMT80-PBAC-RS exhibited only minor surface erosion (Fig. 4.19.3f), the extent of which was lower than with PBAC-RS (Fig. 4.19.2c) granules. Pecos (PE) behaved differently from all other starches in exhibiting only minor corruptions in their native state (PBPE), after 30 min hydrolysis (PBPE-RDS), and after 16 h hydrolysis (PBPE-RS). PBPE-RDS granules exhibited indentations and rugged appearances, with no splitting or cracks evident in any of the other granules (Fig. 4.19.4b). PBPE-RDS granules exhibited only slight erosion at the granule surface. None of the granules exhibited indentations on pecos. HMT80-PBPE-RDS exhibited a greater degree of granule degradation (indentations, splitting and pores) than PBPE-RDS (Fig. 4.19.4b) granules. HMT80-PBPE-RS showed only minor surface erosion (Fig. 4.19.4f), which was comparable to that seen with PBPE-RS (Fig. 4.19.4c) granules. The levels of degradation among the starches (Fig. 4.19.1-4.19.4) paralleled the RDS and RS levels (Table 4.15).

Figure 4.19 Scanning electron microscopy images of FB (Fatima, 4.19.1), BB (Expresso, 4.19.2) and PB (AC pintoba, 4.19.3; Pecos, 4.19.4) starches in their native (a,b,c) and HMT80 (d,e,f) states before and after amylolysis (30 min [b,e] and 16 h [c,f]). Both cultivars of FB and BB exhibited similar granular morphology in their native and HMT states on amylolysis. Therefore, only one cultivar of each starch source is shown in figure 4.19.









Chapter 5

5.1 Summary and conclusions

The structure property relationship study of native pulse starches described here showed that FB starches differed significantly from BB and PB starches with respect to the presence of cracked granules, less well ordered amylopectin double helices and lower extent of molecular order near the granule surface. These differences had a major impact on granular swelling (FB > BB ~ PB), amylose leaching (FB > BB ~ PB), extent of set-back (FB > BB ~ PB), gelatinization transition temperatures (BB ~ PB > FB), enthalpy of gelatinization (BB ~ PB > FB), rate of acid hydrolysis (FB > BB ~ PB), rapidly digestible starch (FB > BB ~ PB), slowly digestible starch (FB > BB ~ PB), resistant starch (BB ~ PB > FB), hydrolysis index (FB > BB ~ PB) and expected glycemic index (FB > BB ~ PB). Differences in physicochemical properties were marginal among FB cultivars, but were significant ($P < 0.05$) among cultivars of BB and PB.

Retrogradation studies showed that the extent of retrogradation (at the end of the storage period) assessed by turbidity, FTIR, DSC, ^{13}C CP/MAS NMR, X-ray and enzyme susceptibility, followed the order: FB > BB ~ PB, PB > BB > FB, PB ~ BB ~ FB, PB ~ BB ~ FB, PB ~ BB ~ FB and PB > BB > FB, respectively. It was interesting to observe, that although both ^{13}C CP/MAS NMR and FTIR monitor conformational changes during storage, both techniques gave a completely different order of retrogradation. This

suggests that ^{13}C CP/MAS NMR is mainly sensitive to conformational changes associated with AP crystallization, whereas, FTIR is sensitive to conformational changes associated with crystallization of both AP-AP and AM-AP chains. This seems plausible, since the order of retrogradation assessed by DSC and X-ray (both of which reflect changes associated with AP crystallization) were in agreement with that obtained by ^{13}C CP/MAS NMR. However, the order of retrogradation assessed by FTIR was identical to that obtained by turbidity measurements which reflect interactions involving amylose chains (AM-AM and AM-AP). This study showed that retrogradation differences among the starch sources were influenced mainly by the extent of amylose leaching during gelatinization, and by the extent of starch chain interactions (AM-AM and AM-AP) and chain mobility during the progress of retrogradation. To the best of our knowledge, this is the first study that clearly demonstrates the influence of amylose on starch retrogradation. Furthermore, it must be emphasized that the different techniques used in this study measured different processes of recrystallization.

HMT of pulse starches showed that amylopectin chain length distribution and gelatinization enthalpy remained unchanged in all starches. However, they differed significantly ($P < 0.05$) with respect to amylose (AM) content, crystalline stability, radial orientation of crystallites, polymorphic composition, molecular order, thermal stability, granular swelling, amylose-leaching, gelatinization properties and *in-vitro* digestibility. This study has filled the gap in the knowledge base with respect to the part played by amylose chains, starch chain flexibility and starch chain interactions during HMT of pulses starches (having similar amylopectin chain length distribution and differing

marginally in amylose content, lipid content, and phosphorus content) at different temperatures of HMT and their impact on physicochemical properties. The results of this study would help food processors to tailor the properties of HMT pulse starches (by different moisture / temperature / time combination) to a level that is presently met by chemical modification. This in turn will add value to pulse starch production in Canada.

5.2 Novelty and Significance

Major novel findings and significance of this investigation are outlined below:

1. Detailed study of pulse starch structure at both the molecular and supramolecular levels of granule organization using a wide variety of analytical techniques.
2. Pulse starches exhibited constancy in amylopectin chain length distribution (APCLD), but wide variations in crystallinity.
3. Relative crystallinity differences among the starches were shown to be influenced by the interplay of several factors such as: 1) amylose/amylopectin ratio, 2) amount of B-type crystallites, 3) Organization of crystallites in the crystalline lamella, 4) crystallite size and 5) crystallite orientation.
4. Susceptibility of pulse starches towards acid and enzyme hydrolysis was influenced by differences in granule morphology, crystallinity, and by the extent of molecular order near the granule surface.
5. Variation in double helical content (double helices formed between AP-AP, AP-AM and AM-AM) among the pulse starches.
6. Molecular distribution of AM and AP within the granule interior.

7. The influence of B-type crystallites on enzyme and acid susceptibility.
8. The mechanism of retrogradation using a multi-technique approach.
9. The influence of amylose on the rate and extent of retrogradation.
10. Many researchers have attempted to probe the mechanism underlying the structural changes on HMT by comparative studies on starches varying widely in APCLD, composition and polymorphic composition. Consequently, it has been difficult to ascertain to what extent amylose content and their packing density within the amorphous domains influence structural changes on HMT. This study was able to show, for the first time, that amylose chains play a significant role in influencing chain realignment and their interactions during HMT.
11. This study showed, for the first time, that structural changes on HMT is first initiated by changes to the flexibility of the spacers linking AP double helices, which is then followed by interactions among and between AM-AM, AM-AP and AP-AP chains.
12. Unlike in cereal and tuber starches, structural changes on HMT did not change significantly beyond 80°C, and was more pronounced at HMT80.
13. Many researchers have assumed that a decrease in WAXS intensity on HMT is indicative of crystalline disruption. However, this investigation showed that this was

erroneous, since a decrease in X-ray intensities on HMT, could also indicate a decrease in crystal size.

14. At the present time, there is intense interest on finding methods for modifying the extent of starch digestibility by amylolytic enzymes. To this end, starches have been modified structurally by enzymatic and chemical methods. This study showed that the HMT was able to modify the nutritional fractions of pulse starches to nearly the same extent as enzymatic and chemical methods.
15. The study on starch nutritional fractions at different temperatures of HMT provided insight into the influence of starch structure on the rate and extent of amylolysis.
16. This study has filled the gap in the knowledge base with respect to pulse starch structure at different levels of granule organization and the mechanism of heat-moisture treatment. It has provided a new way of modifying pulse starch structure without recourse to chemical reagents. This in turn will add value to pulse starch production in Canada, which currently primarily relies on the sale of the raw material.

5.3 Directions for future research

1. This study showed that the structural organization of starch chains within the amorphous and crystalline domains is altered on HMT. It will be interesting to investigate, to what extent reagents such as acetic anhydride and POCl_3 (which are used widely in the food industry to chemically modify starch structure) are able to penetrate the amorphous and crystalline domains of HMT starches.
2. Complete removal of the amorphous region by acid hydrolysis, followed by HMT on the crystalline residue could provide new insights into the extent to which amorphous regions influence structural reorganization of starch chains on HMT.
3. Modification of pulse starches with HMT followed by other physical/chemical modification techniques such as annealing, ultra-high pressure, cross-linking, substitution may pave the way for production of starches with novel properties and, hence new food and industrial applications.

References

- AACC (2000). Approved methods of the AACC (10th ed.), St. Paul, MN, USA: American Association of Cereal Chemists.
- Abeysekera, S., Chilibeck, P. D., Vatanparast, H. and Zello, G. A. (2012). A pulse-based diet is effective for reducing total and LDL-cholesterol in older adults. *The British Journal of Nutrition*, 108, S103 - S110.
- Abd Karim, A., Norziah, M.H. and Seow, C.C. (2000). Methods for the study of starch retrogradation. *Food Chemistry*, 71, 9-36.
- Abraham, T. E. (1993). Stabilization of paste viscosity of cassava starch by heat-moisture treatment. *Starch/Stärke*, 43, 131-135.
- Adebowale, K. O., Afolabi, T. A. and Olu-Owolabi, B. I. (2005). Hydrothermal treatment of finger millet (*Eleusine coracana*) starch. *Food Hydrocolloids*, 19, 974-983.
- Adebowale, K. O. and Lawal, O. S. (2003). Microstructure, physicochemical properties and retrogradation behaviour of mucuna bean (*Mucuna puriens*) starch on heat moisture treatment. *Food Hydrocolloid*, 17, 265-272.
- American Association of Cereal Chemists. (2000). *Approved methods of the AACC* (10th ed.). St. Paul, MN, USA.
- Anderson, A. K., Guraya, H. S. (2006). Effects of microwave heat-moisture treatment on properties of waxy and non-waxy rice starches. *Food Chemistry*, 97, 318-323.
- Angellier, H., Choisnard, L., Molina-Boisseau, S., Ozil, P. and Dufresne, A. (2004). Optimization of the preparation of aqueous suspensions of waxy maize starch nanocrystals using a response surface methodology. *Biomacromolecules*, 5, 1545-1551.
- Appelqvist, I. A. M. and Debet, M. R. M. (2000). Starch-biopolymer interactions- A review. *Food Reviews International*, 13, 163-224.
- Atkin, N. J., Cheng, S. L., Abeysekera, R. M. and Robards, A. W. (1999). Localization of amylose and amylopectin in starch granules using enzyme-gold labeling. *Starch/Stärke*, 51, 163-172.

- Atichokudomchai, N. and Varavinit, S. (2003). Characterization and utilization of acid-modified cross-linked Tapioca starch in pharmaceutical tablets. *Carbohydrate Polymers*, 53, 263-270.
- Atwell, W. A., Hood, L. F., Lineback, D. R., Varriano-Marston, E. and Zobel, H. E. (1988). The terminology and methodology associated with basic starch phenomena. *Cereal Foods World*, 33, 306-311.
- Baik, M. Y., Dickinson, C. L. and Chinachoti, P. (2003). Solid-state ^{13}C CP/MAS NMR studies on aging of starch in white bread. *Journal of Agricultural Food Chemistry*, 51, 1242-1248.
- Baldwin, P. M. (2001). Starch granule-associated proteins and polypeptides: A review. *Starch/Stärke*, 53, 475-503.
- Banks, W. and Greenwood, C. T. (1975). Starch and its components. Edinburgh University Press, Edinburgh, pp. 309-325.
- Banks, W. and Greenwood, C. T. (1971). Amylose: a non-helical biopolymer in aqueous solution. *Polymer*, 12, 141-145.
- Banks, W., Greenwood, C. T. and Khan, K. M. (1971). The interaction of linear amylose oligomers with iodine. *Carbohydrate Research*, 17, 25-33.
- Banks, W., Greenwood, C. T. and Walker, J. T. (1970). Studies on the starches of barley cultivars: The waxy starch. *Starch*, 22, 149-152.
- Bello-Pérez, L. A., Ottenhof, M. A., Agama-Acevedo, E. and Farhat, I. A. (2005). Effect of storage time on the retrogradation of banana starch extrudate. *Journal of Agricultural and Food Chemistry*, 53, 1081-1086.
- Bergthaller, W. and Hollmann, J. (2007). Starch. *Comprehensive Glycoscience*, 2, 579-612.
- Bertoft, E. (2004). Lintnerization of two amylose-free starches of A- and B-crystalline types, respectively. *Starch/Stärke*, 56, 167-180.
- Bertoft, E. and Qin, Z. (1993). Studies on the structure of pea starches Part 4: Intermediate material of wrinkled pea starch. *Starch/Stärke*, 45, 420-425.

- Bertoft, E. and Wiik, D. (2004). Acid treatment of starch granules. In *Starch: progress in structural studies, modifications and applications*. P. Tomasik, V. P. YÛr'ev, E. Bertoft, Eds., Polish Society of Food Technologists, Cracow, Poland. pp. 289-300.
- Biliaderis, C. G. (1982). Physical characteristics, digestibility and structure of chemically-modified smooth pea and waxy maize starches. *Journal of Agricultural and Food Chemistry*, 30, 925-930.
- Biliaderis, C. G. (1992). Structures and phase transitions of starch in food systems. *Food Technology*, 46, 98-109.
- Biliaderis, C. G. (1998). Structures and phase transitions of starch polymers. In *Polysaccharide Association Structures in Foods*, R. H. Walter, Ed., Marcel Dekker, New York, NY, pp. 57-168.
- Biliaderis, C. G. (2009). Structural transitions and related physical properties of starch. In *Starch chemistry and Technology*, J. BeMiller, R. Whistler, Eds., Academic press, NY, pp. 293-359.
- Biliaderis, C. G., and Galloway, G. (1989). Crystallization behaviour of amylose-V complexes: structure-property relationships. *Carbohydrate Research*, 189, 31-48.
- Biliaderis, C. G. Grant, D. R. and Vose, J. R. (1981). Structure characterization of legume starches. II. Studies on acid treated starches. *Cereal Chemistry*, 58, 502-507.
- Biliaderis, C. G., Page, C. M., Slade, L. and Sirett, R. R. (1985). Thermal-behavior of amylose-lipid complexes, *Carbohydrate Polymers*, 5, 367-389.
- Biliaderis, C. G. and Prokopowich, D. J. (1994). Effect of polyhydroxy compounds on structure formation in waxy starch gels- a calorimetric study. *Carbohydrate Polymers*, 23, 193-202.
- Biliaderis, C. G. and Tonogai, J. R. (1991). Influence of lipids on the thermal and mechanical properties of concentrated starch gels. *Journal of Agricultural and Food Chemistry*, 39, 833-840.
- Biliaderis, C. G. and Zawistowski, J. (1990). Viscoelastic behavior of aging starch gels; effect of concentration, temperature and starch hydrolysates on network properties. *Cereal Chemistry*, 67, 240-246.

- Bird, A. R., Lopez-Rubio, A., Shrestha, A. K., and Gidley, M. J. (2009). Resistant starch in vitro and in vivo: Factors determining yield, structure, and physiological relevance. In *Modern biopolymer sciences*. S. Kasapis, I. T. Norton, and J. B. Ubbink., Eds., Academic Press, London. pp. 449–512.
- Blanshard, J. M. V. (1986). The significance of structure and function of the starch granule in baked products. In *Chemistry and Physics of Baking*, J. M. V. Blanshards, Ed. Royal Society of Chemistry, London, pp. 1-13.
- Blazek, J. and Copeland, L. (2010). Amylolysis of wheat starches. II. Degradation patterns of native starch granules with varying functional properties. *Journal of Cereal Science*, 52, 295-302.
- Blazek, J. and Gilbert, E. P. (2010). Effect of enzymatic hydrolysis on native starch granule structure. *Biomacromolecules*, 11, 3275-3289.
- Blennow, A., Bay-Smidt, A. M., Wischmann, B., Olsen, C. E. and Lindberg-Møller, B. (1998). The degree of starch phosphorylation is related to the chain length distribution of the neutral and the phosphorylated chains of amylopectin. *Carbohydrate Research*, 307, 45–54.
- Blennow, A., Engelsen, S. B., Nielsen, T. H., Baunsgaard, L. and Mikkelsen, R. (2000). Starch phosphorylation: a new front line in starch research. *Trends in Plant Sciences*, 7, 445-450.
- Blennow, A., Hansen, M., Schulz, A., Jørgensen, K., Donald, A. M. and Sanderson, J. (2003). The molecular deposition of transgenically modified starch in the starch granule as imaged by functional microscopy. *Journal of Structural Biology*, 143, 229– 241.
- Bligh, E. G. and Dyer, W. J. (1959). A rapid method for total lipid extraction and purification. *Canadian Journal of Biochemistry and Physiology*, 37, 911-917.
- Bogacheva, T. Y., Morris, V. J., Ring, S. G. and Hedley, C. L. (1998). The granular structure of C-type pea starch and its role in gelatinization. *Biopolymers*, 45, 323– 332.
- Bogacheva, T. Y. Wang Y. L. and Hedley, C. L. (2001). The effect of water content on the ordered/disordered structures in starches. *Biopolymers*, 58, 247–259.

- Boyer, C. d., Simpson, E. k. G. and Damewood, P. A. (1982). The possible relationship of starch and phytoglycogen in sweet corn. II. The role of branching enzyme I. *Starch/Stärke*, 34, 81-85.
- Brumovsky, J. O. and Thompson, D. B. (2001). Production of boiling stable granular resistant starch by partial acid hydrolysis and hydrothermal treatments of high amylose maize starch. *Cereal Chemistry*, 79, 680–689.
- Bruner, R.L. (1964). Determination of reducing value. In R.L. Whistler (Ed), *Methods in Carbohydrate Chemistry: Starch* (Vol. IV). Academic Press, NY, pp. 67-71.
- Buléon, A. Colonna, P. Planchot V. and Ball, S. (1998). Starch granules: Structure and biosynthesis. *International Journal of Biological Macromolecules*, 23, 85–112.
- Buléon, A., Bizot, H., Delage, M. M. and Multon, J. L. (1982). Evolution of crystallinity and specific gravity of potato starch versus water ad- and desorption. *Starch/Stärke*, 34, 361–366.
- Bulpin, P. V., Welsh, E. J. and Morris, E. R. (1982). Physical characterization of amylose-fatty acid complexes in granules and in solution. *Starch/Stärke*, 34, 335-339.
- Burrell, M. M. (2003). Starch: the need for improved quality or quantity: an overview. *Journal of Experimental Botany*, 54, 451-456.
- Burton, R. A., Bewley, J. D., Smith, A. M., Bhattacharyya, M. K., Tatge, H., Ring, S., Bull, V., Hamilton, W. D. O. and Martin, C. (1995). Starch branching enzymes belonging to distinct enzyme families are differentially expressed during pea embryo development. *The Plant Journal*, 7, 3-15.
- Calabrese, V. T. and Khan, A. (1999). Amylose–iodine complex formation without KI: evidence for absence of iodide ions within the complex. *Journal of Polymer Science: Part A*, 37, 2711–2717.
- Capron, I., Robert, P., Colonna, P., Brogly, M. and Planchot, V. (2007). Starch in rubbery and glassy states by FTIR spectroscopy. *Carbohydrate Polymers*, 68, 249-259.
- Carlson, T. L. G., Larsson, K., Dinhnguyen, N. and Krog, N. (1979). Study of the amylose–monoglyceride complex by Raman-spectroscopy, *Starch*, 31, 222–224.

- Cheetham, N. W. H. and Tao, L. P. (1998). Amylose conformational transitions in binary DMSO/water mixtures. *Carbohydrate Polymers*, 35, 287–295.
- Chung, J. H., Han, J. A., Yoo, B., Seib, P. A. and Lim, S. T. (2008). Effects of molecular size and chain profile of waxy cereal amylopectins on paste rheology during retrogradation. *Carbohydrate Polymers*, 71, 365-371.
- Chung, H. J., Hoover, R. and Liu, Q. (2009). The impact of single and dual hydrothermal modifications on the molecular structure and physicochemical properties of normal corn starch. *International Journal of Biological Macromolecules*, 44, 203-210.
- Chung, H. J., Liu, Q. and Hoover, R. (2009). Impact of annealing and heat-moisture treatment on rapidly digestible, slowly digestible and resistant starch levels in native and gelatinized corn, pea and lentil starches. *Carbohydrate Polymers*, 75, 436–447.
- Chung, H. J., Liu, Q. and Hoover, R. (2010). Effect of single and dual hydrothermal treatments on the crystalline structure, thermal properties, and nutritional fractions of pea, lentil, and navy bean starches. *Food Research International*, 43, 501-508.
- Chung, H. J., Liu, Q., Donner, E., Hoover, R., Warkentin, T. D. and Vandenberg, B. (2008). Composition, molecular structure, properties and in vitro digestibility of starches from newly released Canadian pulse cultivars. *Cereal Chemistry*, 85, 471–479.
- Collado, L.S. and Corke, H. (1999). Heat-moisture treatment effects on sweet potato starches differing in amylose content. *Food Chemistry*, 65, 339–346.
- Colonna, P. and Buléon, A. (2009). Thermal transitions of starches. In A. C. Bertolini, (Ed), *Starches: Characterization, properties and applications*, CRC Press, Boca Raton, FL, pp 72-95.
- Colonna, P., Buléon, A. and Lemarié, F. (1988). Action of *Bacillus subtilis* α -amylase on native wheat starch. *Biotechnology and Bioengineering*, 31, 895–904.
- Colonna, P., Leloup, V. and Buléon, A. (1992). Limiting factors of starch hydrolysis. *European Journal of Clinical Nutrition*, 46, S17-S32.

- Colonna, P. and Mercier, C. (1984). Macromolecular structure of wrinkled-and smooth-pea starch components. *Carbohydrate Research*, 126, 233–247.
- Cooke, D. and Gidley, M. (1992). Loss of crystallinity and molecular order during starch gelatinization: origin of the enthalpic transition. *Carbohydrate Research*, 227, 103-112.
- Craig, S. A. S., Maninget, C. C., Seib, P. A. and Hosney, R. C. (1989). Starch paste clarity. *Cereal Chemistry*, 66, 173-182.
- Dang, J. M. C. and Copeland, L. (2003). Imaging rice grains using atomic force microscopy. *Journal of Cereal Science*, 37, 165-170.
- Daniels, D. R. and Donald, A. M. (2004). Soft material characterization of the lamellar properties of starch: Smectic side-chain liquid-crystalline polymeric approach. *Macromolecules*, 37, 1312-1318.
- Davis, J. P., Supatcharee, N., Khanddelwal, R. L. and Chibbar, R. N. (2003). Synthesis of novel starches in Planta: Opportunities and challenges. *Starch/Stärke*, 55, 107-120.
- Debet, M. R. and Gidley, M. J. (2006). Three classes of starch granule swelling: Influence of surface proteins and lipids. *Carbohydrate Polymers*, 64, 452-465.
- Demeke, T., Hucl, P., Abdel-Aal, E. S. M., Baga, M. and Chibbar, R. N. (1999). Biochemical characterization of the wheat waxy A protein and its effect on starch properties. *Cereal Chemistry*, 76, 694-698.
- Dhital, S., Shrestha, A. K. and Gidley, M. J. (2010). Effect of cryo-milling on starches: functionality and digestibility. *Food Hydrocolloids*, 24, 152-163.
- Dickinson, L. C., Morganelli, P., Chu, C. W., Petrovic, Z., Macknight, J. and Chen, J. C. W. (1998). Molecular motions in model network polymers. *Macromolecules*, 21, 338-346.
- Dona, A. C., pages, G., Gilbert, R. G., and Kuchel, P. W. (2010). Digestion of starch: *in vivo* and *in vitro* kinetic models used to characterize oligosaccharide or glucose release. *Carbohydrate Polymers*, 80, 599-617.
- Donovan, J. W. (1979). Phase transitions of the starch-water system. *Biopolymers* 18, 263–275.

- Donovan, J. W. and Mapes, C. J. (1980). Multiple phase transitions of starches and Naegeli amyloextrins. *Starch/Stärke*, 32,190-193.
- Donovan, J. W., Lorenz, K. and Kulp, K. (1983). Differential scanning calorimetry of heat-moisture treated wheat and potato starches. *Cereal Chemistry*, 60, 381-387.
- Doublier, J. L. (1987). A rheological comparison of wheat, maize, faba bean and smooth pea starches. *Journal of Cereal Science*, 5, 247-262.
- Doublier, J. L., Llamas, G. and LeMeur, M. (1987). A rheological investigation of cereal pastes and gels. Effect of pasting procedures. *Carbohydrate Polymers*, 7, 251-275.
- Eckel, R. H., Grundy, S. M. and Zimmet, P. Z. (2005). The metabolic syndrome. *Lancet*, 365, 1415-1428.
- Eerlingen, R.C., Jacobs, H., Van Win, H. and Delcour, J.A. (1996). Effect of hydrothermal treatment on the gelatinization properties of potato starch as measured by differential scanning calorimetry. *Journal of Thermal Analysis*, 47, 1229-1246.
- Ek, K. L., Miller, J. B. and Copeland, L. (2012). Glycemic effect of potatoes. *Food Chemistry*, 133, 1230-1240.
- El-Faki, H. A., Desikachar, H. S. R., Tareen, J. A. K. and Tharanathan, R. N. (1983). Scanning electron microscopy of in vivo and in vitro digested starch granules of chickpea, cowpea and horse gram. *Journal of Food Science and Technology*, 17, 276-281.
- Eliasson, A. C. (1986). Viscoelastic behavior during the gelatinization of starch I. comparison of wheat, maize, potato and waxy-barley starches. *Journal of Texture Studies*, 17, 253-265.
- Eliasson, A. C. and Gudmundsson, M. (1996). Starch: physicochemical and functional aspects. In A. C. Eliasson, (Ed), *Carbohydrates in Food*. Marcel Dekker, New York, NY, pp. 431-503.
- Eliasson, A. C. and Krog, N. (1985). Physical properties of amylose-monoglyceride complexes. *Journal of Cereal Science*, 3, 239-248.

- Ellis, R. P., Cochrane, M. P., Dale, M. F. B., Duffus, C. M., Lynn, A., Morrison, I. M., Prentice, R. D. M., Swanston, J. S. and Tiller, S. A. (1998). Starch production and industrial use. *Journal of Science and Food Agriculture*, 77, 289-311.
- Englyst, K. N., Liu, S. and Englyst, H. N. (2007). Nutritional characterization and measurement of dietary carbohydrates. *European Journal of Clinical Nutrition*, 61, S19-S39.
- Eerlingen, R. C., Jacobs, H., Block, K. and Delcour, J. A. (1997). Effects of hydrothermal treatment on the rheological properties of potato starch. *Carbohydrate Research*, 297, 347-356.
- Evans, I. D. and Haisman, D. R. (1982). The effect of solutes on the gelatinization temperature range of potato starch. *Starch/Stärke*, 34, 224-231.
- Fan, J and Marks B. P. (1998). Retrogradation kinetics of rice flours as influenced by cultivar. *Cereal Chemistry*, 75, 153-155.
- FAO/WHO. (1998). Carbohydrates in human nutrition. *Report of a joint FAO/WHO Expert Consultation* (pp.1-140): FAO, Food Nutrition Paper.
- FAO-Food and Agriculture Organization of the United Nations. (2007). *FAOSTAT Statistics database-Agriculture*, Rome, Italy.
- Fisher, D. K. and Thompson, D. B. (1997). Retrogradation of maize starch after thermal treatment within and above the gelatinization temperature range. *Cereal Chemistry*, 75, 344-351.
- Fitzgerald, M. A., Bergman, C. J., Resurreccion, A. P., Möller, J., Jimenez, R., Reinke, Russell, F., Martin, M., Blanco, P., Molina, F., Chen, M. H., Kuri, V., Romero, M. V., Habibi, F., Umemoto, T., Jongdee, S., Graterol, E., Reddy, K. R., Bassinello, P. Z., Sivakami, R., Rani, N. S., Das, S., Wang, Y. J., Indrasari, S. D., Ramli, A., Ahmad, R., Dipti, S. S., Xie, L., Lang, N. T., Singh, P., Toro, D. C., Tavasoli, F. and Mestres, C. (2009). Addressing the dilemmas of measuring amylose in rice. *Cereal Chemistry*, 86, 492-498.
- Flores-Morales, A., Jiménez-Estrada, M. and Mora-Escobedo, R. (2012). Determination of the structural changes by FT-IR, Raman, and CP/MAS ¹³C NMR spectroscopy on retrograded starch of maize tortillas. *Carbohydrate Polymers*, 87, 61-68.

- Forsyth, J. L., Ring, S. G., Noel, T. R., Parker, R., Cairns, P., Findlay, K. and Shewry, P. R. (2002). Characterization of starch from tubers of yam bean (*Pachyrhizus ahipa*). *Journal of Agricultural and Food Chemistry*, *50*, 361–367.
- Franco, C. M. L. and Ciacco, C. F. (1987). Studies on the susceptibility of granular cassava and corn starches to enzymatic attack. *Starch/Starke*, *39*, 432-435.
- Franco, C.M.L., Ciacco, C.F., and Tavares, D.Q. (1995). Effect of the heat- moisture treatment on the enzymatic susceptibility of corn starch granules. *Starch*, *47*, 223–228.
- Franco, C. M. L., Wong, K. S., Yoo, S. H. and Jane, J. L. (2002). Structural and functional characteristics of selected soft wheat starches. *Cereal Chemistry*, *79*, 243-248.
- Fredriksson, H., Silverio, J., Andersson, R., Eliasson, A.-C. and Åman, P. (1998). The influence of amylose and amylopectin characteristics on gelatinization and rétrogradation properties of different starches. *Carbohydrate Polymers*, *35*, 119-134.
- Fuentes-Zaragoza, E., Sánchez-Zapata, E., Sendra, E., Sayas, E., Navarro, C., Fernández-López, J. and Pérez-Alvarez, J. A. (2011). Resistant starch as prebiotic: A review. *Starch/Starke*, *63*, 406-415.
- Fukui, T. and Nikuni, Z. (1969). Heat-moisture treatment of cereal starch observed by X-ray diffraction. *Agricultural and Biological Chemistry*, *33*, 460–462.
- Galliard, T. and Bowler, P. (1987). Morphology and composition of starch. In T. Galliard, (Ed), *Starch, Properties and Potential*, John Wiley, Chichester, UK, pp. 55-78.
- Gallant, D. J., Bouchet, B. and Baldwin, P. M. (1997). Microscopy of starch: evidence of a new level of granule organization. *Carbohydrate Polymers*, *32*, 177-191.
- Gallant, D. J., Bouchet, B., Buléon A. and Pérez, S. (1992). Physical characteristics of starch granules and susceptibility to enzymatic degradation. *European Journal of Clinical Nutrition*, *46*, S3–S16.
- Gao, J., Vasanthan, T., Hoover, R. and Li, J. (2012). Structural modification of waxy, regular and high-amylose maize and hullless barley starches on partial acid

- hydrolysis and their impact on physicochemical properties and chemical modification. *Starch/Stärke*, *64*, 313-325.
- Gerard, C., Barron, C., Colonna, P. and Planchot, V. (2001a). Amylose determination in genetically modified starches. *Carbohydrate Polymers*, *44*, 19-27.
- Gérard, C., Colonna, P., Buléon, A. and Planchot, V. (2001b). Amylolysis of maize mutant starches. *Journal of the Science of Food and Agriculture*, *81*, 1281-1287.
- Gérard, C., Colonna, P., Buléon, A. and Planchot, V. (2002). Order in maize mutant starches revealed by mild acid hydrolysis. *Carbohydrate Polymers*, *48*, 131-141.
- Gernat, C., Radosta, S., Damaschun, G. and Schierbaum, F. (1990). Supramolecular structure of legume starches revealed by X-ray scattering, *Starch/Stärke*, *42*, 175-178.
- Ghiasi, K., Varriano-Marston, E. and Hosney, R.C. (1982). Gelatinization of wheat starch. 2. Starch surfactant interaction. *Cereal Chemistry*, *59*, 86-88.
- Gidley, M. J. (1987). Factors affecting the crystalline type (A-C) of native starches and model compounds: a rationalisation of observed effects in terms of polymorphic structures. *Carbohydrate Research*, *161*, 301-304.
- Gidley, M.J. and Bociek, S.M. (1985). Molecular organization in starches: A ^{13}C .CP/MAS NMR study. *Journal of the American Chemical Society*, *107*, 7040-7044.
- Gidley, M. J. and Bociek, S. M. (1988). ^{13}C CP/MAS NMR Studies of amylose inclusion complexes, cyclodextrins, and the amorphous phase of starch granules: relationships between glycosidic linkage conformation and solid-state ^{13}C chemical shifts. *Journal of the American Chemical Society*, *110*, 3820-3829.
- Gidley, M. J., and Bulpin, P. V. (1987). Crystallization of malto-oligosaccharides as model of the crystalline forms of starch: minimum chain-length requirement for the formation of double helices. *Carbohydrate Research*, *161*, 291-300.
- Gidley, M. J., Cooke, D., Darke, A. H., Hoffmann, R. A., Russell, A. L. and Greenwell, P. (1995). Molecular order and structure in enzyme-resistant retrograded starch. *Carbohydrate Polymers*, *28*, 23-31.

- Glaring, M. A., Koch, C. B. and Blennow, A. (2006). Genotype-specific spatial distribution of starch molecules in the starch granule: a combined CLSM and SEM approach, *Biomacromolecules*, 7, 2310–2320.
- Godet, M. C., Bizot, H. and Buléon, A. (1995). Crystallization of amylose-fatty acid complexes prepared with different amylose chain lengths. *Carbohydrate Polymers*, 27, 47–52.
- Godet, M. C., Bouchet, B., Colonna, P., Gallant, D. J. and Buléon, A. (1996). Crystalline amylose fatty acid complexes: morphology and crystal thickness, *Journal of Food Science*, 61, 1196–1201.
- Gomand, S. V., Lamberts, L., Visser, R. G. F. and Delcour, J. A. (2010). Physicochemical properties of potato and cassava starches and their mutants in relation to their structural properties. *Food Hydrocolloids*, 24, 424-433.
- Goni, I., Garcia-Alonso, A. and Saura-Calixto, F. (1997). A starch hydrolysis procedure to estimate glycemic index. *Nutrition Research*, 17, 427-437.
- Grandfeldt, Y., Björck, I., Drews, A. Q. and Tovar, J. (1992). An *in-vitro* procedure based on chewing to predict metabolic responses to starch in cereal and legume products. *European Journal of Clinical Nutrition*, 46, 649-660.
- Gray, J. A. and BeMiller, J. N. (2004). Development and utilization of reflectance confocal laser scanning microscopy to locate reaction sites in modified starch granules. *Cereal Chemistry*, 81, 278–286.
- Greenwell, P., Evers, A. D., Gough, B. M. and Russell, P. L. (1985). Amyloglucosidase-catalysed erosion of native, surface-modified and chlorine-treated wheat starch granules. The influence of surface protein. *Journal of Cereal Science*, 3, 279–293.
- Greenwell, P. and Scofield, J. D. (1986). A starch granule protein associated with endosperm softness in wheat. *Cereal Chemistry*, 63, 379-380.
- Guan, H. P. and Preiss, J. (1993). Differentiation of the properties of the branching isozymes from maize (*Zea mays*). *Plant Physiology*, 102, 1269–1273.
- Gudmundsson, M. E. and Eliasson, L. C. (1991). The effects of water soluble arabinoxylan on gelatinization and retrogradation of starch, *Starch/Starke*, 43, 5-10.

- Gunaratne, A. and Corke, H. (2007). Gelatinizing, pasting and gelling properties of potato and amaranth starch mixtures. *Cereal Chemistry*, 84, 22–29.
- Gunaratne, A. and Hoover, R. (2002). Effect of heat-moisture treatment on the structure and physicochemical properties of tuber and root starches. *Carbohydrate Polymers*, 40, 425-437.
- Guzel, D. and Sayar, S. (2010). Digestion profiles and some physicochemical properties of native and modified borlotti bean, chickpea and white kidney bean starches. *Food Research International*, 43, 2132-2137.
- Haase, N. U. and Shi, H. L. (1991). Characterization of faba bean starch (*Vicia faba L.*), *Starch/Stärke*, 43, 205–208.
- Hagenimana, A. and Ding, X. (2005). A comparative study on pasting and hydration properties of native rice starches and their mixtures. *Cereal Chemistry*, 82, 72–76.
- Han, X. Z. and Hamaker, B. R. (2001). Amylopectin fine structure and rice starch paste breakdown. *Journal of Cereal Science*, 34, 279-284.
- Hanashiro, I., Shinohara, H. and Takeda, Y. (2003). Application of fluorescent labeling HPSEC method of structural characterization of the product from amylose by starch branching enzyme. *Journal of Applied Glycoscience*, 50, 487-491.
- Hanashiro, I., Tagawa, M., Shibahara, S., Iwata, K., Takeda, Y. (2002). Examination of molar-based distribution of A, B and C chains of amylopectin by fluorescent labelling with 2-aminopyridine. *Carbohydrate Research*, 337, 1211–1215.
- Hanes, C. S. (1937). The action of amylases in relation to the structure of starch and its metabolism in the plant. Parts I-III. *New Phytologist*, 36, 101–141.
- Haase, N. U. and Shi, H. L. (1991). Characterization of faba bean starch (*Vicia faba L.*). *Starch/Stärke*, 43, 205–208.
- Hayashi, A., Kinoshita, K. and Miyake, Y. (1981). The conformation of amylose in solution. *Polymer Journal*, 13, 537–541.
- Hedley, L., Bogracheva, T. Y. and Wang, T. L. (2002). A genetic approach to studying the morphology, structure and function of starch granules using pea as a model. *Starch/Stärke*, 54, 235–242.

- Heinemann, C., Conde-Petit, B., Nuessli, J. and Escher, F. (2001). Evidence of starch inclusion complexation with lactones, *Journal of Agricultural and Food Chemistry*, 49, 1370–1376.
- Herrero-Martínez, J. M., Schoenmakers, P. J. and Kok, W. T. (2004). Determination of the amylose–amylopectin ratio of starches by iodine-affinity capillary electrophoresis. *Journal of Chromatography A*, 1053, 227-234.
- Higgins, J. A. (2004). Resistant starch: Metabolic effects and potential health benefits. *Journal of AOAC International*, 87, 761-768.
- Hill, R. D. and Dronzek, B. L. (1973). Scanning electron microscopy studies of wheat, potato and corn starch during gelatinization. *Starch//Stärke*, 25, 367-372.
- Hizukuri, S. (1961). X-ray diffractometer studies on starches. Part VI. Crystalline types of amylopectin and effect of temperature and concentration of mother liquor on crystalline type. *Agricultural Biological Chemistry*, 25, 45-49.
- Hizukuri, S. (1985). Relationship between the distribution of the chain length of amylopectin and the crystalline structure of starch granules. *Carbohydrate Research*, 141, 295–306.
- Hizukuri, S. (1986). Polymodal distribution of the chain lengths of amylopectins, and its significance. *Carbohydrate Research*, 147, 342–347.
- Hizukuri, S., Kaneko, T. and Takeda, Y. (1983). Measurement of the chain length of amylopectin and its relevance to the origin or crystalline polymorphism of starch granules. *Biochemica et Biophysica Acta*, 760, 188–191.
- Hizukuri, S., Tabata, S. and Nikuni, Z. (1970). Studies on starch phosphate. Part 1. Estimation of glucose-6-phosphate residues in starch and the presence of other bound phosphate(s). *Starch*, 22, 338-343.
- Hizukuri, S., Takeda, Y., Abe, J., Hanashiro, I., Matsunobu, G. and Kiyota, H. (1997). Analytical developments: molecular and microstructural characterization. In *Starch: Structure and Functionality*. P. J. Frazier, P. Richmond, A. M. Donald., Eds., London: Royal Society of Chemistry, pp. 121.

- Hizukuri, S., Takeda, Y., Yasuda, M. and Suzuki, A. (1981). Multibranched nature of amylose and the action of de-branching enzymes. *Carbohydrate Research*, 94, 205–213.
- Holt, S. H. A., Miller, J. C. B., Petocz, P. and Farmakalidis, E. (1995). A satiety index of common foods. *European journal of clinical nutrition*, 49, 675–690.
- Hoover, R. (1995). Starch retrogradation. *Food Reviews International*, 11, 331-346.
- Hoover, R. (2000). Acid treated starches. *Food Reviews International*, 16, 369-392.
- Hoover, R. (2010). The impact of heat-moisture treatment on molecular structures and properties of starches isolated from different botanical sources. *Critical Reviews in Food Science and Nutrition*, 50, 1-13.
- Hoover, R. (2001). Composition, molecular structure, and physico-chemical properties of tuber and root starches: a review. *Carbohydrate Polymers* 45, 253–267.
- Hoover, R. and Hadziyev, D. (1981). Characterization of potato starch and its monoglyceride complexes. *Starch/Stärke*, 33, 290–330.
- Hoover, R., Hynes, Y.X. , Li, G. and Senanayake, N. (1997). Physicochemical characterization of mung bean starch. *Food Hydrocolloids*, 11: 401–408.
- Hoover, R., Hughes, T., Chung, H. J. and Liu, Q. (2010). Composition, molecular structure, properties and modification of pulse starches- A review. *Food Research International*, 43, 399-413.
- Hoover, R., Li, Y., Hynes, G. and Senanayake, N. (1997). Physicochemical characterization of mung bean starch. *Food Hydrocolloids*, 11:401–408.
- Hoover, R. and Manuel, H. (1996a). Effect of heat-moisture treatment on the structure and physicochemical properties of legume starches. *Food Research International*, 29, 731–750.
- Hoover, R. and Manuel, H. (1996b). The effect of heat-moisture treatment on the structure and physicochemical properties of normal maize, waxy maize, dull waxy maize and amylo maize V starches. *Journal of Cereal Science*, 23, 153-162.
- Hoover, R. and Manuel, H. (1995). A comparative study of the physicochemical properties of starches from two lentil cultivars. *Food Chemistry*, 53:275–284.

- Hoover, R. and Ratnayake, W. S. (2002). Starch characteristics of black bean, chickpea, lentil, navy bean and pinto bean cultivars grown in Canada. *Food Chemistry*, 78, 489–498.
- Hoover, R. and Ratnayake, W.S. (2004). Determination of total amylose content of starch. In *Handbook of Food Analytical Chemistry – Water, protein, enzymes, lipids, and carbohydrates*, Wrolstad *et al.* (Eds.), Wiley-Interscience, Hoboken. NJ, pp. 689-691.
- Hoover, R. and Sosulski, F. W. (1985). Studies on the functional characteristics and digestibility of starches from phaseolus vulgaris biotypes. *Starch*, 37, 181–191.
- Hoover, R. and Sosulski, F. W. (1991). Composition, structure, functionality, and chemical modification of legume starches: A review. *Canadian Journal of Physiology and Pharmacology*, 69, 79-92.
- Hoover, R., Swamidas, G. and Vasanthan, T. (1993). Studies on the physicochemical properties of native, defatted, and heat-moisture treated pigeon pea (*Cajanus cajan* L.) starch. *Carbohydrate Research*, 246, 185–203.
- Hoover, R., Vasanthan, T., Senanayake, N. J. and Martin, A. M. (1994). The effects of defatting and heat–moisture treatment on the retrogradation of starch gels from wheat, oat, potato and lentil. *Carbohydrate Research*, 26, 13–24.
- Hoover, R. and Vasanthan, T. (1994a). Effect of heat-moisture treatment on the structure and physicochemical properties of cereal, legume and tuber starches. *Carbohydrate Research*, 252, 33-53.
- Hoover, R., and Vasanthan, T. (1994b). The flow properties of native, heat– moisture treated and annealed starches from wheat, oat, potato and lentil. *Journal of Food Biochemistry*, 18, 67–82.
- Hoover, R. and Zhou, Y. (2003). *In vitro* and *in vivo* hydrolysis of legume starches by α -amylase and resistant starch formation in legumes, A review. *Carbohydrate Polymers*, 54, 401-417.
- Hormdok, R. and Noomhorm, A. (2007). Hydrothermal treatments of rice starch for improvement of rice noodle quality, *LWT – Food Science and Technology*, 40, 1723–1731.

- Htoon, A., Shrestha, A. K., Flanagan, B. M., Lopez-Rubio, A., Bird, A. R., Gilbert, E. P. and Gidley, M. J. (2009). Effects of processing high amylose maize starches under controlled conditions on structural organisation and amylase digestibility. *Carbohydrate Polymers*, 75, 236-245.
- Huang, J., Schols, H. A., Van Soest, J. J. G., Jin, Z., Sulmann, E. and Voragen, G. J. A. (2007). Physicochemical properties and amylopectin chain profiles of cowpea, chickpea and yellow pea starches. *Food Chemistry*, 101, 1338–1345.
- Huber, K. C. and BeMiller, J. N. (2000). Channels of maize and sorghum starch granules. *Carbohydrate Polymers*, 41, 269-276.
- Hughes, T., Hoover, R., Liu, Q., Donner, E., Chibbar, R. and Jaiswal, S. (2009). Composition, morphology, molecular structure, and physicochemical properties of starches from newly released chickpea (*Cicer arietinum* L.) cultivars grown in Canada. *Food Research International*, 42, 627-635.
- Imberty, A., Buléon, A., Tran, V. and Pérez, S. (1991). Recent advances in knowledge of starch structure. *Starch/Stärke*, 43, 375–384.
- Imberty, A. and Pérez, S. (1988). A revisit to the three dimensional structure of B-type starch. *Biopolymers*, 27, 308–325.
- Imberty, A., Chanzy, H., Pérez, S., Buléon, A. and Tran, V. (1988). The double helical nature of the crystalline part of A-starch. *Journal of Molecular Biology*, 201, 365–378.
- Inouchi, N., Glover, D. V., Sugimoto, Y., Fuwa, H. (1991). DSC characteristics of retrograded starches of single-, double-, and triple-mutants and their normal counterpart in the inbred Oh43 Maize (*Zea mays* L.) background. *Starch/Stärke*, 43, 473-477.
- International Standards Organization. ISO 26,642 (2010). Food products – Determination of the glycaemic index (GI) and recommendation for food classification, *International Standards Organisation*, 2010.
- Jackson, D. S. (2003). Starch–Structure, properties and determination, *Encyclopedia of Food Sciences, Food Technology, and Nutrition*, Academic Press, New York, pp. 5561–5567.

- Jacobasch, G., Dongowski, G., Schmedl, D., and Schmehl, K.M. (2006). Hydrothermal treatment of Novelose 330 results in high yield of resistant starch type 3 with beneficial prebiotic properties and decreased secondary bile acid formation in rats. *British Journal of Nutrition*, *95*, 1068–1074.
- Jacobs, H. and Delcour, J.A. (1998). Hydrothermal modifications of granular starch, with retention of the granular structure: a review. *Journal of Agricultural Food Chemistry*, *46*, 2895–2905.
- Jacobs, H., Eerlingen, R. C., Rouseu, N., Colonna, P. and Delcour, J. A. (1998). Acid hydrolysis of native and annealed wheat, potato and pea starches—DSC melting features and chain length distributions of lintnerised starches. *Carbohydrate Research*, *308*, 359-371.
- Jacobson, M. R., Obanni, M. and BeMiller, J. N. (1997). Retrogradation of starches from different botanical sources. *Cereal Chemistry*, *74*, 571-578.
- Jane, J. (1993). Mechanism of starch gelatinization in neutral salt solutions, *Starch/Starke*, *45*, 161-166.
- Jane, J. L. (2004). Starch: structure and properties. In *Chemical and functional properties of food saccharides*, P. Tomasik, Eds., CRC Press, Washington, D. C. pp. 81-101.
- Jane, J. (2006). Current understanding on starch granule structures. *Journal of Applied Glycoscience*, *53*, 205-213.
- Jane, J. L. (2007). Structure of starch granules, *Journal of Applied Glycoscience*, *54*, 31–36.
- Jane, J. L. (2009). Structural features of starch granules II. In *Starch: Chemistry and Technology*, J. BeMiller and R. Whistler, Eds., Academic Press, New York, NY, pp 193-236.
- Jane, J., Atichokudomchai, N., Park, J. and Suh, D. (2006). Effects of amylopectin structure on the organization and properties of starch granules. In *Advances in Biopolymers: Molecules, clusters, networks and interactions*, M. L. Fisherman, P. X. Qi, and L. Wicker, Eds., ACS Symposium series, Washington D.C. pp.146-164.

- Jane, J. L., Chen, Y. Y., Lee, L. F., McPherson, A. E., Wong, S., Radosavljevic, M. and Kasemsuwan, T. (1999). Effects of amylopectin branch chain length and amylose content on the gelatinization and pasting properties of starch. *Cereal Chemistry*, 76, 629–637.
- Jane, J., Kasemsuwan, T., Chen, J. F. and Juliano, B. O. (1996). Phosphorus in rice and other starches. *Cereal Foods World*, 41, 827–832.
- Jane, J., Kasemsuwan, T., Leas, S., Zobel, H. and Robyt, J. F. (1994). Anthology of starch granule morphology by scanning electron microscopy. *Starch/Stärke*, 46, 121–129.
- Jane, J. L. and Robyt, J. F. (1984). Structure studies of amylose V complexes and retrograded amylose by action of alpha amylase, a new method for preparing amyloextrins. *Carbohydrate Research*, 132, 105–110.
- Jane, J. L. and Shen, J. J. (1993). Internal structure of potato starch granule revealed by chemical gelatinization. *Carbohydrate Research*, 247, 279–290.
- Jane, J. -I., Wong, K. -S. and McPherson, A. E. (1997). Branch-structure difference in starches of A- and B-type X-ray patterns revealed by their Naegeli dextrins. *Carbohydrate Research*, 300, 219–227.
- Jane, J. L., Xu, A., Radosavljevic, M. and Seib, P. A. (1992). Location of amylose in normal starch granules. I: susceptibility of amylose and amylopectin to cross-linking reagents. *Cereal Chemistry*, 69, 405–409.
- Jane, J. L., Wong, K. S. and McPherson, A. E. (1997). Branch-structure difference in starches of A- and B-type X-ray patterns revealed by their Naegeli dextrins. *Carbohydrate Research*, 300, 219–227.
- Jaska, E. (1971). Starch gelatinization as detected by proton magnetic resonance. *Cereal Chemistry*, 48, 437–444.
- Jayakody, L. and Hoover, R. (2002). The effect of lintnerization on cereal starch granules. *Food Research International*, 35, 665–680.
- Jayakody, L., Lan, H., Hoover, R., Liu, Q. and Donner, E. (2007). Composition, molecular structure and physicochemical properties of starches from two grass pea (*Lathyrus sativus* L.) cultivars grown in Canada. *Food Chemistry*, 105, 116–125.

- Jenkins, P. J., Cameron, R. E. and Donald, A. M. (1993). A universal feature in the structure of starch granules from different botanical sources. *Starch/Stärke*, *45*, 417–420.
- Jenkins, P. J. and Donald, A. M. (1995). The influence of amylose on starch granule structure, *International Journal of Biological Macromolecules*, *17*, 315–321.
- Jenkins, D. A., Kendall, C. C., Augustin, L. S., Mitchell, S., Sahye-Pudaruth, S., Blanco Mejia, S., Chiavaroli, L., Mirrahimi, A., Ireland, C., Bashyam, B., Vidgen, E., de Souza, R. J., Sievenpiper, J. L., Coveney, J., Leiter, L. A. and Josse, R. G. (2012). Effect of Legumes as Part of a Low Glycemic Index Diet on Glycemic Control and Cardiovascular Risk Factors in Type 2 Diabetes Mellitus: A Randomized Controlled Trial. *Archives in International Medicine*, *172*, 1653-1660.
- Jenkins, D. J. A., Wolever, T. M. S., Jenkins, A. L., Thorne, M. J., Kalmusky, J. and Reichert, R. (1983). The glycemic index of foods tested in diabetic patients. A new basis for carbohydrate exchange favoring the use of legumes. *Diabetologia*, *34*, 257-264.
- Jenkins, D. J. A., Wolever, T. M. S., Taylor, R. H., Barker, H., Fielder, H., Baldwin, J. M., Bowling, A. C., Newman, H. C., Jenkins, A. L. and Goff, D. V. (1981). Glycemic index of foods: a physiological basis of carbohydrate exchange. *American Journal of Clinical Nutrition*, *34*, 362-366.
- Jeon, J. S., Ryoo, N., Hahn, T. R., Walia, H. and Nakamura, Y. (2010). Starch biosynthesis in cereal endosperm. *Plant Physiology and Biochemistry*, *48*, 383-392.
- Jinglin, Y., Shujun, W., Fengmin, J., Sun, L. and Yu, J. (2009). The structure of C-type *Rhizoma Dioscorea* starch granule revealed by acid hydrolysis method. *Food Chemistry*, *113*, 585-591.
- Jiranuntakul, W., Puttanlek, C., Rungsardthong, V., Pucha-arnon, S. and Uttapap, D. (2011). Microstructural and physicochemical properties of heat-moisture treated waxy and normal starches. *Journal of Food Engineering*, *104*, 246-258.

- John, M., Schmidt, J. and Kneifel, H. (1983). Iodine-maltosaccharide complexes: relation between chain-length and color. *Carbohydrate Research*, 119, 254-257.
- Jouppila, K., Kansikas, J. and Roos, Y. H. (1998). Factors affecting crystallization and crystallization kinetics in amorphous corn starch. *Carbohydrate Polymers*, 36, 143-149.
- Karim, A. A., Toon, L. C., Lee, V. P., Ong, W. Y., Fazilah, A. and Noda, T. (2007). Effects of phosphorus contents on the gelatinization and retrogradation of potato starch. *Journal of Food Science*, 72, C132-138.
- Karkalas J., Ma, S., Morrison, W. and Pethrick, R. A. (1995). Some factors determining the thermal properties of amylose inclusion complexes with fatty acids. *Carbohydrate Research*, 268, 233-247.
- Kasemsuwan, T. and Jane, J. (1994). Location of amylose in normal starch granules. II. Location of phosphodiester cross-linking revealed by phosphorous-31 nuclear magnetic resonance. *Cereal Chemistry*, 71, 282-287.
- Kim, W. J., Eum, C. J., Lim, S. T., Han, J. A., You, S. G. and Lee, S. (2007). Separation of amylose and amylopectin in corn starch using dual-programmed flow field-flow fractionation. *Bulletin of Korean Chemical Society*, 28, 2489-2492.
- Kawabata, A. , Takase, N., Miyoshi, E., Sawayama, S., Kimura, T. and Kudo, K. (1994). Microscopic observation and X-ray diffractometry of heat-moisture treated starch granules. *Starch/Stärke*, 46, 463-469.
- Kay, M., Behall, K. M., Daniel, J., Scholfield, D.J., Hallfrisch, J.G. and Liljeberg-Elmståhl, H.G.M. (2006). Consumption of both resistant starch and β -glucan improves postprandial plasma glucose and insulin in women. *Diabetes Care*, 29, 976- 981.
- Kevate, B. N., Chavan, U. D., Kadam, S. S. and Chavan, J. K. (2007). Isolation and characterization of moth bean. *Journal of Arid Legumes*, 4, 45-48.
- Khunae, P., Tran, T. and Sirivongpaisal, P. (2007). Effect of heat-moisture treatment on structural and thermal properties of rice starches differing in amylose content. *Starch/Stärke*, 59, 593-599.

- Klucinec, J. D. and Thompson, D. B. (1998). Fractionation of high amylose maize starches by differential alcohol precipitation and chromatography of the fractions. *Cereal Chemistry*, 75, 887-896.
- Klucinec, J. D. and Thompson, D. B. (1999). Amylose and amylopectin interact in retrogradation of dispersed high-amylose starches. *Cereal Chemistry*, 76, 282-291.
- Knutson, C. A. (2000). Evaluation of variations in amylose-iodine absorbance spectra. *Carbohydrate Polymers*, 42, 65-72.
- Knutson, C. A., Khoo, U., Cluskey, J. E. and Inglett, G. E. (1982). Variation in enzyme digestibility and gelatinization behavior of corn starch granule fractions. *Cereal Chemistry*, 59, 512-515.
- Kojima, M., Shimizu, H., Ohashi, M. and Ohba, K. (2006). Physico-chemical properties and digestibility of pulse starch after four different treatments. *Journal of Applied Glycoscience*, 53, 105-110.
- Kugimiya, M. and Donovan, J. W. (1981). Calorimetric determination of the amylose content of starches based on the formation and melting of the amylose-lysolecithin complex. *Journal of Food Science*, 46, 765.
- Kulp, K. and Lorenz, K. (1981). Heat-moisture treatment of starches. I. Physicochemical properties. *Cereal Chemistry*, 58, 46-48.
- Kweon, M., Haynes, L., Slade, L. and Levine, H. (2000). The effect of heat and moisture treatments on enzyme digestibility of AeWx, Aewx and aeWx corn starches. *Journal of Thermal Analytical Calorimetry*, 59, 571-586.
- Lan, H., Hoover, R., Jayakody, L., Liu, Q., Donner, E., Baga, M., Asare, E. K., Hucl, P. and Chibbar, R. N. (2008). Impact of annealing on the molecular structure and physicochemical properties of normal, waxy and high amylose bread wheat starches. *Food Chemistry*, 111, 663-675.
- Langton, M. and Hermasson, A. M. (1989). Microstructural changes in wheat starch dispersions during heating and cooling. *Food Microstructure*, 8, 29-39.

- Lansky, S., Kooi, M. and Schoch, T. J. (1949). Properties of the fractions and linear subfractions from various starches. *Journal of the American Chemical Society*, *71*, 4066-4075
- Larson, B. L., Gilles, K. A. and Jenness, R. (1953). Amperometric method for determining the sorption of iodine by starch. *Analytical Chemistry*, *25*, 802-804.
- László, E., Holló, J., Hoschke, A. and Sárosi, G. (1978). A study by means of lactone inhibition of the role of a "half-chair" glycosyl conformation at the active centre of amylolytic enzymes. *Carbohydrate Research*, *61*, 387-394.
- Lawal, O. S. (2005). Studies on the hydrothermal modifications of new cocoyam (*Xanthosoma sagittifolium*) starch. *International Journal of Biological Macromolecules*, *37*, 268-277.
- Lawal, O. S., and Adebowale, K. O. (2005a). An assessment of changes in thermal and physicochemical parameters of jack bean (*Canavalia ensiformis*) starch following hydrothermal modifications. *European Food Research and Technology*, *221*, 631-638.
- Lawal, O. S. and Adebowale, K. O. (2005b). Physicochemical characteristics and thermal properties of chemically modified jack bean (*Canavalia ensiformis*) starch. *Carbohydrate Polymers*, *60*, 331-341.
- Leach, W., McCowen, D. and Schoch, T. J. (1959). Structure of the starch granule. I. Swelling and solubility patterns of various starches. *Cereal Chemistry*, *36*, 534-544.
- Lee, C. J., Kim, Y., Choi, S. J. and Moon, T. W. (2011). Slowly digestible starch from heat-moisture treated waxy potato starch: preparation, structural characteristics, and glucose response in mice. *Food Chemistry*, *133*, 1222-1229.
- Leloup, V. M., Colonna, P. and Buléon, A. (1991). Influence of amylose-amylopectin ratio on gel properties. *Journal of Cereal Science*, *13*, 1-13.
- LeMeste, M., Huang, V. T., Panama, J., Anderson, G., Lentz, R. (1992). Glass transition of bread. *Cereal Foods World*, *37*, 264-267.
- Lewen, S. K., Paeschke, T., Reid, J., Molitor, P. and Schmidt, S. J. (2003). Analysis of the retrogradation of low starch concentration gels using differential scanning

- calorimetry, rheology and Nuclear magnetic Resonance Spectroscopy. *Journal of Agricultural and Food Chemistry*, 51, 2348-2358.
- Li, J. H., Vasanthan, T., Rossnagel, B. and Hoover, R. (2001). Starch from hull-less barley: I. Granule morphology, composition, and amylopectin structure. *Food Chemistry*, 74, 395–405.
- Li, S., Ward, R. and Gao, Q. (2011). Effect of heat-moisture treatment on the formation and physicochemical properties of resistant starches from mung bean (*Phaseolus radiatus*) starch. *Food Hydrocolloids*, 25, 1702-1709.
- Lim, S. T., Chang, E. H. and Chung, H. J. (2001). Thermal transition characteristics of heat-moisture treated maize and potato starches. *Carbohydrate Polymers*, 46, 107–115.
- Lim, S., Kasemsuwan, T. and Jane, J. (1994). Characterization of phosphorus in starch by ³¹P-nuclear magnetic resonance spectroscopy. *Cereal Chemistry*, 71, 488-493.
- Lim, S. T. and Seib, P. A. (1993). Preparation and pasting properties of wheat and corn starch phosphates. *Cereal Chemistry*, 70, 145-152.
- Lindeboom, N., Chang, P. R. and Tyler, R. T (2004). Analytical, biochemical and physicochemical aspects of starch granule size, with emphasis on small granule starches: A review. *Starch*, 56, 89–99.
- Lionetto, F., Maffezzoli, A., Ottenhof, M. A., Farhat, I. A. and Mitchell, J. R. (2005). The retrogradation of concentrated starch systems. *Starch/Stärke*, 57, 16-24.
- Liu, Q., Gu, Z., Donner, E., Tetlow, L. and Emes, M. (2007). Investigation of digestibility in vitro and physicochemical properties of A and B-type starch from soft and hard wheat flour, *Cereal Chemistry*, 84, 15–21.
- Liu, J. and Zhou, S. (1990). Scanning electron microscope study on gelatinization of starch granules in excess water. *Starch*, 42, 96-98.
- Loisel, C., Maache-Rezzoug, Z., Esneault, C. and Doublier, J. L. (2006). Effect of hydrothermaltreatment on the physical and rheological properties of maize starches. *Journal of Food Engineering*, 71, 45–54.

- Longton, D. J. and Legrys, G. A. (1981). Differential scanning calorimetry studies on the crystallinity of ageing wheat starch gels. *Starch/Starke*, 33: 410-414.
- Lopez, E. C., Rolee, A. and Le Meste, M. (2004). Study of starch granules swelling by the blue dextran method and by microscopy. *Starch*, 56, 576-581.
- Lopez-Rubio, A., Flanagan, B. M., Gilbert, E. P., and Gidley, M. J. (2008). A novel approach for calculating starch crystallinity and its correlation with double helical content: A combined XRD and NMR study. *Biopolymers*, 89, 761-768.
- Lorenz, K. and Kulp, K. (1981). Heat-moisture treatment of starches. II. Functional properties and baking potential. *Cereal Chemistry*, 58, 49-52.
- Lorenz, K., and Kulp, K. (1982). Cereal and root starch modification by heat- moisture treatment. 1. physicochemical properties. *Starch* 34, 50-54.
- Lu, S., Chen, C.Y. and Lii, C.Y. (1997). Correlations between the fine structure and physicochemical properties and retrogradation of amylopectins from Taiwan rice varieties. *Cereal Chemistry*, 74, 34-39.
- Lu, Z. H., Yada, R. Y., Liu, Q., Bizimungu, B., Murphy, A., Koeyer, D. D., Li, X. Q. and Pinhero, R. G. (2011). Correlation of physicochemical and nutritional properties of dry matter and starch in potatoes grown in different locations, *Food Chemistry*, 126, 1246-1253.
- Lunn, J. and Buttriss, J. L. (2007). Carbohydrates and dietary fibre. *Nutrition Bulletin*, 32, 21- 64.
- MacGregor, E. A. and MacGregor, A. W. (1985). The action of cereal α -amylases on solubilized starch and cereal starch granules. *Carbohydrate Research*, 142, 223-236.
- Marsh, R. D. L. (1986). A study of the retrogradation of wheat starch systems using X-ray diffraction. Doctoral dissertation, University of Nottingham.
- Matalanis, A. M., Campanella, O. H. and Hamaker, B. R. (2009). Storage retrogradation behaviour of sorghum, maize and rice starch pastes related to amylopectin fine structure. *Journal of Cereal Science*, 50, 74-81.
- Martin, C. and Smith, A. M. (1995). Starch biosynthesis. *The Plant Cell*, 7, 971-985.

- Matheson, N. K. and Welsh, L. A. (1988). Estimation and fractionation of the essentially unbranched (amylose) and branched (amylopectin) components of starch with concanavalin A. *Carbohydrate Research*, 180, 301-313.
- Melo, E. A., Stamford, T. L. M., Silva, M. P. C., Krieger, N. and Stamford, N. P. (2003). Functional properties of yam bean (*Pachyrhizus erosus*) starch. *Bioresource Technology*, 89, 103-106.
- McCue, K. F., Hurkman, W. J., Tanaka, C. K. and Anderson, O. D. (2002). Starch branching enzymes Sbe1 and Sbe2 from wheat (*Triticum aestivum* cv. Cheyenne): molecular characterization, developmental expression and homolog assignment by differential PCR. *Plant Molecular Biology Reporter*, 20, 191-192.
- MacGregor, E. A., Janeček, Š. and Svensson, B. (2001). Relationship of sequence and structure to specificity in the α -amylase family of enzymes. *Biochimica et Biophysica Acta*, 1546, 1-20.
- McPherson A. E. and Jane, J. (1999). Comparison of waxy potato with other root and tuber starches, *Carbohydrate Polymers* 40, 57-70.
- Mestres, C., Matencio, F., Pons, B., Yajid, M. and Fliedel, G. (1996). A rapid method for the determination of amylose content by using differential-scanning calorimetry. *Starch*, 48, 2-6.
- Mizuno, K., Kimura, K., Arai, Y., Kawasaki, T., Shimada, H. and Baba, T. (1992). Starch branching enzymes from immature rice seeds. *Journal of Biochemistry*, 112, 643-651.
- Miyazaki, M. and Morita, N. (2005). Effect of heat-moisture treated maize starch on the properties of dough and bread. *Food Research International*, 38, 369-376.
- Miyoshi, E. (2002). Effect of heat-moisture treatment and lipids on gelatinization and retrogradation of maize and potato starches. *Cereal Chemistry*, 79, 72-77.
- Moorthy, S.N. (1999). Effect of steam pressure treatment on the physicochemical properties of dioscorea starches. *Journal of Agricultural and Food Chemistry*, 47, 1695-1699.

- Morgan, K. R., Furneaux, R. H. and Stanley, R. A. (1992). Observation by solid-state ^{13}C CP MAS NMR-spectroscopy of the transformations of wheat-starch associated with the making and staling of bread. *Carbohydrate Research*, 235, 15–22.
- Morgan, K. R., Gerrard, J., Every, D., Ross, M. and Gilpin, M. (1997). Staling in starch breads: The effect of antistaling α -amylase. *Starch/Stärke*, 49, 54–59.
- Morrison, W.R. (1964). A fast simple and reliable method for the micro determination of phosphorus in biological material. *Analytical Biochemistry*, 7, 218-224.
- Morrison, W. R. (1981). Starch lipids: A reappraisal. *Starch*, 33, 408-410.
- Morrison, W. R. (1988). Lipids in cereal starches: A review. *Journal of Cereal Science*, 8, 1-15.
- Morrison, W. R. and Karkalas, J. (1990). Starch. In *Methods in plant biochemistry: carbohydrates*, P. M. Dey, Eds., Academic Press, London, UK, pp. 252–323.
- Morrison, W. R. and Laignelet, B. (1983). An improved colorimetric procedure for determining apparent and total amylose in cereal and other starches. *Journal of Cereal Science*, 1, 9-20.
- Morrison, W.R., Law, R.V. and Snape, C.E. (1993). Evidence for inclusion complexes of lipids with V-amylose in maize, rice and oat starches. *Journal of Cereal Science*, 18, 107-109.
- Morrison, W. R., Tester, R. F. and Gidley, M. J. (1993). Resistance to acid hydrolysis of lipid complexed amylose and lipid free amylose in lintnerized waxy and non waxy barley starch. *Carbohydrate Research*, 245, 289-302.
- Morrison, W. R., Tester, R. F., Gidley, M. J. and Karkalas, J. (1993a). Resistance to acid hydrolysis of lipid-complexed amylose and lipid-free amylose in lintnerised waxy and non-waxy barley starches. *Carbohydrate Research*, 245, 289-302.
- Morrison, W. R., Tester, R. F., Snape, C. E., Law, R. and Gidley, M. J. (1993b). Swelling and gelatinization of cereal starches: IV. Some effects of lipid complexed amylose and free amylose in waxy and normal barley starches. *Cereal Chemistry*, 70, 385–391.

- Mua, J. P. and Jackson, D. S. (1997). Fine structure of corn amylose and amylopectin fractions with various molecular weights. *Journal of Agricultural and Food Chemistry*, 45, 3840–3847.
- Mua, J. P. and Jackson, D. S. (1998). Retrogradation and gel textural attributes of corn starch amylose and amylopectin fractions. *Journal of Cereal Science*, 25, 157-166.
- Mutungi, C., Onyango, C., Doert, T., Paaschi, S., Thiele, S., Machilli, S., Jaros, D. and Rohm, H. (2011). Long- and short-range structural changes of recrystallized cassava starch subjected to in vitro digestion. *Food Hydrocolloids*, 25, 477-485.
- Nakazawa Y. and Wang, Y. J. (2004). Effect of annealing on starch–palmitic acid interaction, *Carbohydrate Polymers*, 57, 327–335.
- Nikuni, Z. (1978). Studies on starch granules. *Starch*, 30:105-111.
- Noda, T., Takahata, Y., Sato, T., Ikoma, H. and Mochida, H. (1996). Physicochemical properties of starches from purple and orange fleshed sweet potato roots at two levels of fertilizer. *Starch/Stärke*, 48, 395–399.
- Nugent, A. (2005). Health properties of resistant starch. *Nutrition Bulletin*, 30, 27–54.
- Nutting, G. C. (1952). Effect of electrolytes on the viscosity of potato starch pastes. *Journal of Colloidal Science*, 7, 128-139.
- Oates, C. G. (1997). Towards an understanding of starch granule structure and hydrolysis. *Trends in Food Science and Technology*, 82, 375-382.
- Oda, S. and Schofield, J. D. (1997). Characterisation of friabilin polypeptides. *Journal of Cereal Science*, 26, 29-36.
- Okechukwu, P. E. and Rao, M. A. (1996a). Role of granule size and size distribution in the viscosity of cowpea starch dispersions heated in excess water. *Journal of Texture Studies*, 27,159–173.
- Okechukwu, P. E. and Rao, M. A. (1996b). Kinetics of Cowpea starch gelatinization based on granular swelling. *Starch/Stärke*, 48, 43-47.
- Olayinka, O., Adebowale, K. O. and Olu-Owolabi, B. I. (2008). Effect of heat-moisture treatment on physicochemical properties of white sorghum starch. *Food Hydrocolloids*, 22, 225–230.

- Orford, P. D., Ring, S. G., Carroll, V., Miles, M. J. and Morris, V. J. (1987). Effect of concentration and botanical source on the gelation and retrogradation of starch. *Journal of the Science of Food and Agriculture*, 6, 147-158.
- O'Shea, M. G., Samuel, M. S., Konik, C. M. and Morell, M. K. (1998). Fluorophore-assisted carbohydrate electrophoresis (FACE) of oligosaccharides— Efficiency of labelling and high-resolution separation. *Carbohydrate Research*, 307, 1-12.
- Ottenhof, M. A., Hill, S. E. and Farhat, I. A. (2005). Comparative study of the retrogradation of intermediate water content waxy maize, wheat, and potato starches. *Journal of Agricultural and Food Chemistry*, 53, 631-638.
- Palma-Rodriguez, H. M., Agama-Acevedo, E., Mendez-Montealvo, G., Gonzalez-Soto, R. A., Vernon-Carter, E. J., and Bello-Pérez, L. A. (2012). Effect of acid treatment on the physicochemical and structural characteristics of starches from different botanical sources. *Starch/Stärke*, 64, 115-125.
- Paris, M., Bizot, H., Emery, J., Buzare, J. Y. and Buléon, A. (2001). NMR local range investigations in amorphous starchy substrates I. Structural heterogeneity probed by ^{13}C CP-MAS NMR. *International Journal of Biological Macromolecules*, 29, 127-136.
- Patindol, J. A., Guraya, H. S., Champagne, E. T. and McClung, A. M. (2010). Nutritionally important starch fractions of rice cultivars grown in Southern United States. *Journal of Food Science*, 75, 137- 144.
- Patterson, C. A., Maskus, H. and Bassett, C. M. C. (2010). Fortifying foods with pulses. *Cereal Foods World*, 55, 56-62.
- Peat, S., Whelan, W. J., Thomas, G. J. (1952). Evidence of multiple branching in waxy maize starch. *Journal of the Chemical Society Chemical Communications*, 4546-4548.
- Perera, C. and Hoover, R. (1999). Influence of hydroxypropylation on retrogradation properties of native, defatted and heat-moisture treated potato starches. *Food Chemistry*, 64, 361-375.

- Pérez, S. and Bertoft, E. (2010). The molecular structures of starch components and their contribution to the architecture of starch granules: A comprehensive review. *Starch*, 62, 389-420.
- Pfannemuller, B. (1987). Influence of chain length of short mono disperse amylose on the formation of A-type and B-type X-ray diffraction patterns. *International Journal of Biological Macromolecule*, 9, 105–108.
- Planchot, V., Colonna, P., Gallant, D. J. and Bouchet, B. (1995). Extensive degradation of native starch granules by alpha-amylase from *Aspergillus fumigatus*. *Journal of Cereal Science*, 21, 163-171.
- Poulsen, P. and Kreiberg, J. D. (1993). Starch branching enzyme cDNA from *Solanum tuberosum*. *Plant Physiology*, 102, 1053–1054.
- Preiss, J. and Sivak, M. N. (1996). Starch synthesis in sinks and sources. In *Photoasssimilate distribution in plants and crops: source-sink relationship*, E. Zamski and A. A. Schaffer, Eds., Marcel Decker, New York, NY. pp. 63-96.
- Primo-Martin, C., Nieuwenhuijzen, N. H., Hamer, R. J. and VanVliet, T. (2007). Crystallinity changes in wheat starch during the bread making process: starch crystallinity in the bread crust. *Journal of Cereal Science*, 45, 219-226.
- Protserov, V. A., Karpov, V. G., Kozhevnikov, G. O., Wasserman, L. A. and Yuryev, V. P. (2000). Changes of thermodynamic and structural properties of potato starches (Udacha and Acrosil) varieties during biosynthesis. *Starch/Starke*, 52, 461-466.
- Pukkahuta, C. and Varavinit, S. (2007). Structural transformation of sago starch by heat–moisture and osmotic–pressure treatment. *Starch/Stärke*, 59, 624–631.
- Pukkahuta, C., Suwannawat, B., Shobsngob, S. and Varavinit, S. (2008). Comparative study of pasting and thermal transition characteristics of osmotic pressure and heat-moisture treated corn starch. *Carbohydrate Polymers*, 72, 527–536.
- Pulse Canada, Canada and the global pulse industry. (2010). Available from: <http://www.pulsecanada.com/uploads/wv/nr/wvnr5qGWli8Rqbl22UyY8g/Canada-s-Pulse-Industry-in-the-Global-Market-Sep-07.pdf>.

- Puncha-arnon, S. and Uttapap, D. (2013). Rice starch vs. rice flour: Differences in their properties when modified by heat–moisture treatment. *Carbohydrate Polymers*, 91, 85-91.
- Purwani, E.Y., Widaningrum, R., Thahir, and Muslich. (2006). Effect of heat- moisture treatment of sago starch on its noodle quality. *Indonesian Journal of Agricultural Science*, 7, 8–14.
- Putseys, J. A., Lamberts, L. and Delcour, J. A. (2010). Amylose-inclusion complexes: Formation, identity and physic-chemical properties. *Journal of Cereal Science*, 51, 238-247.
- Radosta, S., Kettlitz, B., Schierbaum, F. and Gernat, C. (1992). Studies on rye starch properties and modification. Part II. Swelling and solubility behavior of rye starch granules. *Starch/Stärke*, 44, 8–14.
- Raphaelides, S. and Karkalas, J. (1988). Thermal dissociation of amylose–fatty acid complexes. *Carbohydrate Research*, 172, 65–82.
- Ratnayake, W. S., Hoover, R., Shahidi, F., Perera, C. and Jane, J. (2001). Composition, molecular structure, and physicochemical properties of starches from four field pea (*Pisum sativum* L.) cultivars. *Food Chemistry*, 74, 189–202.
- Ring, S. G., Gee, M. J., Whittam, M., Orford, P. and Johnson, I. T. (1988). Resistant starch: its chemical form in foodstuffs and effect on digestibility *in vitro*. *Food Chemistry*, 28, 97–109.
- Ritte, G., Scharf, A., Eckermann, N., Haebel, S. and Steup, M. (2004) Phosphorylation of transitory starch is increased during degradation. *Plant Physiology*, 135, 2068–2077.
- Robin, J. P., Mercier, C., Charbonnière, R., and Guilbot, A. (1974). Lintnerized starches. Gel-filtration and enzymatic studies of insoluble residues from prolonged acid treatment of potato starch. *Cereal Chemistry*, 51, 389–406.
- Roby, J. F. (2008). Starch: structure, properties, chemistry and enzymology. In *Glycoscience*, Fraser-Reid, B., Tatsuta, K., Thiem, J. Eds, Springer Berlin Heidelberg, pp 1438-1468.

- Roby, J. F. (2009). Enzymes and their action on starch. In *Starch: Chemistry and Technology*, BeMiller, J., Whistler, R. Eds, Academic Press, NY, pp 238-284.
- Roby, J. F. and French, D. (1970). The action pattern of porcine pancreatic α -amylase in relationship to the substrate binding site of the enzyme. *Journal of Biological Chemistry*, 245, 3917-3927.
- Roulet, P. H., MacInnes, W. M., Wursch, P., Sanchez, R. M. and Raemy, A. (1988). A comparative study of the retrogradation kinetics of gelatinized wheat starch in gel and powder form using X-ray, differential scanning calorimetry and dynamic mechanical analysis. *Food Hydrocolloids*, 2, 381-396.
- Rundle, R. E. and French, D. (1943). The configuration of starch in the starch-iodine complex. III. X-ray diffraction studies of the starch-iodine complex. *Journal of the American Chemical Society*, 65, 1707-1710.
- Rutschmann, M. A. and Solms, J. (1990). Formation of inclusion complexes of starch with different organic compounds. 2. Study of ligand binding in binary model systems with decanal, 1-naphthol, monostearate and monopalmitate, *Food Science and Technology*, 23, 70-79.
- Russel, P. L. (1987). The aging of gels from starches of different amylose and amylopectin content studied by differential scanning calorimetry. *Journal of Cereal Science*, 6, 147-158.
- Saenger, W. (1984). The structure of the blue starch-iodine complex. *Naturwissenschaften*, 71, 31-36.
- Saibene, D., Zobel, H. F., Thompson, D. B. and Seetharaman, K. (2008). Iodine binding by granular corn and potato starch: Evidence for differential location of amylose. *Starch/Stärke*, 60, 165-173.
- Sair, L. (1967). Heat-moisture treatment of starch. *Cereal Chemistry*, 44, 8-26.
- Salman, H., Blazek, J., López-Rubio, A., Gilbert, E. P., Hanley, T. and Copeland, L. (2009). Structure-function relationships in A and B granules from wheat starches of similar amylose content. *Carbohydrate Polymers*, 75, 420-427.
- Saltiel, A. R. and Kahn, C. R. (2001). Insulin signalling and the regulation of glucose and lipid metabolism. *Nature*, 414:799-806.

- Sandhu, K. S. and Lim, S. (2008). Digestibility of legume starches as influenced by their physical and structural properties. *Carbohydrate Polymers*, 71, 245–252.
- Sang, Y., and Seib, P.A. (2006). Resistant starches from amylose mutants of corn by simultaneous heat–moisture treatment and phosphorylation. *Carbohydrate Polymers*, 63, 167–175.
- Sasaki, T. and Matsuki, J. (1998). Effect of wheat starch structure on swelling power. *Cereal Chemistry*, 75, 525–529.
- Saskatchewan Pulse Growers. (2013). Available from: <http://www.saskpulse.com/communications/pulse-market-report/>.
- Sandhu, K. S. and Lim, S. (2008). Digestibility of legume starches as influenced by their physical and structural properties, *Carbohydrate Polymers*, 71: 245-252.
- Sarko, A. and Biloski, A. (1980). Packing analysis of carbohydrates and polysaccharides. 10. Crystal-structure of the KOH-amylose complex. *Carbohydrate Research*, 79, 11-21.
- Sathe, S. K. and Salunke, D. K. (1981). Isolation partial characterization and modification of the great northern bean (*Phaseolus vulgaris* L.) starch. *Journal of Food Science*, 46, 617–621.
- Schierbaum, F. and Kettlitz, B. (1994). Studies on rye starch properties on modification. Part III. Viscograph pasting characteristics of rye starches. *Starch/Stärke*, 46, 2–8.
- Schnupf, U., Willett, J. L., Bosma, W. and Momany, F. A. (2009). DFT conformation and energies of amylose fragments at atomic resolution. Part 1: syn forms of α -maltotetraose. *Carbohydrate Research*, 344, 362-373.
- Schoch, T. J. (1964). Iodometric determination of amylose. In *Methods in Carbohydrate Chemistry*, Vol.4. R. L. Whistler. Ed. Academic press, New York, NY, pp. 157-160.
- Schoch, T. J. and Maywald, E. C. (1956). Preparation and properties of various legume starches. *Cereal Chemistry*, 45, 564-571.
- Seigner, C., Prodanov, E. and Machis-Mouren, G. (1987). The determination of subsite binding energies of porcine pancreatic α -amylase by comparing hydrolytic activity towards substrates. *Biochimica Biophysica Acta*, 913, 200-209.

- Sekine, M., Otake, K., Sugiyama, J. and Kawamura, Y. (2000). Effects of heating, vacuum drying and steeping on gelatinization properties and dynamic viscoelasticity of various starches. *Starch/Stärke*, 52, 398–405.
- Senior, M. B. and Hamori, E. (1973). Investigation of the effect of amylose/ iodine complexation on the conformation of amylose in aqueous solution. *Biopolymers*, 12, 65-78.
- Shi, Y.-C. and Seib, P. A. (1992). The structure of four waxy starches related to gelatinization and retrogradation. *Carbohydrate Research*, 227, 131–145.
- Shih, F., King, J., Daigle, K., An, H.J., and Ali, R. (2007). Physicochemical properties of rice starch modified by hydrothermal treatments. *Cereal Chemistry*, 84, 527–53.
- Shin, S. I., Kim, H. J., Ha, H. J., Lee, S. H. and Moon, T. W. (2005). Effect of hydrothermal treatment on formation and structural characteristics of slowly digestible non-pasted granular sweet potato starch. *Starch//Stärke*, 57, 421–430.
- Silverio, J., Fredriksson, H. Andersson, R., Eliasson, A. C. and Åman, P. (2000). The effect of temperature cycling on the amylopectin retrogradation of starches with different amylopectin unit-chain length distribution. *Carbohydrate Polymers*, 42, 175-184.
- Silverio, J., Svensson, E., Eliasson, A. C. and Olofsson, G. (1996). Isothermal microcalorimetry studies on starch retrogradation. *Journal of Thermal Analysis*, 47, 1179-1200.
- Simpson, T.D., Dintzis, F.R. and Taylor, N.W. (1972). V7 conformation of dimethyl sulfoxide amylose complex. *Biopolymers*, 11, 2591-2600.
- Singh, V., and Ali, S. Z. (2000). Acid degradation of starch. The effect of acid and starch type. *Carbohydrate Polymers*, 41, 191-195.
- Singh, J., Kaur, L. and McCarthy, O. J. (2007). Factors influencing the physico-chemical, morphological, thermal and rheological properties of some chemically modified starches for food applications—A review. *Food Hydrocolloids*, 21, 1-22.
- Singh, N., Kaur, M. Sandhu, K. S. and Guraya, H. S. (2004). Physicochemical, thermal, morphological and pasting properties of starches from some Indian black gram (*Phaseolus mungo* L.) cultivars. *Starch/Stärke*, 56, 535–544.

- Singh, S., Raina, C. S., Bawa, A. S., and Saxena, D. C. (2005). Effect of heat- moisture treatment and acid modification on rheological, textural, and differential scanning calorimetry characteristics of sweet potato starch. *Journal of Food Science*, 70, E373–E378.
- Singh, J. Q. and Singh, N. (2003). Studies on the morphological and rheological properties of granular cold water soluble corn and potato starches. *Food Hydrocolloids*, 17, 63-72.
- Sivak, M. N. & Preiss, J. (1998). Physicochemical structure of the starch granule. *Advances in Food Nutrition and Research*, 41, 13-32.
- Skerritt, J. H., Frend, A. J., Robson, L. G. and Greenwell, P. (1990). Immunological homologies between wheat gluten and starch granule proteins. *Journal of Cereal Science*, 12, 123–126.
- Smith, A. M. (1988). Major differences in isoforms of starch branching enzyme between developing embryos of round- and wrinkled-seeded peas (*Pisum sativum* L.). *Planta*, 175, 270-279.
- Smith, A. M., Denyer, K. and Martin, C. R. (1995). What controls the amount and structure of starch in storage organs? *Plant Physiology*, 107, 673-677.
- Snow, P. and O'Dea, K. (1981). Factors affecting the rate of hydrolysis of starch in food. *American Journal of Clinical Nutrition*, 34, 2721–2727.
- Srichuwong, S., Sunarti, T. C., Mishima, T., Isono, N. & Hismatsu, M. (2005a). Starches from different botanical sources. I: Contribution of amylopectin fine structure to thermal properties and enzyme digestibility. *Carbohydrate Polymers*, 60, 529-538.
- Srichuwong, S., Sunarti, T. C., Mishima, T., Isono, N. and Hisamatsu, M. (2005b). Starches from different botanical sources. II: Contribution of starch structure to swelling and pasting properties. *Carbohydrate Polymers*, 62, 25–34.
- Stevens, D. J. and Elton, G. A. H. (1971). Thermal properties of the starch/water system. Part I. Measurement of heat of gelatinisation by differential scanning calorimetry. *Starch/Stärke*, 23, 8–11.

- Stute, R. (1992). Hydrothermal modification of starches: The difference between annealing and heat/moisture-treatment. *Starch/Stärke*, 44, 205- 214.
- Suganuma, T., Matsuno, R., Ohinishi, M. and Hiromi, K. (1978). *Journal of Biochemistry (Tokyo)*, 84, 293-316.
- Sujka, M. and Jamroz, J. (2007). Starch granule porosity and its changes by means of amylolysis. *International Agrophysics*, 21, 107-113.
- Sun, Q., Wang, T., Liu, X. and Zhao, Y. (2013). The effect of heat moisture treatment on physicochemical properties of Early Indica Rice. *Food Chemistry*, <http://dx.doi.org/10.1016/j.foodchem.2013.03.077>.
- Svegmark, K. and Hermansson, A. M. (1993). Microstructure and rheological properties of composites of potato starch granules and amylose: A comparison of observed and predicted structure, *Food Structure*, 12,181–193.
- Svegmark, K., Helmersson, K., Nilsson, G., Nilsson, P.O., Anderson, R., and Svenson, E. (2002). Comparison of potato amylopectin starches and potato starches–influence of year and variety. *Carbohydrate Polymers*, 47, 331–340.
- Swinkels, J. J. M. (1985). Composition and properties of commercial native starches. *Starch/Stärke*, 37, 1–5.
- Szydlowski, N., Ragel, P., Raynaud, S., Lucas, M. M., Roldn, I., Montero, M., Muoz, F. J., Ovecka, M., Bahaji, A., Planchot, V. R., Pozueta-Romero, J., D'Hulst, C. and Murida, Å. (2009). Starch Granule Initiation in Arabidopsis Requires the Presence of Either Class IV or Class III Starch Synthases. *The Plant Cell Online*, 21, 2443-2457.
- Takeda Y. and Hizukuri, S. (1982). Location of phosphate groups in potato amylopectin. *Carbohydrate Research*, 102, 321–327.
- Takeda, Y., Guan, H. P. and Preiss, J. (1993). Branching of amylose by the branching isoenzymes of maize endosperm. *Carbohydrate Research*, 240, 253-263.
- Takeda, Y., Hizukuri, S. and Juliano, B. O. (1987). Structures of rice amylopectins with low and high affinities for iodine. *Carbohydrate Research*, 168, 79-88.

- Takeda, Y., Hizukuri, S., Takeda, C., and Suzuki, A. (1987). Structures of branched molecules of amyloses of various origins and molar fractions of branched and unbranched molecules. *Carbohydrate Research*, 165, 139–145.
- Takeda, Y., Maruta, N. and Hizukuri, S. (1992). Examination of the structure of amylose by tritium labelling of the reducing terminal. *Carbohydrate Research*, 227, 113–120.
- Takeda, Y., Shibahara, S. and Hanashiro, I. (2003). Examination of the structure of amylopectin molecules by fluorescent labelling, *Carbohydrate Research*, 338, 471–475.
- Tan, I., Flanagan, B. M., Halley, P. J., Whittaker, A. K. and Gidley, M. J. (2007). A method for estimating the nature and relative proportions of amorphous, single, and double-helical components in starch granules by ^{13}C CP/MAS NMR. *Biomacromolecules*, 8, 885–891.
- Tatge, H., Marshall, J., Martin, C., Edwards, E. A. and Smith, A. M. (1999). Evidence that amylose synthesis occurs within the matrix of the starch granule in potato tubers, *Plant, Cell and Environment*, 22, 543–550.
- Tattiyakul, J., Naksriaporn, T., Pradipasena, P. and Miyawaki, O. (2006). Effect of moisture on hydrothermal modification of yam *Dioscorea hispider* Dennst starch. *Starch/Stärke*, 58, 170–176.
- Tester, R. F. (1997). Influence of growth conditions on barley starch properties. *International Journal of Biological Macromolecules*, 21, 37–45.
- Tester, R. F. and Karkalas, J. (2002). Starch. In *Biopolymers Volume 6, Polysaccharides II: Polysaccharides from Eukaryotes*, A. Steinbüchel, (series Ed), E. J. Vandamme, S. De Baets and A. Steinbüchel, (volume Eds), Wiley-VCH, Weinheim, pp. 381–438.
- Tester, R. F., Karkalas, J. and Qi, X. (2004). Starch – composition, fine structure and architecture. *Journal of Cereal Science*, 39, 151–165.
- Tester, R. F. and Morrison, W. R. (1990). Swelling and gelatinization of cereal starches. 1. Effects of amylopectin, amylose, and lipids, *Cereal Chemistry* 67, 551–557.

- Tester, R. F., Morrison, W. R. and Schulman, A. H. (1993). Swelling and gelatinization of cereal starches. V. Risø Mutants of Bomi and Carlsberg II Barley Cultivars. *Journal of Cereal Science*, 17, 1-9.
- Tester, R. F., Qi, X. and Karkalas, J. (2006). Hydrolysis of native starches with amylases. *Animal Feed Science and Technology*, 130, 39-54.
- Tetlow, I. J. (2011). Starch biosynthesis in developing seeds. *Seed Science Research*, 21, 5-32.
- Tetlow, I. J., Morell, M. K. and Emes, M. J. (2004). Recent developments in understanding the regulation of starch metabolism in higher plants. *Journal of Experimental Botany*, 55, 2131-2145.
- Thoma, J. A. (1968). A possible mechanism for amylase catalysis. *Journal of Theoretical Biology*, 19, 297-310.
- Thoma, J. A., Rao, G. V. K., Brothers, C. and Spradlin, J. (1971). Subsite mapping of enzymes. *Journal of Biological Chemistry*, 246, 5621-5635.
- Thygesen, L. G., Blennow, A. and Engelsen, S. B. (2003). The effects of amylose and starch phosphate on starch gel retrogradation studied by low field ¹H NMR relaxometry. *Starch/Stärke*, 55, 241-249.
- Tjahjadi, C. and Breene, W. M. (1984). Isolation and characterization of adzuki bean (*Vigna angularis* cv. Takara) starch. *Journal of Food Science*, 49, 558-562.
- Tharanathan, R. N. (2005). Starch - value addition by modification. *Critical Reviews in Food Science and Nutrition*, 45, 371-384.
- Tomlinson, K. L., Llyod, J. R. and Smith, A. M. (1997). Importance of isoforms of starch branching enzymes in determining the structure of starch in pea leaves. *Plant Journal*, 11, 31-43.
- Uthumporn, U., Karim, A. A. and Zaidul, I.S.M. (2010). Hydrolysis of granular starch at sub-gelatinization temperature using a mixture of amylolytic enzymes. *Food and Bioproducts Processing*, 88, 47-54.
- Valetudie, J. C., Colonna, P., Bouchet, B., Gallant, D. J. (1995). Gelatinization of sweet potato, Tania and yam tuber starches. *Starch/Stärke*, 47, 298-306.

- Vandeputte, G. E., Derycke, V., Geeroms, J., and Delcour, J. A. (2003a). Rice starches. II. Structural aspects provide insight into swelling and pasting properties. *Journal of Cereal Science*, 38, 53–59.
- Vandeputte, G. E., Vermeulen, R., Geeroms, J. and Delcour, J. A. (2003b). Rice starches. III. Structural aspects provide insight in amylopectin retrogradation properties and gel texture. *Journal of Cereal Science*, 38, 61-68.
- van de Velde, F., van Riel, J. and Tromp, R. H. (2002). Visualisation of starch granule morphologies using confocal scanning laser microscopy (CSLM). *Journal of the Science of Food and Agriculture*, 82, 1528-1536.
- Vasanthan, T. and Bhatta, R. S. (1996). Physicochemical properties of small and large granule starches of waxy, regular and high amylose barley. *Cereal Chemistry*, 173, 199-207.
- Vasanthan, T. and Hoover, R. (1992). A comparative study of the composition of lipids associated with starch granules from various botanical sources. *Food Chemistry*, 43, 19-27.
- Varatharajan, V., Hoover, R., Liu, Q. and Seetharaman, K. (2010). The impact of heat-moisture treatment on the molecular structure and physicochemical properties of normal and waxy potato starches. *Carbohydrate Polymers*, 81, 466-475.
- van Soest, J. J. G., de Wit, D., Tournois, H. and Vliegthart, J. F. G. (1994). Retrogradation of potato starch as studied by Fourier transform infrared spectroscopy. *Starch/Stärke*, 46, 453-457.
- van Soest, J. J. G., Tournois, H., de Wit, D., Johannes, F.G. and Vliegthart, J. F. G. (1995). Short-range structure in (partially) crystalline potato starch determined with attenuated total reflectance Fourier-transform IR spectroscopy. *Carbohydrate Research*, 279, 201-214.
- Venn, B. J. and Green, T. J. (2007). Glycemic index and glycemic load: Measurement issues and their effect on diet–disease relationships. *European Journal of Clinical Nutrition*, 61, S122–S131.
- Vermeulen, R., Goderis, B. and Delcour, J.A. (2006). An X-ray study of hydrothermally treated potato starch. *Carbohydrate Polymers*, 64, 364–375.

- Vieira, F. C. and Sarmiento, S. B.S. (2008). Heat-moisture treatment and enzymatic digestibility of Peruvian carrot, sweet potato and ginger starches. *Starch/Stärke*, 60, 223–232.
- Waduge, R. N., Hoover, R., Vasanthan, T., Gao, J. and Li, J. (2006). Effect of annealing on the structure and physicochemical properties of barley starches of varying amylose content. *Food Research International*, 39, 59–77.
- Waigh, T. A., Gidley, M. J., Komanshek B. U. and Donald, A. M. (2000). The phase transformations in starch during gelatinisation: a liquid crystalline approach. *Carbohydrate Research*, 328, 165–176.
- Wang, S. J., Yu, J. L. and Yu, J. G. (2008). The semi-crystalline growth rings of C-type pea starch granule revealed by SEM and HR-TEM during acid hydrolysis. *Carbohydrate Polymers*, 74, 731-739.
- Wankhede, D. B. and Ramtehe, R. S. (1982). Studies on isolation and physicochemical properties of starch from moth bean (*Phaseolus acentifolius*). *Starch/Stärke*, 34, 189–192.
- Wang, S., Blazek, J., Gilbert, E. and Copeland, L. (2012). New insights on the mechanism of acid degradation of pea starch. *Carbohydrate Polymers*, 87, 1941-1949.
- Wang, L. and Seib, P. A. (1996). Australian salt-noodle flours and their starches compared to US wheat flours and their starches. *Cereal Chemistry*, 73, 167–175.
- Wang, L. Z. and White, P. J. (1994). Structure and properties of amylose, amylopectin and intermediate material of oat starches. *Cereal Chemistry*, 71, 263–268.
- Watcharatewinkul, Y., Puttanlek, C., Rungsardthong, V. and Uttapap, D. (2009). Pasting properties of a heat-moisture treated canna starch in relation to its structural characteristics. *Carbohydrate Polymers*, 75, 505-511.
- Whistler, R. L. and BeMiller, J. N. (1997). Carbohydrate chemistry for food scientists. American association of cereal chemists. Minnesota, USA. Pp. 117-151.
- Whistler, R. L. and Daniel, J. R. (1984). Molecular structure of starch. In *Starch: Chemistry and Technology*, R. L. Whistler, J. N. Bemiller and E. F. Paschall, Eds., Academic press, Inc. New York, NY, pp. 153-182.

- Whistler, R. L. and Doane, W. M. (1961). Characterization of intermediate fractions of high- amylose corn starches. *Cereal Chemistry*, 38, 251-255.
- Whitaker, J. R. (1994). The glycoside hydrolases. In *Principles of Enzymology for the Food Science*, 2nd Ed. Marcel Dekker Inc. New York, NY. Pp. 391-423.
- Whittam, M. A., Orford, P. D., Ring, S. G., Clark, S. A., Parker, M. L., Cairns, P. and Miles, M. J. (1989). Aqueous dissolution of crystalline and amorphous amylose alcohol complexes. *International Journal of Biological Macromolecules*, 11, 339-344.
- Withers, S. G. and Aebersold, R. (1995). Approaches to labeling and identification of active-site residues in glycosidases. *Protein Science*, 4, 361-372.
- Wu, H.C.H., and Sarko, A. (1978a). The double helical molecular structure of crystalline B-amylose. *Carbohydrate Research*, 61, 7-25.
- Wu, H.C.H., and Sarko, A. (1978b). The double helical molecular structure of crystalline A-amylose. *Carbohydrate Research*, 61, 27-40.
- Wursch, P. and Gumy, D. (1994). Inhibition of amylopectin retrogradation by partial beta-amyloslysis. *Carbohydrate Research*. 256, 129-137.
- Xia, L., Wenyan, G., Juan, W., Qianqian, J. and Luqi, H. (2010). Comparison of the morphological, crystalline, and thermal properties of different crystalline types of starches after acid hydrolysis. *Starch/Stärke*, 62, 686-696.
- Xijun, L., Lin, L., Kunsheng, Z., Ying, X. and Jiabin, L. (2012). A new proposed sweet potato starch granule structure—Pomegranate concept. *International Journal of Biological Macromolecules*, 50, 471-475.
- Yamada, T. and Taki, M. (1976). Fractionation of maize starch by gel chromatography. *Starch/Stärke*, 28, 374-377.
- Yamamoto, M. Sano, T. and Yasunaga, T. (1982). Interaction of amylose with iodine. I. Characterization of cooperativity binding isotherms for amyloses. *Bulletin of the Chemical Society of Japan*, 55, 1886-1889.
- Yao, N., Paez, A. V. and White, P. J. (2009). Structure and function of starch and resistant starch from corn with different doses of mutant amylose-extender and floury-1 alleles. *Journal of Agricultural and Food Chemistry*, 57, 2040- 2048.

- Yao, Y., Guiltinan, M. J. and Thompson, D. B. (2005). High-performance size-exclusion chromatography (HPSEC) and fluorophore-assisted carbohydrate electrophoresis (FACE) to describe the chain-length distribution of debranched starch. *Carbohydrate Research*, 340, 701-710.
- Yoo, S. H. and Jane, J. L. (2002). Structural and physical characteristics of waxy and other wheat starches. *Carbohydrate Polymers*, 49, 297-305.
- Yook, C. and Robyt, J. F. (2002). Reactions of alpha amylase with starch granules in aqueous suspension giving products in solution and in a minimum amount of water giving products inside the granule. *Carbohydrate Research*, 337, 1113-1117.
- Yoshida, H., Nozaki, K., Hanashiro, I., Yagi, F., Ito, H., Honma, M., Matsui, H. and Takeda, Y. (2003). Structure and physicochemical properties of starches from kidney bean seeds at immature, premature and mature stages of development, *Carbohydrate Research*, 38, 463-469.
- Yoshimoto, Y., Tashiro, J., Takenouchi, T. and Takeda, Y. (2000). Molecular structure and some physicochemical properties of high-amylose barley starch. *Cereal Chemistry*, 77, 279-285.
- You, S., Stevenson, S. G., Izydorczyk, M. S. and Preston, K. R. (2002). Separation and characterization of barley starch polymers by a flow field-flow fractionation technique in combination with multi angle light scattering and differential refractive index detection. *Cereal Chemistry*, 79, 624-630.
- Yu, X., Houtman, C. and Atalla, R. H. (1996). The complex of amylose and iodine. *Carbohydrate Research*, 292, 129-141.
- Yuan, R. C., Thompson, D. B. and Boyer, C. D. (1993). Fine structure of amylopectin in relation to gelatinization and retrogradation behaviour of maize starches from three wax-containing cultivars in two inbred lines. *Cereal Chemistry*, 70, 81-89.
- Yuan, R. C. and Thompson, D. B. (1998). Freeze-thaw stability of three waxy maize starch pastes measured by centrifugation and calorimetry. *Cereal Chemistry*, 75, 571-573.

- Yun, S. and Matheson, N. K. (1993). Structures of the amylopectins of waxy, normal, amylose-extender, and wx:ae cultivars and of the phytyloglycogen of maize. *Carbohydrate Research*, 243, 307-321.
- Yuryev, V. P., Krivandin, A. V., Kiseleva, V. I., Wasserman, L. A., Genkina, N. K., Fornal, J., Blaszczyk, W. and Schiraldi, A. (2004). Structural parameters of amylopectin clusters and semi-crystalline growth rings in wheat starches with different amylose content. *Carbohydrate Research*, 339, 2683–2691.
- Yuryev, V.P., Kozlov, S.S., Noda, T., Bertoft, E., and Blennow, A. (2007). Influence of different GBSS1 and GWD combinations on the amylose localization within wheat and potato starch granules. In V. P. Yuryev, P. Tomasik and E. Bertoft, (Eds), *Starch: Achievements in Under-standing of Structure*. Nova Science, NY, pp. 1–47.
- Zavareze, E. R. and Dias, A. R. G. (2011). Impact of heat-moisture treatment and annealing in starches: A review. *Carbohydrate Polymers*, 83, 317-328.
- Zavareze, E. R., Storck, C. R., Castro, L. A. S., Schirmer, M. A. and Dias, A. R. G. (2010). Effect of heat-moisture treatment on rice starch of varying amylose content. *Food Chemistry*, 121, 358-365.
- Zeeman, S. C., Kossmann, J., and Smith, A. M. (2010). Starch: Its Metabolism, Evolution, and Biotechnological Modification in Plants. *Annual Review of Plant Biology*, 61(1), 209-234.
- Zeeman, S. C., Smith, S. M. and Smith, A. M. (2007). The diurnal metabolism of leaf starch. *Biochemistry Journal*, 401, 13-28.
- Zhang, G., Venkatachalam, M. and Hamaker, B. R. (2006). Structural basis for the slow digestion property of native cereal starches. *Biomacromolecules*, 7, 3259-3266.
- Zheng, G. H. and Sosulski, F. W. (1998). Determination of water separation from cooked starch and flour pastes after refrigeration and freeze-thaw. *Journal of Food Science*, 63, 134-139.
- Zhou, Y., Hoover, R. and Liu, Q. (2004). Relationship between α -amylase degradation and the structure and physicochemical properties of legume starches. *Carbohydrate Polymers*, 57, 299–317.

- Ziegler, G. R., Thompson, D. B. and Casasnovas, J. (1993). Dynamic measurement of starch granule swelling during gelatinisation. *Cereal Chemistry*, 70, 247–261.
- Zobel, H. F. (1992). Starch granule structure. In *Developments in Carbohydrate Chemistry*, R. J. Alexander and H. F. Zobel, Eds., American Association of Cereal Chemists, St. Paul, MN. Pp. 1-36.
- Zobel, H. F. (1988a). Molecules to granules: A comprehensive starch review, *Starch/Stärke*, 40, 44–50.
- Zobel, H. F., (1988b). Starch crystal transformations and their industrial importance. *Starch/Stärke*, 40, 1-7.

List of refereed publications and conference proceedings

Publications

- **Ambigaipalan, P.**, Hoover, R., Donner, E. and Liu, Q. (2014). Starch chain interactions within the amorphous and crystalline domains of pulse starches on heat-moisture treatment at different temperatures and their impact on thermal, rheological and digestibility properties. *Food Chemistry*, 143, 175-184.
- **Ambigaipalan, P.**, Hoover, R., Donner, E. and Liu, Q. (2013). Retrogradation characteristics of pulse starches. *Food Research International*, 54, 203-212.
- **Ambigaipalan, P.**, Hoover, R., Donner, E., Liu, Q., Jasiwal, S., Chibbar, R., Nantanaga, K. K. M. and Seetharaman, K. (2011). Structure of faba bean, black bean and pinto bean starches at different levels of granule organization and their physicochemical properties. *Food Research International*, 44:2962-2974.
- Chibbar, R. N., **Priyatharini, A.** and Hoover, R. (2010). Molecular diversity in pulse seed starch and complex carbohydrates and its role in human nutrition and health. *Cereal Chemistry*, 87:342-352.
- Yalagama, L. L. W. C., **Ambigaipalan, P.** and Arampath, P. C. (2009). Physico-chemical and shelf life evaluation of pasteurized coconut milk. *Indian Coconut Journal*, 52:16-21.
- Yalagama, L. L. W. C., **Ambigaipalan, P.** and Arampath, P. C. (2008). Physico-chemical and shelf life evaluation of pasteurized coconut milk. *Proceedings of the Second Symposium on Plantation Crop Research*: 342-349.

Conference Presentations:

- **Priyatharini, A.**, Hoover, R., Donner, E. and Liu, Q. (2013). Starch chain interactions within the amorphous and crystalline domains of pulse starches on heat-moisture treatment at different temperatures and their impact on thermal, rheological and digestibility properties. IFT Food Annual & Expo, Chicago, LA, USA, July15, 2013.

- **Priyatharini, A.**, Hoover, R., Donner, E. and Liu, Q. (2013). A multi-technique study of pulse starch retrogradation. IFT Food Annual & Expo, Chicago, LA, USA, July15, 2013.

- **Priyatharini, A.**, Hoover, R., Donner, E., Liu, Q., (2012). Impact of pulse starch structure at different levels of granule organization on starch digestibility. Biochemistry summer symposium, St. John's, NL, CA, Aug 17, 2012.

- **Priyatharini, A.**, Hoover, R., Donner, E., Liu, Q., Jasiwal, S., Chibbar, R., Nantanaga, K. K. M. and Seetharaman, K. (2011). A study of structure of pulse starches at different levels of granule organization and their properties. IFT Food Annual & Expo, New Orleans, LA, USA, June 11-14, 2011.

- **Priyatharini, A.**, Yalegama, L. L. W. C. and Arampath, P. C. (2008). Development of pasteurized coconut milk pouches for domestic consumption. *Proceedings of the Sri Lanka Association for the Advancement of Science (SLASS)*, Colombo, Sri Lanka, Dec. 3-6, 2008.

- Yalegama, L. L. W. C., **Ambigaipalan, P.** and Arampath, P. C. (2008). Physico-chemical and shelf life evaluation of pasteurized coconut milk. *Proceedings of the Second Symposium on Plantation Crop Research*, Colombo, Sri Lanka, Oct. 16-17, 2008.

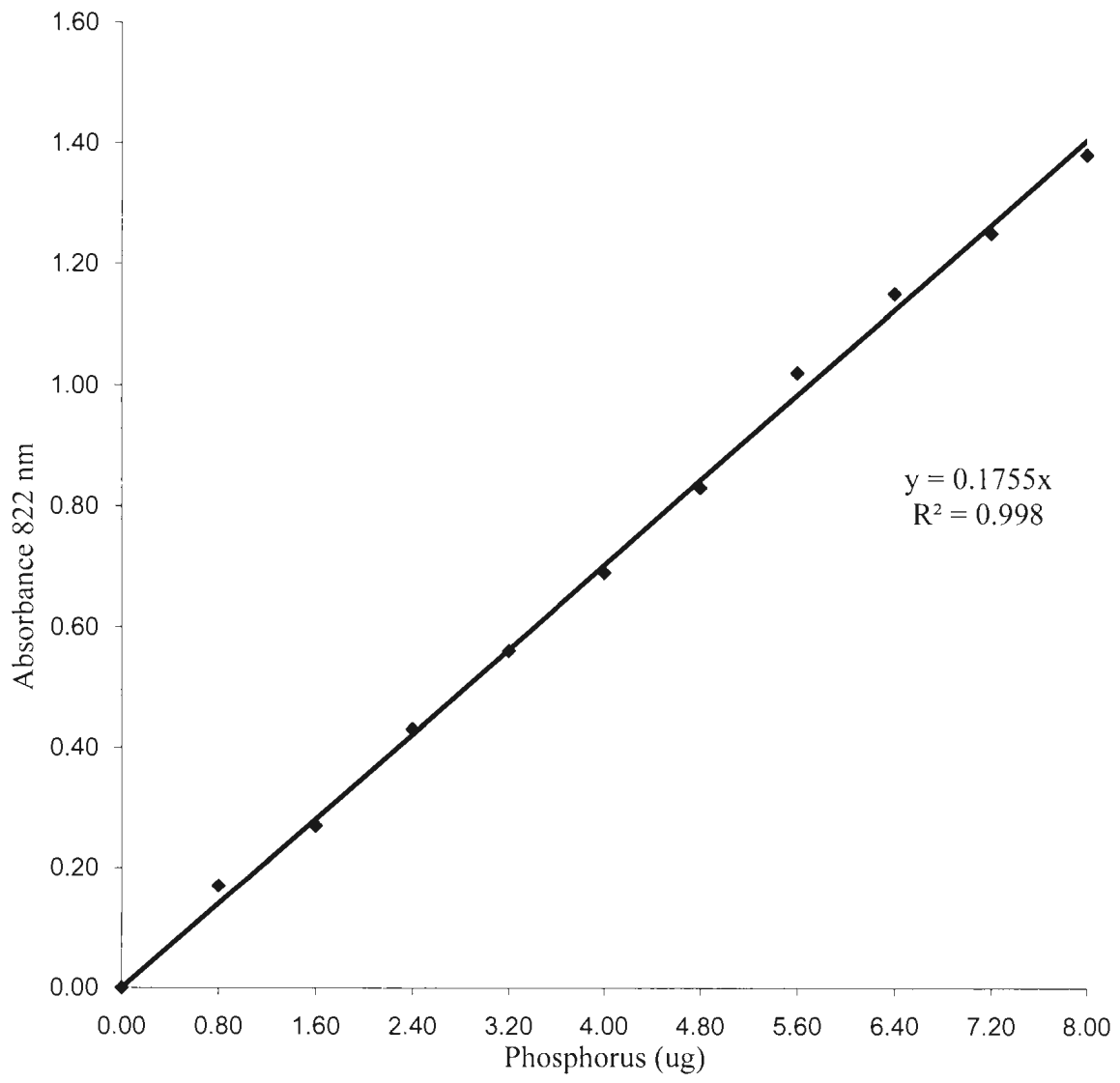
Academic Honors, Awards and Fellowships

- The Barrowman Biochemistry Graduate Travel Award,
Memorial University of NL, CA 2013
- IFT award, Carbohydrate division graduate poster competition finalist,
IFT Annual Meeting & Food Expo 2013, Chicago, USA 2013
- International Graduate Student of the Year,
Memorial University of NL, CA 2012
- Distinction, Comprehensive examination
Memorial University of NL, CA 2012
- The J.Beryl Truscott Graduate Scholarship,
Memorial University of NL, CA 2012
- The Barrowman Biochemistry Graduate Travel Award,
Memorial University of NL, CA 2011
- **First place**, Carbohydrate division graduate poster competition,
IFT Annual Meeting & Food Expo 2011, New Orleans, USA 2011
- Phi Tau Sigma Honors, Carbohydrate division, IFT Annual
Meeting & Food Expo 2011, New Orleans, USA 2011
- Selected as one of the 30 applicants (among 150) in the student oral Professional development
session in Food Chemistry research papers submitted for the IFT Annual Meeting & Food Expo
2011, New Orleans, USA
- Fellow of the school of graduate studies,
Memorial University of NL, CA 2011
- Graduate Fellowship, Dept. of Biochemistry,
Memorial University of NL, CA 2009-2013
- Higher Education (Merit) Scholarship
Mahapola Higher Education Scholarship Trust fund, Sri Lanka 2004-2008

APPENDICES

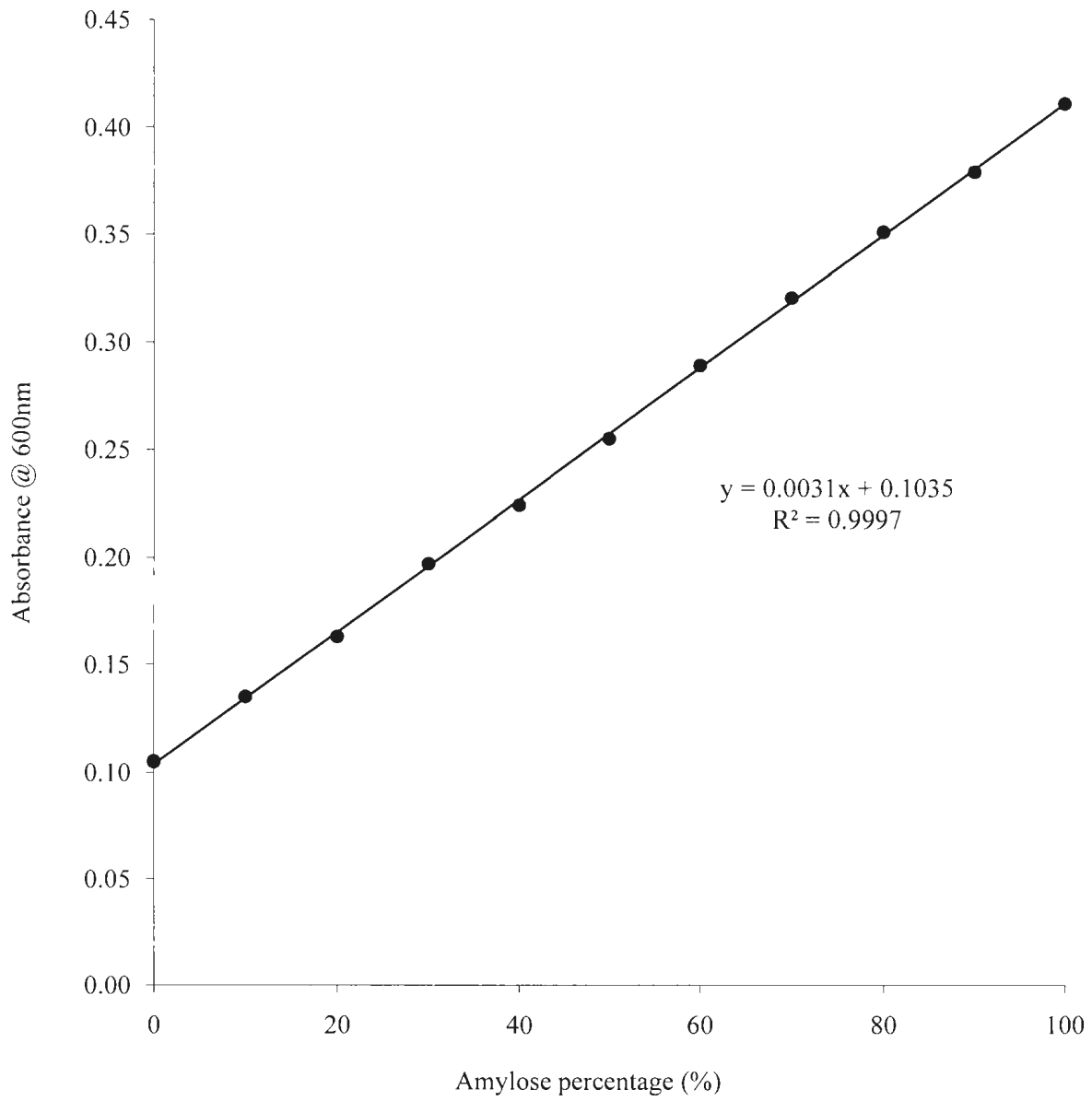
Appendix I

Phosphorus calibration curve (Morrison, 1964)



Appendix II

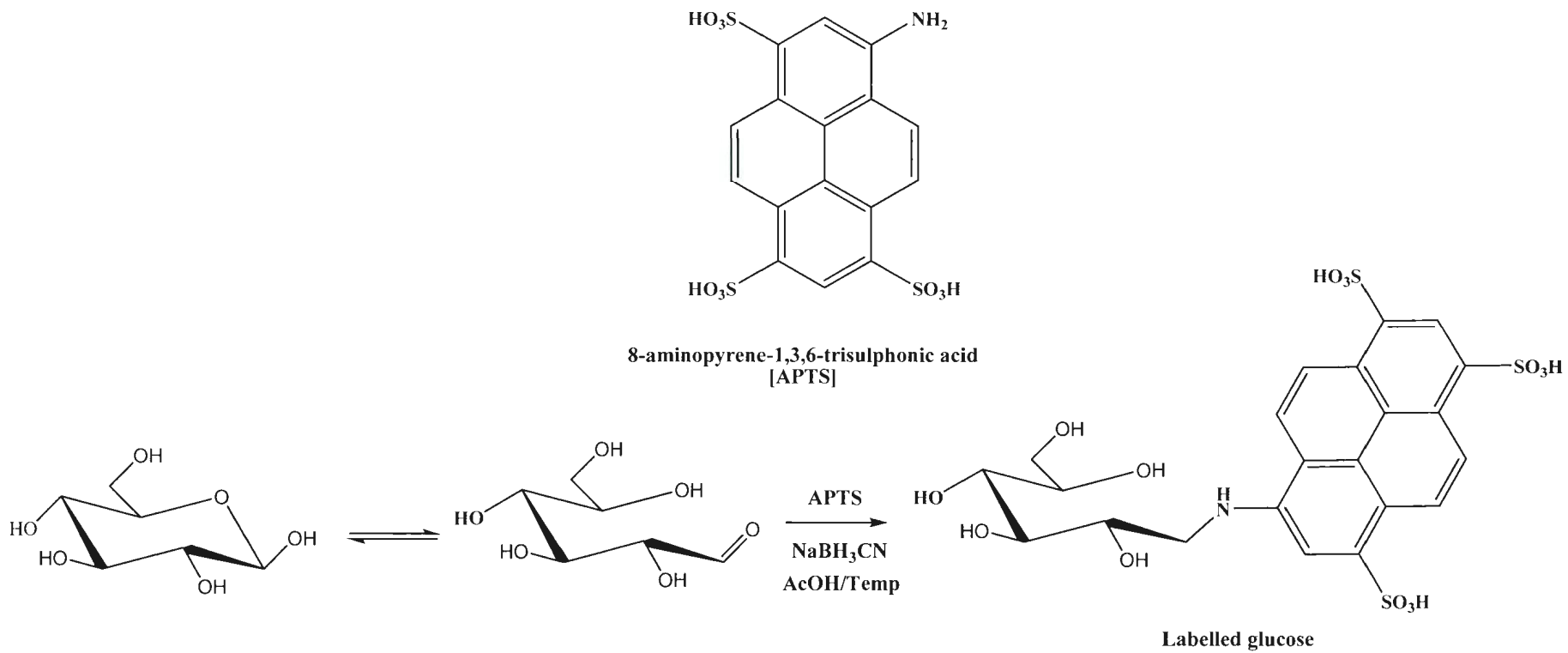
Standard curve for determination of amylose content (Hoover and Ratnayake, 2004)



Appendix III

Labelling reaction of glucose with 8-aminopyrene-1,3,6-trisulfonic acid (APTS)

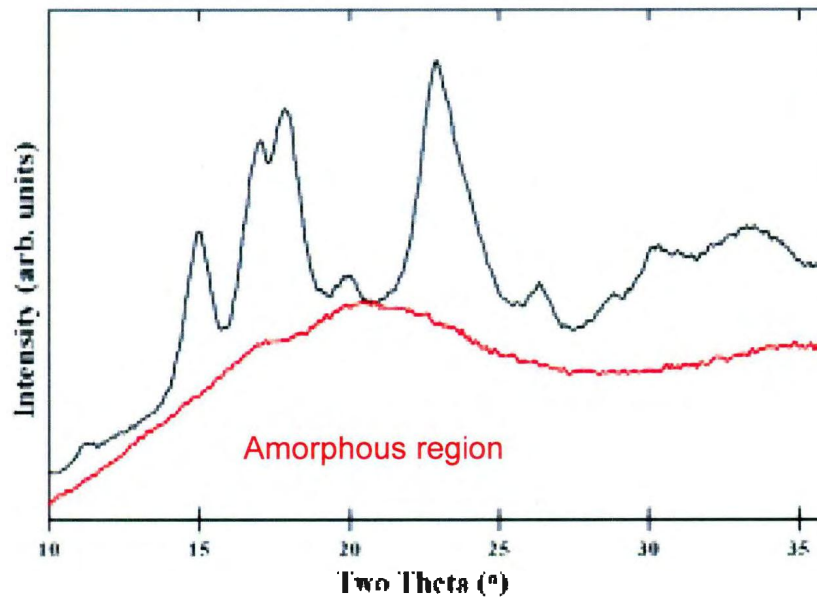
(adapted from O'Shea et al.,1998)



Appendix IV

Curve fitting for XRD using Gaussian function

X-ray spectrum of starch

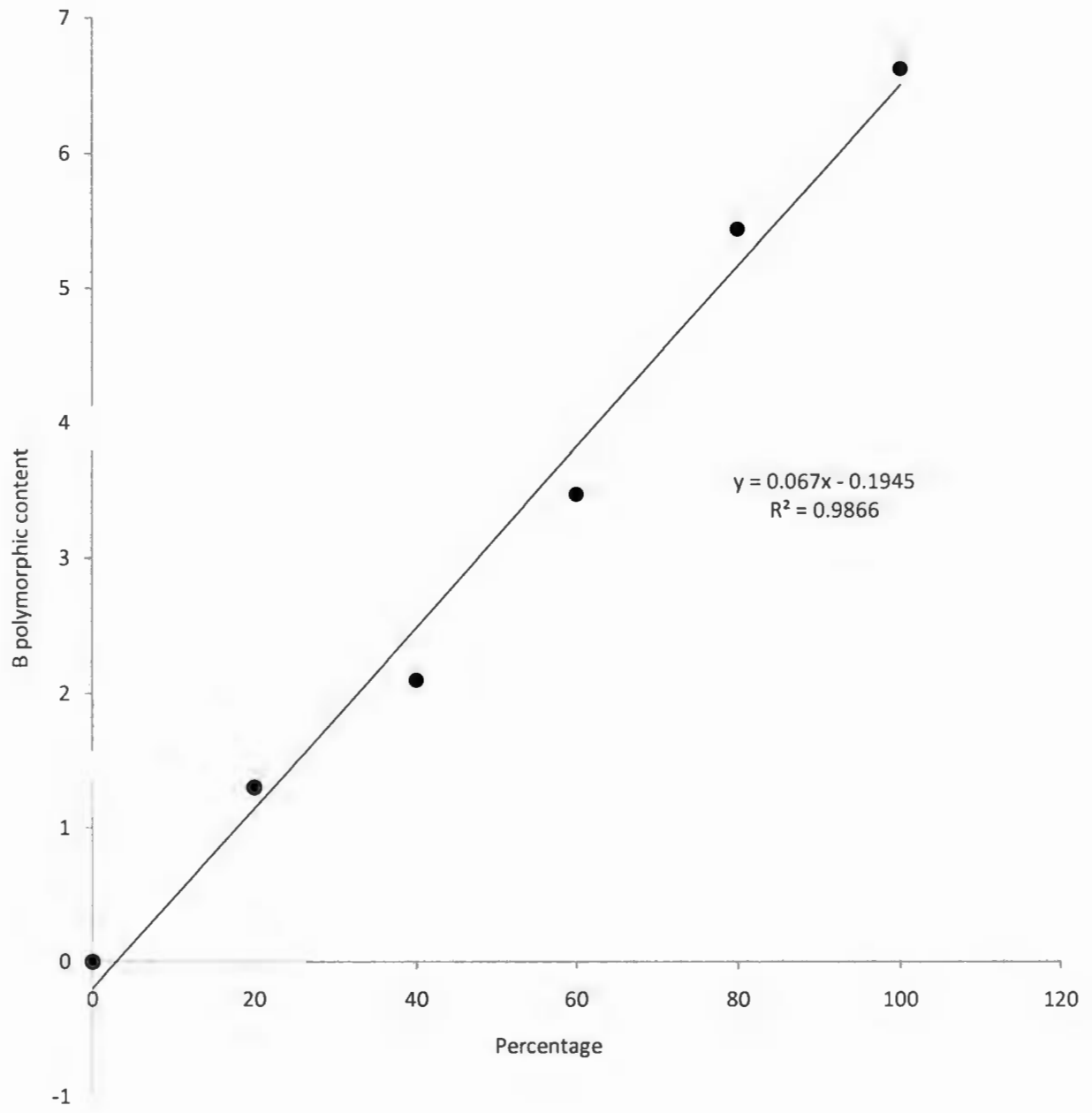


Relative crystallinity will be calculated after subtracting the amorphous background.

$$\text{Relative crystallinity \%} = \frac{\text{Total peak area} - \text{Amorphous peak area}}{\text{Total peak area}} \times 100$$

Appendix V

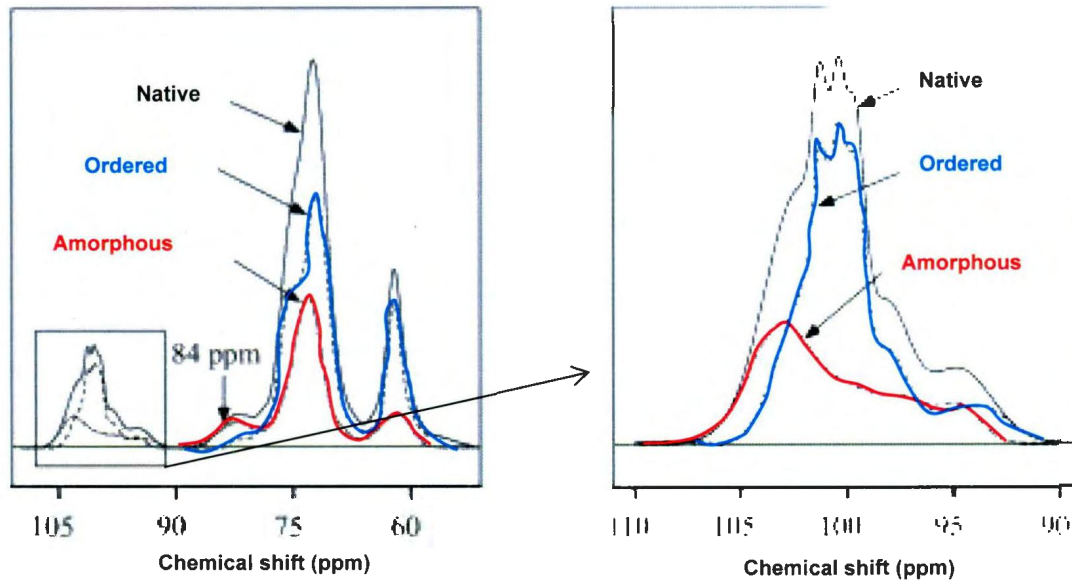
Standard curve for determination of B polymorphic content (Hoover and Ratnayake, 2004)



Appendix VI

^{13}C CP/MAS NMR spectrum decomposition (Tan et al. 2007)

^{13}C CP/MAS NMR spectrum decomposition into amorphous and ordered phases (a) and (b)



$$\text{Double helix \%} = \frac{\text{Area for the C1 signals in the ordered subspectrum}}{\text{Area for the C1 signals in the native spectrum}} * 100$$

$$\text{Amorphous \%} = 100 - (\text{double helix} + \text{V type helix}) \%$$

Appendix VII

Standard curve for determination of reducing sugar as maltose (Bruner, 1964)

